The role of Toll-like Receptor 4 in diabetic foot ulceration

Mark James Portou

Thesis submitted for the degree Doctor of Philosophy

2019

University College London

Division of Surgery and Interventional Science

Royal Free Hospital

Pond Street

London

NW3 2QG

Declaration

I, Mark James Portou confirm the work presented in this thesis is my own, with the guidance of my supervisors, Miss Janice Tsui, Professor David Abraham and Mr Daryll Baker. Where information has been derived from other sources, I confirm this has been indicated in the thesis.

Mark J Portou

Abstract

Diabetes Mellitus has reached epidemic proportions. Foot ulceration is a multifactorial complication of diabetes associated with marked morbidity and mortality. Innate-immune Toll-like receptor 4 (TLR4) mediated inflammation has been implicated in the systemic pathogenesis of diabetes and may contribute to impairment of wound healing. This thesis investigates the effect of high glucose and hypoxic conditions on TLR4 activation and signalling *in vitro* and *in vivo*.

Human skin biopsies were stained for H&E and TLR4. Fibroblasts cultured at physiological glucose concentration (5.5mM) were exposed to pathological glucose concentrations (25mM), with duplicate samples placed in a hypoxia chamber. The effect of TLR4 and its signalling pathway was assessed through specific inhibitors. Diabetes was induced in wild-type (WT) and TLR4 knock-out C57BL/6 mice by intra-peritoneal injection of low-dose streptozocin. Hindlimb ischaemia was induced by femoral artery ligation four weeks post- streptozocin, and full thickness skin wounds initiated below the knee. Wound healing was assessed via digital planimetry at days 3, 7 and 14 post surgery.

Diabetic-ischaemic ulcers demonstrated greater inflammatory cell infiltration ($p=0.0001$) and TLR4 expression ($p=0.038$). Hypoxic and high glucose (25mM), conditions led to an increase in TLR4 protein expression, apoptosis and IL-6 release. Inhibition with MyD88 inhibitory-peptide, TLR4 neutralising-antibody and specific TLR4 antagonist ameliorated the effects of high glucose and ischaemia ($p<0.05$). In vivo, wound healing was significantly impaired in the diabetic-ischaemic group at day 14 ($p<0.05$). Diabetic-ischaemic wounds in TLR4 KO mice exhibited significantly improved healing rates compared to those in WT mice at all time points.

Diabetic-ischaemic ulceration is associated with increased cellular inflammation and TLR4 expression. Hypoxia stimulates up-regulation of TLR4 protein expression and this effect is exaggerated by hyperglycaemia. Inhibition of TLR4 significantly reduced TLR4 protein expression, apoptosis and IL-6 release, suggesting a protective effect. In TLR4 KO mice, there was a significant improvement in the healing of diabetic-ischaemic wounds compared to WT. We propose a synergistic effect between

hypoxia and hyperglycaemia impairing wound healing exists, through TLR4-mediated inflammation.

Impact statement

With a current estimate of 450 million diabetics worldwide, diabetes will remain one of the biggest challenges facing healthcare providers throughout both the developed and developing worlds for the foreseeable future. With this number rising rapidly, the 15-25% of diabetics that will develop foot ulceration throughout their life will continue to place an ever-increasing financial burden on healthcare systems. In 2014 an estimated $13 Billion was spent in the US on managing diabetic foot ulceration (DFU) alone (1). Diabetic complications do not develop in isolation, however. The impact of retinopathy, neuropathy, nephropathy and the need for renal replacement therapy and the increased risk of cardiovascular disease ensures diabetes remains a challenging, expensive and serious condition leading to significant morbidity, disability and excess mortality.

The link between the development of these micro and macrovascular complications and abnormal inflammatory responses mediated via the innate immune system are established. In this project the role of Toll-like receptor 4 in DFU was examined using observational studies of human skin, in vitro models of hyperglycaemia and hypoxia and finally a murine model of diabetic ischaemic distal limb ulceration. We found TLR4 is upregulated and activated by exposure to high glucose conditions and hypoxia. The consequences of the pro-inflammatory effect observed, such as increased cellular apoptosis and IL-6 release are mediated via TLR4 signalling pathways and reduced by specific inhibition of these pathways. In vivo, diabetic ischaemic conditions resulted in a significant impairment in wound healing. The effect of combined diabetes and ischaemia were ameliorated in TLR4 endogenously deleted animals, with a significant improvement in wound healing.

These results suggest a potential benefit for the pharmacological inhibition of TLR4 in diabetic-ischaemic wounds. One of the most obvious utilisations for this therapy is in the form of an impregnated dressing, ensuring local delivery of the drug despite the presence of micro and macro vascular disease. This principle aims to terminate the positive feedback cycle of inflammation-tissue damage-inflammation mediated via pathologically up regulated TLR4 signalling pathways. Thereby restoring the

hyperinflammatory environment of the chronic wound to a physiological state and allowing the normal wound healing process to progress beyond the excessive and prolonged inflammatory phase. Such TLR4 antagonist drugs have been developed and in some cases been subjected to phase 3 clinical trials for alternative uses.

The principles discovered in this project such as the synergistic relationship between hyperglycaemia and ischaemia have implications beyond foot ulceration. Diabetics are subjected to significantly worse clinical outcomes across the whole range of ischaemic pathologies including myocardial infarction and stroke. The widespread expression of TLR4 across immune and non-immune cells in tissues throughout the body, and the multisystemic reach of hyperglycaemia in diabetes suggest that excessive TLR4 mediated inflammation may occur following a latent or asymptomatic pre-clinical 'priming' phase of hyperglycaemia exposure. There may therefore be a survival benefit for the use of systemic TLR4 antagonists in diabetic patients suffering any acute ischaemic event, perhaps even pre-emptively.

Acknowledgements

I cannot adequately express the gratitude I have for my supervisor, mentor and friend Miss Janice Tsui. Your patience knows no bounds and your enduring support, guidance and unwavering faith in me has been an inspiration. I would also like to thank Professor David Abraham for his help and guidance, and Dr Xu Shi-wen for his incredible ability to teach lab techniques, that at first were so unfamiliar to me. I must also thank Mr Daryll Baker for his guidance, advice and mentoring.

I am incredibly grateful to all those in the centre for Rheumatology and Connective Tissue Diseases, and Comparative Biology Unit, UCL that have been on hand for advice and help over the years. I would particularly like to thank Dr Rebekah Yu, Dr Alan Holmes, Dr Markella Ponticos, Dr Ioannis Papaioannou, Dr Svetlana Nihtyanova, Dr Adrian Gilbane, Dr Sandra Guerra, Dr Richard Stratton, Mrs Korsa Khan and everyone else I've had the pleasure to work alongside throughout this journey.

Finally, I'd like to thank my family. Thank you to my parents, whose hard work and sacrifice have provided me with every opportunity in life, to my mum in particular for never letting my motivation drop and whose calming words helped me through difficult times. Thank you to my wife Katie, your patience and support have been essential, I could not have done it without you. The two of us are now four, and to Henry and Alexander, you are my inspiration for everything.

Table of Contents

List of figures

List of tables

List of abbreviations

αSMA	Alpha smooth muscle actin
ABPI	Ankle-brachial pressure index
ACE	Angiotensin converting enzyme
AGE	Advanced glycation end-products
AIDS	Acquired immune deficiency syndrome
ARB	Angiotensin receptor blocker
ASA	American society of anaesthesiologists
BCA	Bicinchoninic acid assay
BME	Beta-mercaptoethanol
BMI	Body Mass Index
C5	Complement component 5
CAD	Coronary artery disease
CABG	Coronary artery bypass graft
CBG	Capillary blood glucose
CCL5	Chemokine (C-C motif) ligand 5
Ck	Cytokeratin
CD4	Cluster of differentiation 4
CD8	Cluster of differentiation 8
CFA	Common femoral artery
CKD	Chronic kidney disease
CLI	Critical limb ischaemia
CLR	C-type lectin receptor
COPD	Chronic obstructive pulmonary disease
CTA	Computed tomography angiography
CVA	Cerebral vascular accident
CXCL9	C-X-C motif chemokine 9
CXCL10	C-X-C motif chemokine 10
DAB	Diaminobenzidine

DAG	Diacylglycerol
DAMP	Damage associated molecular pattern
DAPI	4’,6-diamidino-2-phenylindole
DFU	Diabetic foot ulceration
DM	Diabetes mellitus
DM-I	Diabetic ischaemic
DM-N	Diabetic non-ischaemic
DMEM	Dulbecco’s modified Eagle’s medium
DMSO	Dimethyl sulfoxide
DNA	Deoxyribonucleic acid
DSA	Digital subtraction angiography
eGFR	Estimated glomerular filtration rate
ECM	Extracellular matrix
EDTA	Ethylenediaminetetraacetic acid
EGF	Epidermal growth factor
EIA	External iliac artery
ELISA	Enzyme linked immunosorbent assay
ESKD	End stage kidney disease
FCS	Foetal calf serum
FFPE	Formalin-fixed paraffin embedded
FGF	Fibroblast growth factor
FSP	Fibroblast specific protein
GADA	Glutamic acid decarboxylase antibodies
GADPH	Glyceraldehyde 3-phosphate dehydrogenase
H&E	Haematoxylin and eosin
HbA1C	Haemoglobin A1C (Glycosylated haemoglobin fraction)
HEPES	N-2-hydroxyethylpiperazine--2-ethanesulfonic acid
HIV	Human immunodeficiency virus
HMBG1	High mobility box group 1

HMDEC	Human microvascular dermal endothelial cells
HRP	Horse radish peroxidase
HSP	Heat shock protein
IGF1	Insulin-like growth factor 1
IgG	Immunoglobulin G
IHC	Immunohistochemistry
IL-1	Interleukin 1
IL-6	Interleukin 6
IL-8	Interleukin 8
IRAK	Interleukin receptor-associated kinase
JNK	c-Jun N-terminal kinase
KGF	Keratinocyte growth factor
KO	Knock out
LADA	Latent autoimmune diabetes of adults
LASER	Light amplification by stimulated emission of radiation
LDS	lithium dodecyl sulfate
LG	Low glucose
LPS	Lipopolysaccharide
M	Mannitol
MAL	MyD88 adaptor like
MAPK	Mitogen activated protein kinase
MCP	Monocyte chemotactic protein
MDT	Multidisciplinary team
MI	Myocardial infarction
mM	Mmol/L
MMC	Mitomycin C
MMP	Matrix metalloprotease
MODY	Mature onset diabetes of the young
MRA	Magnetic resonance angiography

MyD88	Myeloid differentiation factor 88
NADPH	Nicotinamide adenine dinucleotide phosphate
NF	Normal fibroblast
NFκB	Nuclear factor kappa light chain enhancer of activated B cells
NLR	NOD-like receptors
NK	Natural killer
NPDR	Non proliferative diabetic retinopathy
NICE	National institute for health and clinical excellence
NOD	Non-obese diabetic
PAD	Peripheral artery disease
PAMP	Pathogen associated molecular pattern
PBS	Phosphate buffered saline
PDGF	Platelet derived growth factor
PDR	Proliferative diabetic retinopathy
PKC	Protein kinase C
PMN	Polymorphonuclear neutrophils
pNFκB	Phosphorylated Nuclear factor kappa light chain enhancer of activated B cells
PRR	Pattern recognition receptors
RAGE	Receptors for glycation end-products
RCT	Randomised controlled trial
RIPA	Radioimmunoprecipitation assay buffer
RNA	Ribonucleic acid
ROS	Reactive oxygen species
RT-PCR	Reverse transcriptase polymerase chain reaction
SDS-PAGE	Sodium dodecyl sulphate polyacrylamide gel electrophoresis
SFA	Superficial femoral artery
STZ	Streptozotocin
TGF-β	Tissue transforming growth factor beta
TIMP1	TIMP matrix metalloprotease inhibitor 1

TLR	Toll-like receptor
TNF-α	Tissue necrosis factor alpha
TRAM	TRIF adaptor molecule
TRIF	TIR domain-containing adaptor-inducing interferon-β
VEGF	Vascular endothelial growth factor
VHG	Very high glucose
WHO	World health organisation
WT	Wild type

Chapter 1

Introduction

1.1 General introduction

The dawn of the 21st century has seen a continued increase in global life expectancy rates, with the average in 2015 (combining both genders) estimated at 71.5 years, increased from 65.3 years in 1990 (2). Considerable regional variations exist and observed increases in life expectancy were not evenly distributed between the developing and high-income developed worlds (2). The developing world saw average life expectancy improve mostly through a dramatic reduction in child and maternal mortality, the high-income world through reduction in cardiovascular, cancer and chronic respiratory disease related deaths (2). In 2016, Ischaemic heart disease remained the single most common cause of death worldwide, followed by stroke, lower respiratory tract infections and chronic obstructive pulmonary disease (COPD) (3).

Despite the improvement in global life expectancies overall, several important causes of death were observed to have dramatically increased. HIV/AIDS as a cause of death worldwide peaked in 2005 and has been declining since, however ominously death rates from hepatocellular carcinoma, pancreatic adenocarcinoma, atrial fibrillation, drug use disorders, chronic kidney disease, sickle cell disorders and diabetes mellitus are continuing to rapidly rise, with little sign of improvement (2).

When considering the major healthcare challenges of the years to come, it remains possible that increasing incidences of these conditions, particularly diabetes, may lead to a plateau or even reversal of decades of improvement in global life expectancy.

1.2 Diabetes Mellitus

Diabetes is one of the earliest documented human diseases. Ancient Egyptian physicians described a condition of “too great emptying of the urine” in the Ebers papyrus, written approximately 1500BC. (4). Ancient Indian physicians from around the same time recognised the urine from diabetics attracted flies and ants and termed the condition “mudhumeha” or “honey urine” (4).

In modern times, diabetes has now reached epidemic proportions. According to World Health Organisation (WHO) data, in 2014 an estimated 422 million people were living with diabetes worldwide (3). This estimate had increased to 451 million by 2017 and is projected to exceed 693 million by 2045 (5). However, even recent predictions consistently underestimate the seemingly exponential increase in prevalence. It is anticipated that currently, approximately half of all people with diabetes are currently undiagnosed, and a further 374 million are living with impaired glucose tolerance or ‘pre-diabetes’ (5).

The concept or use of ‘diabetes’ to imply a single condition or pathology is a misnomer. It is in fact a term used to describe a group of metabolic disorders that result in chronic hyperglycaemia and disordered glucose homeostasis (6). Three classic types of diabetes are commonly described, Type 1 diabetes, where autoimmune destruction of pancreatic beta cells results in absolute insulin deficiency, type 2 diabetes, characterised by insulin resistance (and relative insulin deficiency) and gestational diabetes, manifested during the second trimester of pregnancy. This classification does not include other, less common ‘types’ or ‘subtypes’ and may persist because of historical familiarity. Distinct diabetes subtypes such as mature onset diabetes of the young (MODY), latent autoimmune diabetes of adults (LADA), steroid induced diabetes, diabetes secondary to pancreatic disorders (pancreatitis, pancreatectomy, haemochromatosis) and monogenic diabetes (including MODY, cystic fibrosis, mitochondrial disorders) are now widely recognised.

Using the conventional taxonomy, type 1 and type 2 diabetes are by far the most common, with type 2 comprising approximately 90% of cases (7). The aetiology of

type 2 diabetes is largely unknown. There is a strong genetic preponderance with a polygenic influence, but an individual's risk of developing type 2 diabetes is still closely associated with obesity, lifestyle and dietary factors. Insulin resistance remains poorly understood however. In type 2 diabetes, pancreatic paracrine secretion of insulin is initially maintained, the loss of sensitivity to insulin by certain peripheral tissues such as muscle results in a compensatory increase in insulin production until the beta cells capacity is overwhelmed (8). In contrast, Type 1 diabetes is caused by autoimmune or idiopathic destruction of beta cells in the pancreatic islets of Langerhans and results in hyperglycaemia and loss of glucose regulation through the absence of insulin (9).

A recent study has further demonstrated the heterogeneity of the classically labelled 'type 2' diabetic population. This group measured blood parameters such as c-peptide, glutamic acid decarboxylase antibodies (GADA), HBA1C and creatinine, coupled with clinical data such as age of onset, body mass index (BMI) and performed genotyping on diabetics within 2 years of diagnosis. Ongoing measurement of microalbuminuria, estimated glomerular filtration rate (eGFR) and the presence of retinopathy was undertaken. They concluded that 5 distinct and replicable 'clusters' or subtypes of type 2 diabetes exist, each with subtly different characteristics and risk of developing diabetic complications. For instance, they identified an older sub group with severe insulin resistance that is at significantly higher risk of developing diabetic nephropathy, likewise a young relatively insulin deficient population with very poor metabolic control (10). Currently these patients are treated under the same diagnosis.

The implications of this more refined classification are a better appreciation of the potential differences in aetiology, and thus targeting clinical therapies in a more focussed and tailored approach. Evidence from sub-group analysis of the older but still relevant UKPDS study showed tight glycaemic control reduced microvascular complications of diabetes, but had no effect on mortality, whereas aggressive management of hypertension had a significantly beneficial effect on both morbidity and mortality (11). What is clear is that our understanding, diagnoses and management of 'diabetes' is currently drastically oversimplified.

1.2.1 Complications of diabetes

It is estimated an adult patient diagnosed with type 2 diabetes has reduction in life expectancy of between 5-10 years (12). This is increased to 12 years in type 1 diabetes (13). The principle cause of death in both type 1 and type 2 diabetics remains cardio-vascular disease (14, 15). In addition to excess early mortality, diabetes is associated with several complications that result in significant morbidity and disability. These are broadly categorised into microvascular and macrovascular, and often develop and present simultaneously (16). Management of the complications of diabetes presents a considerable economic burden to healthcare systems, with an estimated $237 billion directly spent on diabetes care in the US in 2017 (17). At a cost of £14 billion in the UK, diabetes care represents approximately 10% of the entire NHS budget.

1.2.1.1 Microvascular complications of diabetes

As mentioned in 1.2.1, the complications associated with diabetes are categorised into microvascular which include retinopathy, nephropathy and neuropathy and macrovascular including coronary artery disease, peripheral arterial disease and stroke (18). These do not develop in isolation and micro and macrovascular complications are recognised to co-exist. Reports in the literature vary, but estimations of type 2 diabetic complications already present at diagnosis such as neuropathy range from 3%, 10-15% up to 52% in certain populations (19-21). The presence of other microvascular complications at diagnosis are more consistent, with nephropathy and retinopathy rates reported at 10% (19, 20). Using data extrapolated from studies of retinopathy, it is estimated the delay from onset of type 2 diabetes to diagnosis is 4 to 6 years, even in advanced healthcare systems (22).

Diabetic retinopathy is the most common diabetic microvascular complication, and manifests as non-proliferative diabetic (NPDR) or proliferative diabetic retinopathy (PDR) and represents a leading cause of blindness worldwide (23). NPDR is characterised by formation of microaneurysms, haemorrhages and hard exudates, all of which may still be asymptomatic. NPDR will progress into PDR and is defined by

the presence of neovascularisation (23). The fragile abnormal vessels are prone to bleeding and may lead to vision loss through vitreous haemorrhage or retinal detachment (23). Neovascularisation also results in a breakdown of the blood-retinal barrier and the formation of diabetic macular oedema, leading to loss of visual acuity (23).

Diabetic nephropathy is the leading cause of end-stage kidney disease (ESKD) in many parts of the world including the US, having overtaken hypertension (24). Diabetic nephropathy typically begins with microalbuminuria and progresses to proteinuria and then the overt nephropathy found in ESKD (21). In the process of developing nephropathy, structural and functional changes occur to the nephron. These include glomerular basement membrane thickening, interstitial fibrosis, mesangial expansion, and in advanced cases macrophage and T-lymphocyte infiltration. Podocyte loss and decreased endothelial fenestration also occur. These glomerular structural changes lead to increasing protein loss and decreasing glomerular filtration rate (24). The development of ESKD also known as chronic kidney disease stage 5 (CKD 5), defined as an eGFR <15ml/min/1.73m^2 requires renal replacement therapy. This is administered in the form of dialysis (haemodialysis or peritoneal dialysis) or renal transplantation.

Diabetic neuropathy is an encompassing term that describes motor, sensory and autonomic nerve dysfunction that develops related to chronic hyperglycaemia, in the absence of other causes (25). Autonomic nerve dysfunction clinically manifest in conditions such as gastroparesis, chronic constipation and other bowel disorders, erectile dysfunction and bladder dysfunction represents a considerable morbidity. Cardiac autonomic dysfunction can result in exercise intolerance, resting tachycardia and sudden death from arrhythmia (26). Pure sensory or motor neuropathies are uncommon, as are mononeuropathies, which are often sudden onset and typically affect nerves of the upper limb (21). More commonly diabetic neuropathy manifests as sensorimotor symmetrical polyneuropathies, frequently affecting the lower limbs (27). Diabetic polyneuropathies can present as ‘painful’, with symptoms of pain and burning, often worse at night, or ‘painless’ with paraesthesia and numbness, the latter of which may be asymptomatic (28). Neuropathy is strongly associated with

diabetic foot ulceration and increased risk of major amputation. This will be covered in more detail in section 1.4.

The development of all diabetic microvascular complications is proportional to the degree of abnormal glycaemic control and the length of exposure (duration of diabetes) (29). The diabetes control and complications trial (DCCT) demonstrated that in type 1 diabetics, a treatment regime of intensive tight glycaemic control aiming for normoglycaemia achieved a 35-75% reduction in the development of microvascular complications compared to a regime with less rigorous glucose and HbA1C targets (30). Similar results demonstrating the benefit of tight glycaemic control in reducing microvascular complications in type 2 diabetics were demonstrated in the UKPDS trial (11) and Veterens Affairs Diabetes Trial (VADT) (31). The results of tight glycaemic control on the development of macrovascular disease are less clear however and will be covered in section 1.2.1.2.

An interesting outcome from extended follow up in these trials comparing intensive tight glycaemic control and 'standard' treatment is the observation that patients with initial poor glycaemic control, despite later switching to tight control were still associated with an increase in the development of diabetic micro and macrovascular complications (32). This phenomenon was termed glycaemic or metabolic memory (33).

Several epigenetic mechanisms have been identified to explain glycaemic memory. These include altered methylation of DNA by DNA methyltransferases and post translational histone modifications, both of which are irreversibly influenced by high glucose (32). Other potential mechanisms include the altered regulation of gene expression by micro-RNAs, which have been shown to contribute to chronic inflammation and are directly affected by hyperglycaemic states in human observational studies (34). Compelling evidence is emerging regarding the use of microRNAs as biomarkers or potential therapeutic targets in diabetes (35).

Other theories proposed to explain glycaemic memory include the glycation of mitochondrial proteins, oxidative stress and formation of advanced glycation end-products (AGE) (35). Another proposed mechanism relates to activation of NFkB

mediated inflammatory gene expression by hyperglycaemic conditions, with toll-like receptors particularly implicated (35). The concept of hyperglycaemia provoked TLR mediated inflammation forms the basis of this thesis and will be explored in detail in subsequent chapters.

1.2.1.2 Macrovascular complications of diabetes

The macrovascular complications of diabetes are coronary artery disease, cerebrovascular disease and peripheral arterial disease (PAD). We will consider peripheral arterial disease separately in section 1.3, however these complications arise through the similar mechanism of arterial atherosclerosis resulting in plaque formation, stenosis or occlusion.

As mentioned previously, cardio-vascular disease is the primary cause of death in type 1 and type 2 diabetics (14, 15). Coronary artery disease (CAD) can lead to angina and myocardial infarction (MI), cerebrovascular disease in diabetes manifests as ischaemic stroke secondary to cerebral large and small vessel atherosclerotic disease (36). Diabetes represents a significant risk factor for the accelerated development of atheroma. The observed 7-year MI risk for a diabetic is 22% compared to 3.5% for non-diabetics (37). Once established, CAD intervention is also less successful. Outcomes after percutaneous coronary intervention are significantly worse than for non-diabetics with an observed increase in subsequent MI and all cause mortality (38). Type 2 diabetes increases the risk of stroke by 1.5 to 4 times compared to non-diabetics (36) and is associated with significantly increased risk of vascular dementia, recurrent stroke and stroke related mortality (39).

Large clinical trials such as the diabetes control and complications trial (DCCT) (type 1) and the UKPDS study (type 2) showed a clear benefit for tight glycaemic control in reducing microvascular complications. Such a benefit however was not demonstrated for macrovascular outcomes. There was however a non-significant trend towards a reduction in MI observed in the UKPDS study. The ADVANCE trial was designed to test this further by applying even stricter glycaemic control targets in type 2 diabetics. Again, no statistical benefit to strict glycaemic control on

macrovascular outcomes was found (40). The same conclusion was reached from the veteran's affairs diabetes trial (VADT) (41). The ACCORD study in type 2 diabetics reported an excess mortality in the intensive glycaemic control group with no reduction in cardiovascular events (42). Metanalysis confirmed that intense glycaemic control in type 2 diabetics does not reduce all-cause mortality or cardiovascular death and is associated with significant risks of hypoglycaemia (43).

1.2.1.3 Potential mechanisms for the development of diabetic complications

Clinical studies have conclusively shown the microvascular complications of diabetes are primarily caused by prolonged exposure to high glucose. The endothelium of retinal, renal and nerve vascular beds appear to be particularly susceptible, possibly through a reduced ability by these tissues to regulate the influx of glucose into cells in high glucose conditions (44). Oxidative stress through mitochondrial superoxide overproduction has been proposed as a unifying mechanism to explain the development of both micro and macrovascular diabetic complications. Several hyperglycaemia induced pathological pathways have been described that stem from inhibition of GADPH through the overproduction of the superoxide free radical by the mitochondrial electron transport chain (45). Briefly described these are:

The 'polyol pathway', where hyperglycaemia results in a depletion of NADPH, resulting in inhibited production of reduced glutathione, an important antioxidant and scavenger of reactive oxygen species (ROS) (44).

The production of AGE through non-enzymic binding of glucose directly inhibits both intra and extra cellular protein function, through alteration of protein structure. In addition, AGE binding with RAGE receptors and TLR4 cross-talk results in activation of NFkB mediated inflammatory pathways (44, 45).

The increased activity of protein kinase C (PKC) isoforms through the accumulation of the PKC potentiating factor diacylglycerol (DAG), which occurs following the inhibition of the glycolytic enzyme GADPH. PKC leads to increased expression of VEGF and TGF-β in target tissues (44, 45).

An increase in hexosamine pathway flux, where the physiological glycolysis pathway produces fructose-6-phosphate, in high glucose conditions excess is converted to uridine diphosphate N-acetyl glucosamine, which results in alterations to gene transcription factors such as Sp1, resulting in increased expression of TGF-β1 and plasminogen-activating factor1 (44).

The evidence for early aggressive tight glycaemic control to reduce the development of diabetic microvascular complications and their consequences such as blindness, renal dialysis and limb loss is clear. Macrovascular complications however have a more complex influence of contributing risk factors, and all need to be aggressively individually addressed.

1.3 Peripheral artery disease

Peripheral artery disease (PAD) refers to a collection of conditions of varying severity caused by atherosclerotic stenosis or occlusion of a peripheral limb (46). 13% of people over 50 years are affected with PAD (46, 47).

The majority of patients remain asymptomatic however and symptoms range from intermittent claudication, defined as exercise induced ischaemic pain relieved by rest to critical limb ischaemia (CLI) is defined as ischaemic pain at rest or arterial ulceration or gangrene (tissue loss) (48). CLI is associated with a significant increased risk of limb loss.

Diabetes is a significant risk factor for the development of PAD (46), comparable to the relative risk of smoking (49). Diabetic patients are often asymptomatic due to the co-existing presence of peripheral neuropathy (49). There is a significant tendency in diabetics towards the disproportionate development of crural vessel disease, often with significant calcium burden. This is irrespective of gender, although older age is associated with greater progression to pedal arch involvement (50). The pathophysiology of this tendency is unclear.

1.4 Diabetic foot ulceration

Foot ulceration (DFU) and a wide spectrum of associated diabetic foot diseases result in an enormous morbidity and excess mortality for diabetic patients. DFU is a common presentation, with a 12-25% lifetime risk of developing an ulcer in diabetes (51, 52). It remains the most common cause of hospitalisation in diabetics (51) and confers 15-20-fold risk of major amputation over non diabetics, responsible for 85% of all non-traumatic amputations (53). Annually an estimated 6000 diabetic patients undergo amputation in England, with a 50% mortality in this population within 2 years of amputation (54). There is a significantly reduced life expectancy associated with DFU without amputation, with only 56% alive at 5 years following development of ulceration (54).

The aetiology of DFU is multifactorial. DFU is classically and broadly described as either neuropathic or ischaemic with neuropathy or purely ischaemic, the reality however is significantly more complicated (55). As described in section 1.2.1.1, neuropathy is a common microvascular complication of diabetes, describing a combination of sensory, motor and autonomic neuropathy. Sensory neuropathy results in numbness and paraesthesia leaving the foot vulnerable to trauma and skin breakdown through reduced or absent sensation (56). Loss of joint proprioception compounds the ability to compensate for abnormal joint loads and pressure. Simultaneous motor neuropathy results in denervation and wasting of the intrinsic muscles of the foot, causing muscle imbalance and structural changes in foot architecture (57). Common structural abnormalities are claw and hammer toes, subluxed and prominent metatarsal heads, pes cavus and equinus and hallux valgus (58). These anatomical deformities result in abnormal pressure loads distributed through previously non-load bearing tissues, which react through hyperkeratinisation, forming callus and predisposing to ulceration (59). Autonomic neuropathy reduces local vasodilatation and sweating, resulting in dry and fissured skin and increases local temperature, leaving the foot more prone to ulceration and infection (56).

The presence of macrovascular disease in the form of PAD is an independent risk factor for the development of DFU (60). PAD is present in 50% of patients with DFU and recent evidence from the EURODIALE group suggests this is increasing (61). Unsurprisingly, diabetic ulcer healing rates are significantly impaired with co-existing PAD, with a greater incidence of major amputation and higher mortality (61). This effect is significantly worse in the presence of infection (61).

Given the impact on outcome, it is important to identify PAD in patients presenting with DFU. A clinical history of pre-existing symptomatic PAD will include intermittent claudication, previous ulceration and ischaemic rest pain. Simple tests such as hand-held doppler, ABPI and or toe/brachial (TBI) measurement are recommended to all patients with DFU. Absence of palpable pulses, monophasic doppler signals or an ABPI <0.9 should prompt further investigation, ABPI measurement may not be accurate in diabetic patients however. Arterial duplex scanning is recommended as the first line investigation by the national institute for health and clinical excellence (NICE) (62). Subsequent investigation may include gandolinium contrasted magnetic resonance angiography (MRA), computed tomography angiography (CTA) or digital subtraction angiography (DSA) (60).

Despite optimum medical therapy and revascularisation approximately one third of diabetic ulcers will never heal (63). Other important aetiological factors in addition to neuropathy, abnormal pressure loads, and micro and macrovascular dysfunction include the presence of infection, including chronic osteomyelitis (60). The role of immunological dysfunction and innate immune mediated hyperinflammation in these chronic wounds will be explored in section 1.6.1.

In certain studies, the location of ulcers on the foot has impacted on median healing times. Toe ulceration was associated with faster healing times than midfoot ulcers, which healed more quickly than heel ulceration (64).

1.4.1 Classification of DFU

Many classification systems for DFU have been described for the purposes of clinical description or comparison, research or audit (65). Two classifications recommended for clinical use by NICE are the SINBAD and University of Texas classifications (62).

SINBAD Score:

Category	Definition	SINBAD score	Equivalent S(AD)SAD categories
Site	Forefoot	0	—
	Midfoot and hindfoot	1	—
Ischemia	Pedal blood flow intact: at least one pulse palpable	0	0–1
	Clinical evidence of reduced pedal blood flow	1	2–3
Neuropathy	Protective sensation intact	0	0–1
	Protective sensation lost	1	2–3
Bacterial infection	None	0	0–1
	Present	1	2–3
Area	Ulcer $<1cm^2$	0	0–1
	Ulcer $\geq 1cm^2$	1	2–3
Depth	Ulcer confined to skin and subcutaneous tissue	0	0–1
	Ulcer reaching muscle, tendon or deeper	1	2–3
Total possible score		6	—

Table 1.4.1 Reproduced from: Diabetes Care. 2008 May;31(5):964-7 (66).

University of Texas classification:

	Grade			
Class	0	I	II	III
A	Preulcerative or postulcerative lesion, completely epithelialized	Superficial wound, not involving tendon, capsule, or bone	Wound penetrating to tendon or capsule	Wound penetrating to bone or joint
B	Preulcerative or postulcerative lesion, completely epithelialized with infection	Superficial wound, not involving tendon, capsule, or bone, with infection	Wound penetrating to tendon or capsule with infection	Wound penetrating to bone or joint with infection
C	Preulcerative or postulcerative lesion, completely epithelialized with ischemia	Superficial wound, not involving tendon, capsule, or bone, with ischemia	Wound penetrating to tendon or capsule with ischemia	Wound penetrating to bone or joint with ischemia
D	Preulcerative or postulcerative lesion, completely epithelialized with infection and ischemia	Superficial wound, not involving tendon, capsule, or bone, with infection and ischemia	Wound penetrating to tendon or capsule with infection and ischemia	Wound penetrating to bone or joint with infection and ischemia

Table 1.4.2 Reproduced from: J Foot Ankle Surg. 1996 Nov-Dec;35(6):528-31 (67)

The SINBAD score compares multiple wound factors such as ischaemia, neuropathy, infection as well as ulcer size, site and depth. It is simple and has a binary scoring method which allows the classification to be used for outcome prediction and comparisons and research/audit purposes. The Texas classification is well established and simplifies the clinical assessment of individual wounds, while recognising the influence of infection and ischaemia as well as wound depth.

1.5 Management of diabetic foot ulceration

The development of DFU is multifactorial, and best management must strive to address each of the contributing factors. Broad principles for the treatment strategies that form current best therapy include tight glycaemic control, wound offloading, debridement, infection control and revascularisation where required.

There are also a variety of adjunctive therapies such as negative pressure dressings (VAC pumps) and skin substitutes currently approved by the national institute for health and clinical excellence (NICE), other novel therapies such as hyperbaric oxygen, growth factors and electrical stimulation therapies are not currently recommended unless part of a clinical trial (62).

There is a dearth of quality evidence in wound care interventions as randomised controlled trials in wound healing are notoriously difficult to design and perform. Clinical trials are often subject to considerable bias, in outcome measure and patient selection, and often the results of promising pre-RCT studies cannot be replicated (68).

Foot wounds are highly heterogenous. There is little conclusive evidence favouring one broad treatment strategy over another. For instance, wound characteristics such as size, location, or exudate will inform off-loading method. Bedside wound debridement is comparable to operative surgery if tolerated and depending on extent. Antibiotic regimes are tailored to the individual bacterial species following microbiological sampling.

Re-vascularisation interventions are broadly classified as surgical or endovascular. Surgical options are endarterectomy or bypass. Endovascular approaches involve angioplasty or stenting. Comparison of these approaches or detailed discussion regarding the techniques used (vein vs prosthetic bypass, drug eluting vs plain balloon angioplasty) are beyond the scope of this brief overview.

Comprehensive management of this complex and challenging multifactorial condition must involve multidisciplinary input from vascular surgeons, diabetologists, podiatrists, specialist nurses, orthopaedic surgeons, microbiologists, radiologists, vascular scientists, physiotherapists and plaster technicians.

1.6 Wound healing

Wound healing is a complex physiological process comprised of discreet but inter-related and overlapping stages, requiring exact timing and regulation to successfully progress, yet occurs spontaneously in response to injury. It is characterised by four phases, coagulation, inflammation, proliferation and remodelling. Each phase is predominated by particular cell types, cytokines and chemokines.

Immediately following trauma to the skin, platelets aggregate at the site of injury with haemostasis achieved following local vasoconstriction and activation of the clotting cascade, resulting in fibrin clot formation (69). The inflammatory phase of wound healing begins with release of proinflammatory cytokines such as Platelet derived growth factor (PDGF), transforming growth factor (TGF-β), fibroblast growth factor (FGF), epidermal growth factor (EGF) and Interleukin 8 (IL-8/CXCL-8) from the newly formed clot and directly from the damaged tissues (70). These act as potent chemotactic signals to immediately recruit neutrophils to the wound (71). Circulating polymorphonuclear neutrophils (PMN) begin migration within minutes from the blood into the immature wound bed formed by the clot, peaking within the first 24 hours (72). The neutrophils now present in the wound provide a crucial defence against microbial invasion following disruption to the skin's natural barrier function, clearing both pathogen and tissue debris by phagocytosis (70, 73).

The process of platelet de-granulation, activation of the complement cascade, and the migration and signalling of PMNs results in the further production of chemotactic factors such as complement component 5 (C5), fibrin by products and TGF-β (53). These chemokines along with chemokine (C-C motif) ligand 5 (CCL5) produced by keratinocytes, recruit monocytes to the wound, which under the influence of local cytokines undergo differentiation to become mature wound macrophages (53, 74). By days three to five following injury, tissue macrophages become the dominant cell type (75). Wound macrophages continue the process of wound bed clearance through phagocytosis of apoptotic cells including the early phase PMNs, tissue debris and microbial organisms (75). In addition, macrophages also directly aide the debridement of injured and devitalised tissue through release of protease and

metalloprotease enzymes (75, 76). Over and above their phagocytic role, an important initial function of wound macrophages is the release of cytokines which further aid the recruitment and activation of inflammatory cells (70, 75). As the inflammatory phase progresses, macrophages produce important growth factors such as KGF, TGF-β, VEGF and PDGF which stimulate fibroblast and keratinocyte growth and migration and the process of angiogenesis (69). It is therefore considered that macrophages are responsible for the transition to the proliferative phase of wound healing (70, 75).

The late inflammatory phase becomes characterised by infiltration of T-lymphocytes under the influence of IL-1, which peak at day 7 after injury. At this stage there is considerable temporal overlap between the late inflammatory, proliferative and early remodelling phases of normal wound healing (77). As described, the inflammatory phase involves a well characterised sequence of immune cell infiltration, neutrophils followed by macrophages then finally T-lymphocytes (70).

Like macrophages, T-lymphocytes appear to have a complex yet significant role in the normal process of wound healing, however these processes, functions and pathways remain poorly understood. Studies utilising *in vivo* murine knock-out models have suggested that absent or delayed T-lymphocyte wound infiltration results in an impairment of the healing process (68). However there appears to be differential roles of CD4+ T helper and CD8+ cytotoxic T cells, with CD4+ cells found to have a positive promoting effect on healing, and CD8+ cells an inhibitory effect (78). In addition, T-lymphocytes have a regulatory effect on inflammation and fibrosis and a dermal subgroup of gamma delta T cells produce keratinocyte growth factor (KGF) and insulin-like growth factor 1 which stimulate keratinocyte proliferation, promoting healing (79).

Central to the proliferative phase of wound healing is the formation of granulation tissue. Dermal fibroblast proliferation, migration and differentiation (into contractile myofibroblasts) occurs under the influence of growth factors such as fibronectin, PDGF, FGF, TGF-β and C5a, as inflammatory cytokine release diminishes (80). Fibroblasts are crucial for the production of extracellular matrix comprised of

collagen, glycosaminoglycans, proteoglycans, fibronectin and elastin (81). Angiogenesis occurs as dermal endothelial cells migrate into the newly forming extracellular matrix under the influence of macrophage derived angiogenic factor, forming new capillaries (75).

During the proliferative phase, wound contraction is an important process that occurs through the action of myofibroblasts, differentiated from mesenchymal fibroblast cell lines (82). Myofibroblasts, unlike fibroblasts express the contractile protein α smooth muscle actin (αSMA) and as the wound matures are gradually lost from the granulation tissue (82).

Restoration of the skins crucial barrier function requires successful epidermal keratinocyte migration, proliferation and differentiation to cover the newly formed granulation tissue and extracellular matrix in a process termed re-epithelialisation (83). In intact skin, keratinocytes are closely attached to adjacent epithelial cells through desmosomes, and to the extra cellular matrix of the underlying basement membrane by hemidesmosomes (84). Following injury, keratinocytes become mobilized by undergoing phenotypic changes favouring detachment in a process that remains incompletely understood. However cytokines such as IL-1, IL-6 and TNF-α produced in inflammatory phase seem to help modulate the migratory phenotype of keratinocytes (84). Migration and proliferation are influenced by growth factors such as IGF1 and epidermal growth factors (EGF) (85). In addition, EGF, KGF and TGF-β have important pro-migratory or pro-proliferative effects on keratinocytes (84). Essential to the process of keratinocyte migration is production of proteases such as collagenases and matrix metaloproteases (86). These degrade adjacent adherent sections of the newly formed extracellular matrix to permit cell movement (83). Disruption of the basement membrane after injury requires migrating keratinocytes to utilize fibronectin, vitreonectin and fibrin components of the provisional extracellular matrix for attachment through focal integrin receptors (83). Closely following migration is rapid proliferation and basement membrane repair through laminin production (87). Keratinocyte differentiation and keratin production occurs as the epidermal barrier and normal stratified architecture is restored (88).

The remodelling phase is the longest phase of the wound healing process, continuing for weeks to months (75). This phase is characterised by reduced proliferation and inflammation, active re-organisation of the extra cellular matrix and regression of the newly formed capillaries as the nutrient requirements of the wound site reduce (75).

Type III collagen produced by fibroblasts during the proliferative phase is gradually replaced by structural type I collagen, through the action of collagenases and matrix-metalloproteases (83). During remodelling, collagen becomes more organised and increasingly cross-linked strengthening the scar; fibronectin disappears, and hyaluronic acid and glycosaminoglycans are replaced by proteoglycans. The result is the re-organisation of the extracelluar matrix to an architecture more closely resembling normal tissue (70, 75).

1.6.1 Wound Healing in diabetes

The diabetic wound environment differs from the normal acute wound process through a prolonged and persistent inflammatory phase, represented in figure 1.6.1. There is an exaggerated and sustained neutrophil and macrophage infiltration, which in a db/db mouse model was demonstrated to be associated with deregulated and prolonged chemokine expression, such as macrophage inflammatory protein 2 and macrophage chemoattractant protein 1 (89).

Although the initial infiltration of immune cells is impaired, once activated the result is a hyperinflammatory response with elevated inflammatory cytokine production of TNF-α, IL-1β and IL-6, and increased NFkB regulated matrix metalloprotease (MMP) production leading to excessive extracellular matrix destruction and grossly impaired granulation tissue formation (53). Neutrophils in particular appear to contribute to these destructive wound conditions through upregulated release of MMP-8 and downregulated release of the MMP inhibitor TIMP1 in chronic wounds (90). The resulting hostile environment of excess inflammatory cytokine production (TNF-α, IL-6) also impairs other events and processes crucial to healing such as fibroblast migration and proliferation, collagen synthesis and promotes apoptosis in fibroblasts

and vascular precurser cells (53). Diabetic ulceration is an example of chronic inflammation directly leading to a significant impairment in the healing process and the creation of a chronic non-healing wound. There is compelling evidence this pathological inflammation is mediated via excessive activation of pattern recognition receptors of the innate immune system such as toll-like receptors.

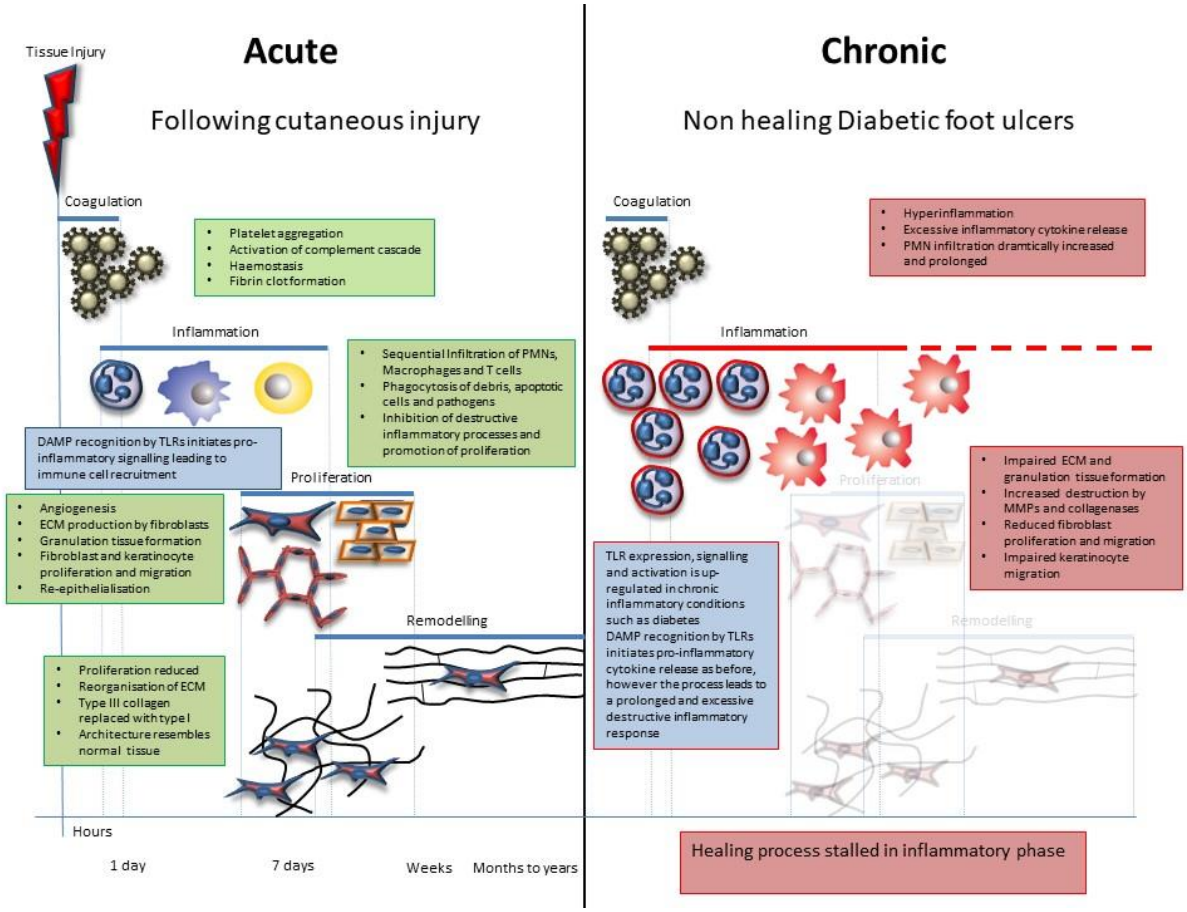

Figure 1.6.1 Wound healing in diabetes (Reproduced from Portou et al, 2014) (91)

1.7 The innate immune system and pattern-recognition receptors

Mammals and other higher vertebrate organisms have evolved complex immune defences against invading pathogenic microorganisms, comprised of the innate and adaptive immune systems (92). The innate immune system is in evolutionary terms primitive and unlike the clonal selection antibody-based response of the adaptive

immune system, is entirely encoded within the genome (93). Innate immunity comprises the entire immune response of invertebrate organisms, however in higher species it provides the first line of defence against infectious pathogens and aides adaptive responses through antigen presentation, with the adaptive response concerned with later stages of infection, providing a targeted and specific response and immunological memory (92).

The innate immune system is comprised of numerous different cellular components such as neutrophils, eosinophils, basophils, mast cells, monocytes, macrophages, dendritic cells, NK cells, gamma delta T cells, B-1 cells (94). Rather than co-ordinating a non-specific pro-inflammatory or phagocyte response, cell activation, pathogen recognition and a specificity of the innate immunity is conferred by the presence of specific receptors expressed by these immune cells termed pattern recognition receptors (PRRs) (95, 96).

1.7.1 Toll-like receptors

Toll-like receptors (TLRs) are key pattern recognition receptors of the innate immune system (97). Other examples of PRRs include scavenger receptors (SRs), C-type lectin receptors (CLRs), NOD-like receptors (NLRs) and B2 integrins (96). These receptors are highly conserved in evolution and recognise discreet molecular components of invading pathogens termed pathogen associated molecular patterns (PAMPs), such as lipids, lipopeptides, proteins and nucleic acids (92, 97). The recognition of microbial PAMPs by PRRs leads to activation of specific signalling pathways and a variety of cell dependant responses, including pro-inflammatory cytokine release, phagocytosis and antigen presentation (96).

The Toll-like receptor family consists of thirteen identified members of which ten are expressed in humans (94). TLRs are located either at the cell surface (TLRs 1,2, 4, 5, 6) or in the intracellular compartment (TLRs 3, 7, 8, 9) primarily on exosomes and endoplasmic reticulum (98, 99). TLRs are transmembrane proteins comprised of an ectodomain comprising leucine-rich repeats, a transmembrane domain and an intracellular (TIR) domain (98). The binding of TLR ligands results in activation

through the recruitment of specific adaptor molecules such as myeloid differentiation factor 88 (MyD88), MyD88 adaptor like (MAL), TIR domain-containing adapter-inducing interferon-β (TRIF) and TRIF adaptor molecule (TRAM) to the intracellular domain (98, 100). All TLRs except TLR3 utilise one of two signalling pathways, the MyD88 dependent and MyD88 independent (TRIF) pathways, resulting in the activation of nuclear transcription factors such as NFkB, JNK and MAPK (98). TLR3 signals solely through the TRIF pathway (97). TLR4 signals through both MyD88 and TRIF pathways, as represented in figure 1.7.1. The result is proinflammatory cytokine and type 1 interferon gene induction (92).

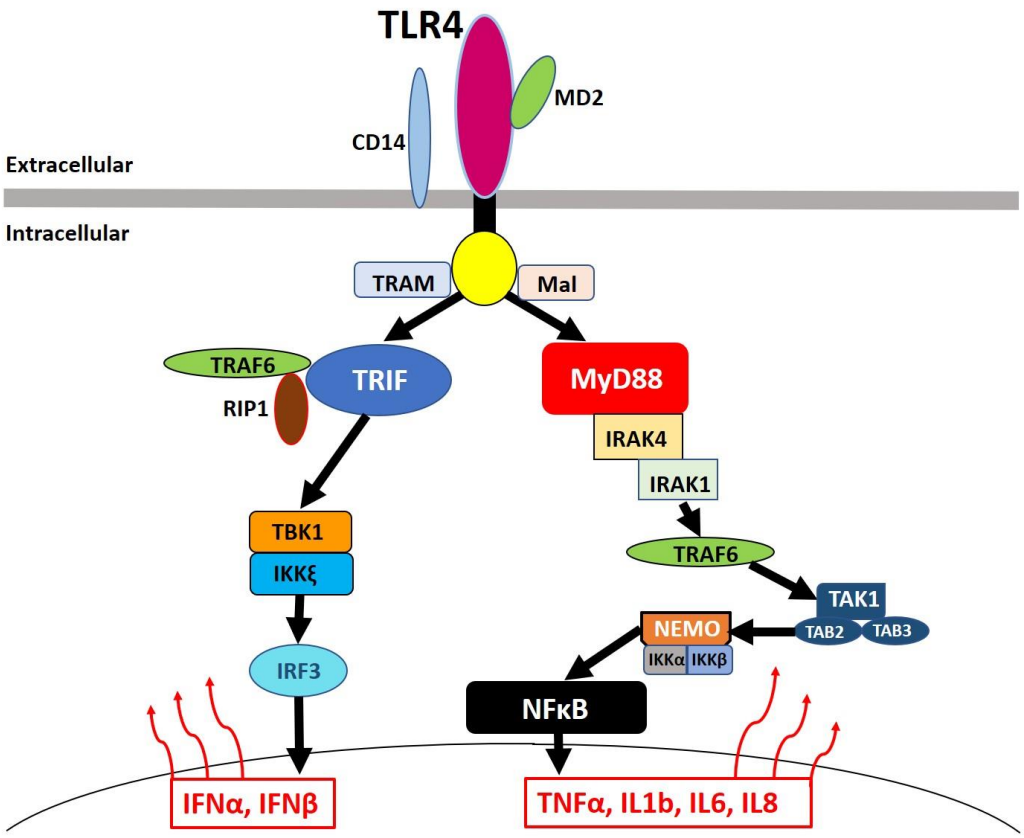

Figure 1.7.1 Schematic representation of TLR4 signalling pathway

TLRs efficiently recognise distinct components of pathogens that are essential to their metabolism, preventing mutations rendering them undetectable (101). TLRs 1, 2 and 6 recognise gram positive bacteria cell wall constituents such as lipoproteins, peptidoglycans and lipoteichoic acid (101). TLR4 is activated by the gram negative

bacteria cell wall component lipopolysaccharide (LPS) (102) and TLR5 bacterial flagellin (101). The intracellular TLRs 3, 7 and 8 recognise double and single stranded viral RNA, and TLR9 non-methylated CpG dinucleotides present in bacterial DNA (101, 103).

In addition to exogenous microbial PAMP ligands, TLRs are also activated by a range of endogenous ligands released as a result of tissue and cellular injury termed damage associated molecular patterns (DAMPs). These are usually hidden from recognition, however following injury they are released or revealed, triggering a TLR mediated inflammatory response (101). It has been suggested DAMPs act as danger signals, released by injured tissues, alerting the immune system of damage (104). The resulting sterile inflammation is a key stimulator for the recruitment of innate immune inflammatory cells and initiation of the wound healing process (101). DAMPs identified as TLR ligands include the extracellular matrix constituent hyaluronic acid, HMGB1 (a nuclear protein), Heat shock proteins (HSPs) 60 and 70, oxidised LDL, fibrinogen and fibronectin (105).

1.7.1.1 Toll-Like receptors and apoptosis

As described in section 1.7.1, Toll-like receptors trigger crucial pro-inflammatory immune responses in response to stimulation by pathogen and damage-associated ligands. In addition, TLR activation directly induces cellular apoptosis (106). Apoptosis is the process of 'programmed cell death' and occurs through a sequential proteolytic cleavage of caspases, a family of cysteine proteases (106, 107). Immune-initiated apoptosis is thought to reduce microbial spread throughout the organism and prevent overwhelming autoimmune reactions (106).

TLR4 has been identified as the dominant pro-apoptotic signal transducer of immune mediated cell death (108). Additionally, TLR4 activation has been directly linked to cleaved caspase 3 associated apoptosis, in macrophages (108), cardiac myocytes (109), microglia (110) and ischaemic neurones in a cerebral infarction model (111).

1.7.2 Toll-like receptors and the skin

Intact skin provides an external barrier to the environment, preventing infection by the majority of pathogenic bacteria, viruses and fungi (112). In addition to this physical defence, cells of the innate immune system present in skin such as dermal mast cells, phagocytes and dendritic cells such as Langerhans cells of the epidermis, and those readily recruited from blood such as neutrophils, macrophages, basophils, eosinophils, NK cells and gamma-delta T cells all express TLRs for pattern recognition (101). On detection of invading microbial pathogens through recognition of PAMPs, TLR activation results in the initiation of a pro-inflammatory defence response, promoting phagocytosis, immune cell recruitment and antigen presentation (112). In addition to immune cells, TLRs are also widely expressed by a variety of non-immune cells contained within both the epidermis and dermis and vital to wound healing (113).

The epidermis is primarily comprised of keratinocytes, which have been demonstrated to express TLRs 1-6 and TLR9 and 10 (114). Unlike specialist immune cells, keratinocytes and other epithelial cells comprise the boundary and interface with the external environment and are under constant exposure to microbes and PAMPS (101). They are able to maintain a delicate balance between tolerance of commensal organisms and the detection of infection and injury and subsequent inflammatory response (101). The relative expression of TLRs by keratinocytes also seems to vary depending on position of the cell, for instance TLR5 is predominantly expressed in the basal layers, whereas TLR9 is expressed to a greater degree by more differentiated cells of the upper epidermal layers (115). It does appear however all TLRs are functional, and produce distinct immune responses (116). For instance, activation of keratinocyte TLRs 3, 4, 5 and 9 resulted in TNF-α, IL-8, CCL2 (basophil chemokine) and CCL20 (macrophage inflammatory protein-3) release (116). TLR3 and TLR9 activation produced CXCL9 and CXCL10, involved in T-memory cell activation and type 1 interferon production (116).

Fibroblasts located in the dermis produce extra cellular matrix constituents, cytokines, growth factors and have a crucial role in the wound healing process as described above. They have been found to express the full range of human TLRs from

1 to 10 (117). Studies have demonstrated *in vitro* activation of TLRs 2, 3, 4, 5 and 9 resulted in production of interferon-γ, CXCL9, CXCL10 and CXCL11, important in the recruitment of T-cells and NK cells (116). TLR4 activation in dermal fibroblasts has been demonstrated to result in IL-6, IL-8 and monocyte chemotactic protein (MCP) (118). Microvascular cells such as dermal endothelial cells have been shown to highly express TLR4 and to a lesser extent TLR2. *In vitro* treatment of the exogenous TLR4 ligand LPS resulted in NFkB activation and exposure to the endogenous derived hyaluronan induced IL-8, a potent chemokine, stimulating the recognition of tissue injury and promoting initiation of the early stages of the wound healing process (119).

1.7.3 Toll-like receptors and wound healing

As described in 1.7.1, recognition of endogenous ligands by TLRs on both immune and non-immune cells of the skin provide alarm signals via TLR activation and resulting sterile inflammation alerting to tissue injury. However, the effect of TLR activation on the wound healing process extends beyond the initial recognition of cellular damage, and it appears depending on the location, timing and degree of activation may have a promoting or inhibiting effect on the process of wound healing and tissue regeneration (120).

In vitro and *in vivo* data has suggested that TLR4 becomes upregulated within the first 12-24 hours following injury and slowly decreases to baseline at day 10, and is primarily concentrated in epidermal keratinocytes (121). The same study demonstrated significantly impaired wound healing in TLR4 deficient mice at days 1-5, with no difference seen from wild type at 10 days (121). An altered pattern of cytokine release and inflammatory cell infiltration was observed with decreased IL-1β and IL-6, and an increase in neutrophil, macrophage and T-cell infiltrates at discreet time points (121). Another study also observed impairment in wound healing in TLR2 and TLR4 deficient mice at days 3 and 7, but observed a decrease in neutrophil and macrophage infiltration, and reduced TGF-β and CCL5 expression (74). Activation of TLRs 4 and 2 appears therefore to have a beneficial effect on

wound healing in the early stages following acute injury, at least in absence of other influences on TLR expression, signalling and activation.

Controversy exists however as to the exact effect of TLR4 and TLR2 in the wound healing process. Given the seemingly important regulatory role of TLR4 and TLR2 in initiating the early stages of wound healing, it perhaps seems counter-intuitive that wound healing was significantly improved in TLR2 deficient mice with induced diabetes compared to diabetic wild-type animals (122). The same effect was also observed in diabetic TLR4 deficient mice (123) in apparent contradiction of the studies described above.

In addition to decreased healing time, the wounds from TLR2 deficient mice also demonstrated significantly reduced NFkB activation, IL-6 and TNF-α release (122). In the same study when comparing wild-type diabetic mice to non-diabetic controls, TLR2 mRNA and protein expression was significantly increased, along with markers of activation such as increased expression of MyD88, IRAK and NFkB (122). Likewise, TLR4 mRNA and protein expression, IL-6, TNF-α and NFkB activation was increased in wild-type diabetic compared to non-diabetic animals, with a corresponding reduction in IL-6, TNF-α and NFkB activity in the TLR4 deficient diabetic populations (123).

These studies demonstrated significantly increased TLR (2 and 4) and MyD88 expression in diabetic compared to non-diabetic wounds and suggests in diabetes, TLR2 and 4 mediated hyperinflammation results in an impairment of wound healing. Persistent activation of TLRs 2 and 4 is also associated with other chronic non-healing wounds such as chronic venous ulceration (124).

Wound healing studies utilising TLR 3 deficient mice resulted in significantly delayed wound healing compared to wild-type controls, led to decreased neutrophil and macrophage recruitment, and reduced CXCL2, CCL2 and CCL3 chemokines (125). Further to this effect, the TLR3 agonist poly(I:C) significantly accelerated wound healing when applied topically to human and mouse wounds compared to control and resulted in greater neutrophil and macrophage recruitment and upregulated CXCL2 (126).

TLR9 deficient mice demonstrated delayed wound healing compared to wild-type (103). In addition, topical administration of the TLR9 agonist CpG ODN to wounds resulted in significantly improved healing times, increased macrophage infiltration and increased production of VEGF (103).

Chapter 2

Materials and Methods

2.1 Human Tissue

With approval by the local ethics committee of the Royal Free Hospital and medical school (REC reference 29-2000), samples of human skin were collected from amputated lower limbs.

Donor patients were categorised as diabetic or non-diabetic depending whether they had received a formal diagnosis documented in their medical notes. Recruitment of donor patients occurred pre-operatively following identification of suitable individuals by senior members of the Royal Free hospital vascular surgery team and following informed, written consent. Information material was provided to every patient.

All consenting patients were included irrespective of their drug therapies, duration of diabetes, HBA1C, the presence or absence of a co-existent diagnosis of PAD and infection status. Data on patient demographics, co-morbidity, medications, severity of ischaemia and smoking history was collected (see Appendix).

2.1.1 Sample collection

Human skin biopsies were taken following surgical removal of the limb using standardised aseptic technique. Full thickness skin samples incorporating the epidermis and dermis, down to and including subcutaneous fat were obtained by sharp dissection. Prior to processing, all fat was removed using sharp dissection with either surgical scissors or a scalpel blade. In diabetic patients undergoing amputation for skin ulceration wide local excision of the entire ulcer incorporating its base were

taken. These were subsequently divided into 1cm square samples through the ulcer including its edge and base. In non-diabetic patients, similar excision biopsies were taken through ischaemic ulcerated tissue if present, or intact distal ischaemic skin from the foot if no ulceration was found, 1cm^2 samples were then prepared. In both diabetic and non-diabetic patients, a second intact sample was taken from the non-ischaemic proximal skin edge, to provide a non-ischaemic control. Additional samples of non-diabetic non-ischaemic proximal skin were collected for subsequent primary cell culture.

2.1.2 Tissue preparation

Skin and ulcerated biopsy samples were divided into 1cm^2 sections and fixed immediately in 10% formal saline (Cell Path, UK). Additional samples were placed in Eppendorf cryo tubes and snap frozen in liquid nitrogen, before transferring to a -80°C freezer. Further samples were placed in RNALater® (Thermofisher, Ma, US) at 4°C overnight and then transferred to -80°C freezers for possible future RNA analysis.

The tissue samples from the non-diabetic non-ischaemic proximal skin described above in 2.1.1 were immediately placed in a culture medium of Dulbecco's modified Eagle's medium 4.5g/dL glucose (25mM), (DMEM), 10% fetal calf serum (FCS), 100 U/ml penicillin (pen) and 100 g/ml streptomycin (strep). The dermis and epidermis were separated by scalpel dissection, and tissue from the dermal layer finely chopped. This tissue was then seeded in a T75 flask with 25ml of culture medium and incubated in a humidified atmosphere of 21% O2 and 5% CO2 at 37°C. A more detailed description of the primary culture process is provided in section 2.2.1.1.

2.1.3 Tissue analysis

2.1.3.1 Homogenisation of human skin samples

Human skin samples were thawed on ice and weighed. After removal of subcutaneous fat with sharp dissection, between 0.5 – 1g of skin tissue was placed

in a 2ml round bottom eppendorf, and 10-volumes of radio-immunoprecipitation assay (RIPA) buffer (150 mM NaCl, 1.0% IGEPAL® CA-630, 0.5% sodium deoxycholate, 0.1% SDS, and 50 mM Tris, pH 8.0; Sigma-Aldrich, UK) with 1x complete mini EDTA-free protease inhibitor (Roche) and 10 µL/ml each of phosphatase inhibitor cocktail 2 and 3 (Sigma-Aldrich) were added.

A stainless-steel metal ball was added, and the samples arranged in the TissueLyser (Qiagen, Nl). Tissue was disrupted by mechanical homogenisation for a total of 6 minutes (2 x 3 minutes) at 30 Hz. To ensure even homogenisation, samples were rearranged throughout the TissueLyser reaction-tube holder after 3 minutes. Homogenised samples were subsequently centrifuged at 13,000 rpm for 15 minutes at 4°C. The supernatant was removed, and the pellet discarded. The concentration of liberated protein was then determined using a bicinchoninic acid assay (BCA, Thermo-scientific) performed according to manufacturer's protocols.

The Pierce BCA assay working reagent is created by a 50:1 mixing of reagent A and reagent B. Standardised protein standards are prepared by serial dilution of known concentrations of albumin (BCA). Protein standard or test samples are loaded in duplicate onto a 96 well plate to 200µl of working reagent and incubated at 37°C for 30 minutes. The protein in the samples reduces Cu2+ to Cu+ in an alkaline medium. The BCA chelates the Cu+ ion forming a purple reaction product, the light absorbance of which has a linear relationship with protein concentration (127). The light absorbance of test samples at 460nm is determined using a microplate reader (Mithras LB940 microplate reader, Berthold Technologies, Switzerland). Protein concentrations are calculated from the standard curve.

Protein concentrations are then normalised to the sample with the lowest value by addition of further RIPA lysis buffer. NuPAGE LDS (x4) sample buffer (Invitrogen, UK) and Beta-mercaptoethanol (BME) were then added to each sample and heated to 80°C for 5 minutes to denature the proteins. The samples were subsequently stored in -80°C.

2.1.3.2 Western blot

The expression of specific individual cellular proteins with homogenised epidermal and dermal tissue was identified and quantified using western blot analysis from cell lysates (2.2.5). Protein concentrations were standardised following BCA assay as described above and added to NuPAGE LDS sample buffer (Invitrogen) before heating. A sodium dodecyl sulphate polyacrylamide gel electrophoresis (SDS-PAGE) method was used to separate denatured proteins based on their molecular weight (128). In the sample preparation stage, the addition of SDS detergent results in an unravelling of the three-dimensional structure of proteins to form a negatively charged linear structure. The addition of a reducing agent such as beta-mercaptoethanol (BME) to the lysis homogenate-LDS sample buffer solution disrupts disulphide bonds between protein complex's to further unravel and denature the protein structure after heating as described in 2.2.5 (129).

The process of sodium dodecyl sulphate-polyacrylamide gel electrophoresis (SDS-PAGE) was undertaken using a gel cartridge manufactured to comprise stacking and separating gel components, and (on removal of the packaging combs) 10, 12 or 15 wells in which to load protein-sample buffer homogenates. The gels used were pre-made 4-12% bis-tris gels (Invitrogen) or self-made tris-glycine gels (method used described below in 2.2.11.1). The application of an electric current across the gel causes the negatively charged proteins to move towards the anode to different degrees relative to their molecular weight (128). A reference ladder (SeeBlue®Plus2 Pre-stained standard, Invitrogen) was added to the first well in each gel. Equal volumes of lysed protein-sample buffer homogenates were added to other wells as per the requirements of that individual experiment.

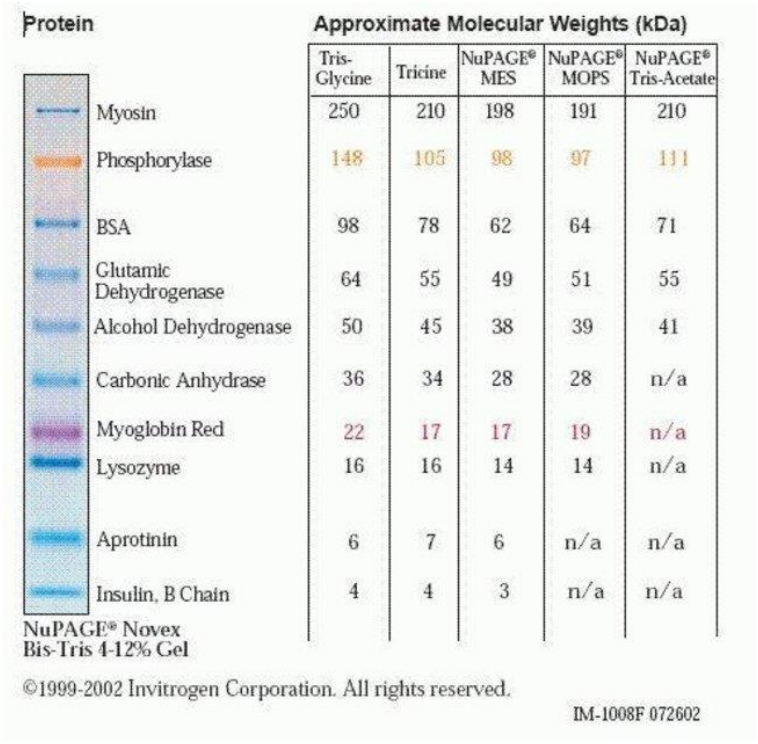

Protein	Approximate Molecular Weights (kDa)				
	Tris-Glycine	Tricine	NuPAGE® MES	NuPAGE® MOPS	NuPAGE® Tris-Acetate
Myosin	250	210	198	191	210
Phosphorylase	148	105	98	97	111
BSA	98	78	62	64	71
Glutamic Dehydrogenase	64	55	49	51	55
Alcohol Dehydrogenase	50	45	38	39	41
Carbonic Anhydrase	36	34	28	28	n/a
Myoglobin Red	22	17	17	19	n/a
Lysozyme	16	16	14	14	n/a
Aprotinin	6	7	6	n/a	n/a
Insulin, B Chain	4	4	3	n/a	n/a

NuPAGE® Novex
Bis-Tris 4-12% Gel

IM-1008F 072602

Figure 2.1.3.2 SeeBlue® Plus2 Pre-stained Standard

Protein bands have different mobilities depending on the SDS-PAGE buffer system used. (Invitrogen)

NuPage MES running buffer x20 (Invitrogen) was diluted 50ml up to 1L with distilled water. The tanks were assembled and filled with diluted running buffer, the combs removed, and wells loaded as explained above with 10µl SeeBlue® Plus2 ladder control. Protein samples were loaded at 20µl per well in 12 well gels, or 15µl per well in 15 well gels. Electrophoresis was initiated by the application of 180V over 1 hour for Bis-Tris gels or 120V over 1 hour 30 minutes for Tris-glycine gels.

Once complete, transfer of proteins from gels to a nitro-cellulose membrane (Hybond-C Extra, GE Healthcare, Amersham, UK) occurred via electroblotting. Transfer buffer was prepared through the addition of 50ml NuPage transfer buffer (Invitrogen) to 100ml of methanol and diluted with distilled water to 1L total volume. Gels were carefully removed from cassettes and placed onto membranes, sandwiched between filter paper and transfer buffer-soaked sponges. Once loaded into transfer tanks, 35V was applied for 1 hour 30 minutes. Adequate transfer of proteins was assessed using Ponceau S solution (Sigma-Aldrich). Membranes were washed with a solution of phosphate-buffered saline (PBS) with 0.1% Tween (Sigma-Aldrich) (PBS-T).

Non-specific antibody binding was reduced by blocking the membranes with 5% milk protein reconstituted with PBS-T for a period of 1 hour at room temperature with gentle agitation. After blocking, primary antibody diluted into reconstituted 5% milk was applied to the membrane, at the antibody dilutions recommended by manufacturers. Primary antibodies were applied overnight and stored at 4°C with constant gentle agitation.

Multiple primary antibodies were on occasions applied simultaneously to each membrane. If the proteins in question were a sufficiently different molecular size, then the membrane was carefully cut to allow separation and application of different primaries as per the method described above. Beta-tubulin was used as a loading control for all membranes at a dilution of 1 in 50000.

Following incubation, the membranes were removed from the primary antibody and thoroughly washed with submergence in 50ml PBS-T for at least ten minutes on a tube roller at room temperature. This process was repeated twice more. Following washing, the species-specific HRP linked secondary antibody was applied diluted in 5% milk at a concentration of 1 in 1000 for 1 hour at room temperature. The washing process described above was then repeated three times.

A luminescence based protein band detection method was used, by the application of ECL™ western blotting detection reagents (GE Amersham). This occurs through the oxidation of luminol via HRP/peroxidase catalysm in alkaline conditions. Chemical enhancers such as phenols increase light output and duration of luminescence (130). After addition of the combined detection reagent mixture, the membranes were placed in a detection cassette with photographic film (Hyperfilm ECL, GE Amersham) in dark-room conditions. Exposure duration was determined by the strength of the protein bands, with stronger signals requiring less exposure time. An automatic film developer was used to produce final western blot films. Protein band density was determined after digital scanning using densitometry software (VisionWorkLS) and expressed as a ratio of the corresponding beta-tubulin band density.

2.1.3.3 Histology

Samples collected and prepared as described in section 2.1.2 were removed from 10% formal saline containing 4% formaldehyde (CellPath, UK). Fixed tissues were processed and dehydrated overnight and embedded in molten paraffin wax to generate the formalin-fixed paraffin embedded (FFPE) samples. Following this 3µm sections were cut using a microtome (Leica, UK) and mounted onto polylysine-coated slides (VWR, UK). Sections were heated overnight at 42°C and then used to perform staining.

Haematoxylin and Eosin

FFPE sections were dewaxed in xylene (Genta Medical, York, UK) and passed through a series of graded ethanols and then transferred to water. To ensure correct cross-sectional orientation of the embedded muscle tissue, and also to assess tissue architecture, haematoxylin and eosin (H&E) staining was performed using standard protocol. Following H&E staining, sections were dehydrated by passing through graded alcohols, cleared in xylene, and then mounted in permanent DePeX mountant (VWR, UK).

Immunohistochemistry

All immunohistochemistry undertaken was performed on FFPE sections prepared as described above. After dewaxing, slides were immersed in 0.5% hydrogen peroxide in methanol for 10 minutes to quench endogenous peroxidase activity. Antigen retrieval was achieved through a heat-mediated method by microwave heating of sections submersed in 10mM Citrate buffer (pH 6.0) for 10 – 20 minutes.

Reduction of non-specific antibody binding was achieved through the addition of a blocking serum to tissue samples for 15 minutes, horse serum was chosen as the secondary anti-rabbit antibody was horse derived. A rabbit derived human anti-TLR4 primary antibody was applied to the samples at a concentration of 1:100, and incubated overnight at 5°C.

After warming to room temperature, the slide is repeatedly washed in PBS, before a non-biotin polymer conjugated anti-rabbit secondary antibody at 1:200

concentration (Immpress reagent kit, Vector laboratories, UK) was added for 30 minutes. After washing, a DAB (Diaminobenzidine) peroxidase substrate solution was added for a period of 10 minutes. Following further PBS wash, the slide was placed into Mayers haematoxylin for 5 minutes. Finally, the slides were dipped into acid alcohol and bluing solution and passed through the reversal of the de-waxing process utilising graded alcohols and xylene.

2.2 *In vitro* model of diabetic ischaemic conditions

In the context of a complex and multifactorial pathology such as diabetic foot ulceration, *in vitro* studies allow modelling and individual control of many of the variables concerned. Observation and assessment of these variables on individual cell function, processes and signalling pathways and the effect of manipulation of these pathways is possible, accepting that skin is a complex tissue containing multiple interacting cell types, extracellular matrix, immune and vascular cells. The complexity of interaction between these constituent components of whole tissue such as skin is not possible to adequately replicate *in vitro* but will at least provides proof of concept to direct and inform whole organism *in vivo* studies.

2.2.1 Cell culture

2.2.1.1 Culture of Human dermal fibroblasts

Primary cultured normal Human dermal fibroblasts were obtained from the proximal wound edges of non-diabetic patients as previously described. After overnight refrigeration in a culture medium containing 25mM DMEM, 10% FCS, 1% pen/strep, mechanical separation of the dermis from epidermis was undertaken. The epidermal layer was discarded, and the dermal tissue finely chopped and placed as multiple islands of tissue within a T75 flask with 25ml of culture medium and incubated in a humidified atmosphere of 21% O2 and 5% CO2 at 37°C. Cultures were checked daily under light microscopy and media changed every 48 hours.

High glucose DMEM culture medium (25mM) was required for successful primary culture, as the primary obtained dermal fibroblasts failed to survive in low glucose (5.5mM) DMEM conditions. Once established however, at passage 2 to 3 all cells were successfully transferred to a low glucose media (5.5mM), and further cultured for at least two weeks to limit the phenotypic changes that might occur in prolonged high glucose conditions during the process of achieving culture.

Cell passage

At 90% confluence, cell cultures were passaged utilising an established lab protocol. The culture medium was aspirated and discarded, and the cell layer washed with 3ml of 0.25% trypsin/1mM EDTA to mitigate the neutralising effect of any residual FCS in the T75 flask. After aspiration of this fluid, a further 10ml of 0.25% trypsin/1mM EDTA was added and incubated for 5 minutes. The detachment and round appearance of the cells were confirmed by light microscopy. Trypsin was inactivated by the addition of 5ml of normal culture medium (outlined above), suspensions were then split into equal volumes and centrifuged at 1000rpm for 5 minutes. Following this, the fluid was discarded and the cellular pellet resuspended in 5ml of normal media, which can be further split and diluted with growth medium depending on the required use of the cells.

Cell cryopreservation

Samples of cultured cell lines were preserved in liquid nitrogen at low passage. A solution of 1ml 10% dimethyl sulfoxide (DMSO) (Sigma-Aldrich), 2ml 20% FCS and 7ml normal culture medium is prepared and filtered through a 2µm filter using a sterile syringe. A 2ml volume of this cryosolution is added to the cellular pellet, following the passage procedure outlined above. 1ml volumes are transferred to Nalgene cryoware cryogenic vials (ThermoFisher), placed within cryofreezing containers and stored in -80°C freezers for at least 6 hours before transfer into liquid nitrogen.

2.2.1.2 Culture of HaCat epithelial cells

HaCat cells are a commercially available immortalised human keratinocyte cell line, with a high capacity for differentiation and potential for proliferation (131). HaCat cells were successfully cultured in both very high (25mM) and low (5.5mM) glucose DMEM media, with 10% FCS and 1% pen/strep, maintained with 48-hour media changes. They were passaged at 90% confluence utilising the above described method.

2.2.1.3 Culture of human microvascular dermal endothelial cells (HMDEC)

HMDEC cells are commercially available human endothelial cells derived from juvenile foreskin or adult skin of various source locations (Promocell, Germany). HMDEC cells were successfully cultured in 25mM very high glucose DMEM with 10% FCS and 1% pen/strep media, however HMDEC cells would not proliferate in lower glucose concentrations. Cells were passaged at 90% confluence utilising the before mentioned protocol.

2.2.2 Simulation of tissue ischaemia

Our research group has considerable experience in developing protocols for the simulation of the local hypoxic environment of ischaemic tissues in PAD and has utilised these in a variety of human cell lines (132). This validated protocol was therefore employed to replicate the hypoxic conditions in diabetic-ischaemic ulceration using a hypoxic chamber (Modular Incubator Chamber, MIC-101; Billups-Rothenberg, Del Mar, CA, USA). Cell cultures are placed in this air-tight container and flushed with a gas mixture of 20% CO_2 and 80% N_2 (BOC Ltd, UK) and a rate of 15L/min for 15 minutes, before sealing. The modular chamber is then placed in an incubator at 37°C for 8 hours.

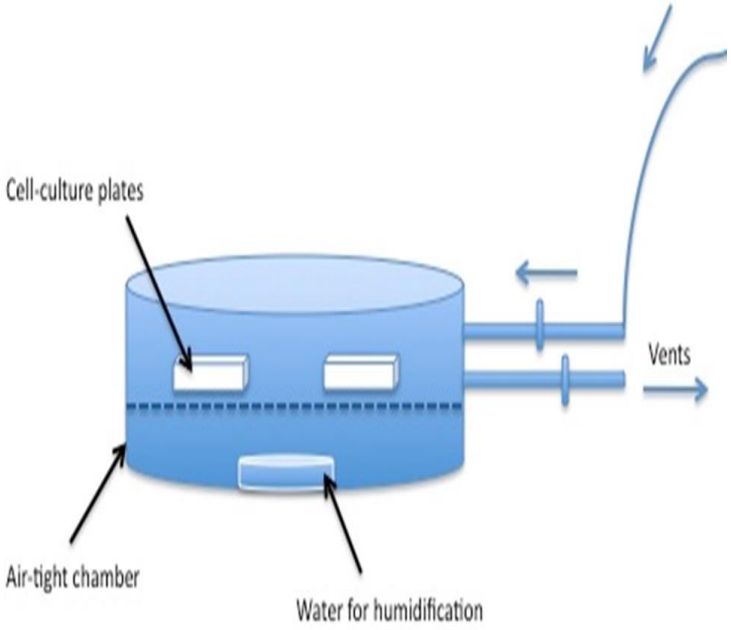

Figure 2.2.2 Hypoxic chamber (reproduced from Joshi et al, 2011) (132)

2.2.3 Glucose treatments and simulation of hyperglycaemia

The cell culture medium utilised in this project for all cell types was based on DMEM. The medium was completed by the addition of varying concentrations of FCS and 1% penicillin/streptomycin. Importantly, the standard DMEM media contains 4.5g/dL of glucose, which translates to a glucose concentration of 25mM, or extrapolated in clinical terms, the blood glycaemic concentration of a very poorly controlled diabetic patient. To model the physiological environment as closely as possible a 'resting' physiological glucose concentration of 5.5mM was chosen, as this represents the mid-point of the normal human physiological glycaemic range of 4-7mM. This low glucose concentration media was therefore utilised throughout the cell culture process and for low glucose controls during experiments.

The bespoke glucose concentration media were created through relative dilution of the DMEM 4.5g/dL glucose solution with DMEM no glucose (Invitrogen, UK) as illustrated in table 2.2.3 below.

Target concentration	Proportion of DMEM 4.5g/dL	Proportion of DMEM no glucose
O mM	0	45
5.5 mM	10	35
15 mM	27	18
25mM	45	0

Table 2.2.3 shows the relative proportions of each DMEM solution required to create the desired glucose concentration solution. For instance, to mix a final media volume of 500ml containing 10% FCS, 1% pen/strep, the desired DMEM volume required is 450ml to allow for the addition of 45ml FCS and 5ml pen/strep.

2.2.3.1 Glucose dose-response relationship on TLR4 expression

Low glucose (5.5mM) cultured dermal fibroblasts were seeded into 6 well plates at a density of 80,000 cells per well. The media was changed daily and at 90% confluence a low serum media (0.1% FCS) was applied 24 hours before commencing the experiment. The fibroblasts were subsequently exposed to a 2ml volume of DMEM, 10% FCS 1% pen/strep culture media containing glucose concentrations of 0mM, 5.5mM, 15mM and 25mM for 24 hours and included 14mM mannitol in low glucose (5.5mM) as an osmotic control in accordance with published studies employing a similar protocol. In early preliminary experiments an additional 6^{th} group was included containing 25mM glucose and LPS (Sigma Aldrich, UK), to provide a positive control for TLR4.

2.2.3.2 Very high glucose treatment exposure duration

Several published studies examining the effect of hyperglycaemia on TLR4 expression in human monocytes and gingival fibroblasts selected 24 hours as the very high glucose treatment exposure duration (133-135). A time course experiment to examine optimum exposure duration of very high glucose conditions on TLR4 expression in dermal fibroblasts was therefore required. In accordance with the above method, 3 different cell lines of low glucose cultured dermal fibroblasts were seeded into 6 well plates, at a density of 80,000 cells per well. Identical plates across all cell line repeats were created for the 6-hour, 12-hour, 24-hour and 48-hour glucose exposure time points. At 90% confluence, a low serum medium (0.1% FCS) was applied for 24 hours. A 2ml volume of DMEM, 10% FCS 1% pen/strep culture media was added at the start of the experiment, at glucose concentrations of 5.5mM, 5.5mM plus 14mM mannitol, and 25mM. The experiment was stopped at each of the 4 time points for the corresponding plates within each cell line, the cell cultures washed and lysed according to the standard protocol described below (2.2.5).

2.2.4 Inhibitor treatments

2.2.4.1 TLR4 Antagonists

The effect of TLR4 inhibition was assessed through the addition of a selective TLR4 inhibitor (LPS-RS, Invivogen, Ca, US) and neutralising antibody (mabg-htlr4, Invivogen) to the glucose-dosed cell cultures. The dose utilised was derived from optimisation experiments conducted in cell migration studies (explained in more detail in 2.2.7), corroborated with similar experiments conducted by others within our research group (on different cell lines), and based on manufacturers recommendations. The inclusion of both a TLR4 antagonist and neutralising antibody in these studies provided selective but different mechanisms of inhibition of TLR4. A dose of 1µg/ml of the TLR4 neutralising antibody and 10µg/ml of the LPS-RS TLR4 antagonist was used.

2.2.4.2 MyD88 and TRIF inhibitors

Further inhibitor compounds were utilised to determine the pathway through which TLR4 activation results in the observed effects. MyD88 and TRIF inhibitory peptides (Invivogen) were added to the very high glucose (25mM) media. Early experiments (migration studies 2.2.7) to optimise dose measured the response of these compounds based on the recommended working concentration range advised by the compounds data sheet (5µM-50µM). 50µM doses of both peptides were observed to be lethal to the fibroblasts. Subsequently, doses of 5, 10 and 20µM of both peptides were retested using the same method, and an optimal dose of 10µM was chosen.

The experiments were conducted with low-glucose cultivated human dermal fibroblasts seeded into 6 well plates at a density of 80,000 cells per well. As before, at 90% confluence cells were serum starved for 24 hours in 0.1% FCS containing media. High glucose treatment media at a concentration of 25mM was then added containing 2ml DMEM, 10% FCS and 1% pen/strep, and the inhibitor compounds at the previously mentioned doses, to the cell cultures for a period of 24 hours. Low glucose (5.5mM) and very high glucose only (25mM) controls were also included. This method was repeated across three different human dermal fibroblast cell lines, and conducted in both normoxia and in the hypoxic chamber as per the previous protocol described in 2.2.2.

2.2.5 Cell lysis

Following the completion of the exposure and inhibitor experiments, the supernatant from individual wells was aspirated, decanted to appropriately labelled Eppendorf's and immediately stored in -20°C overnight, before being moved to -80°C. Cellular protein was harvested using a well-established lab protocol.

A lysis buffer mixture was prepared containing RIPA lysis buffer (Thermo-scientific, UK), Pierce protease inhibitor (Thermo-scientific) and phosphatase inhibitor cocktails 2 and 3 (Sigma-Aldrich, UK). Test wells were washed and aspirated three times with sterile phosphate buffered saline (PBS, Sigma-Aldrich). A 120µl volume of the pre-

prepared lysis buffer was added to each well. Cell scraping was performed using the barrel of a sterile, single use 3ml syringe. After physical disruption of the cells, the lysis buffer-protein mixture was repeatedly drawn into the 3ml syringe through a 23 gauge needle (Terumo). The mixture was transferred to an appropriately labelled Eppendorf and cooled on ice. Samples were centrifuged at 15,000rpm for 15 minutes at 4°C. The protein-lysate liquid was removed and the solid pellet discarded. Samples were stored in -20°C overnight before being transferred to -80°C.

The protein concentration of each lysis sample was subsequently determined using a BCA Assay (Thermo-scientific) using the protocol described in section 2.1.3.1. Protein concentrations were then normalised to the sample with the lowest value by addition of further RIPA lysis buffer. NuPAGE LDS (x4) sample buffer (Invitrogen, UK) and Beta-mercaptoethanol (BME) were then added to each sample, and heated to 80°C for 5 minutes to denature the proteins. The samples were subsequently stored in -80°C.

2.2.6 Immunocytochemistry

Immunofluorescence analysis was performed on each of the primary cultured human dermal fibroblast cell lines as a quality control measure to ensure the cultured cells were a correctly identified line of fibroblasts without significant contamination or differentiation. A similar technique was utilised for HaCat cells. Fibroblast populations were seeded into four chamber slides (BD Bioscience, Bedford, MA, USA) after passage, and suspended in 1ml of normal culture medium containing 5.5mM glucose DMEM, 10% FCS and 1% pen/strep. At 90% confluence, the media was removed and the chambers washed and aspirated three times with sterile phosphate-buffered saline (PBS). The cell cultures were then fixed using a solution of freezing 50:50 methanol/acetone (stored at -20°C), and subsequently placed in -20°C freezer for 5 minutes. After further repeated PBS wash, a species specific block (specific to secondary antibody species) was applied for 30 minutes (10% chicken serum).

Primary antibody was then applied for 1 hour at room temperature. Fibroblast specific protein (FSP- Anti S100A4, Abcam, Cambridge, UK) was used for fibroblast cultures at a concentration of 1 in 200 (5µl in 1ml). Pan-Cytokeratin (Thermofisher), a keratin marker antibody cocktail was used for HaCat cells at a concentration of 1 in 100 (10µl in 1ml). An IgG control was used for all cell lines at a concentration of 1 in 200. After one hour of room temperature incubation, further repeated PBS washes are carried out before application of the secondary antibody. A 1 in 2000 concentration of chicken anti-rabbit (fibroblast) and chicken anti-mouse (HaCat) was applied for 30 minutes at room temperature.

After a final repeat of PBS wash, the chamber slides were fixed using Vectashield® mounting medium for fluorescence (Vectorlabs, Burlingame, CA), containing 4',6-diamidino-2-phenylindole (DAPI), a fluorescent stain for DNA. The chamber slide is broken and the chambers discarded, the slide is then stored in the dark. Fluorescence signal was detected using AxioSkop2 fluorescence microscope and Axiovision v4.8 software (Carl Zeiss GmbH, Germany).

2.2.7 Cell migration

Scratch migration assay was undertaken to assess the functional consequences of high glucose concentrations, with or without hypoxia on the migration of dermal fibroblasts. This is a key occurrence in the physiological process of normal wound healing. A simulated high glucose and hypoxic environment models the local conditions found in poorly controlled diabetic and diabetic-ischaemic wounds. The use of selective inhibitors will determine the effect of TLR4 and its down-stream MYD88 and TRIF inflammatory signalling pathways on the process of fibroblast migration.

Low glucose (5.5mM) cultured human dermal fibroblasts were seeded into 24 well plates at a density of 20000 cells per well and incubated at 40°C. The media containing DMEM at a 5.5mM glucose concentration, 10% FCS and 1% pen/strep was changed daily. At 70% confluence the media was removed and replaced with a low-serum media (0.1% FCS) of otherwise identical composition. After 24 hours of serum

starvation, the media was aspirated and a standardised straight-line scratch wound was inflicted across the fibroblast mono-layer using a sterile 20-200µl pipette tip and the plate lid as a straight edged ruler (136, 137). The scratched fibroblast monolayer was washed with sterile PBS to remove debris and aspirated to dryness. Phase contrast microscopy was used to capture images of the scratched wounds (Olympus CDK2 microscope). Treatment media was then applied containing the proliferation inhibitor Mitomycin-C (Merck Millipore, UK). Preliminary dose optimisation experiments determined a dose of 1% mitomycin-C, which was used for all subsequent experiments. Higher doses were lethal to test cells.

Treatments applied were DMEM, 10% FCS 1% pen/strep at glucose concentrations of 5.5mM, 5.5mM with mannitol, 15mM and 25mM. Treatments were added in triplicate and included a 1% FCS control group without the addition of mitomycin-C. All experiments were simultaneously conducted in the hypoxic chamber using the above described protocol (2.2.2).

In addition to increasing glucose concentration and hypoxia, the effect of specific TLR4 inhibition on fibroblast migration was assessed using the selective TLR4 inhibitor (LPS-RS, Invivogen) and neutralising antibody (mabg-htlr4, Invivogen) added to the very high glucose (25mM) media. An optimisation experiment was conducted to determine the working dose for both treatments, this informed all subsequent experiments. Concentrations of 0.01µg/ml, 0.1µg/ml, 1µg/ml and 10µg/ml of both the TLR4 inhibitor and neutralising antibody were added to the high glucose treatment media. After the scratch was inflicted, this media was applied to the fibroblast monolayer and placed in the hypoxic chamber. Following migration analysis, optimised doses of 1µg/ml of the TLR4 neutralising antibody and 10µg/ml of the LPS-RS TLR4 antagonist were chosen.

The effect on fibroblast migration of inhibiting the MYD88 dependant and TRIF downstream signalling pathways of TLR4 was investigated by the addition of MyD88 and TRIF inhibitory peptides. Doses of 10µM were used following preliminary dose optimisation experiments. Images were taken of each well at 24 hours. Cellular migration was estimated by using a blinded visual estimation method, following an established lab protocol. Migration was expressed as a percentage wound coverage.

2.2.8 Cell proliferation

In addition to migration, proliferation is an essential physiological cellular function fundamental to the process of normal wound healing. To determine how fibroblast proliferation was affected by conditions of simulated diabetic-ischaemic conditions *in vitro*, a crystal violet assay was conducted using different lines of primary cultured normal human dermal fibroblasts. Crystal violet binds to DNA located within the cell nuclei. The dye-DNA binding forms a quantifiable colourmetric complex, allowing for comparable measurement of DNA density, and thus indirect assessment of cell proliferation (138).

Fibroblasts were seeded into 96 well plates at a density of 4000 cells per well. The cells were suspended in either a normal low glucose media (5.5mM) or very high glucose (25mM) DMEM, 10% FCS, 1% pen/strep culture medium. Duplicate plates were seeded, all plates were immediately incubated in a humidified atmosphere of 21% O2 and 5% CO2 at 37°C. At 8 hours post trypsinisation, duplicate plates were removed and placed within the hypoxic chamber as per the protocol described in 2.2.2, for a period of 16 hours.

At 24 hours post seeding, the media was aspirated from each well and the cell culture carefully washed with sterile phosphate buffered saline (PBS). Excess moisture was removed and to each well a 50µl volume of a pre-prepared solution of 0.1mg crystal violet and 10ml methanol diluted in 40ml distilled water (20% methanol solution) was added. The plates were then incubated for 10 minutes at room temperature. After thorough repeat distilled water washing, the plates were air dried to complete dryness. Crystal violet-DNA complexes were then solubilised by the addition of 100µl of 33% acetic acid. Light absorption at 560nm was measured on a microplate reader (Mithras LB940 microplate reader, Berthold Technologies). The relative colour density as an indirect measurement of cellular proliferation was then expressed as a factor change from the lowest measured density.

2.2.9 Gel contraction

The ability of a tissue injury with a resulting defect and loss of architecture to heal and restore structural integrity involves a variety of complimentary and inter related cellular functions. Proliferation and migration discussed in 2.2.7 and 2.2.8 are two of these functions, which along with the ability of tissue defects to contract, comprise the major fundamental physiological cellular processes of normal wound healing (139). Fibroblast differentiation into contractile myofibroblasts enables structural tissue defects to physically reduce their incongruity. The effect of high glucose and hypoxic conditions on this functional property of dermal fibroblasts was assessed with a gel contraction assay.

Sterile 24 well plates were pre-coated overnight with filtered 2.5% bovine serum albumin (BSA) at 37°C. The BSA was removed and each well washed and aspirated three times with sterile phosphate buffered saline (PBS). A collagen solution comprising 3mg/ml collagen (Vitrogen-100, Cohension technologies, Ca, US) and 0.2M N-2-hydroxyethylpiperazine--2-ethanesulfonic acid (HEPES) mixed in a 4:1 ratio was mixed. An equal volume of DMEM media, (plus 1% FCS, 1% pen/strep) containing a suspended trypsinised fibroblast culture was added to this collagen/HEPES solution. The final gel composition was therefore 10% HEPES, 40% collagen and 50% cell suspended media.

The glucose dose of the DMEM media was varied between 0mM, 5.5mM and 25mM. In addition, various inhibitor compounds were added to separate solutions containing 25mM glucose. A selective TLR4 neutralising antibody was added at a dose of 1µg/ml, and TLR4 antagonist at 10µg/ml. MYD88 and TRIF inhibitory peptides were also tested in these very high glucose solutions (25mM) at a dose of 10µM. Following component mixing, the plate was incubated at 37°C in a 5% CO2 atmosphere to allow polymerisation of the collagen gel. After an hour, a 1ml solution of DMEM culture medium at the same glucose concentration as the cell suspension was added to detach and float the gel.

All plates were prepared in duplicate, and at the stage of collagen-cell gel detachment, one plate was placed in the hypoxic chamber as per the method

outlined in 2.2.2. After 24 hours contraction was quantified by reduction in gel diameter and loss of gel weight.

2.2.10 Enzyme Linked Immunosorbent Assay (ELISA)

2.2.10.1 Multi analyte ELISArray

Unlike functional assays such as proliferation, scratch migration and gel contraction assays which determine the effect of test conditions on essential physical cellular functions, enzyme linked immunosorbent assay (ELISA) is used to detect and quantify the release of specific inflammatory cytokines in response to these same conditions.

At the time of fibroblast cell lysis described in 2.2.5, treatment supernatant was aspirated and frozen at -20°C. To determine the spectrum and quantity of inflammatory cytokines released by our sample cultures of human dermal fibroblasts into the supernatant, a multi-analyte ELISArray kit (Product number MEH-006A, Qiagen, Nl) was performed according to the manufacturer's protocol. The multi-analyte ELISArray kit allowed simultaneous analysis of 12 pro-inflammatory cytokines through pre-coating of target-specific capture antibodies on a supplied 96-well plate for: IL1α, IL1β, IL2, IL4, IL6, IL8, IL10, IL12, IL17A, IFN-γ, TNF-α, GM-CSF.

To each well, 50µl of the supplied assay buffer was added along with 50µl of the supernatant sample. These samples included supernatant aspirated from fibroblasts cultured in low glucose (5.5mM) normoxia and hypoxia, very high glucose (25mM) normoxia and hypoxia, and very high glucose in hypoxia with a TLR4 neutralising antibody and antagonist (as per 2.2.4.1). These were gently mixed on a plate shaker and incubated at room temperature for 2 hours. The wells were subsequently aspirated and washed with 350µl of the supplied wash buffer. After blotting, this process was repeated twice more. On completion of washing, 100µl of the specific diluted detection antibody was pipetted into the relevant plate row using a 12-channel pipette, gently shaken and incubated for 1 hour at room temperature. The wash process was thereafter repeated as described above. After blotting, 100µl of diluted streptavidin- horse radish peroxidase (Avidin-HRP) was added to each well,

gentle shaken and for 10 seconds for mixing and incubated for 30 minutes in the dark. The wash process was repeated as before but repeated four times.

A 100µl volume of development solution was pipetted into each well at room temperature and incubated in the dark for 15 minutes. Finally, 100µl of stop solution was added in the same order as the development solution. The absorbance at 450nm was then immediately read on a microplate reader (Mithras LB940) and absorbance calculated by subtracting the measured figure for each antibody in the panel from its corresponding negative control.

2.2.10.2 Interleukin-6 ELISA

The multi analyte ELISArray was utilised to profile the predominant cytokine(s) produced by our cultured fibroblast populations. Of specific interest was interleukin-6 (IL- 6), an inflammatory cytokine associated with TLR4 activation (140). To assess the effect of very high glucose and hypoxia, and of TLR4 through a specific antibody and antagonist (2.2.4.1) on IL-6 release by our primary cultured fibroblast cell lines, an IL-6 sandwich ELISA was conducted according to manufacturer's protocols.

A human IL-6 DuoSet ELISA development kit (R&D systems, MN, USA) prepared by adding 100µl of capture antibody to each well of the 96 well plate and incubating overnight at room temperature. Following overnight incubation, each well was aspirated and washed with the supplied wash buffer a total of three times, and after the final wash blotted to dryness. The plate was then blocked using 300µl of reagent diluent and incubated at room temperature for 1 hour. Following this, the wash process was repeated as outlined above. Once prepared, 100µl of supernatant sample was added to the relevant well, covered and incubated at room temperature for 2 hours. The wells were washed as before, following this step was the addition 100µl of diluted detection antibody. This was again covered with an adhesive cover and incubated for 2 further hours at ambient temperature. The aspiration and wash of each well was repeated using the same methodology, 100µl streptavidin-horse radish protein (HRP) was thereafter added to each well and incubated in the dark for 20 minutes. The avidin-HRP was discarded and wells washed as before. Finally, 100µl

of substrate solution (equal mixture of hydrogen peroxide and tetramethylbenzidine) was added and kept in the dark for 20 minutes, before the addition of 50µl stop solution.

The optical density of each well was then measured with a microplate reader (Mithras LB940) at 450nm. The concentrations were calculated from a best fit curve plotting log IL-6 concentration against the log of the measured optical density.

2.2.11 Western blotting

The expression of specific individual cellular proteins by fibroblasts was identified and quantified using western blot analysis from cell lysates (2.2.5). Protein concentrations were standardised following BCA assay as described in 2.2.5 and added to NuPAGE LDS sample buffer (Invitrogen) before heating. As described in more detail above in section 2.1.3.2, equal volumes of protein in LDS sample buffer were fractionated by SDS-polyacrylamide gel electrophoresis using 4-12% bis-tris gels (Invitrogen). A reference ladder (SeeBlue® Plus2 Pre-Stained Standard, Invitrogen) was included, and samples electrophoresed at 180 V for 1 hour. Proteins were transferred by electro-blotting from each gel onto a nitrocellulose membrane (Hybond-C Extra, GE Healthcare). Adequate transfer was assessed by Ponceau S solution (Sigma-Aldrich) staining of each membrane. The membrane was washed with 0.1% phosphate-buffered saline with Tween 20 (PBS-T) (Sigma-Aldrich). Non-specific binding was blocked by incubation with 5% nonfat dry milk in PBS-T for 2 hours at room temperature. Membranes were incubated overnight at 4°C with gentle agitation with primary antibodies. Primary antibodies used are listed in table 2.2.11.

Table 2.2.11 Primary antibodies used for Western blotting

Antibody	Species	Dilution	Manufacturer	Cat. number
Anti-TLR4	Rabbit	1:1000	Abcam	ab47093
Anti-TLR2	Rabbit	1:1000	Abcam	ab24192
Cleaved caspase 3	Rabbit	1:1000	Cell Signalling	#9664
HMBG1	Rabbit	1:1000	Abcam	ab18256
Anti-MyD88	Rabbit	1:1000	Abcam	ab2064
NFκB	Rabbit	1:1000	Cell Signalling	#4764
pNFκB	Rabbit	1:1000	Cell Signalling	#3033
B-Tubulin	Rabbit	1:50000	Abcam	ab24192

Before the addition of a secondary, species-specific antibody, membranes were washed thoroughly with PBS-T. Secondary antibodies were used at 1:1000 dilution in 5% nonfat dry milk solution and incubated for 1 hour at room temperature. Signal was detected using a luminescence kit (ECL detection kit; Amersham) followed by exposure to photographic film (Hyperfilm ECL; Amersham). Exposure duration was determined by the strength of the protein bands, with stronger signals requiring less exposure time. An automatic film developer was used to produce final western blot films. Protein band density was determined after digital scanning using densitometry software (VisionWorkLS) and expressed as a ratio of the corresponding beta-tubulin band density.

2.3 *In vivo* model of chronic diabetic-ischaemic ulceration

As mentioned before, *in vitro* cell-culture based techniques are essential to determine individual cell line response on a functional, receptor and downstream pathway level to the variety of conditions and treatments explored above in 2.2. The ultimate purpose of these experiments is to model as much as possible the local conditions found in chronic diabetic- ischaemic wounds. Given the complex, time critical and multicellular nature of the wound healing process, whole tissue and thus

whole organism studies are required to more accurately understand and influence the effect of diabetes and ischaemia in chronic ulceration.

The *in vivo* studies aim to provide a murine model of non- or poorly healing human diabetic-ischaemic chronic ulceration. Initial experiments are therefore intended to validate this model. Four arms to the initial experiment were therefore chosen as demonstrated in figure 2.3. A non-diabetic, non -ischaemic group, a diabetic non-ischaemic group, a non-diabetic ischaemic group and finally a diabetic-ischaemic group. Three time points are chosen for evaluation of wounds at days 3, 7 and 14 post induction of ischaemia.

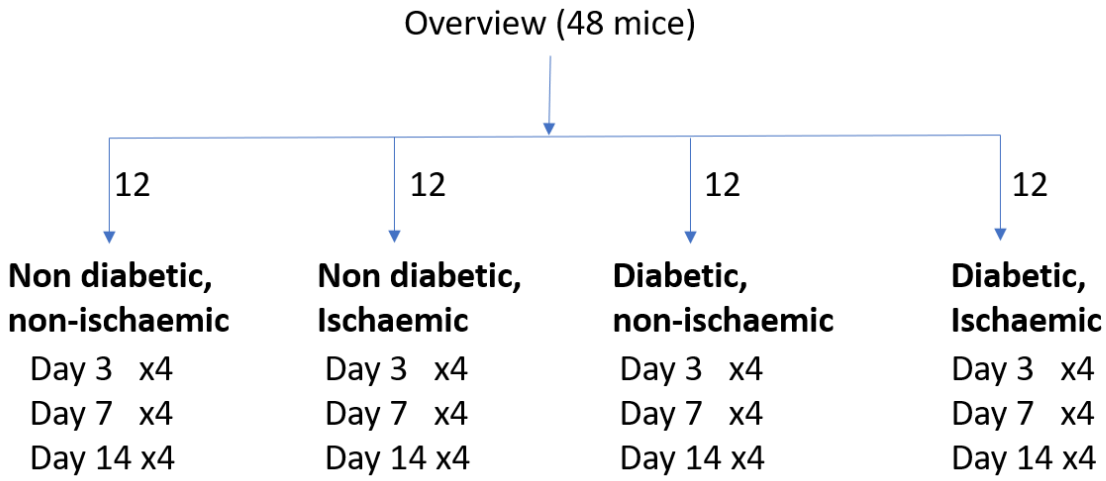

Figure 2.3 *In vivo* experimental plan

2.3.1 Animal housing

All animals were licenced and all procedures were conducted in accordance with UK home office regulations under an Animals (Scientific Procedures) Act 1986 project license and conducted and reported in accordance with ARRIVE guidelines. Home office approval was obtained through the granting of an updated project licence, specifically amended to include the induction of diabetes and hindlimb wounding (project licence number 70/7087).

Male C57Bl/6 mice were sourced due to a greater reported association of female animals of this inbred strain developing dermatitis (141, 142). This was identified as a potential confounding factor within this study, as the outcome focussed primarily on wound healing. All animals were obtained from lab bred in-house stocks at 8 weeks old and transferred to individually ventilated cages with 2-3 animals in each cage. They were exposed to 12 hour light/dark cycles, a temperature and humidity controlled environment, provided with enrichment and allowed standard chow and water *ad libitum*.

2.3.2 Induction of diabetes

Animals were not formally randomised into the treatment groups outlined above, however they were assigned randomly into the individually ventilated cages. Adjacent cages were then assigned to each arm of the study, with a total of 12 per group.

Simulation of type 1 diabetes was achieved through a low dose daily streptozotocin (STZ) intra-peritoneal injection method (143). STZ is an alkylating chemotherapeutic agent, with a potent toxicity for mammalian pancreatic insulin-producing beta cells. Clinical use of STZ as chemo-therapy is therefore restricted to metastatic insulin producing tumours of pancreatic beta cells (144). The induction of type 1 diabetes through the low dose multiple STZ injection method was favoured over the large single dose method to reduce the effects of STZ toxicity. These effects include weight loss, respiratory distress, hypoglycaemia and death (145).

Streptozotocin was purchased from commercial suppliers (Abcam) and reconstituted using a cold (5°C) 0.1M citrate buffer at pH 4.5, created through the addition of trisodium citrate (2.941g in 100ml distilled water) and citric acid monohydrate (2.1g in 100ml distilled water). The citrate buffer was used to reconstitute the STZ at a dose of 1g/ml (146). After aliquoting on ice and away from light into 50x 10mg in 30µl aliquots, they were subsequently stored at -20°C.

At first dosing, the individual 8-week-old male C57Bl/6 mice were weighed and a dose of 40mg/kg body weight STZ injected into the peritoneal cavity. The same dose was given for five consecutive days per animal. The animals were monitored for signs of distress or injury at least twice per day.

2.3.3 Monitoring of diabetic mice

Throughout and after the five consecutive days of low dose STZ injection, the mice were maintained on unrestricted standard feed and water. Monitoring post diabetes induction followed protocols reported by other groups utilising this low-dose STZ method (146). Animals were weighed on day 1 of dosing, for correct volumes to be administered to give a 40mg/kg dose daily and as a baseline pre-diabetes value. Weights were repeated on day 7. Day 14 post dosing the animals were weighed again, had urine checked for glycosuria and capillary tail blood sampling was performed for random capillary blood glucose (CBG) testing.

2.3.3.1 Urinalysis

The presence of urinary glucose is a pathological marker of elevated blood glucose levels, as glucose is efficiently reabsorbed in the proximal convoluted tubule of the nephron. The ability of the nephron to reabsorb excreted glucose is limited and at glucose thresholds exceeding 160mg/dL (8.6mmol/L) the active transport process is overwhelmed, leading to urinary loss of glucose (147).

The individual animals were removed from their housing and placed on a cleaned bench. If they had not spontaneously micturated then they were picked up and

'scruffed'. This was sufficient to provoke a micturition response. Standard human urine test strips (Bayer) were used and urine droplets placed directly on the relevant glucose test. After 30 seconds the colour change was compared to the standard chart, and the glucosuria recorded. A urinary glucose concentration of 500mg/dL (2+) was used as the threshold for confirming the successful induction of diabetes.

2.3.3.2 Capillary blood glucose sampling

The successful induction of diabetes was also confirmed through random non-fasted capillary blood glucose monitoring (CBG). A commercially available human glycometer (ACCU CHEK® Performa, Roche, Germany) with corresponding test strips was purchased and calibrated according to manufacturers instructions.

Animal tail capillary samples were obtained by pin prick at the base of the tail using a 23g hypodermic needle (BD microlance, Becton Dickenson, UK). Test strips were then applied directly to the blood spot and the result recorded. A value of >11.1mmol/L was taken to indicate successful induction of diabetes, in line with the World Health Organisation (WHO) human diagnostic criteria (148).

2.3.4 Induction of hindlimb ischaemia and creation of lower limb wound

2.3.4.1 Anaesthetic

Induction of anaesthesia occurred in a specialist anaesthetic chamber in an adjacent room to the operating room. Individuals were placed inside the anaesthetic chamber, where 2l/min O2 was applied as a pre-oxygenation step. Isoflurane gas was introduced, increasing gradually to a minimum flow setting of 2 (maximum 5) on the anaesthetic machine. Once anaesthetised the animal was removed and placed on a warming mat and transferred to nasal gas anaesthetic using a scavenger circuit. Isoflurane anaesthesia was delivered driven via 2l/min O2 at setting of 2-5. Anaesthesia was confirmed by applying toe pressure.

Hind limb fur was shaved on the left limb (or both if bilateral wounds were created) and the limbs were fully extended and taped in place. The skin was cleansed with aqueous chlorhexidine. From this point full aseptic technique was observed.

2.3.4.2 Operative procedure

Full aseptic technique was utilised. Instruments were cleansed in alcoholic chlorhexidine, and heat sterilised using hot bead sterilisation. The animal was positioned supine on an isothermal heating pad, and the surgical area prepared using alcoholic chlorhexidine. Under x10 magnification, a 1 cm longitudinal incision was made in the left groin at the level of the inguinal ligament, and down the leg to above the knee. The subcutaneous fat pad overlying the groin was swept away to reveal the femoral artery, vein and nerve, covered by a thin layer of fascia. The fascia was divided to expose the neurovascular bundle. The external iliac artery was mobilised, avoiding damage to the vein. It was ligated between two 7-0 prolene ligatures (Ethicon, Johnson and Johnson, UK). The superficial femoral artery (SFA), just distal to bifurcation was ligated using a 7-0 prolene (Ethicon) with the popliteal artery just proximal to the knee joint ligated the same way. The SFA between the two ligatures was excised. Skin closure was with interrupted 3-0 vicryl rapide (Ethicon).

2.3.4.3 Hindlimb wound

While still anaesthetised, the animal was rotated exposing the lateral left lower leg. A 4mm full thickness punch biopsy was taken below the knee using a standardised sterile disposable punch biopsy (Stiefel, Glaxo-SmithKlien, UK).

2.3.5 Wound assessment

2.3.5.1 Wound photography

Prior to recovery from anaesthesia, a Day 0 digital photograph was taken for wound area measurement. A sterile measuring tape was placed in the image area to later allow size standardisation. Repeat wound imaging was subsequently repeated post mortem following euthanasia observing schedule 1 methods at time points of 3-, 7- and 14-days post infliction of wound.

2.3.5.2 Sample collection

Following euthanasia under terminal anaesthesia, skin wounds were completely excised using sharp dissection. The samples were mounted on filter paper to maintain architecture and placed into 10% formal saline (Cell Path). Skin immediately distal to the excised specimens was harvested by sharp dissection and snap frozen in liquid nitrogen.

2.3.6 Homogenisation of murine skin samples

Protein samples were liberated from homogenised mouse skin samples utilising the TissueLyser (Qiagen) protocol. After thawing, any residual hair was removed and the samples were weighed. The skin sample was placed in a 2ml round bottom Eppendorf tube, and a weight corresponding volume of RIPA buffer/protease and phosphatase inhibitor cocktail solution was added along with a steel ball bearing. Tissue was then disrupted by mechanical homogenisation for a total of 6 minutes at 30 Hz. Homogenised samples were then centrifuged at 13,000 rpm for 15 minutes at 4°C and the protein supernatant collected. The protein concentration was measured using a BCA assay as previously described.

2.3.7 Wound area planimetry

Wound areas were measured from digital photographs using ImageJ software. The Jpeg images loaded into ImageJ were enlarged via the 'Image' 'Zoom' toolbar function to improve accuracy. The tape measure contained within each image was used to calibrate the scale, using the 'analyse' and 'set scale' dropdown option to ensure standardised measurement of each individual image. Wound area was measured using the 'freehand selection' tool in the main taskbar, and area obtained through the 'analyse' 'measure' function.

Figure 2.3.7 Image J wound area measurement with standard for accurate scale

The variation between individuals of the day 0 starting wound area, and the subsequent inability to identify individual animals required a mean area for each test group, at each time point, to be calculated. Subsequent individual wound area measurements within groups were normalised against the starting day 0 mean of that group. This ensured all groups day 0 wound area was assigned a value of 1, and comparisons between test groups was then possible.

2.4 Statistical analysis

2.4.1 Power calculations

Required sample sizes for human sample collection and *in vivo* animal numbers were estimated using data from prior similar experiments conducted within this research group, to provide a 90% power of detecting a difference at the 5% significance level.

$$n = \frac{2\sigma^2}{\delta^2} f(\alpha,\beta)$$

Where

δ is the true difference

σ is the standard deviation of the outcome

α is 5% (significance level)

1-β is power

Based on mean values and SD of prior studies, required sample sizes were estimated to be approximately 6 patients per group for human tissue analysis, 12 animals per group for *in vivo* validation.

2.4.2 Statistical analyses

Non-parametric data were expressed as median + ranges. Statistical analyses were performed using GraphPad Prism (GraphPad Software). Comparisons between two groups were performed using two-tailed Mann-Whitney test. Comparisons between multiple independent groups were performed using the Kruskall-Wallis test. A p-value < 0.05 was considered statistically significant.

Chapter 3

Effect of diabetic ischaemia on human skin and TLR4 expression

3.1 Introduction

This physiological process of wound healing occurs following tissue injury and is described in detail in section 1.6. It is characterised by overlapping and inter-dependent phases with differing dominant cell types, cytokines and processes. The rapid initial response is haemostasis through coagulation where platelet aggregation and degranulation results in cytokine release, leading to progression to the inflammatory phase of the process.

This stimulates a rapid recruitment of inflammatory cells to the site of injury. This crucial physiological reaction is mediated via innate immune cell surface receptor signalling, through pattern-recognition receptors such as toll-like receptors (TLR). TLR4 is widely expressed throughout skin and is closely associated with initiation of the wound healing process.

The migration of innate immune cells such as polymorphonuclear neutrophils into the areas of tissue damage within minutes following injury helps to prevent bacterial invasion following skin breach, and initiates phagocytosis of tissue debris. Further chemokine and cytokine release from neutrophils recruit monocytes, which differentiate into wound macrophages. Mature wound macrophages continue phagocytosis, recruitment of further inflammatory cells and importantly launch the proliferative phase of healing, through the release of growth factors that stimulate fibroblast, keratinocyte and endothelial cell proliferation. By day 7 post-injury T-lymphocytes have become the most numerous inflammatory cell type, inflammatory effects start waning, and proliferative processes dominate.

In diabetes, the inflammatory response to tissue injury appears to be excessive and pathological. This is discussed in more detail in section 1.6.1. Histological studies in genetically diabetic mice have illustrated a sustained and excessive neutrophil and macrophage infiltration (89), and an excessive production of destructive MMPs and pro-inflammatory cytokines leads to impaired granulation tissue formation (53).

Human histology studies of chronic diabetic ulcers have demonstrated the preponderance of infiltrating neutrophils and macrophages, with a localisation around capillaries and absence of granulation tissue (53). Direct comparison between diabetic wounds and proximal intact skin margins of amputated limbs reveals the same pattern of increased inflammatory cell infiltration in the chronic diabetic wounds compared to normal diabetic skin (149). In addition to the peri-capillary inflammation, significant occlusive microvascular disease was observed in diabetic ulcerated samples with intimal hyperplasia and medial fibrosis, compared to non-diabetic ulcerated (venous) tissue (149). Studies comparing neuropathic, pressure and diabetic-ischaemic ulcer histology have identified a 'typical' pattern characterising diabetic-ischaemic ulcers, with the same pericapillary inflammation previously described, intimal thickening, scarcity of endothelial cells in abnormal granulation tissue and significantly greater infiltration of mononuclear inflammatory cells (150).

There is observational evidence through immunohistochemistry (IHC) analysis for the detrimental involvement of TLR4 in diabetes. While no direct IHC studies have been reported in diabetic skin, intact or ulcerated, a murine model of diabetic bladder dysfunction demonstrated significantly increased TLR4 staining in diabetic animals compared to non-diabetic in bladder muscle (151). Similar IHC studies in human patients with nephropathy revealed an increase in TLR4 staining in diabetic nephropathy vs diabetes alone or non diabetic controls (151). Further histological evidence for the pathological effect of TLR4 in diabetes was reported in KO animals, where reduced infiltration of inflammatory cells in TLR4 KO was observed compared to WT (74).

These histological features provide compelling evidence of the excessive and destructive inflammatory conditions that characterise chronic diabetic-ischaemic

wounds, where healing fails to progress, and the wounds become stalled in the inflammatory phase. Evidence from IHC studies cannot ascertain causality, however the strong association between increased TLR4 expression and diabetes-related processes and complications warrants further study.

3.2 Aims

Human tissue analysis, while entirely observational, is important to establish whether the outcomes of the hypothesised associations to be tested *in vitro* and *in vivo* are present in real world human samples. The aim of this chapter is therefore to observe the relative difference in cellular inflammation and TLR4 expression between diabetic and non-diabetic, ischaemic and non-ischaemic tissues. We hypothesise that increased inflammatory cell infiltrate and increased expression of TLR4 will be present in diabetic ischaemic skin.

3.3 Methods

3.3.1 Human skin sample collection

Human skin cell biopsies were obtained after written consent from patients undergoing either above or below knee amputation. As described in section 2.2.1, full thickness skin samples were taken from the most proximal margin of the amputation specimen, just along the incision. A second sample was taken distally, from the edges of ulcers or from intact but ischaemic skin. Specimens were placed in 10% formal saline containing 4% formaldehyde (CellPath, UK) immediately after collection. Further duplicate $1cm^2$ samples were taken and immediately snap frozen in liquid nitrogen.

3.3.2 Patient demographics

A total of 13 patients undergoing major amputation were recruited to this study. All patients were male, mean ages were comparable across groups. Seven patients were diabetic. All recruited irrespective of diabetes status had a documented diagnosis of ischaemic heart disease, which varied from previous MI and CABG, to previous coronary stent insertion and atrial fibrillation. Two diabetic patients had end-stage renal failure on haemodialysis, each of the diabetic patients not on dialysis had an identified degree of nephropathy and a diagnosis of chronic kidney disease (CKD). All patients across both groups were diagnosed with hypertension. Three of the non-diabetic patients were current smokers, the rest were ex-smokers, the diabetic group contained no active smokers, six ex-smokers and one never smoker.

Most diabetic patients (5/7) were taking an antiplatelet agent and the same number a statin. Three patients in the non-diabetic group were taking an antiplatelet and four a statin.

Table 3.3.2 Summary of patient demographics/ characteristics

	Diabetic	**Non-diabetic**
Male/Female	7/0	6/0
Age	67	68
Ischaemic Heart disease	7	6
ESKD on dialysis	2*	0
Hypertension	7	6
Smoking (Current/Ex/Never)	0/6/1	3/3/0
Anticoagulant	1	0
Antiplatelet	5	3

Statin	5	4
ASA grade 1/2/3/4	0/1/5/1	0/1/5/0

All patients undergoing major amputation in the non-diabetic group had confirmed critical limb ischaemia, in the form of either rest pain (2/6) or tissue loss (4/6). Arterial duplex, angiogram or computed tomography (CT) examinations demonstrated unreconstructable peripheral artery disease and the decision to proceed to major amputation was confirmed in a peripheral vascular multidisciplinary team (MDT) meeting.

3.3.3 Sample preparation

Formalin fixed tissues were dehydrated overnight and embeded in molten paraffin wax to create formalin-fixed paraffin embeded histology samples. Thin 3µm slices were cut using a microtome (Leica, UK) and mounted onto polylysine- coated microscopy slides (VWR, UK). When required to perform staining, skin histology sections were heated overnight at 42°C.

Snap-frozen skin samples were removed from liquid nitrogen and placed in -80°C freezers. These samples were used for protein analysis, with protein homogenates processed as described in section 2.1.3.1.

3.3.3.1 Haematoxylin and Eosin

Haematoxylin and eosin (H&E) staining was performed using a standard lab protocol. Skin histology sections were dewaxed in xylene (Genta Medical, York, UK) and passed through graded ethanols before transfer to water. After immersion in running tap water, sections were immersed in Harris haematoxylin for 5 minutes before dipping in a weak acid alcohol solution (20mM HCl in 70% ethanol). Sections were then rinsed in running tap water before immersion in eosin for 1 minute. Sections were then rinsed and dehydrated by passing through graded alcohols, cleared in xylene,

and then mounted in permanent DePeX mountant (VWR, UK).

3.3.3.2 Immunohistochemistry

As above, prepared skin sample slides were dewaxed in xylene and graded ethanol baths before tap water rinsing. Residual endogenous perioxidase activity was blocked by soaking samples in methanol and hydrogen peroxide for 10 minutes, before tap water wash. Antigen retrieval was achieved through submersing samples in heated 10mM citrate buffer and microwaving for 10minutes.

Reduction of non-specific antibody binding was achieved through the addition of a blocking serum to tissue samples for 15 minutes, horse serum was chosen as the secondary anti-rabbit antibody was horse derived. A rabbit derived human anti-TLR4 primary antibody was applied to the samples at a concentration of 1:100, and incubated overnight at 5°C. After warming to room temperature, the slide is repeatedly washed in PBS, before a non-biotin polymer conjugated anti-rabbit secondary antibody at 1:200 concentration (Immpress reagent kit, Vector laboratories, UK) was added for 30 minutes. After washing, a DAB (Diaminobenzidine) peroxidase substrate solution was added for a period of 10 minutes. Following further PBS wash, the slide was placed into Mayers haematoxylin for 5 minutes. Finally, the slides were dipped into acid alcohol and bluing solution and passed through the reversal of the de-waxing process utilising graded alcohols and xylene.

3.3.3.3 Inflammatory cell quantification

The semi-quantitative analysis of inflammatory cell infiltration was compared between samples taken from proximal (non-ischaemic) and distal (ischaemic) tissue in both diabetic and non-diabetic donors after the H&E staining process described in section 3.3.3.1. Slide preparations were photographed under light microscopy at x100 magnification.

Three areas of each slide were sampled by applying an identical template over individual slides. This standardised method was used to prevent sampling bias, and

to maximise the accuracy of analysis. A semi-quantitative blinded scoring system was then employed to categorise inflammatory cell density on H&E staining in each of the sampled areas. Slides were anonymised and placed in a random order. The scoring was done by a single independent individual who was blinded to the slide origin, and who had participated in a prior series of on-line multimedia tutorials in cell identification. Inflammatory cells were then identified based on their morphology and their density assigned to a score measured against provided standards. 0= Absent, 1= Mild, 2= Moderate, 3= Severe.

3.3.3.4 TLR4 Staining intensity measurement

Following the immunohistochemistry preparation and staining process described in 2.1.3.3, slides stained using TLR4 antibody were photographed under microscopy at x100 magnification. All samples from all patient groups were processed together, employing an identical staining protocol. This was to ensure valid comparison of results between the groups by reducing any potential bias in the staining process, that may lead to differences in staining intensity.

Image J software was used to compare the brown pigment staining intensity of each slide, expressed in relative units.

3.4 Results

3.4.1 Inflammatory cell infiltration in H&E Stained Human skin samples

To explore the presence and relative number of inflammatory cells in Human skin biopsies, samples were collected and prepared as described in section 3.3 and stained for haematoxylin and eosin. Figure 3.4.1 demonstrates representative samples taken from proximal (non-ischaemic) and distal (ischaemic) tissue and in both diabetic and non-diabetic patients. Figures 3.4.1 A and C are taken from proximal amputation margins and represent healthy intact, non-ischaemic skin. Figures 3.4.1 B and D are biopsied from distal tissues at the site of ulceration.

A

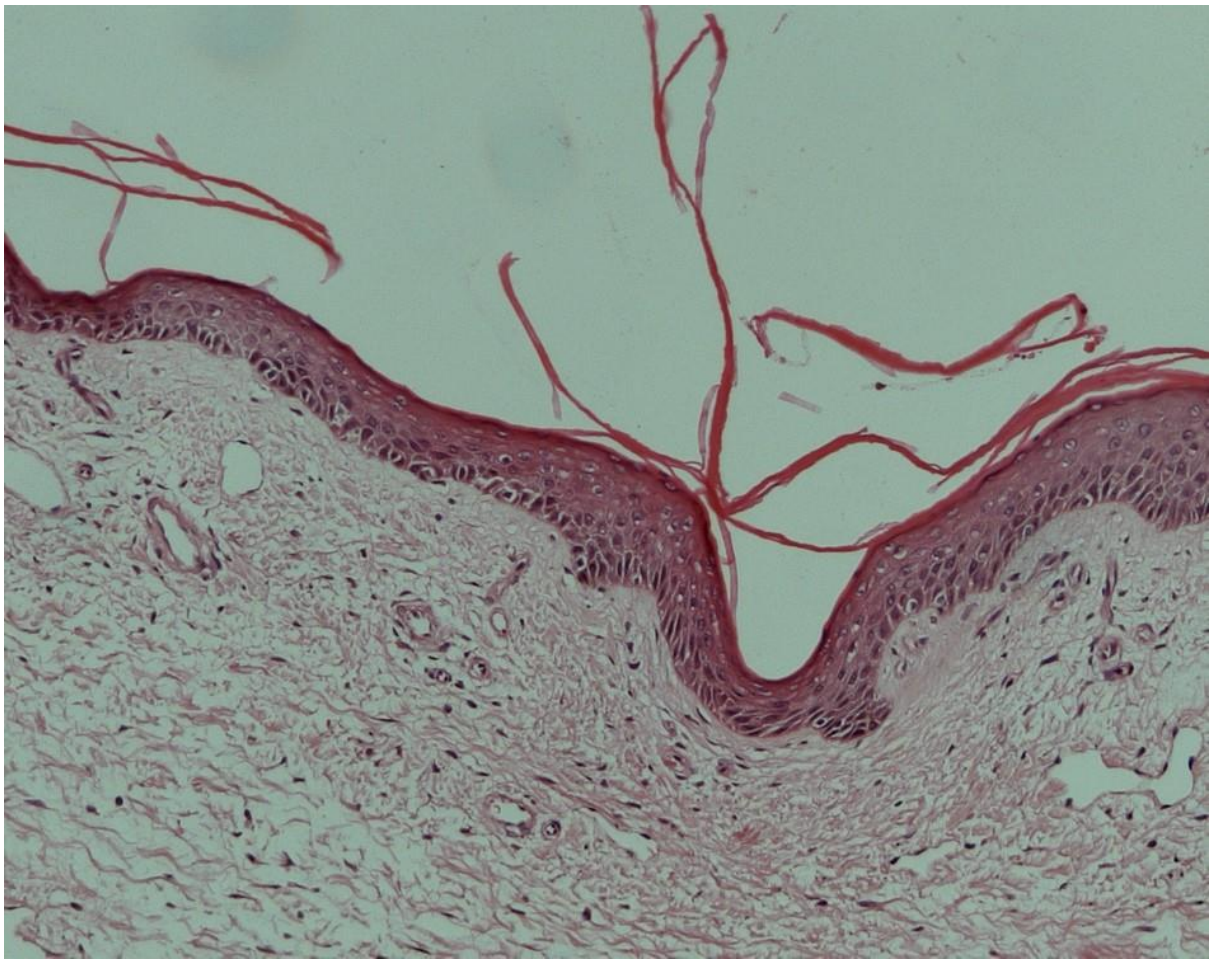

x100

B

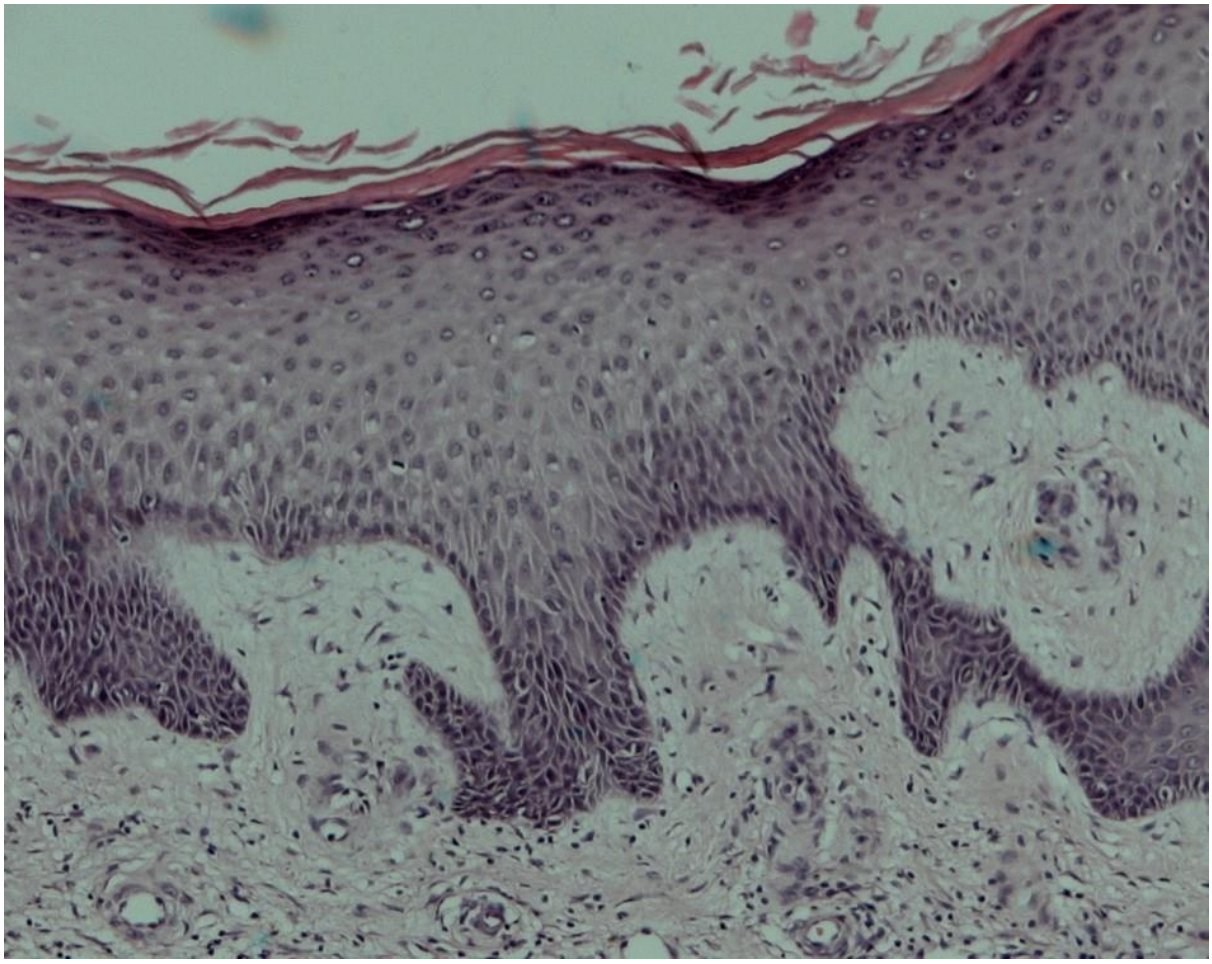

x100

C

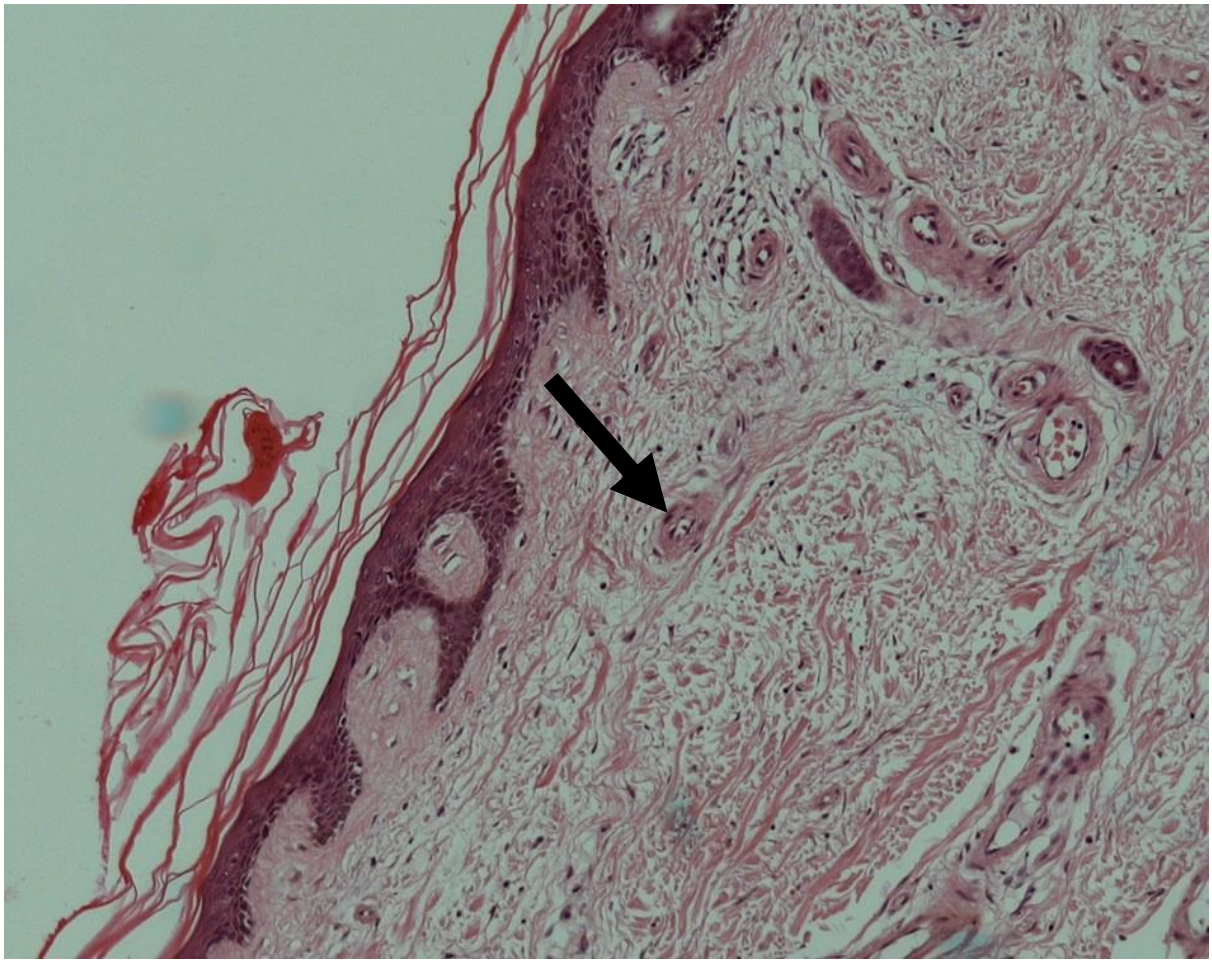

x100

D

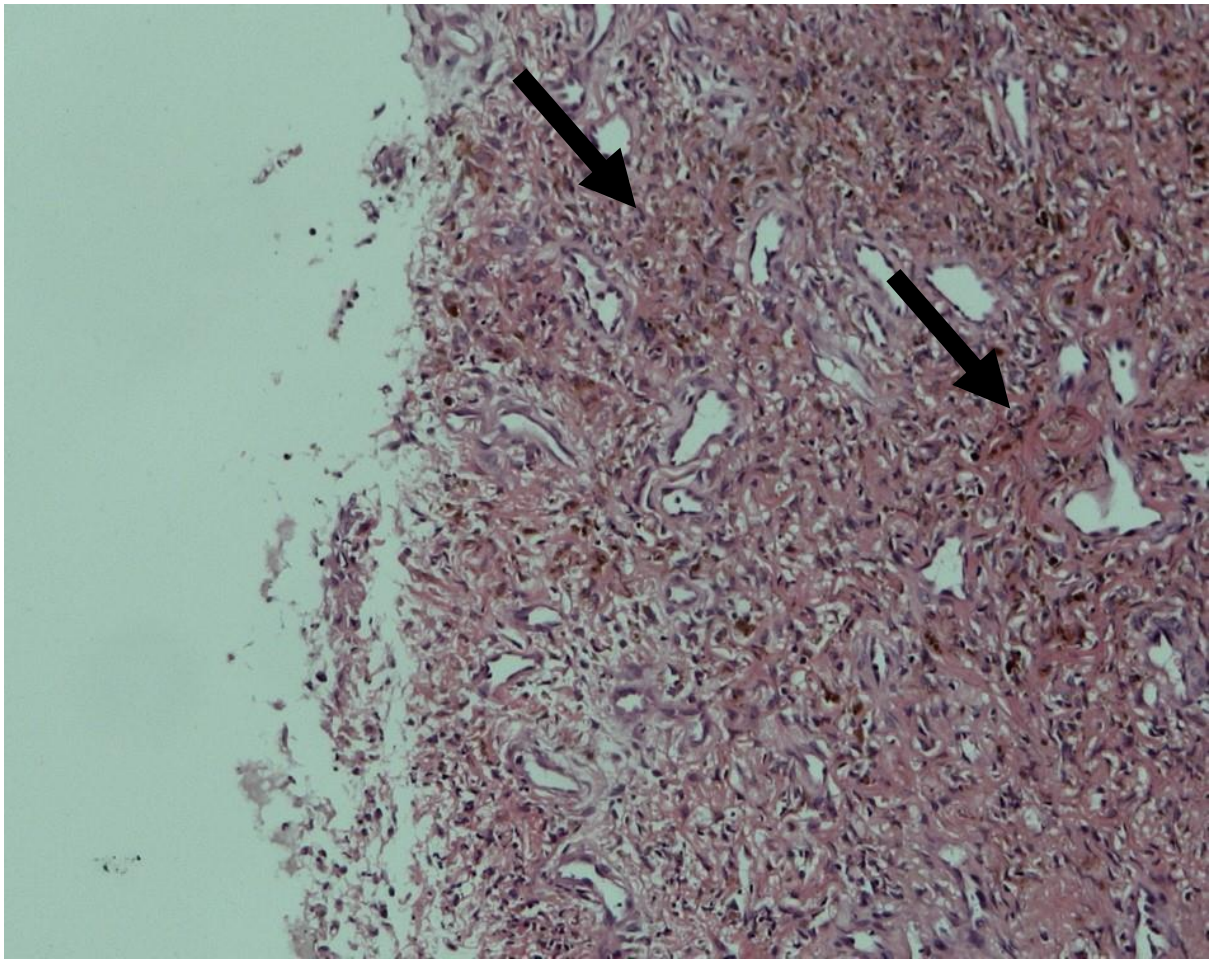

x100

E

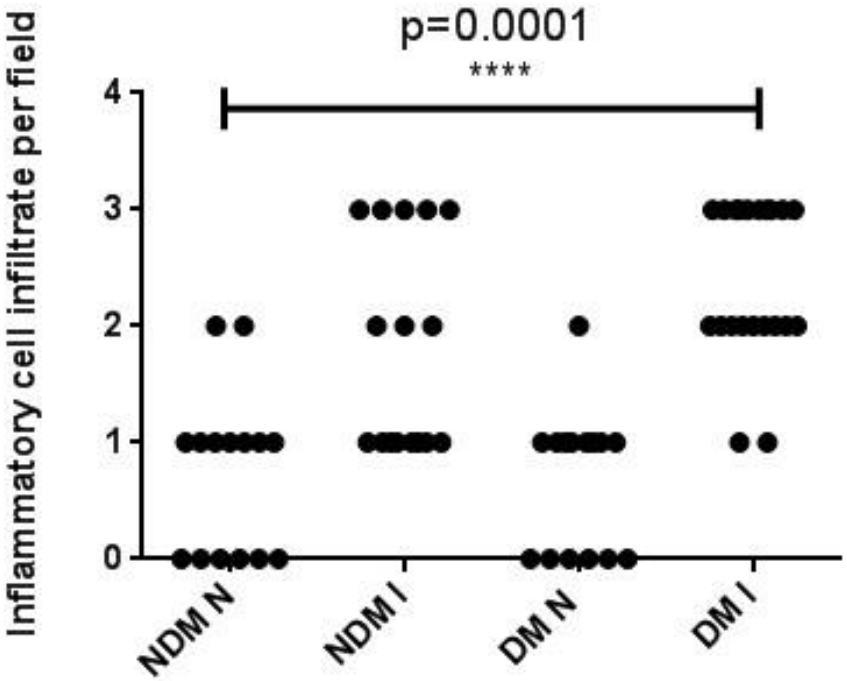
p=0.0001
****
Inflammatory cell infiltrate per field
4
3
2
1
0
NDM N
NDM I
DM N
DM I

Figure 3.4.1 Haematoxylin and Eosin staining inflammatory cell infiltrate

Figure 3.4.1 **A** Representative H&E staining image of non-diabetic, proximal non-ischaemic tissue. **B** Non-diabetic, distal ischaemic tissue sample. **C** Diabetic proximal non-ischaemic skin sample, arrow denotes pericapillary thickening. **D** Diabetic, distal ulcerated ischaemic tissue. **E** Semi-quantitative Inflammatory cell infiltrate score. Inflammatory cells seen on H&E staining include neutrophils and macrophages (arrowed). (****p=0.0001, Kruskall-Wallis test, n=7). Key: NDM N- Non diabetic non ischaemic, NDM I- Non diabetic ischaemic, DM N- Diabetic non ischaemic, DM I Diabetic ischaemic.

There was a significant difference in inflammatory cell infiltration observed across patient sample sub-types, with increased inflammatory cell density in the diabetic ulcerated distal ischaemic tissues (Figure 3.4.1 E, Kruskal-Wallis test n=7). In addition, figure 3.4.1 C demonstrates greater peri-capillary thickening (arrowed) compared to the non-diabetic dermal capillaries found in figure 3.4.1 A. Inflammatory cell infiltrates were concentrated in the dermis (Figure 3.4.1 A, B, C, D) and were greatest in ischaemic distal tissues (Figure 3.4.1 E). Individual dots in figure 3.4.1 E correspond to each individually scored sample section. As mentioned in section 3.3.3.3, each slide prepared following H&E staining was sampled in three places by the application of a set template, hence three samples per patient. The positioning of the histology sample on certain slides meant no specimen was contained within the template border, hence the differing number of dots within each group.

3.4.2 TLR4 immunohistochemistry staining

Skin samples were mounted on slides and stained for Toll-Like receptor 4 to observe the relative density of TLR4 expression in each of the four experimental conditions of interest. As before, samples of proximal non-ischaemic and distal ischaemic skin in diabetic and non-diabetic patients were tested. The intensity of TLR4 expression was assessed across the whole sample using image J software.

A

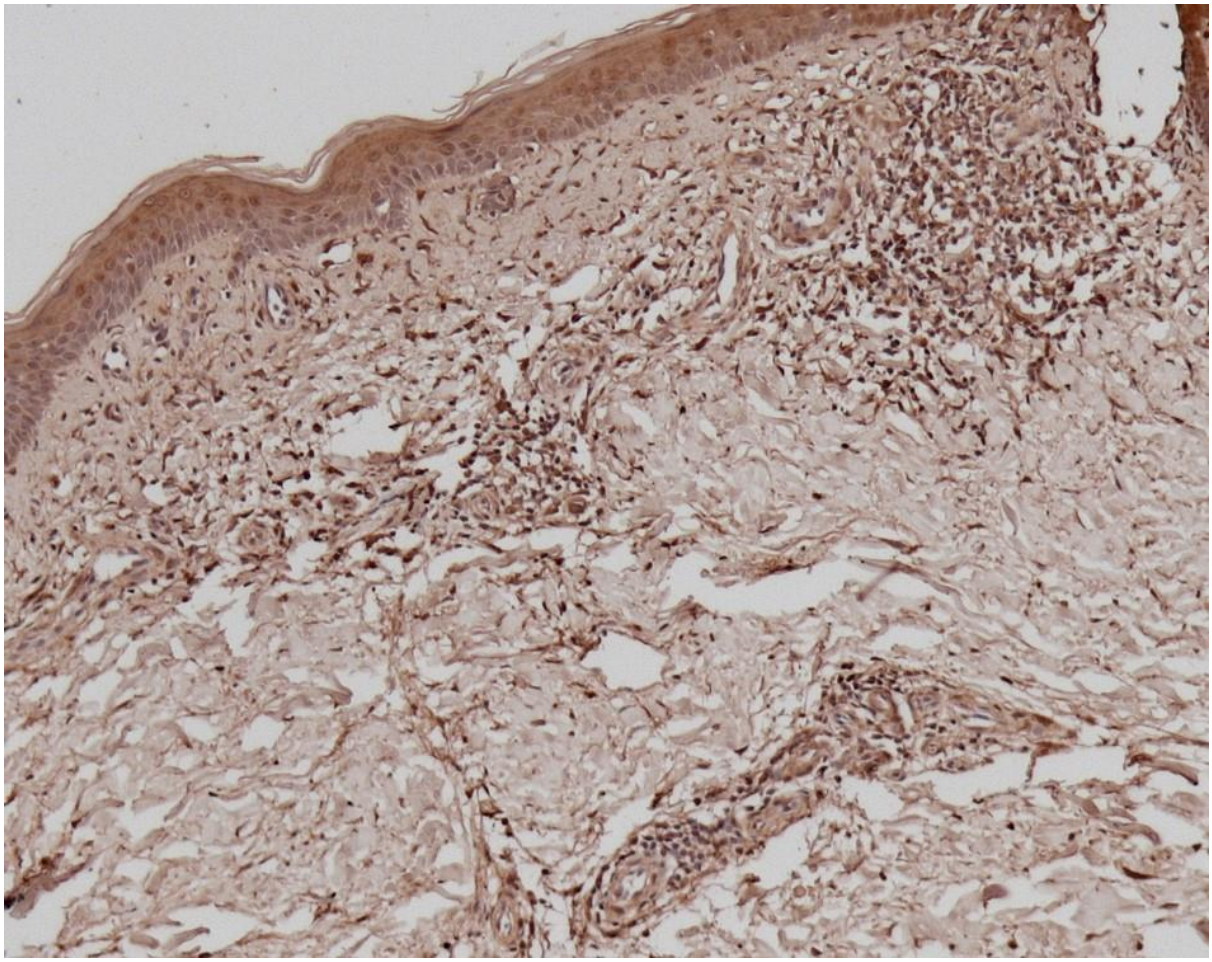

x100

B

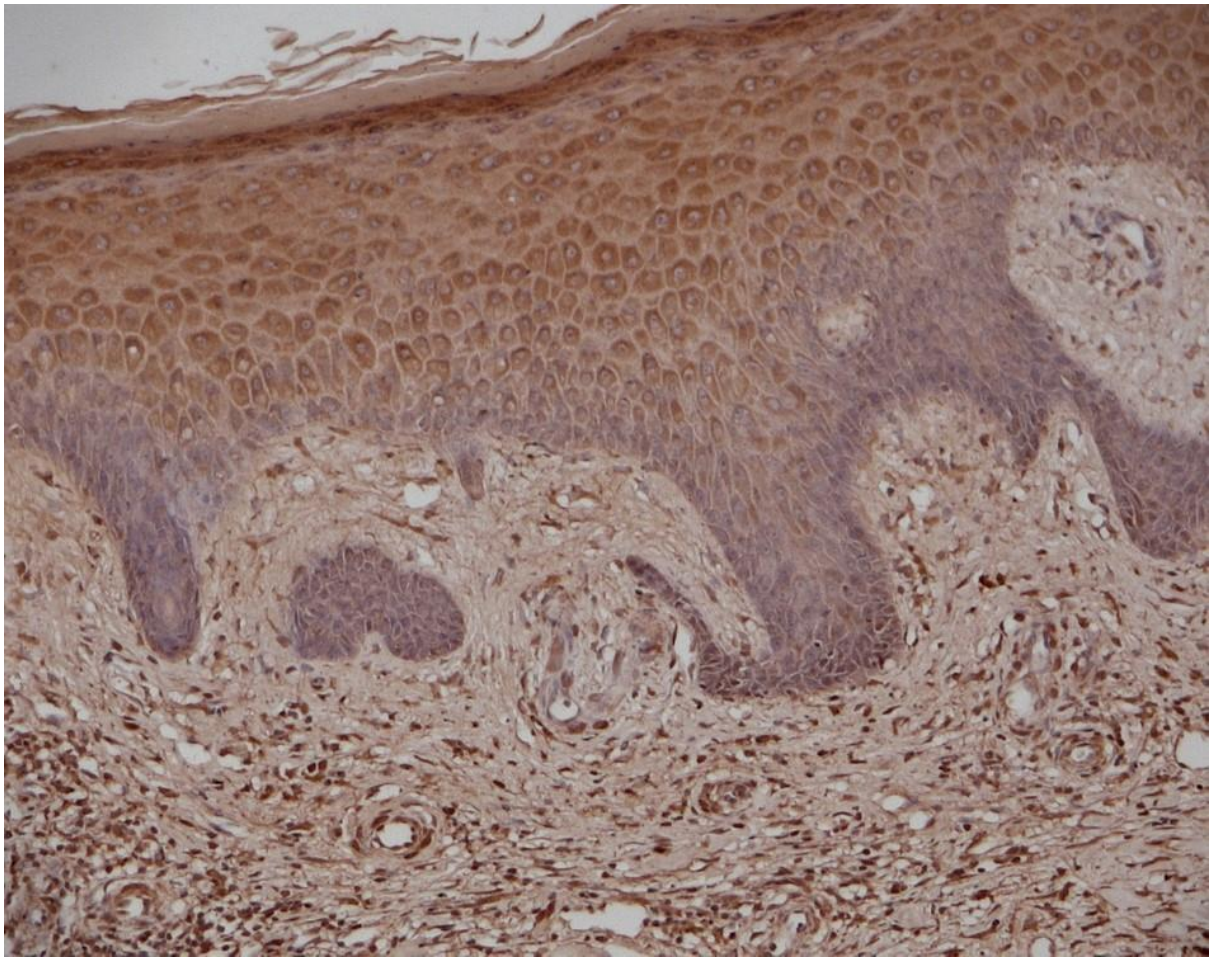

x100

C

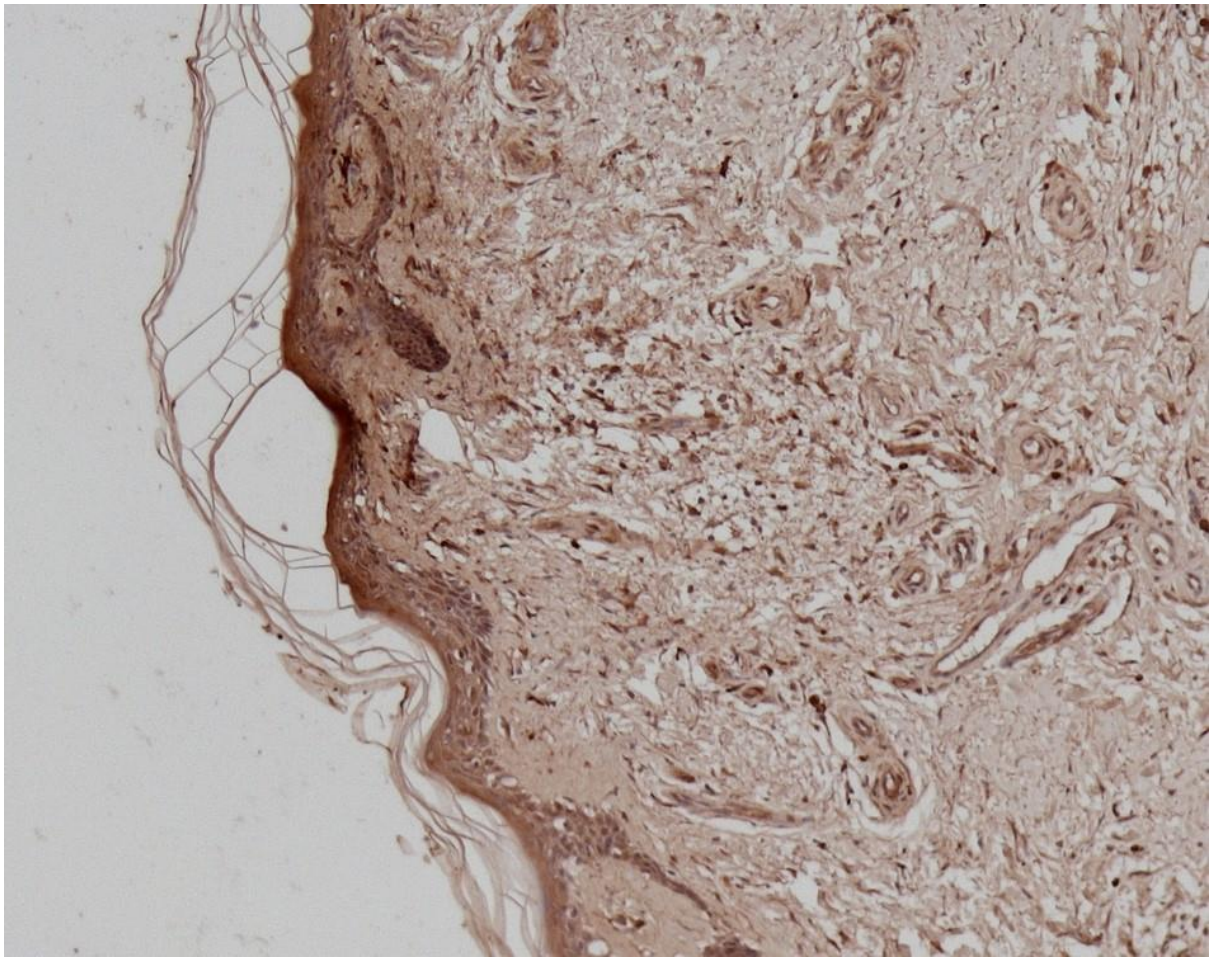

x100

D

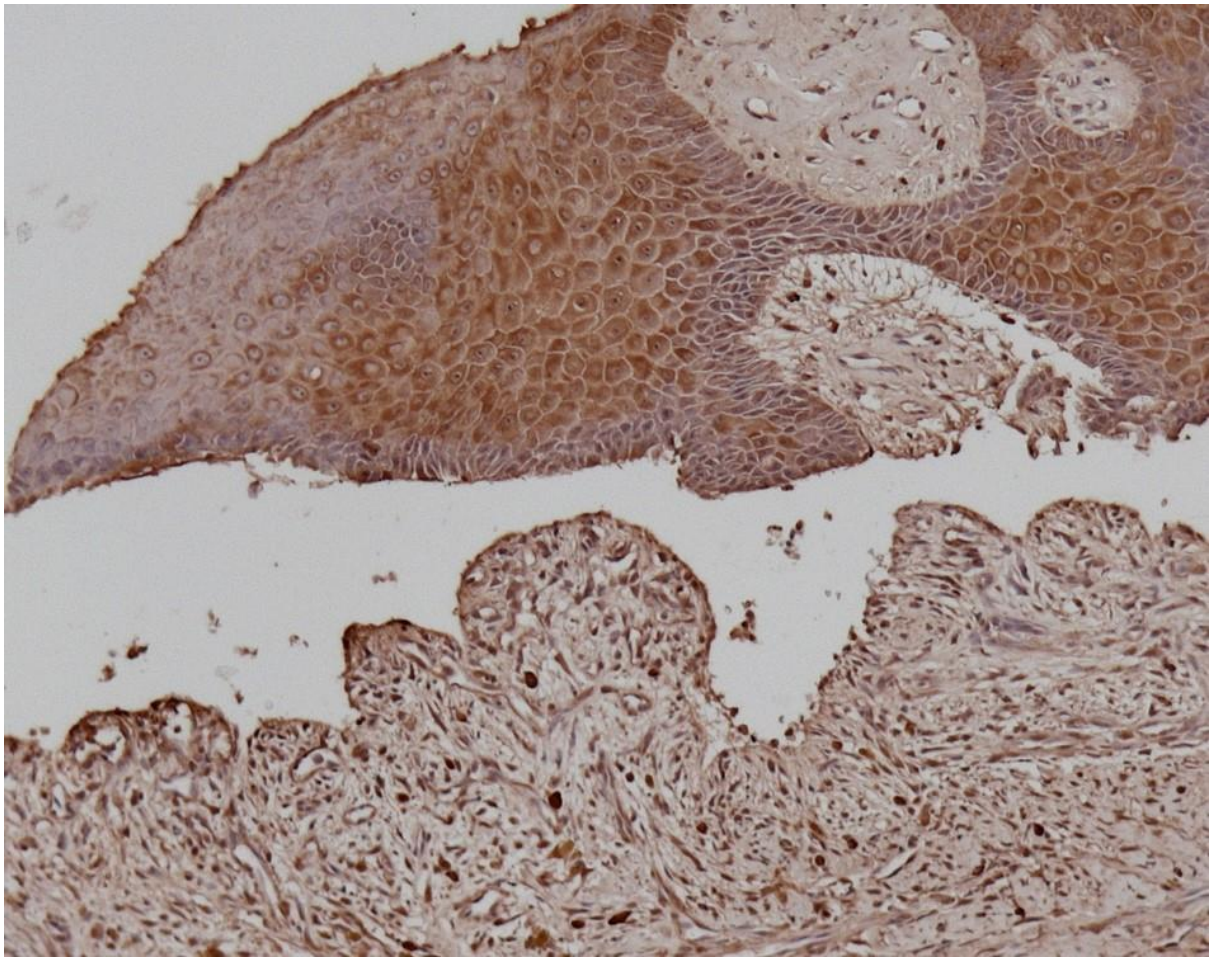

x100

E

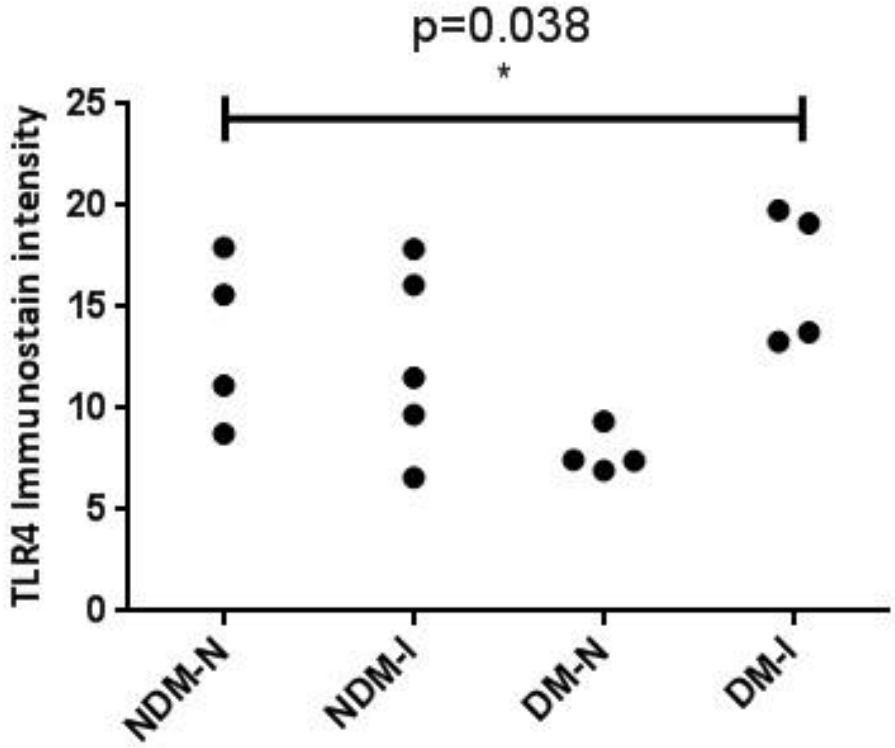
p=0.038
*
TLR4 Immunostain intensity
25
20
15
10
5
0
NDM-N
NDM-I
DM-N
DM-I

Figure 3.4.2 Relative Toll-like receptor 4 expression density

Figure 3.4.2 **A** Representative TLR4 immunostaining image of non-diabetic, proximal non-ischaemic skin sample. **B** Non-diabetic distal ischaemic. **C** Diabetic proximal non-ischaemic. **D** Diabetic distal ulcerated and ischaemic. **E** Quantitative TLR4 staining densities. Brown colour immunostaining was measured across all sample using Image J software. (*p=0.038, Kruskall-Wallis test n=4). More intense TLR4 staining was observed in the diabetic-ischaemic group. Key: NDM N- Non diabetic non ischaemic, NDM I- Non diabetic ischaemic, DM N- Diabetic non ischaemic, DM I Diabetic ischaemic.

TLR4 immunohistochemistry staining revealed a greater observed intensity of TLR4 expression in the diabetic- distal ischaemic biopsy samples compared to non-diabetic and non-ischaemic samples. This observation is consistent with the results shown in figure 3.4.1 which demonstrated a higher density of innate immune inflammatory cells in the diabetic ischaemic samples. While no firm conclusions can be drawn from these observations, these results are consistent with an excessive pro-inflammatory environment characterised by increased inflammatory cell infiltration and excess expression of pro-inflammatory TLR4 receptors in diabetic-ischaemic conditions. Four patient samples per group are represented by individual dots in figure 3.4.2 E. Only four samples in each patient group were tested for TLR4 immunohistochemistry, as all sixteen were analysed together simultaneously to reduce variability in the staining protocol process.

3.4.3 Toll-like receptor 4 staining density and distribution

In addition to the quantified relative TLR4 staining density, immunohistochemistry can also be used to determine the distribution of TLR4 expression within the skin tissue. The cells which express TLR4 to the greatest degree stain darker, indicating a higher expression density. A direct visual comparison of TLR4 staining intensity in non-diabetic proximal non-ischaemic tissue and diabetic distal tissues reveals an increase in TLR4 staining intensity throughout all skin structures.

A

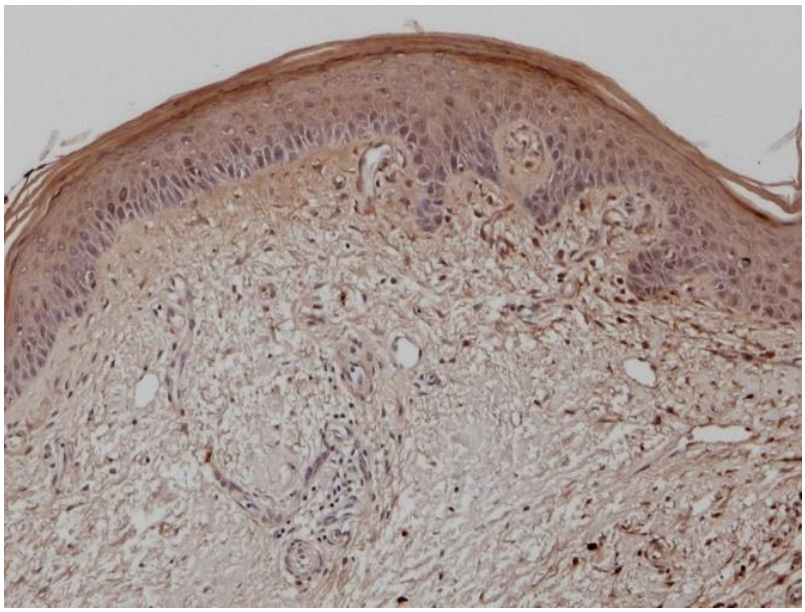

B

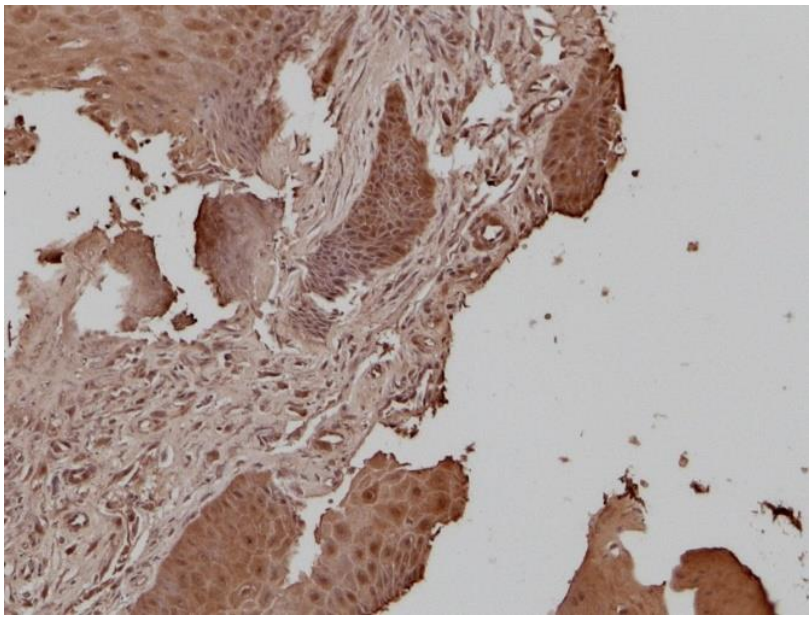

C

Non diabetic
Non ischaemic

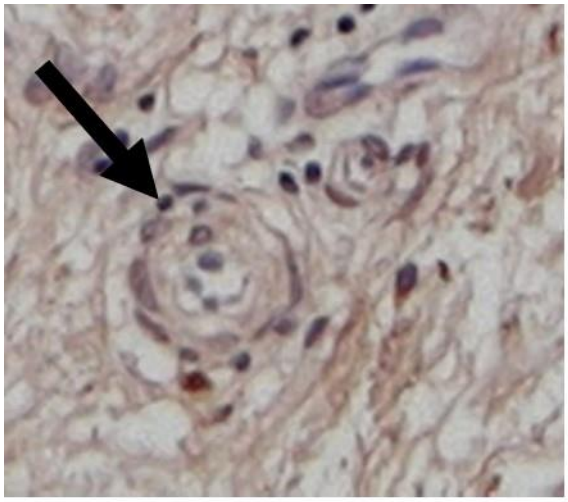

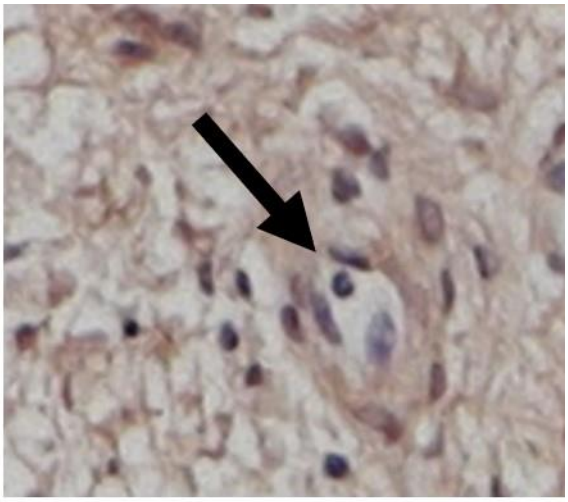

Diabetic
Ischaemic

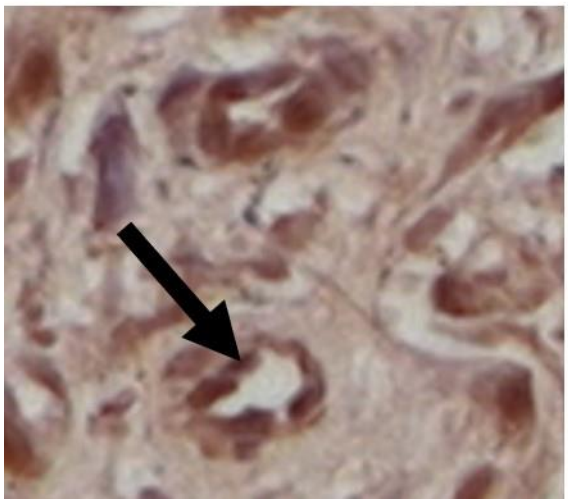

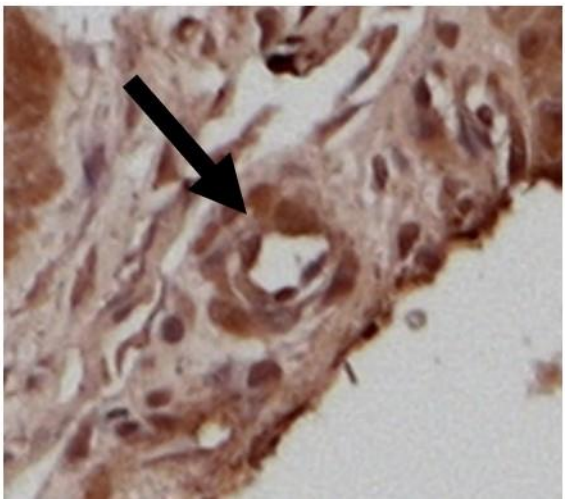

x200

D

Non diabetic
Non ischaemic

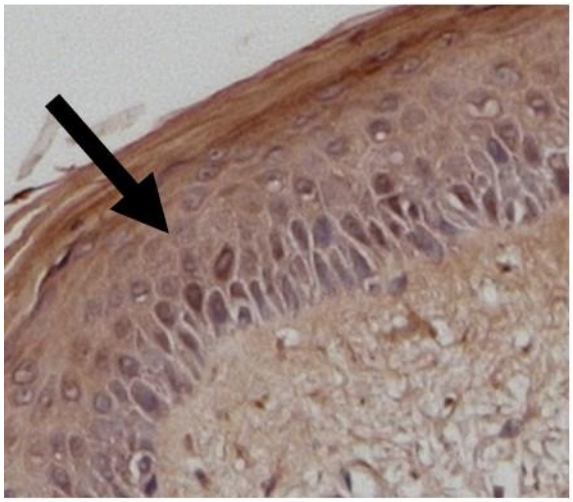

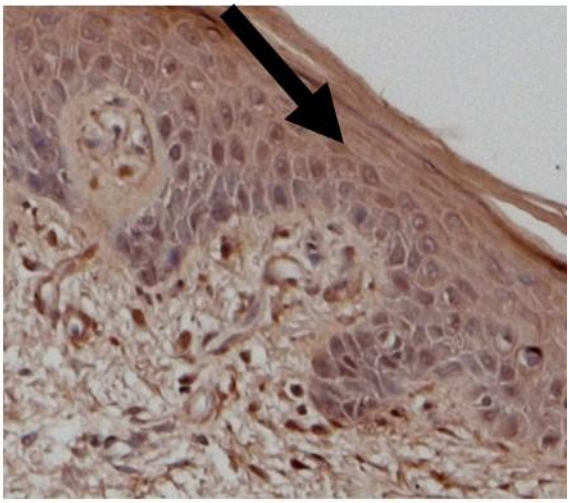

Diabetic
Ischaemic

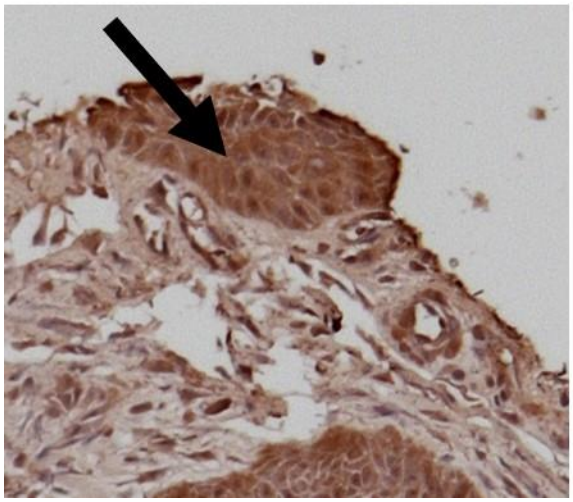

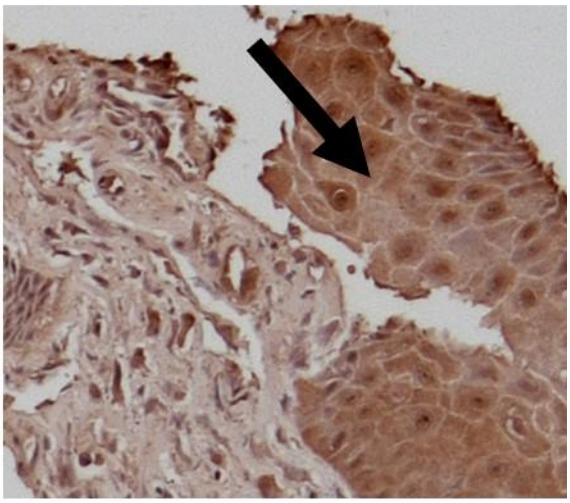

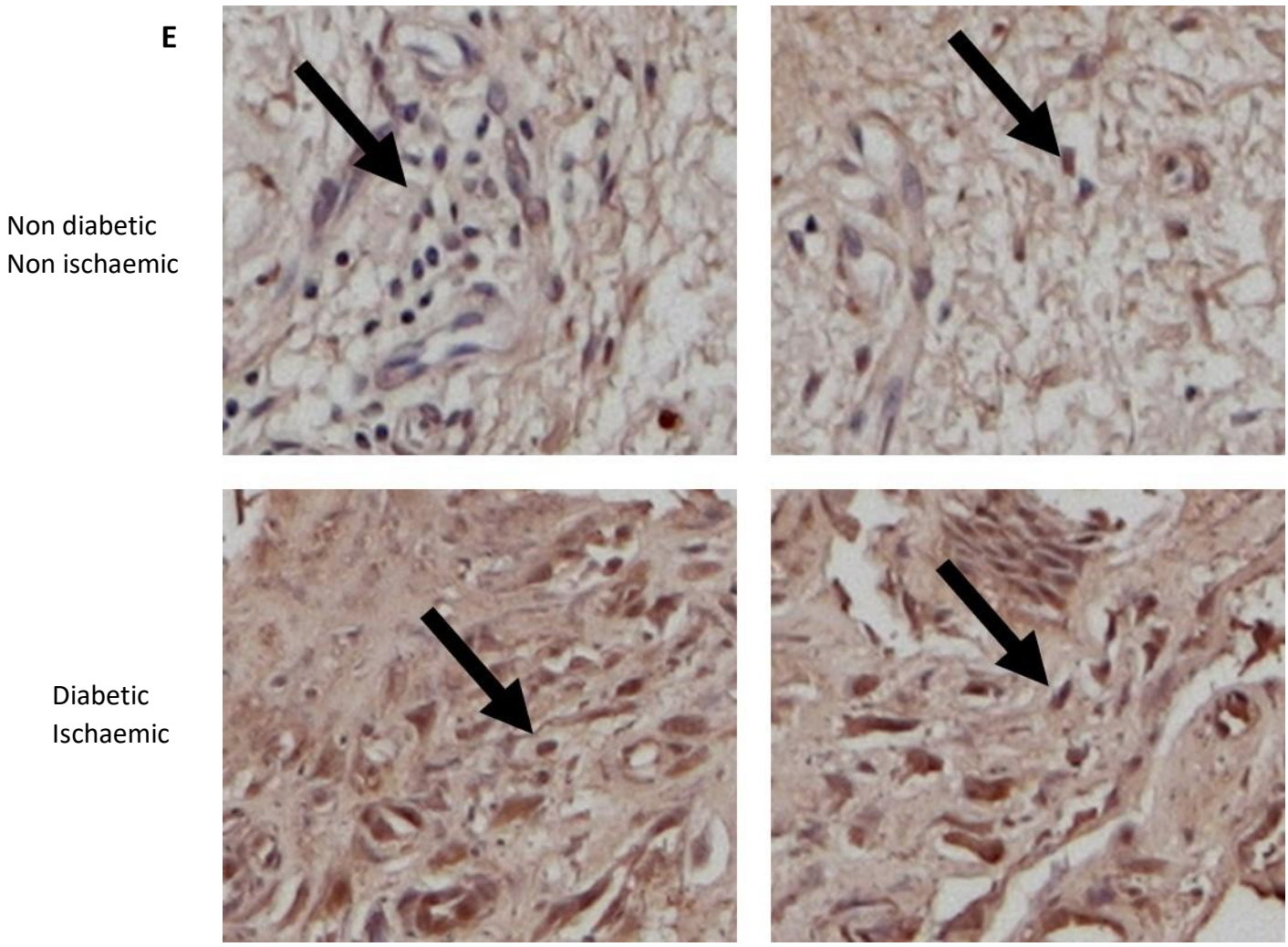

Figure 3.4.3 Distribution and staining intensity of TLR4

Figure 3.4.3 **A** representative TLR4 immunohistochemistry staining image of a non-diabetic, proximal non-ischaemic skin sample. **B** Diabetic distal ischaemic sample. **C** Comparison between TLR4 staining intensity in capillary endothelial cells in diabetic ischaemic tissue and non-diabetic non ischaemic tissue. **D** Differential TLR4 staining density in epidermal keratinocytes. **E** TLR4 staining intensity in inflammatory cells.

Visual comparison of TLR4 staining in the immunohistochemistry slides shown in figures 3.4.3 **A** representing non-diabetic proximal non-ischaemic skin and diabetic distal ischaemic skin (figure 3.4.3 **B**) clearly shows increased background staining density throughout the epidermis and dermis in the diabetic- ischaemic sample.

Observational comparison between the individual structures in these two samples reveals increased concentration density of TLR4 expression in epidermal keratinocytes (figure 3.4.3 **D**), endothelial cells (figure 3.4.3 **C**) and inflammatory cells which include neutrophils and monocytes figure 3.4.3 **E**). These cells types, along with fibroblasts (not identified in these samples) are well recognised to highly express TLR4 (120, 152).

The observation in diabetic-ischaemic human tissue samples of increased TLR4 expression by cell types crucial to the physiological process of wound healing, gives real world correlation to the hypothesised association between diabetes, ischaemia and increased TLR4 expression, and the inhibitory effect on wound healing of excessive TLR4 mediated inflammation.

3.5 Discussion

This chapter examines the relationship between inflammatory cell recruitment and infiltration and the presence of diabetes, ischaemia or both combined in human patients undergoing major amputation for end-stage disease. The relative expression and distribution of TLR4 was ascertained through IHC studies.

The observation of increased inflammatory cell infiltrate in the diabetic-ischaemic human skin samples compared to non-ischaemic and non-diabetic samples in figure 3.4.1 is consistent with the published findings of other groups utilising similar methodology (153). Morphological changes in diabetic non-ischaemic or ulcerated tissues are also evident, such as the peri-capillary tissue thickening observed in figure 3.4.1 C, when compared to non-ischaemic non-diabetic dermal capillaries.

The hyperinflammatory and pathological nature of the healing process in diabetes is characterised by excessive and prolonged infiltration of innate immune cells such as neutrophils and macrophages, and absence of normal granulation tissue formation. It is hypothesised the lack of progression of the healing process, through inhibited cellular proliferation and failure of termination of the inflammatory phase of healing leads to a chronic, non-healing wound. The data presented in this chapter is consistent with this proposed mechanism.

The association between exaggerated cellular inflammation and diabetes is evident, however the underlying mechanism of this pathological process is unclear. Pattern recognition receptors of the innate immune system such as TLR4 have been implicated, through evidence of their crucial role in the normal healing process and observation through IHC studies of their over expression in diabetic-ischaemic pathologies. Figure 3.4.2 demonstrated an increased TLR4 expression in diabetic-ischaemic skin tissues when compared across groups. While no comparable results in Human skin could be found in the literature, the increased IHC expression of TLR4 in diabetes has been observed in other tissue types.

The distribution of TLR4 expression concentrated within keratinocytes, endothelial and inflammatory cells is consistent with cell types well known to express TLR4. The

higher staining intensity observed in diabetic tissues compared to non-diabetic suggests a greater TLR4 expression in diabetic conditions.

The comparison of TLR4 staining intensity through image J software in sample groups highlighted a significant difference between diabetic ischaemic and non-diabetic non-ischaemic groups, however there was less variation than was expected. One explanation for this is the small sample size, recognised as a major limitation to the validity of any conclusions drawn from this data. Another potential but unquantifiable limitation to these results is the potential confounding influence of patient's medications on TLR4 expression. Drugs commonly prescribed to diabetic patients such as statins and ACE inhibitors have been shown to have anti-inflammatory effects through anti-TLR4 activity.

Atorvastatin and simvastatin reduced TLR4 expression and inhibited signalling in human monocytes (154), similarly aortic valve interstitial cells demonstrated reduced TLR4 induced pro-inflammatory activity when treated with simvastatin (155). Atorvastatin inhibited HMGB1 mediated TLR4 activation and expression in human endothelial cells (156), with similar effects discovered in mouse hepatocytes (157). Likewise, TLR4 expression was significantly reduced in endothelial cells, macrophages and smooth muscle cells taken from carotid artery plaques of patients taking statins vs those of non-statin users (158). Angiotensin II is also associated with systemic pro-inflammatory effects mediated via TLR4 signalling (159). There is evidence for the anti-inflammatory effect of ACE inhibitors through inhibition of the TLR4/NFkB signalling pathway in human monocytes (160), and cardiac myocytes where ramipril reduced TLR4 expression in hypertensive rats (161). The benefit of statin and ACE inhibitor use on cardiovascular mortality in diabetes appears to be over and above that of the cholesterol and blood pressure lowering effects of these drugs respectively (162).

Of the patients recruited for this study 5/7 of the diabetic group and 4/6 of the non-diabetic were prescribed statins and no information regarding dose was recorded. Information regarding the use of ACE inhibitors or angiotensin receptor blockers (ARBs) was incomplete. The effect of dose, individual variability in efficacy of each drug, compliance and duration of prescription are all potential confounding factors.

Comparisons and conclusions from this human tissue data are therefore limited and should be considered descriptive only.

The further confounding effect of infection on TLR4 expression has not be discussed so far in this study. It is inevitable that chronic, non-healing diabetic wounds will be exposed to bacterial colonisation, if not overt infection. TLR4 expression and activation will occur through the processes of infection and trauma, resulting in the introduction of many different variables, impossible to control for. This is an important factor that limits the direct comparison of human tissue samples.

A crucial piece of data missing from this chapter is the quantification of protein concentrations through Western Blot analysis. The protein was collected as a full-thickness skin biopsy sample from the amputated limbs in the same manner as histology samples, and immediately snap frozen in liquid nitrogen. After thawing from -80°C, the skin sample was separated from underlying subcutaneous fat tissue using a scalpel blade. The protein was homogenised as described in section 2.1.3.1, utilising protease and phosphatase inhibitors. Unfortunately, despite concentration adjustment through BCA assay as described in section 2.2.5, the sample proteins had completely degraded, and no results were obtained from successive Western blot attempts.

The failure of the protein quantification experiments almost certainly lies in the significant degradation of the proteins that occurred during both the storage, thawing and homogenising processes. These samples were collected over a period of 18 months from consenting patients undergoing major amputations, and in hindsight the protein samples should have been prepared shortly after collection, avoiding the damaging effect of prolonged storage. In any future analysis utilising similar methodology, samples must be prepared contemporaneously.

3.6 Summary

In conclusion, this chapter has examined and compared the histological appearance of human skin in diabetic-ischaemic, diabetic only, ischaemic only, and non-diabetic,

non-ischaemic skin. There was an increase in the density of inflammatory cell infiltrate in the diabetic-ischaemic tissues. The relative expression and location of TLR4 was also examined, demonstrating an increase in TLR4 expression in diabetic-ischaemic skin throughout both the epidermal keratinocytes, and dermal structures such as endothelial cells and inflammatory cells.

These experiments show a consistency with published work from other groups reporting similar findings in other tissues, and suggest an excessive inflammatory response mediated by TLR4 expression and signalling in diabetic conditions. Caution is required when interpreting this data however, as no conclusions regarding causality can be drawn from this observational study. However, the wider association between TLR4 over-expression and excessive inflammation leading to wound non-healing is compelling.

Chapter 4

The effect of hyperglycaemia and ischaemia on TLR4 expression, signalling and activation *in vitro*

4.1 Introduction

Diabetes is now recognised as a systemic pro-inflammatory condition. There is compelling evidence this effect is mediated through pattern recognition receptors (PRRs) of the innate immune system (163). Toll-like receptor 4 (TLR4) has been particularly implicated in the systemic pathogenesis of diabetes and its complications (105). TLRs are key PRRs of the innate immune system and activate through recognition of exogenous microbial components termed pathogen associated molecular patterns (PAMPS) (97). Binding PAMPS leads to activation of downstream signaling pathways, ultimately resulting in the release of pro-inflammatory cytokines such as interleukin-6 (IL-6) and tissue necrosis factor alpha (TNF-α) (98). In addition to the PAMPs, TLRs are also activated by a variety of host derived endogenous ligands termed damage associated molecular patterns (DAMPs). These are usually hidden from immune recognition but are exposed by tissue damage alerting the innate immune system to injury (91). The resulting inflammatory response is a physiological mechanism for the recruitment of immune cells and stimulation of the normal process of wound healing (91).

The crucial role of TLR2 and 4 in initiating the early physiological stages of wound healing is recognised, if not fully understood (74). There is evidence to suggest that in the presence of diabetes, the process of TLR2 and 4 activation seems to produce the opposite effect, becoming pathological and impeding wound healing. In animal

studies of induced diabetes, wound healing was significantly improved in TLR2 deficient mice compared to diabetic wild-type animals (122) with the same effect observed in diabetic TLR4 deficient mice (123). Other studies have demonstrated significantly increased TLR2, TLR4 and MyD88 expression in diabetic compared to non-diabetic wounds and suggest that in diabetes, TLR2 and TLR4 mediated pathological inflammation results in an impairment of wound healing.

The effect of hyperglycaemia on the expression, signalling and activation of TLR4 in cells comprising the skin *in vitro* is therefore of particular interest in chronic non-healing wounds, which in the case of diabetic patients is often co-associated with ischaemia.

4.2 Aims

In this chapter we aim to ascertain the effect of increasing glucose concentrations on cultures of human cells present in skin and essential for wound healing. In addition, we will also examine the effect of hypoxia; these simulated diabetic-ischaemic conditions aim to model the local wound environment of diabetic wounds *in vitro*. Specifically, we will examine the effect on the expression, signalling and function of toll-like receptor 4 (TLR4) within these dermal and epidermal cells in these conditions.

4.3 Methods

Normal human dermal fibroblasts from non-ischaemic skin of patients without diabetes were primary cultured as per the protocol outlined in 2.2.1.1. Immortalised HaCat keratinocytes and human microvascular dermal endothelial cells (HMDEC) were purchased (Promocell).

Detailed protocols utilised in this chapter are provided in chapter 2. Briefly, low glucose (LG, 5.5mM) cultured dermal fibroblasts were seeded into 6 well plates (Falcon product code #353046) at a density of 80,000 cells per well. The media was

changed daily and at 90% confluence a low serum media (0.1% FCS) was applied 24 hours before commencing the experiment. The cells were subsequently exposed to media containing glucose concentrations of 0mM to 25mM for 24 hours and included 14.5mM mannitol in low glucose as an osmotic control. Identical plates were simultaneously placed in a hypoxic chamber (Modular Incubator Chamber, MIC-101) with a gas mixture of 20% CO_2 and 80% N_2 for 8 hours.

For subsequent experiments, low glucose cultured fibroblasts were exposed to a very high glucose (VHG, 25mM) media for 24 hours utilising the above described protocol. Various inhibitors were added to the VHG treatment media. A selective TLR4 neutralising antibody (Anti-hTLR4 IgG, Invivogen) and inhibitor (LPS-RS, Invivogen) were used. Identical plates were once again simultaneously placed in a hypoxic chamber.

Protein lysates were prepared from the cultured fibroblasts following completion of the 24 hours of treatment exposure. Fibroblast monolayers were placed on ice and washed with PBS before addition of a 175µl volume of lysis buffer, containing RIPA buffer, protease and phosphatase inhibitors and 2-mercaptoethanol. The lysates were liberated using a cell scraper and agitation through a 23G needle and syringe. The lysates were placed into 1.5ml Eppendorff tubes and centrifuged at 10,000rpm for 4mins at 4°C.

Western blot analysis of protein lysates was undertaken following normalisation of protein concentrations by BCA assay (Thermo-scientific), and densitometric analysis conducted using VisionWorkLS software.

IL-6 concentrations were measured from the supernatants of treated human dermal fibroblasts by ELISA (R&D systems) and analysed using Mithras LB940 microplate reader. All Statistical analyses were performed using GraphPad Prism (GraphPad Software).

A multianalyte ELISArray (Qiagen) was performed according to manufacturer's protocol, allowing simultaneous non-quantitative analysis of 12 pro-inflammatory cytokines. Results were read by microplate reader and normalised to the lowest observed absorbance. Further assessments of IL-8 and TNF-α concentrations in the

supernatants of treated human dermal fibroblasts were measured using ELISAs (R&D Systems).

4.4 Results

4.4.1 Effect of glucose treatments on cell cultures

Preliminary experiments were conducted on all three chosen human dermal and epidermal cell types to determine their ability to survive and proliferate in subsequent experiments.

Primary cultured normal human dermal fibroblasts

Fibroblasts at low passage following primary culture placed in culture media at 0mM glucose concentration did not survive. They did however survive and proliferate after transfer to low glucose (5.5mM) media once passaged 2-3 times in the very high glucose media (25mM) required for successful primary culture. Images seen in figure 4.1 are after 48 hours of culture. This indicated fibroblasts cultured directly from human non-diabetic skin samples are suitable for subsequent analysis.

HaCat Keritinocytes

The Immortalised HaCat keratinocyte cell line did not survive in 0mM glucose conditions. After 48 hours this cell line achieved 90% confluence in culture media at 5.5mM glucose concentration. In very high glucose (25mM) media, cells exceeded 100% confluence and clusters detached.

Human microvascular dermal endothelial cells (HMDEC)

This commercially purchased human cell line was extremely sensitive to low glucose conditions. Cells exhibited in figure 4.4.1 were photographed after 1 week of culture. No glucose (0mM) conditions was fatal for HMDEC cells. Cultures in low glucose (5.5mM) media failed to proliferate, even after 1 week. Cells in very high glucose conditions did not reach 90% confluence at 1 week but demonstrated proliferation over longer time spans. The inhibition of proliferation in low glucose conditions

prohibited further study of this cell line and no further experiments were conducted utilising HMDEC.

Primary cultured human dermal fibroblasts

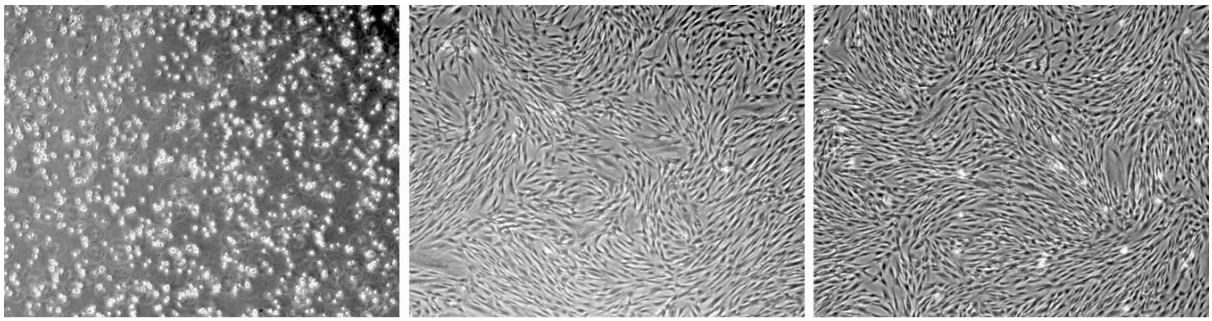

0mM 5.5mM 25mM

HaCat kerintocytes

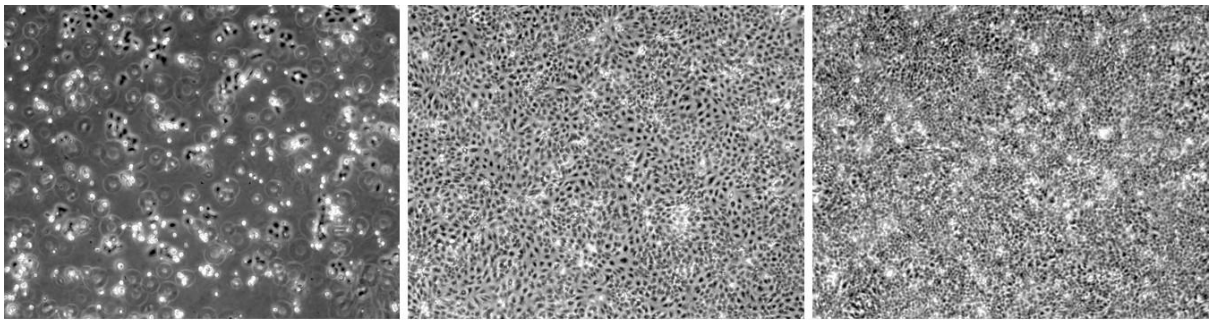

0mM 5.5mM 25mM

HMDEC

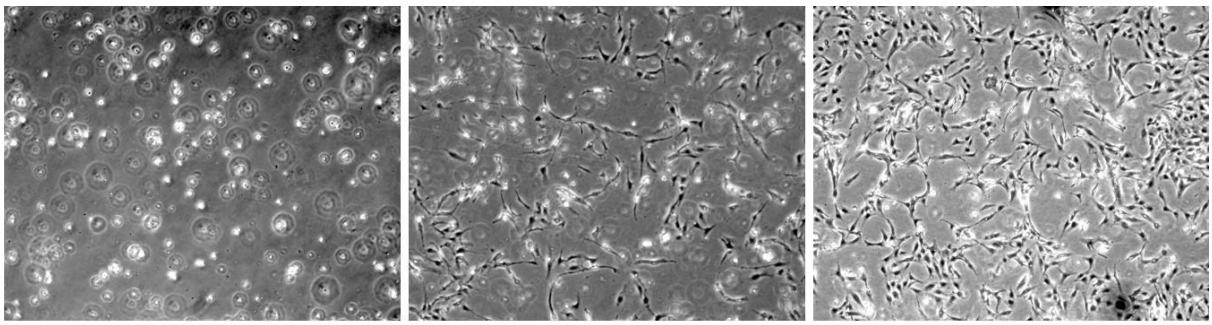

0mM 5.5mM 25mM

Figure 4.4.1 Glucose treatment influences culture success of all three test cell types

Preliminary experiments all conducted in a normoxic environment demonstrated primary cultured fibroblasts could be successfully cultured in low glucose conditions. The proliferation of HaCat cells was also maintained, however this proliferation was not inhibited on attainment of 100% confluence in very high glucose media, raising suspicions of cell differentiation. HMDEC cells did not tolerate low glucose conditions.

4.4.2 Immunocytochemistry

Following primary culture, all fibroblast cell lines were checked for purity and homogeneity culture using immunocytochemistry staining for the Anti-S100A4 fibroblast specific protein (FSP) marker. Suspicions of HaCat cell differentiation were raised given their unregulated growth in very high glucose conditions. Multiple samples of this immortalised keratinocyte cell line were stained for keratin markers using the Pan-CK cocktail antibody.

Fibroblasts

A

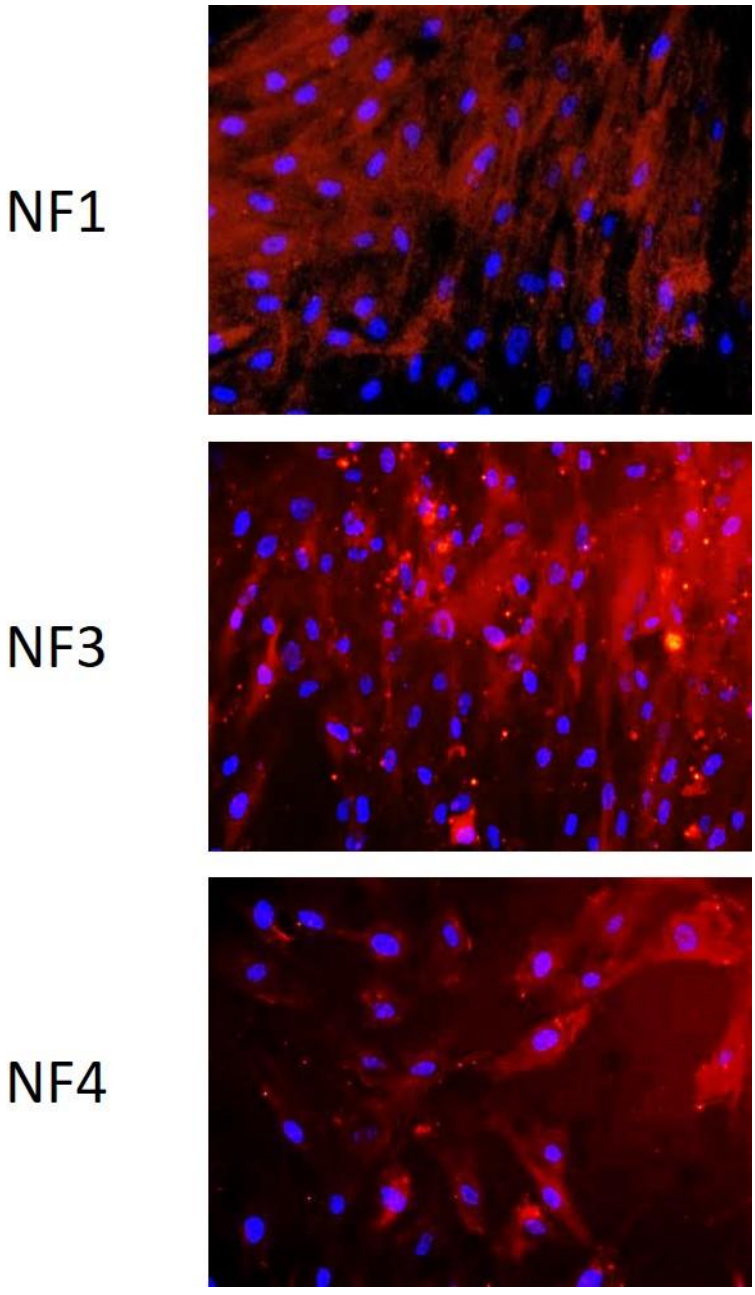

Hacat

B

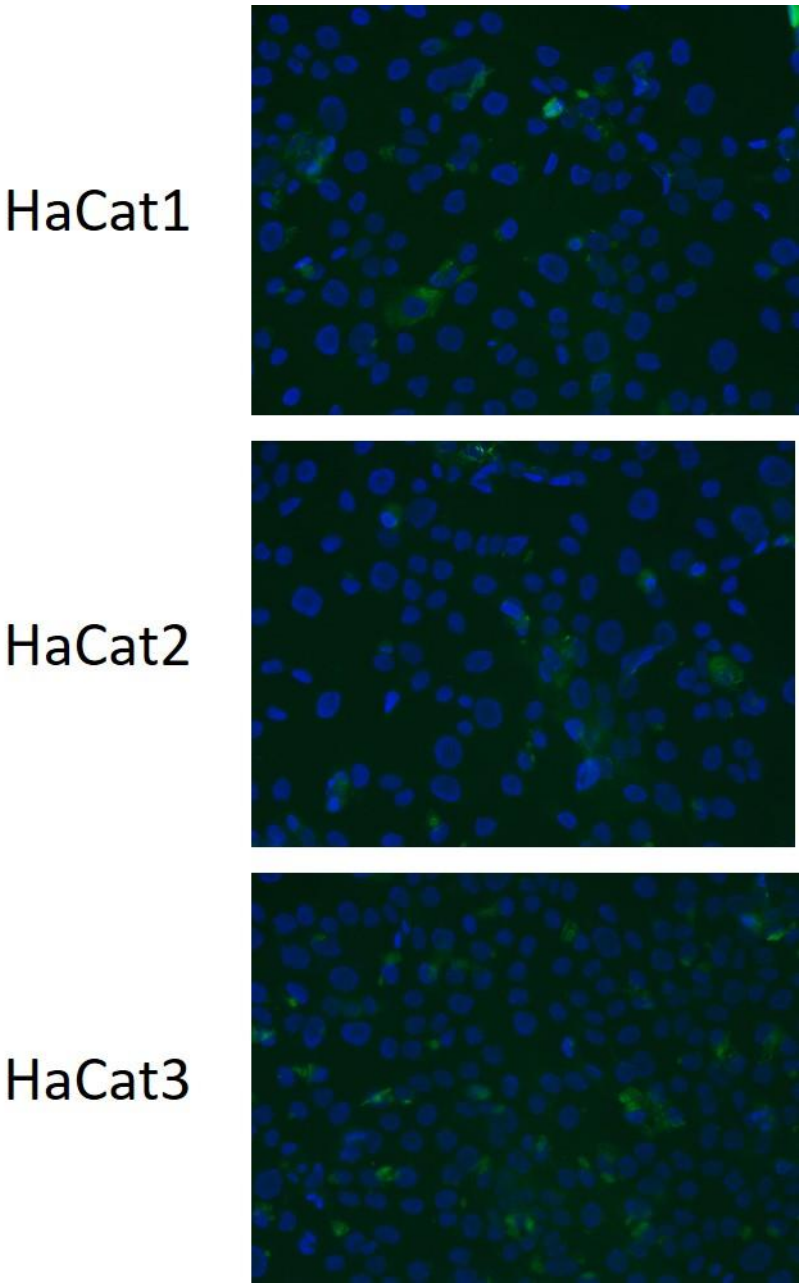

Figure 4.4.2 Immunocytochemistry identification of experimental cell lines

(**A**) Successfully cultured primary cell lines of different donor origin named NF1, NF3 and NF4 all strongly stained positive for FSP indicating a homogenous culture of fibroblasts. (**B**) The samples of HaCat cells, derived from the same initial cell line, demonstrated variable, but generally poor expression of keratin markers. It was concluded the samples could not be used for further experiments.

4.4.3 Effect of glucose concentration on TLR4 protein levels

Increasing concentrations of glucose increased TLR4 protein levels in fibroblasts in a dose response fashion. The addition of 14.5mM mannitol to 5.5mM glucose media as an osmotic control had no significant effect on TLR4 protein levels. The effect on TLR4 is therefore independent of the increased osmotic effect of higher glucose concentrations.

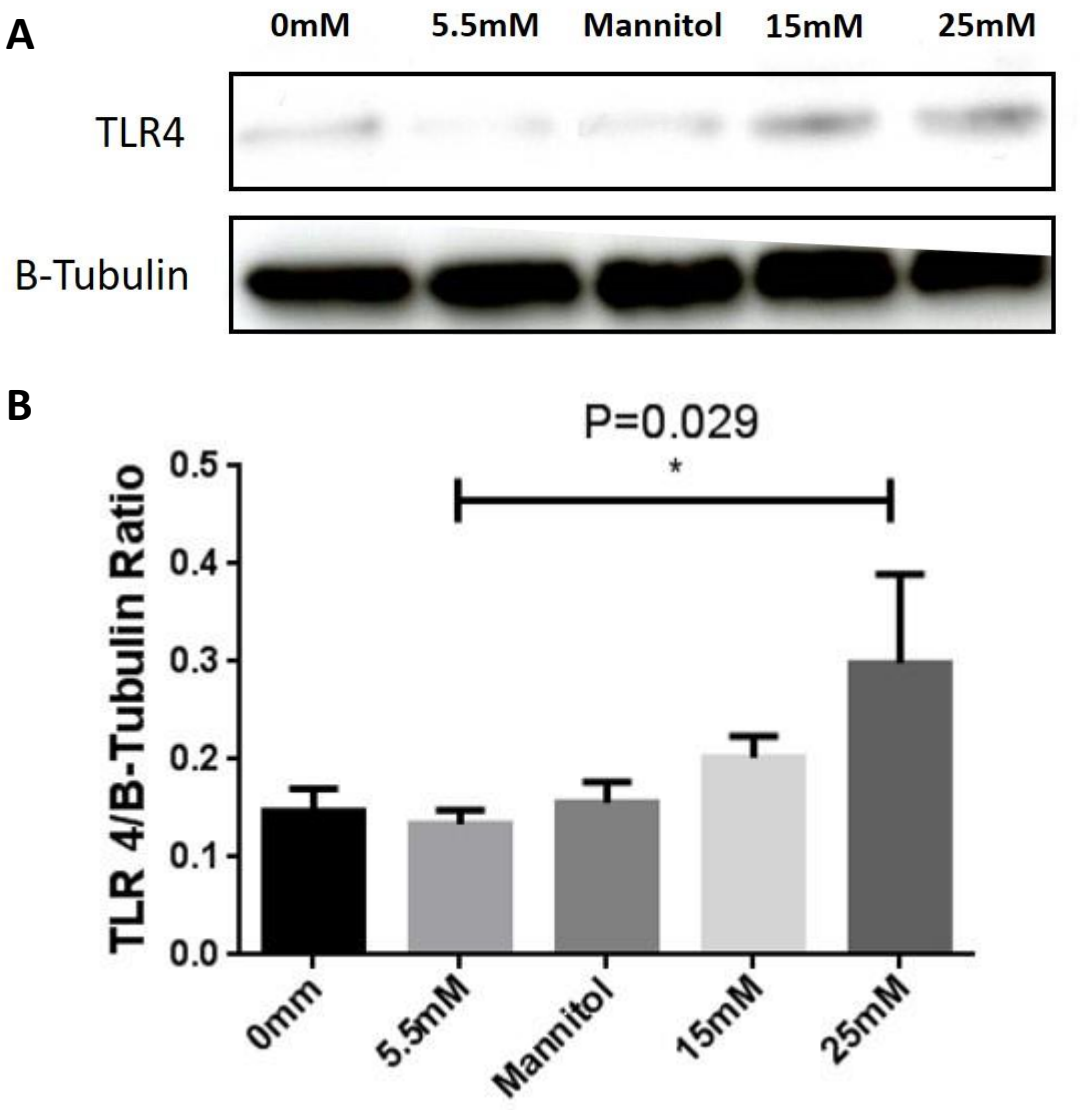

Figure 4.4.3 Dose response relationship between glucose and TLR4 protein levels in fibroblasts

(**A**) Representative western blot analysis demonstrating the effect of increasing glucose concentration on TLR4 protein levels by fibroblasts. (**B**) Densitometric analysis of western blots. (n=9, p=0.029, Mann-Whitney U test).

4.4.4 Glucose dose-exposure time-trial

A dose-time exposure experiment was carried out to determine the optimum duration for the exposure of fibroblasts to very high glucose conditions (25mM) necessary to observe the statistically significant increase in TLR4 protein levels shown in figure 4.4.3.

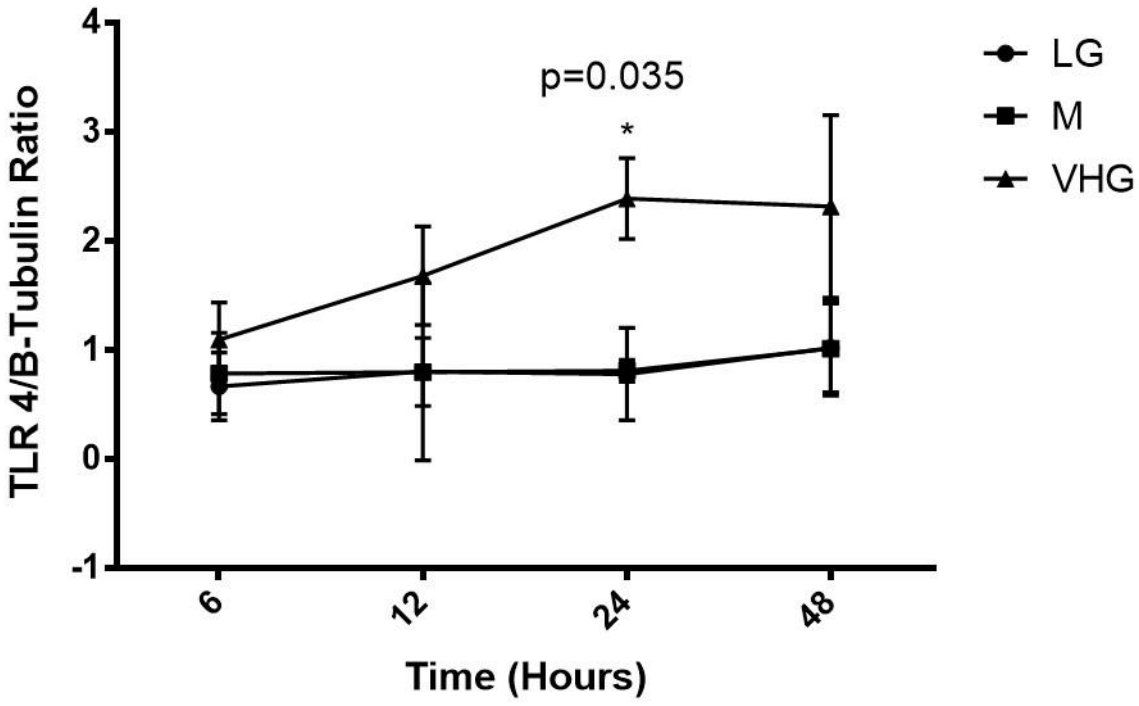

Figure 4.4.4 Effect of very high glucose becomes significant after 24 hours

Densitometric analysis of western blots of TLR4 protein levels after exposure to 5.5mM (LG), 5.5mM and 14.5mM mannitol (M) and 25mM (VHG) at set time points indicated. (n=9, 3 fibroblast cell lines with 3 experimental repeats, *p=0.035, Mann-Whitney U Test).

A time course analysis to determine the optimum duration of exposure to very high glucose (25mM) on TLR4 levels was performed (figure 4.4.4). The difference between the VHG group time points reached significance at 24 hours (p=0.035); Subsequent experiments were conducted for this duration.

4.4.5 The effect of very high glucose and hypoxia on TLR4 protein levels

Comparing the effect of LG (5.5mM) glucose and VHG (25mM) exposure on TLR4 protein levels in nomoxia and hypoxia, hypoxic conditions led to an increase in TLR4 protein expression. This effect was significantly increased (p=0.017) in very high glucose concentrations (25mM).

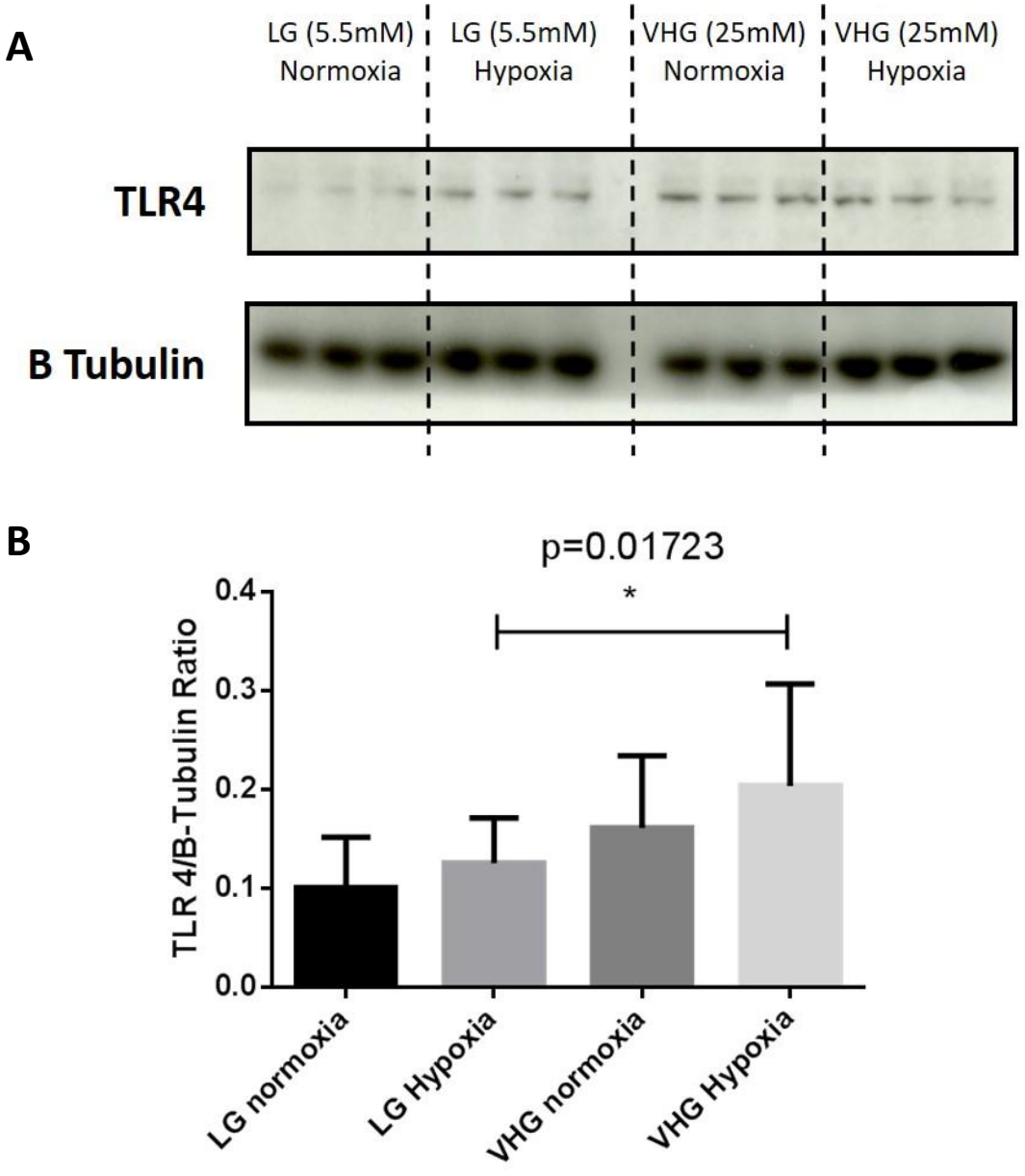

Figure 4.5.5 Effect of LG vs VHG in normoxia and hypoxia on TLR4 protein levels

Figure 4.5.5. (A) Representative Western Blot comparing the effect of LG (5.5mM) glucose and VHG (25mM) exposure in normoxia and hypoxia on expression of TLR4. (**B**). Densitometric analysis of TLR4 expression. (n=9, *p=0.017, Mann-Whitney U test).

4.5.6 The effect of very high glucose and hypoxia on the TLR4 signalling pathway

Hypoxia results in increased TLR4 expression (figure 4.5.5) and signalling and this effect is exaggerated in very high glucose conditions (figure 4.5.6).

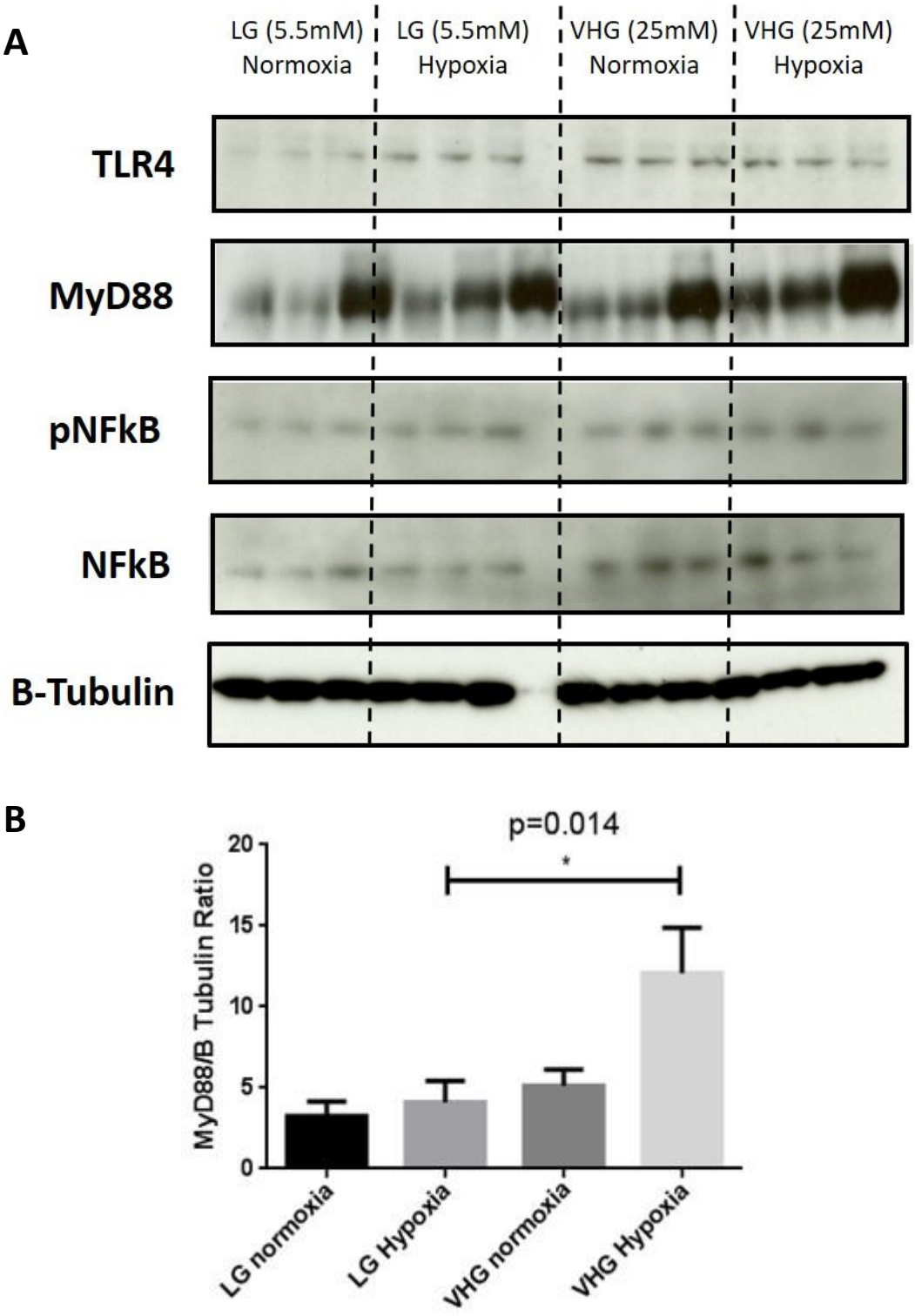

C

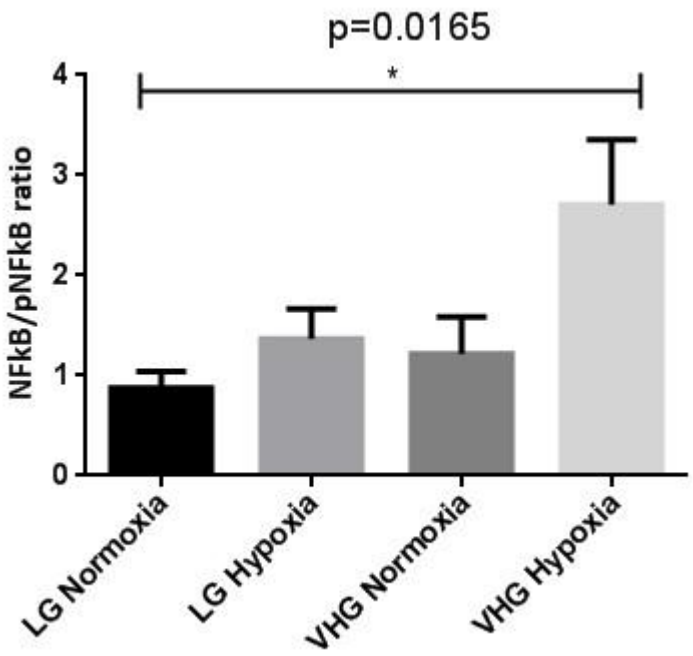

Figure 4.5.6 Effect of LG vs VHG in normoxia and hypoxia on TLR4 signalling pathway

(**A)** Representative Western Blots comparing the effect of LG (5.5mM) and VHG (25mM) exposure in normoxia and hypoxia on expression of TLR4, MyD88, NFkB and phosphorylated NFkB, a marker of NFkB activation. (B) Densitometric analysis of MyD88 expression and (**C**) NFkB activation.

Hypoxic, VHG (25mM) conditions results in increased expression of MyD88 (figure 4.5.6 B) (p=0.014, n=6) and phosphorylation of NFkB (figure 4.5.6 **C**) suggesting increased activation of TLR4 in addition to the observed increase in expression, through the NFkB mediated MYD88 dependent pathway.

4.5.7 The effect of very high glucose and hypoxia on TLR4 endogenous ligands

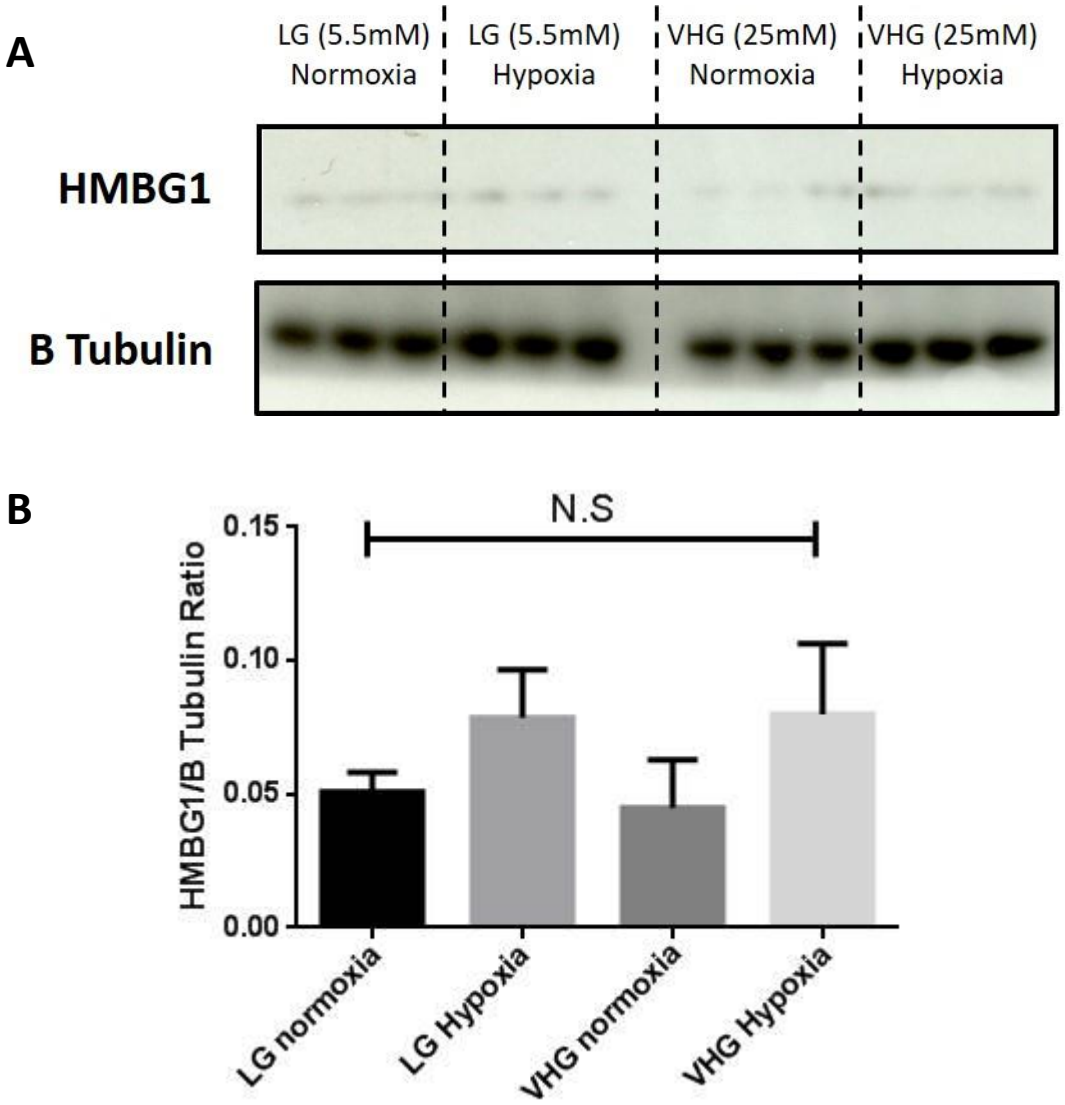

Figure 4.5.7 Effect of LG vs VHG in normoxia and hypoxia on TLR4 endogenous ligand HMBG1

(**A**) Representative Western blots comparing the effect of LG (5,5mM) and VHG (25mM) exposure in normoxia and hypoxia on HMBG1, a potent endogenous ligand of TLR4. (**B**) Densitometric analysis of HMBG1 protein bands.

Results for the comparison of HMBG1 expression between groups did not reach statistical significance (n=6, P= 0.3, Krusal-wallis test). There was a trend towards an increase in HMBG1 release in hypoxia, with a non-significant increase in VHG conditions (figure 4.5.7 B).

4.5.8 The effect of very high glucose and hypoxia on apoptosis and IL-6 release

Hypoxic VHG (25mM) conditions resulted in a significant increase in cell apoptosis represented by cleaved caspase 3 (apoptotic marker) when compared to low glucose (5.5mM) in hypoxia (p=0.0001). The same conditions led to a significantly increased concentration of the pro-inflammatory cytokine IL-6, released into fibroblast supernatant (p=0.043).

A

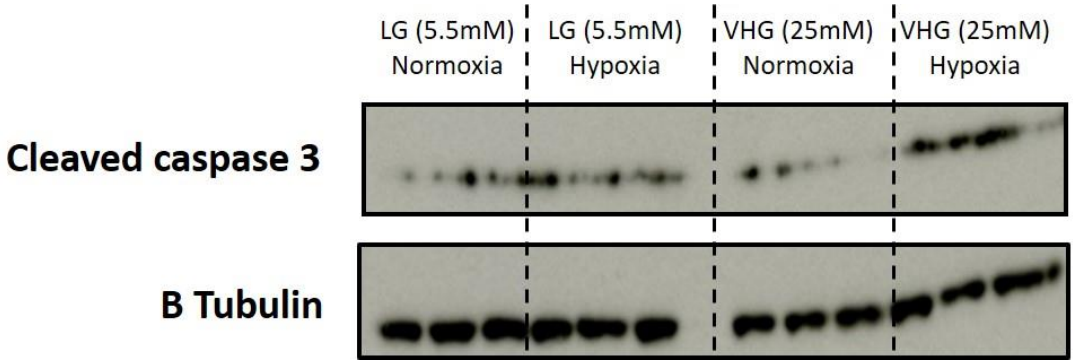

B

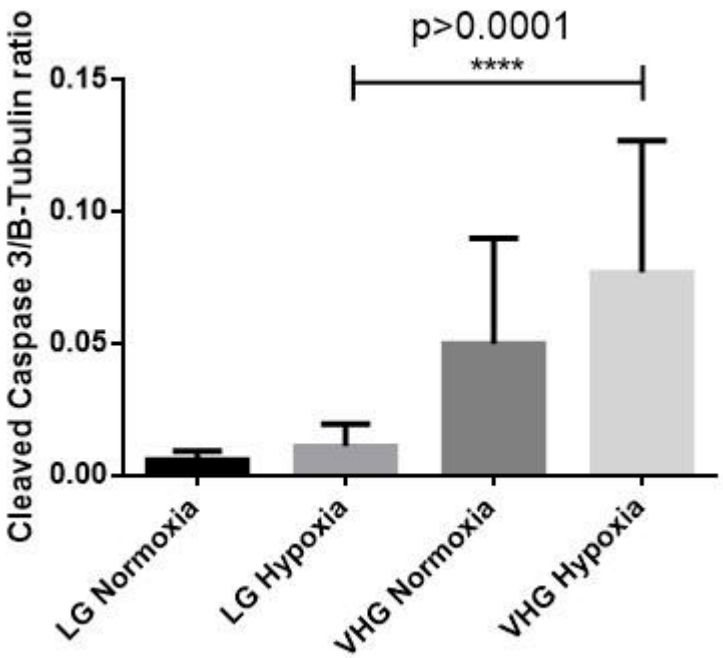

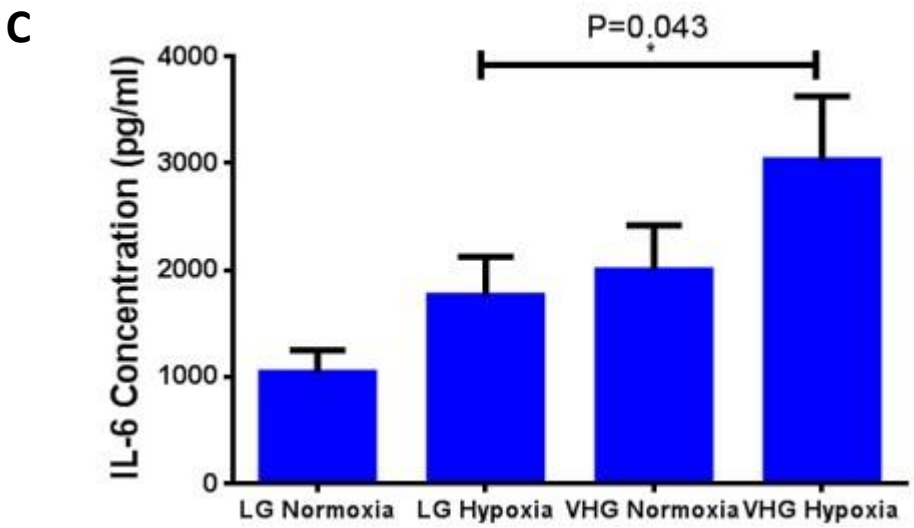

Figure 4.5.8 Effect of LG vs VHG in normoxia and hypoxia on apoptosis and IL-6 release

(**A**) Representative Western Blots comparing the effect of LG (5.5mM) and VHG (25mM) exposure in normoxia and hypoxia on cleaved caspase 3 expression (apoptosis). (**B**) Densitometric analysis of cleaved caspase 3 expression (p=0.0001, n=6 Mann-Whitney U Test) (**C**) IL-6 concentration of cell supernatant samples. VHG conditions resulted in a greater release of IL-6 compared to LG. Hypoxia increased IL-6 release in both LG and VHG conditions. (n = 12, p = 0.043, Mann-Whitney U test).

4.5.9 Effect of TLR4 inhibition in VHG and hypoxia and effect on TLR expression

The use of a specific TLR4 antagonist and neutralising antibody in very high glucose hypoxic conditions resulted in a significant decrease in TLR4 protein expression (p=0.003). There was a corresponding increase in TLR2 expression observed.

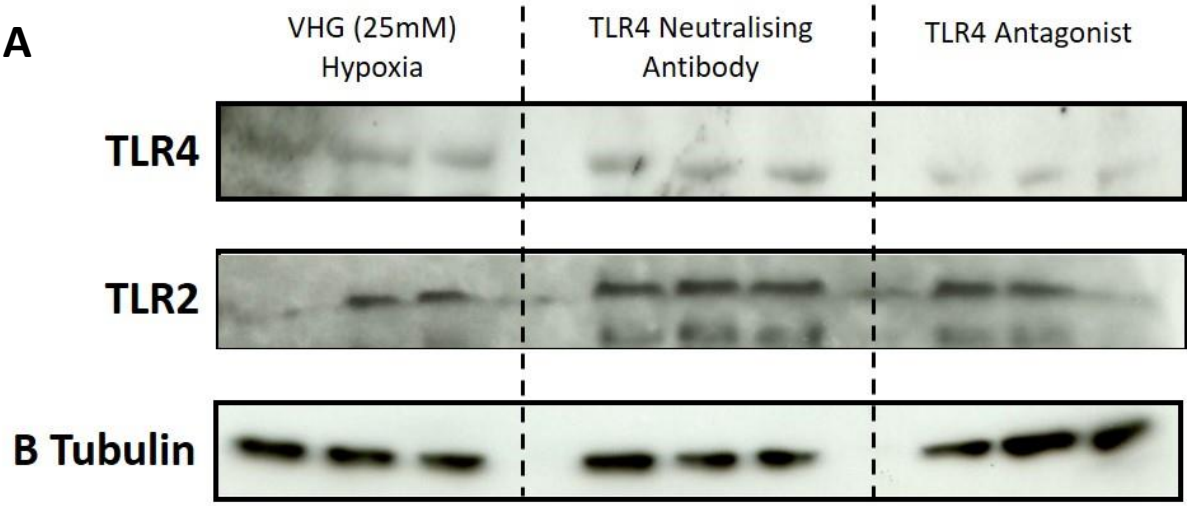

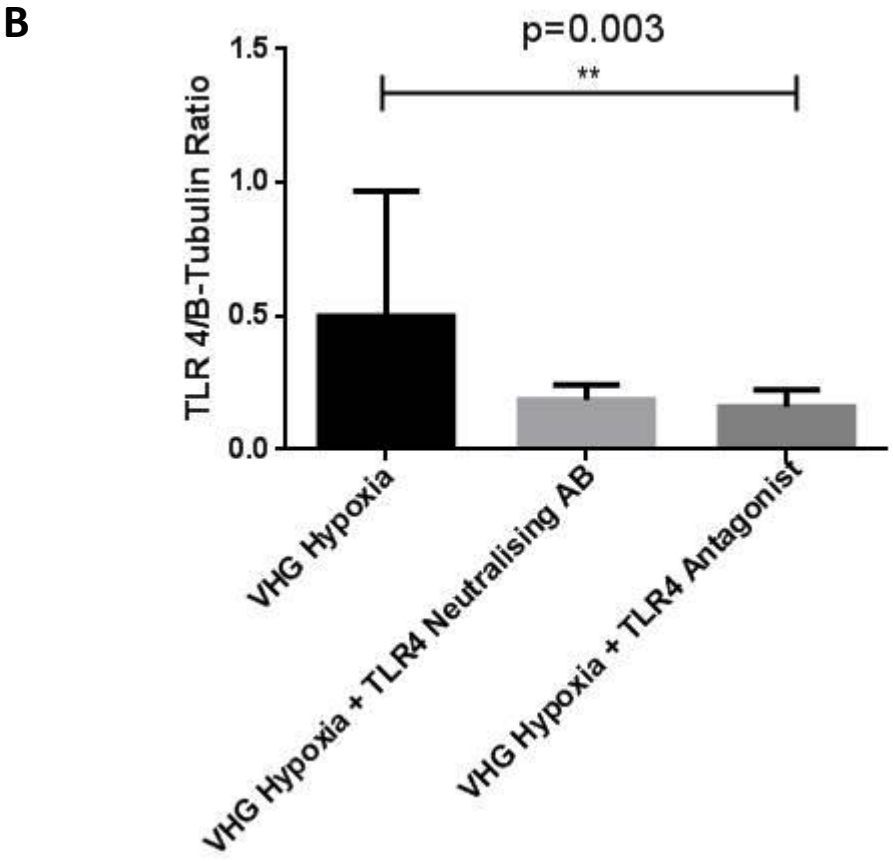

Figure 4.5.9 Effect of TLR4 inhibitors in VHG and hypoxia on TLR4 protein expression

(**A**) Representative Western Blots comparing VHG vs. VHG + specific inhibitor treatment in hypoxic conditions on TLR4 and TLR2. (**B**). Densitometric analysis of TLR4 (**p=0.003, n=9 Kruskal-Wallis test).

4.5.10 Effect of TLR4 inhibition in VHG and hypoxia and effect on TLR4 endogenous ligands

HMBG1 is a potent endogenous ligand of TLR4. An increase in the protein expression of HMBG1 was observed in response to a very high glucose hypoxic environment seen in figure 4.5.7 when compared to low glucose and normoxic conditions. The addition of TLR4 antagonists results in significant decrease in HMBG1 expression by fibroblasts in hyperglycaemic hypoxic conditions (p=0.025).

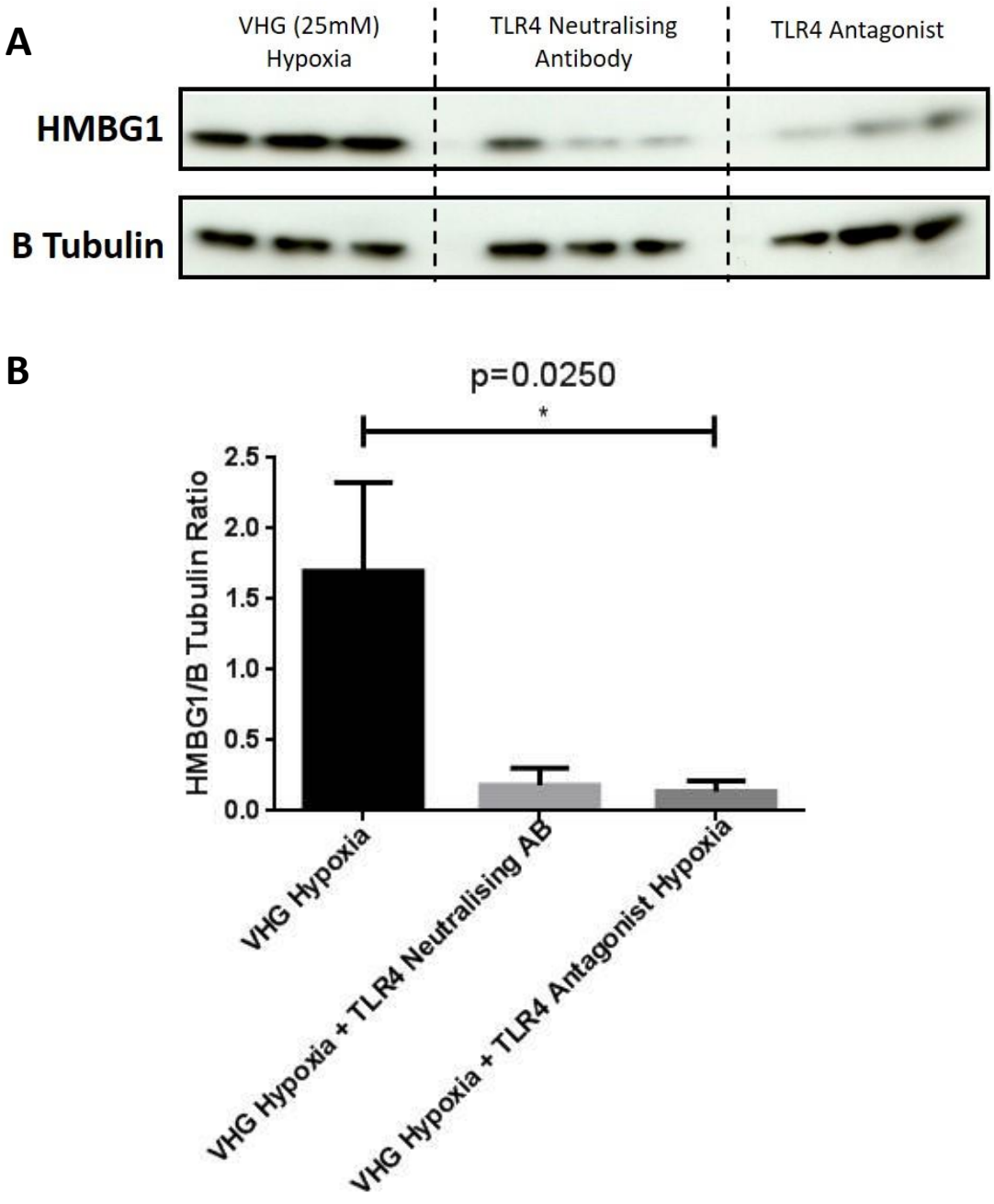

Figure 4.5.10 Effect of TLR4 inhibitors in VHG and hypoxia on TLR4 endogenous ligand HMBG1

(**A**) Representative Western Blots comparing VHG vs. VHG + specific inhibitor treatment in hypoxic conditions on HMBG1. (**B**) Densitometric analysis of HMBG1. The use of TLR4 inhibitors in VHG and hypoxia resulted in a significant decrease in HMBG1 release, a potent TLR4 endogenous ligand (n= 6, p=0.025 Kruskal-Wallis test).

4.5.11 Effect of TLR4 inhibition in VHG and hypoxia and effect on apoptosis and IL-6

An increase in cellular apoptosis through cleaved caspase 3 was observed in a very high glucose (25mM) hypoxic environment (figure 4.5.8). The addition of TLR4 inhibitors resulted in a significant decrease in cell apoptosis in these same conditions (p=0.003). IL-6 release was also significantly decreased by the selective antagonism of TLR4.

A

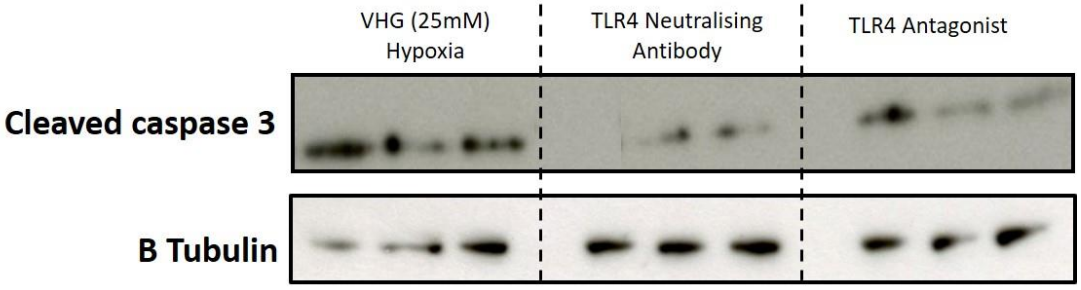

B

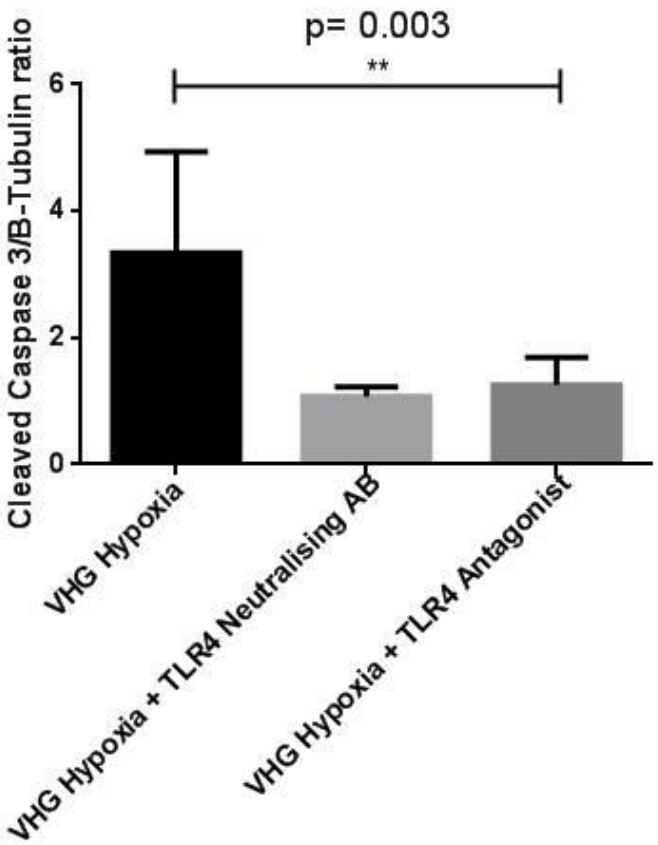

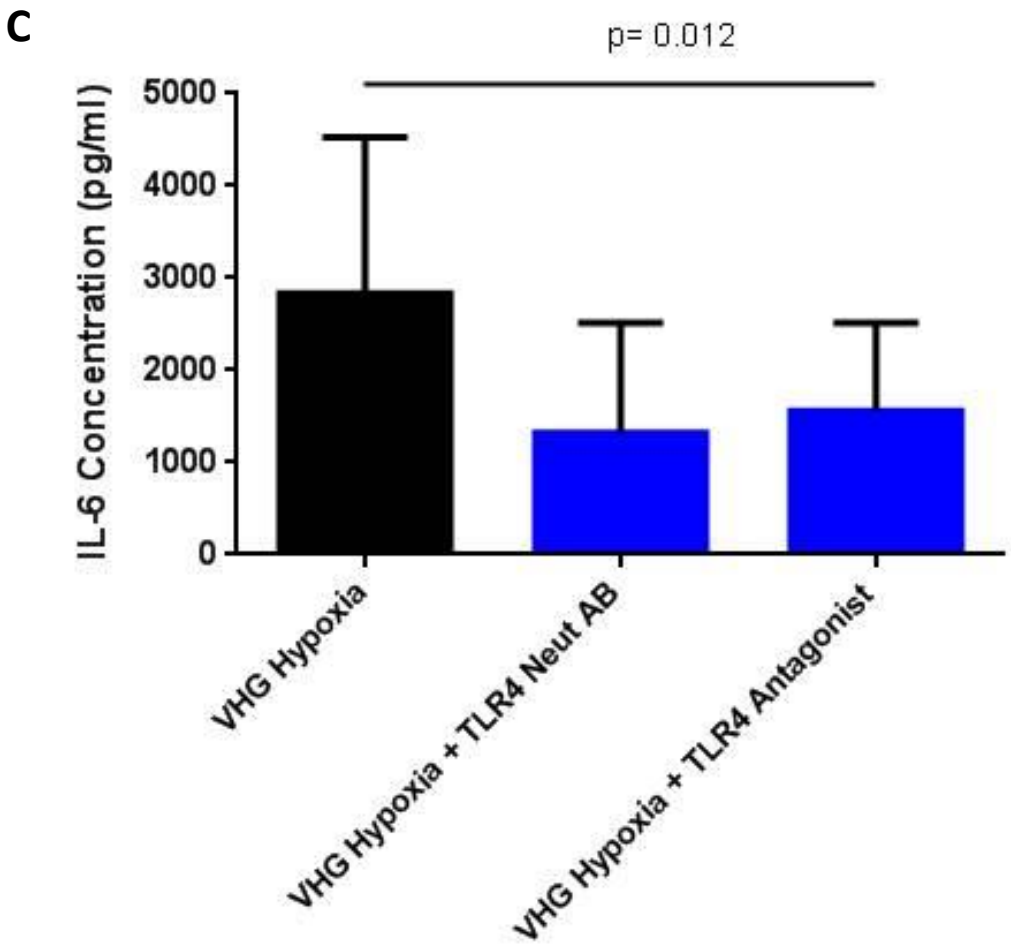

Figure 4.5.11 Effect of TLR4 inhibitors in VHG and hypoxia on apoptosis and IL-6 release

(**A**) Representative Western Blots comparing VHG vs. VHG + specific inhibitor treatment in hypoxic conditions on cleaved caspase 3 expression. (**B**) Densitometric analysis of cleaved caspase 3 expression. (**C**) IL-6 concentration of cell supernatant samples. TLR4 inhibition resulted in a significant reduction in the release of IL-6, ameliorating the inflammatory effect of hyperglycaemia + hypoxia. (n= 11, Kruskal-Wallis test).

4.5.12 Multi-analyte ELISArray

To determine the spectrum and quantity of inflammatory cytokines released by cultured human dermal fibroblasts into the supernatant, a multi-analyte ELISArray kit was used initially which allowed simultaneous analysis of 12 pro-inflammatory cytokines: IL1α, IL1β, IL2, IL4, IL6, IL8, IL10, IL12, IL17A, IFN-γ, TNF-α, GM-CSF.

The NF1, NF3 and NF4 primary cultured cell lines were utilised, and strongly demonstrated fibroblast production of IL-6 and IL-8 and to a lesser degree GM-CSF. TNF-α was not detected by this ELISArray. Values presented are relative values and not concentrations.

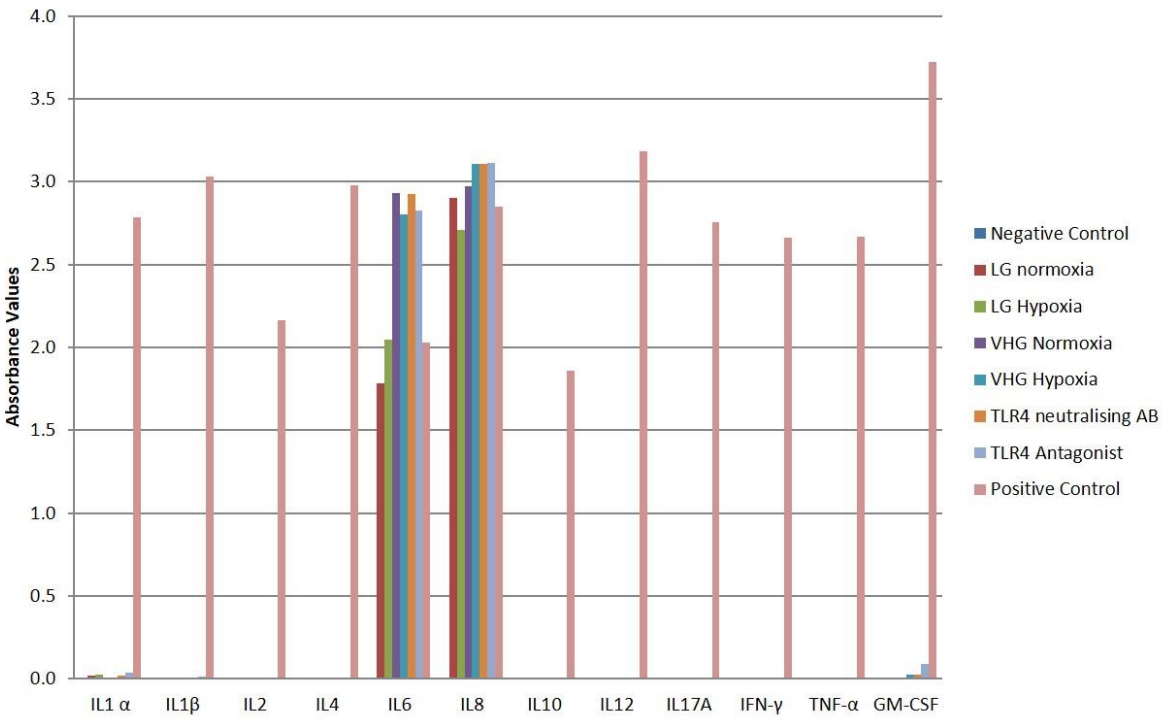

Figure 4.5.12 Multicytokine ELISA array for pro-inflammatory cytokines

This assay is not quantitative but indicates IL-6 and IL8 are produced to the greatest degree by our fibroblast population across the whole range of test environments.

4.5.13 IL-8 and TNF-α ELISA

The multi-analyte inflammatory cytokine array presented in 4.5.12 demonstrated IL-8 release by fibroblasts in addition to IL-6. Individual IL-8 enzyme-linked immunosorbent assay (ELISA) examination allowed for quantitative comparison of cytokine release. A TNF-α ELISA was also conducted due to the known association between TLR4 activation and TNF-α release. No significant difference between glucose concentration and the presence/absence of hypoxia was seen.

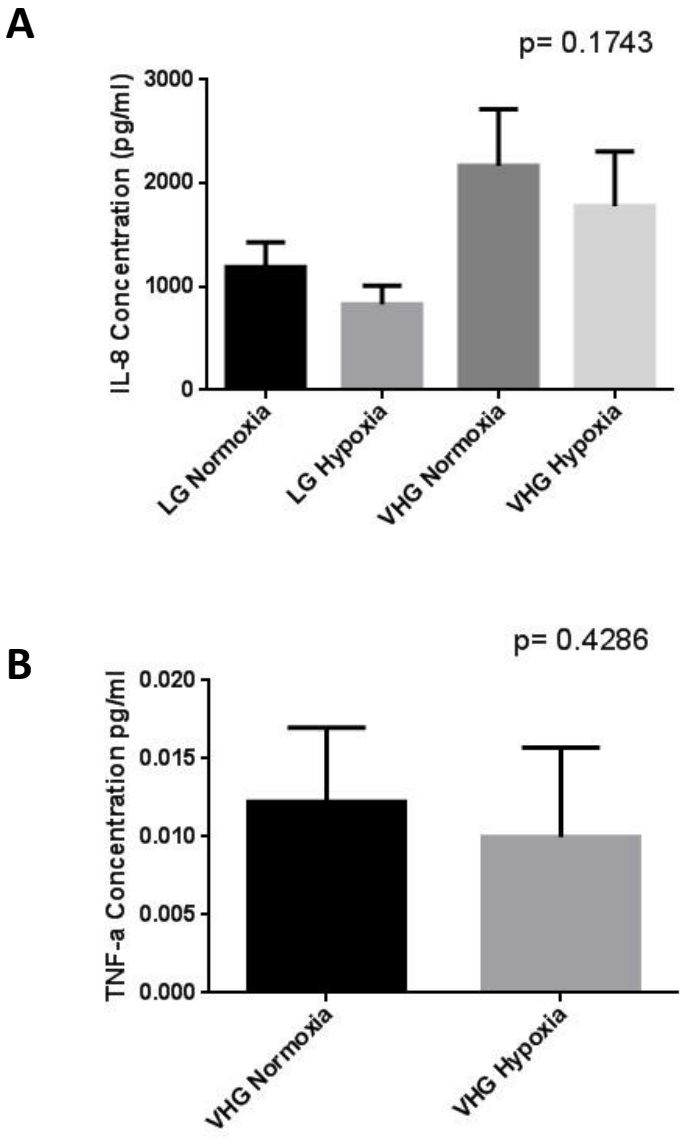

Figure 4.5.13 IL-8 and TNF-α concentration in fibroblast supernatant

There was no significant difference in the release of IL-8 (**A**) (p=0.17, n=6 Kruskal-Wallis test) or TNF- α (**B**) between treatment groups observed (n=6, p= 0.43 Mann-Whitney test).

4.5 Discussion

Three cell types found in the dermis and epidermis of the skin were initially identified for examination in this study. Human microvascular dermal endothelial cells (HMDEC) were very sensitive to low glucose conditions, with complete arresting of proliferation observed. The 'low glucose' concentration utilised in this *in vitro* model is physiological, corresponding to a value of 5.5mM and within the normal non-diabetic human glucose homeostatic range. It is therefore likely the difficulty in utilising HMDEC cells is an artefact of the *in vitro* process.

Given the high degree to which TLR4 is expressed by endothelial cells, and the implication in the development of diabetic macro and microvascular complications of abnormal TLR4 mediated endothelial inflammation, further study is necessary. It may be possible for this methodology to be adapted successfully by comparing very high glucose (25mM) and ultra-high glucose (>35mM) concentrations.

The HaCat immortalised keratinocyte cell line was used to model epidermal cells. Suspicions regarding the suitability of the available cell samples, particularly abnormal proliferation and failure to adequately express keratinocyte markers led to the decision not to pursue further experiments with this cell line. Primary culture of keratinocytes from human donor skin samples is possible but precluded by time constraints in this project. Like HMDEC cells, keratinocytes highly express TLR4, and given the importance of the re-epithelialisation process in wound healing, warrant further study.

From our data, increasing concentrations of glucose increased TLR4 protein levels in a dose response fashion in fibroblasts (figure 4.5.3). Very high glucose conditions (VHG, 25mM) significantly increased TLR4 protein levels compared to physiological 'low glucose' (LG, 5.5mM) conditions (Figure 4.5.3 **B**). The addition of 14.5mM mannitol to 5.5mM glucose media as an osmotic control had no significant effect on TLR4 protein expression, indicating this effect is not driven by the increased osmotic potential of higher glucose concentrations. A similar effect on TLR4 gene expression has been observed in gingival fibroblasts (135) , monocytes (134) and adipocytes (164). In accordance with these other published studies which utilised a similar

methodology on different cell types, our data indicated 24 hours of very high glucose exposure is sufficient for a clear biological difference to be observed (134, 135, 164).

The exposure of dermal fibroblasts to very high glucose and hypoxic conditions led to an increase in TLR4 protein levels (figure 4.5.5). MyD88 is a crucial adaptor molecule recruited to the intracellular domain of TLR4 following activation and NFkB is an essential nuclear transcription factor in the production of pro-inflammatory cytokines such as IL-6. In addition to TLR4 upregulation, there was an observed increase in MyD88, NFkB phosphorylation and IL-6 release. This suggests very high glucose and hypoxic conditions lead to an increase in TLR4 activation and signalling through the MYD88 dependant NFkB pathway, resulting in a significant increase in pro-inflammatory cytokine (IL-6) release. A significant increase in apoptosis and a trend towards an increased release of HMBG1, a potent endogenous ligand of TLR4, was also observed, offering a possible mechanism for the increased expression and activation of TLR4.

To examine further the effect of very high glucose and hypoxic conditions on TLR4 activation and signalling, a specific TLR4 neutralising antibody and an antagonist were utilised. TLR4 inhibition resulted in a significant reduction in TLR4 protein expression (figure 4.5.9 **A**). There was a corresponding increase in TLR2 protein expression in the TLR4 antagonist groups (figure 4.5.9 **A**). There is considerable co-activation and cross-talk between TLR4 and TLR2 via NFkB (165), and compensatory upregulation of TLR2 has been reported in TLR4 knockout mice and in human adipocytes ((166, 167).

Selective blocking of TLR4 mediated pathways in VHG-hypoxic conditions led to a significant reduction in IL-6 release, apoptosis and release of HMGB1. These findings suggest the harmful pro-inflammatory effects of simulated high glucose hypoxic conditions are ameliorated by inhibition of TLR4.

The range of inflammatory cytokines released by our primary cultured cell lines are consistent with other published studies, observing IL-6 and IL-8 as commonly associated inflammatory cytokines (168, 169). It is surprising this data did not show an association between IL-8 and TNF-α release and very high glucose hypoxic

conditions, as both cytokines are associated with TLR4 activation, like IL-6 (170, 171). An explanation for this discrepancy may be down to lack of experimental repeats due to cost constraints, and further examination is desirable.

It has been demonstrated by other groups that high glucose results in an increase in TLR4 mediated inflammation, however the novel observation from these results is the effect of adding a second noxious variable, hypoxia. Data from others in this research group have demonstrated hypoxia induces TLR2, 4 and 6 expression and activation in skeletal muscle (97, 172).

These results in dermal fibroblasts suggest this effect is significantly exaggerated by concurrent exposure to high glucose. This inflammatory effect signals and actions via the TLR4 MYD88 dependant pathway, and as previously described leads to increased and excessive inflammation via downstream production of cytokines such as IL-6.

In clinical situations of chronic non-healing diabetic-ischaemic ulceration, it is possible to see the consequences of this dysregulated process. The release of pro-inflammatory cytokines via TLR4 activation, and the subsequent recruitment of the innate immune cellular response results in tissue damage and cellular apoptosis and the release of damage associated molecular patterns (DAMPS) such as HMGB1. These DAMPS act as potent ligands for TLR4 activation, resulting in the release of further pro-inflammatory cytokines, perpetuating a dysregulated positive feedback cycle of tissue damage-inflammation-tissue damage.

The aim of this chapter was to model the local wound environment of a chronic diabetic-ischaemic wound, however there have not been any direct physiological studies of wound fluid/environment measuring these *in-vivo* conditions. Studies of chronic venous wounds demonstrated a significant reduction in wound glucose concentration compared to serum, however these were non-diabetic subjects (173). For the purposes of this study therefore, the assumption was tissue glucose concentration was equal to that of serum concentration. PAD has been shown to significantly decrease the tissue oxygen levels (174) and increase carbon dioxide (CO_2) levels (175) in skin measured at the foot compared to normal control subjects.

The hypoxia protocol utilised for these *in-vitro* experiments has been shown to model reduced tissue oxygen and increased CO_2 levels (132).

4.6 Summary

Very high glucose culture media lead to an increase in TLR4 protein expression in human dermal fibroblasts. Simulated diabetic-ischaemic conditions resulted in a significant increase in TLR4 protein expression, signalling through the MyD88 adaptor pathway and activation of NFkB, with corresponding increase in pro-inflammatory cytokine (IL-6) release. This resulted in increased cellular apoptosis and release of endogenous TLR4 ligands. Inhibition of TLR4 ameliorated the pro-inflammatory effect of very high glucose hypoxic conditions with a reduction in TLR4 expression, apoptosis, endogenous ligand and IL-6 release. There can be little doubt diabetes is an innate immune induced pro-inflammatory condition, however in addition there appears to be a synergistic effect between this innate inflammatory reaction to high glucose, and hypoxia.

Chapter 5

Effect of hyperglycaemia, ischaemia and TLR4 on cell function *in vitro*

5.1 Introduction

Dermal fibroblasts are essential cellular components of the normal process of skin wound healing through the production of extracellular matrix comprised of collagen, glycosaminosglycans, proteoglycans, fibronectin and elastin essential for the development of granulation tissue. In addition they undergo the crucial functional processes of proliferation, migration and differentiation into contractile myofibroblasts in response to tissue injury (176).

Fibroblasts are the most important cellular constituent of connective tissues and maintain skin homeostasis through a balance between proliferation and differentiation (177). Following tissue damage, growth factors such as platelet derived growth factor (PDGF) and tissue transforming growth factor β1 (TGF-β1) stimulate fibroblast proliferation and migration into the wound (178). Fibroblast proliferation characterises the proliferative phase of wound healing. During this phase fibroblasts rapidly produce extracellular matrix (ECM) which provides the matrix framework for the formation of granulation tissue (179).

In response to tissue injury, fibroblasts migrate from the surrounding undamaged dermal tissues (180). Chemoattractant signals released by platelets and macrophages located in the newly formed fibrin clot direct fibroblasts towards the site of injury (181). It has been observed that fibroblasts migrate in an ordered fashion along the fibronectin structures of the extracellular matrix using specific fibronectin binding integrins (182). The stimulus for fibroblast migration results in a

down-regulation and internalisation of desmosomes that tightly link fibroblasts to adjacent extra cellular matrix proteins allowing migration, although this mechanism is poorly understood (183).

Contraction is another important tissue property that occurs during the proliferative phase of wound healing (184). As mentioned above, fibroblast proliferation and ECM production leads to the formation of early granulation tissue and within granulation tissue fibroblasts undergo differentiation to myofibroblasts, under the influence of transforming growth factor β (TGF-β) (177, 185). A combination of fibroblast traction and myofibroblast contraction then acts to reduce the wound area size (186). Myofibroblasts, like fibroblasts also secrete extra cellular matrix proteins (184).

Many of these essential processes are impaired in fibroblasts taken from diabetic human donors (187). Fibroblasts isolated from diabetics demonstrated reduced proliferation capacity compared to non-diabetics. This effect persisted even when both cell groups were cultured in high glucose media, implying a pre-existing phenotypic change to the cell cultured from diabetic donors (187).

Likewise, cardiac fibroblasts isolated from diabetic rats exhibited a greater contractile property than non-diabetic controls, this was associated with an increased expression of α smooth muscle actin (αSMA) suggesting differentiation to a myofibroblast phenotype (188). Studies of fibroblasts cultured from diabetic db/db mice were compared to wild-type and exhibited significantly impaired migration, in both normoxia and hypoxia (189).

5.2 Aims

The aim of this chapter was to assess the consequences of very high glucose and hypoxia on important functional abilities of fibroblasts, essential to the wound healing process. Proliferative capacity, contraction and migratory potential will be investigated. Given the importance of TLR4 in wound healing, the role of TLR4 was explored through selective inhibition and its consequences on the functional properties of the cells.

5.3 Methods

Methodologies are explained in more detail in chapter 2, sections 2.2.7, 2.2.8, 2.2.9 and 2.2.10.1.

Cell proliferation was measured via the crystal violet assay: fibroblasts were seeded into 96 well plates after re-suspension in either low glucose (5.5mM) or very high glucose (25mM) media, and subsequently cultured for 24 hours. Simultaneously, duplicate plates were placed in a hypoxic chamber. Crystal violet dissolved in 20% methanol was added to each well for 10 minutes, after which the solution was aspirated, and wells washed and air dried. DNA-crystal binding was then measured by microplate reader after re-constitution with acetic acid.

Collagen gels containing collagen, HEPES, DMEM media at variable glucose concentrations and suspended trypsinised fibroblast cells were created and added to pre-BSA coated 24 well plates. Inhibitors were added to media at very high glucose concentrations. After polymerisation a further 1ml of media was added to each well to float the gels. Duplicate plates were simultaneously placed within a hypoxic chamber. After 24 hours contraction was measured by gel weight.

Scratch migration assay was performed by seeding low glucose cultured dermal fibroblasts into 24 well plates, culturing to 90% confluence and inflicting a standardised scratch wound. Following PBS wash, treatment media at glucose concentrations of 5.5mM, 25mM and 25mM with inhibitors, were added in addition to 0.1% mM mitomycin c as a proliferation inhibitor. Duplicate plates were placed in a hypoxic chamber for 24 hours as previously described. Fibroblast migration was assessed via camera microscopy and percentage migration measured using a visual optical method.

5.4 Results

5.4.1 Crystal violet proliferation assay

The effect of variable glucose concentrations in a normoxic and hypoxic environment on fibroblast proliferation was measured via crystal violet assay. There was a significant increase in fibroblast proliferation between very high glucose and low glucose control groups in normoxic conditions (p=0.0002), however no difference was observed in hypoxia (figure 5.4.3). In very high glucose media, fibroblasts subjected to hypoxia demonstrated significantly reduced proliferation compared to normoxia (p=0.01). There was no statistically significant difference between normoxia and hypoxia in low glucose treatment groups (figure 5.4.3).

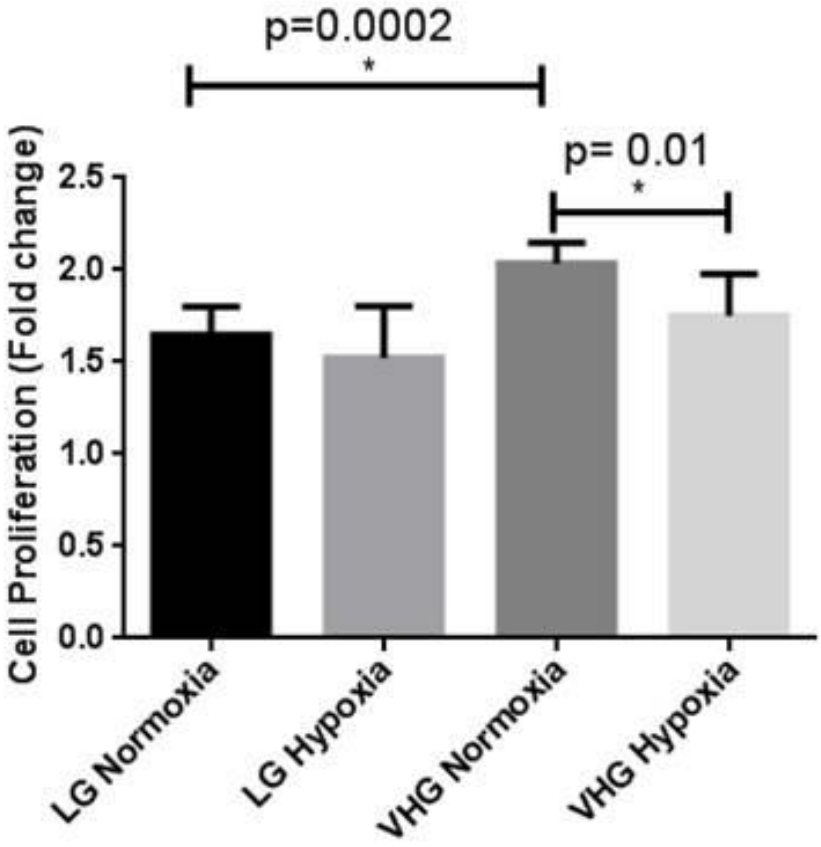

Figure 5.4.1 Effect of simulated hyperglycaemia and ischaemia on fibroblast proliferation

Fibroblasts subjected to very high glucose demonstrated a greater proliferative response compared to low glucose in normoxia (p=0.0002, n=32 Mann-Whitney test). In very high

glucose conditions, simulated ischaemia inhibited fibroblast proliferation ($p=0.01$, $n=32$ Mann-Whitney test). This effect was not seen in normoxia.

5.4.2 Gel contraction assay

Gel contraction assay analysis of fibroblast contraction was performed using all three primary cell lines, comparing contraction between normoxic and hypoxic conditions in low glucose and very high glucose media. Gels in hypoxic environments demonstrated an increase in contraction compared to normoxia, in both low glucose or very high glucose groups, however these differences did not reach statistical significance (figure 5.4.2 **A** and **B**). Comparison of gel contraction between low and high glucose groups in normoxia suggested a trend towards impaired contraction in very high glucose, however this did not reach significance (figure 5.4.2 **D**). There was a significant difference observed however when comparing differences across all groups (figure 5.4.2 **B**).

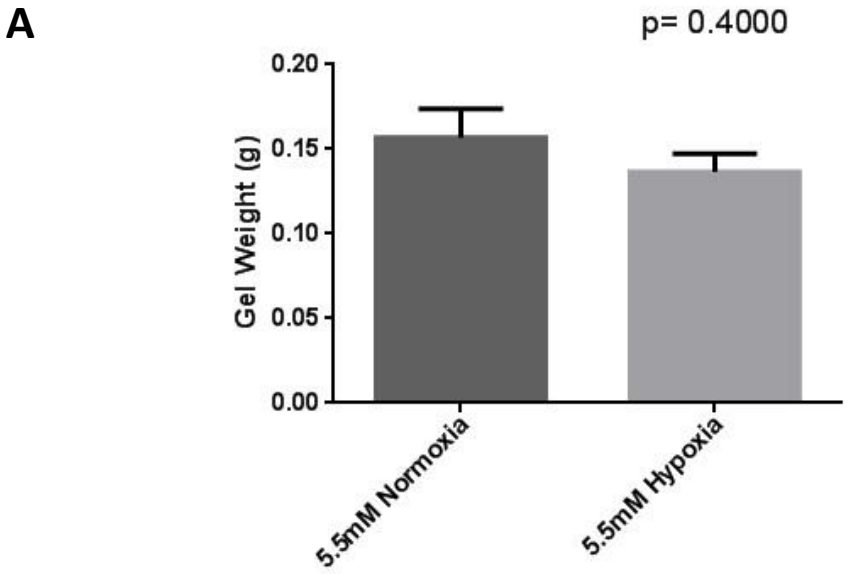

B

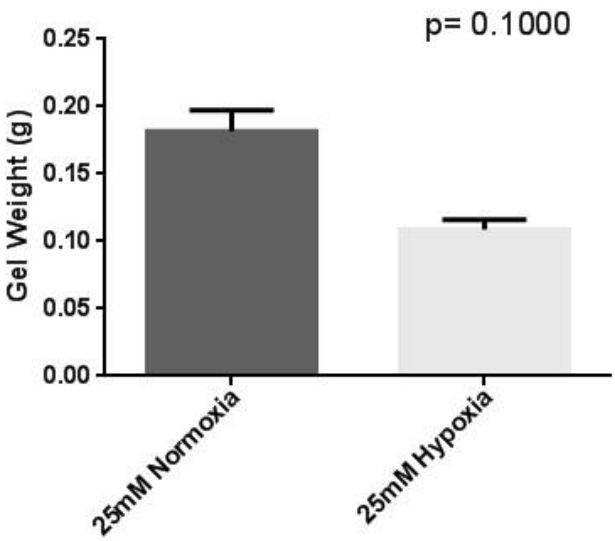
p= 0.1000
Gel Weight (g)
0.25
0.20
0.15
0.10
0.05
0.00
25mM Normoxia
25mM Hypoxia

C

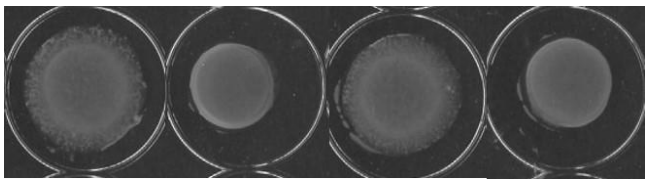

D

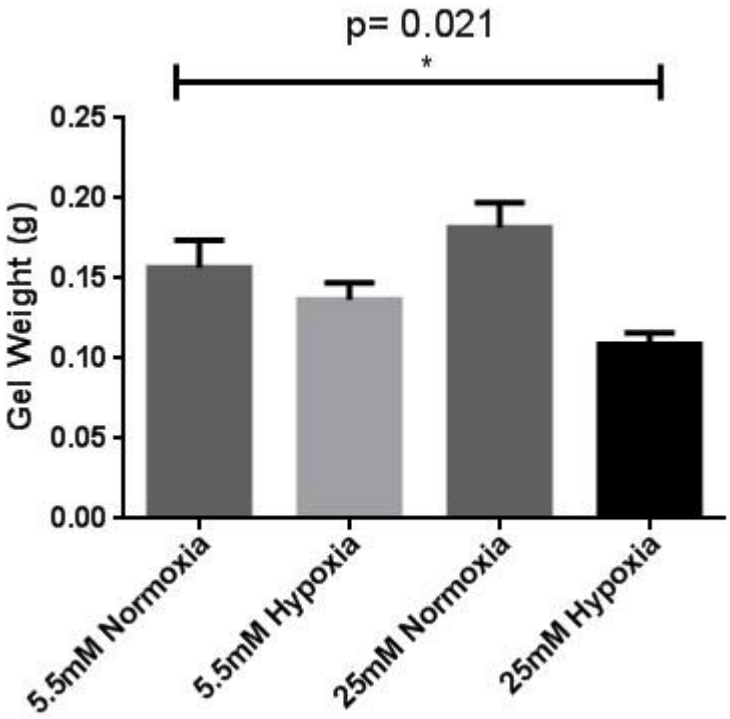
p= 0.021
*
Gel Weight (g)
0.25
0.20
0.15
0.10
0.05
0.00
5.5mM Normoxia
5.5mM Hypoxia
25mM Normoxia
25mM Hypoxia

Figure 5.4.2 Effect of LG vs VHG in normoxia and hypoxia on fibroblast contraction

Gel contraction assay comparing fibroblast contraction in low glucose (5.5mM) and very high glucose (25mM) conditions, with and without hypoxia. There was no significant difference observed when directly comparing normoxia and hypoxia in either low glucose (**A**) or very high glucose (**B**) conditions p=0.4 and p=0.1 respectively (n=9 Mann-Whitney test). (**C**) Representative scan of collagen gels, corresponding to treatment groups, labelled in (**D**). Kruskal-Wallis test analysis demonstrated a significant difference across all the treatment groups (p= 0.021, n= 9) (**D**).

5.4.3 Effect of TLR4 pathway inhibition on fibroblast gel contraction

To determine the effect of TLR4 inhibition on fibroblast contraction, a specific TLR4 neutralising antibody and antagonist were added to very high glucose treatment media. There was no significant difference in contraction in either normoxia or hypoxia (p=0.086). The addition of specific MyD88 and TRIF inhibitory peptides similarly demonstrated no difference compared to very high glucose hypoxic conditions (p=0.99). This provides conclusive evidence fibroblast contraction is not related to TLR4 activation, signalling and function.

A

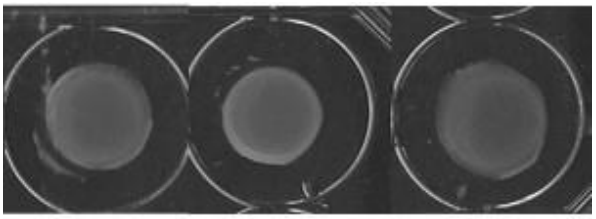

B

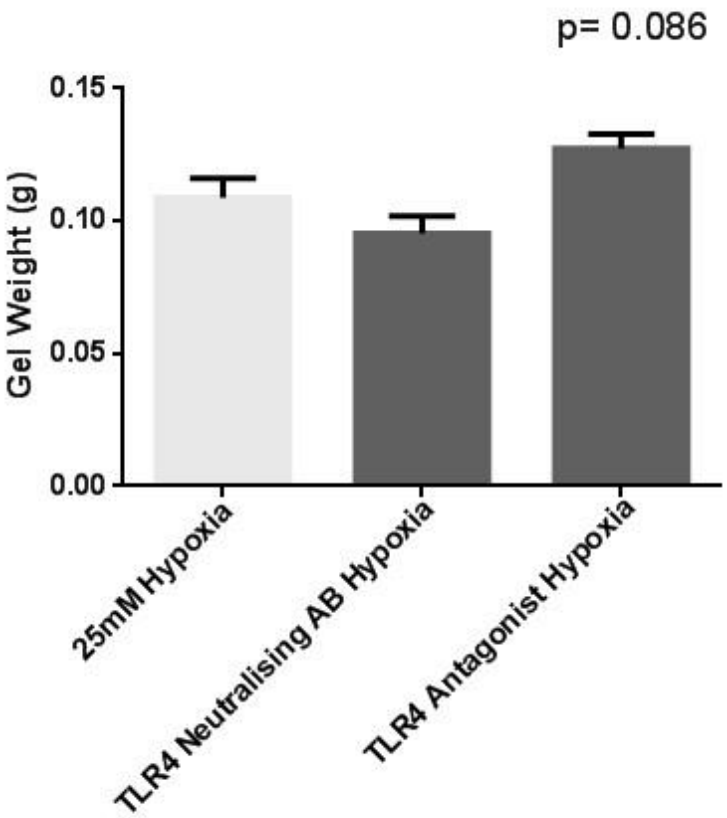

C

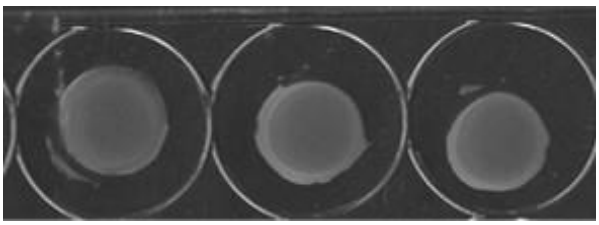

D

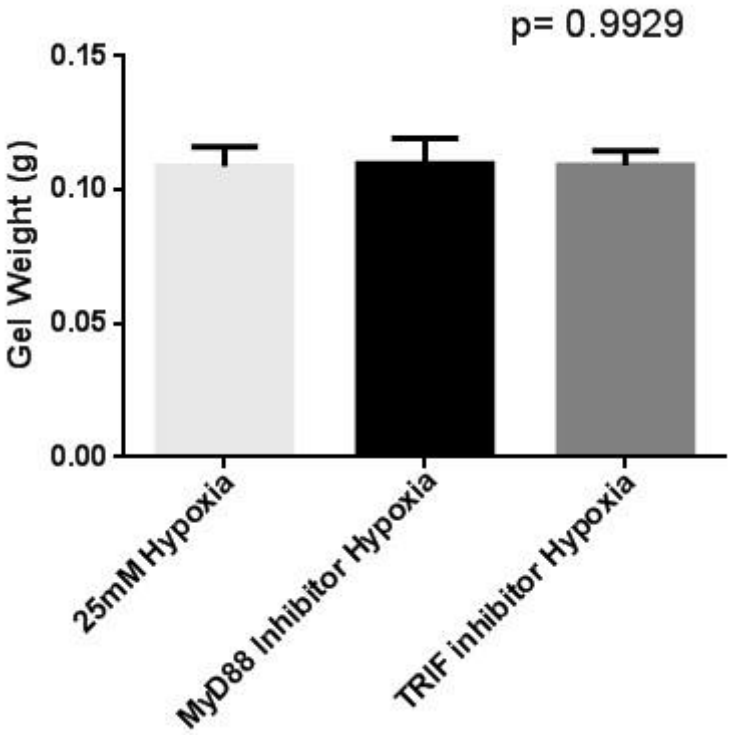

Figure 5.4.3 Effect of TLR4 pathway inhibition on fibroblast contraction

(**A**) Representative scan of collagen gels corresponding to treatment groups labelled in (**B**). (**B**) gel weight comparison between very high glucose hypoxic control and TLR4 inhibitor treatments. No difference was observed between groups (p=0.086, n=6 Kruskal-Wallis test). (**C**) Representative scan of collagen gels corresponding to treatment groups labelled in (**D**). (D) Very high glucose hypoxia and MyD88 and TRIF inhibitors. No difference in contraction was seen in these conditions with the addition of MyD88 and TRIF inhibitors (p=0.99, n=6 Kruskal-Wallis test).

5.4.4 Scratch migration assay

Fibroblast migration was assessed using a scratch assay. The proliferation inhibitor mitomycin c (MMC) was added to remove the effect of proliferation from the scratch closure process, allowing the effect observed to be isolated cell migration. Fibroblast migration was inhibited by simulated ischaemia (figure 5.4.4 **B**) p=0.01, and this effect was significantly exaggerated in very high glucose concentrations (figure 5.4.4 **D**) p=0.01. In a normoxic environment very high glucose led to an increase in cell migration figure 5.4.4 **C**) p=0.05.

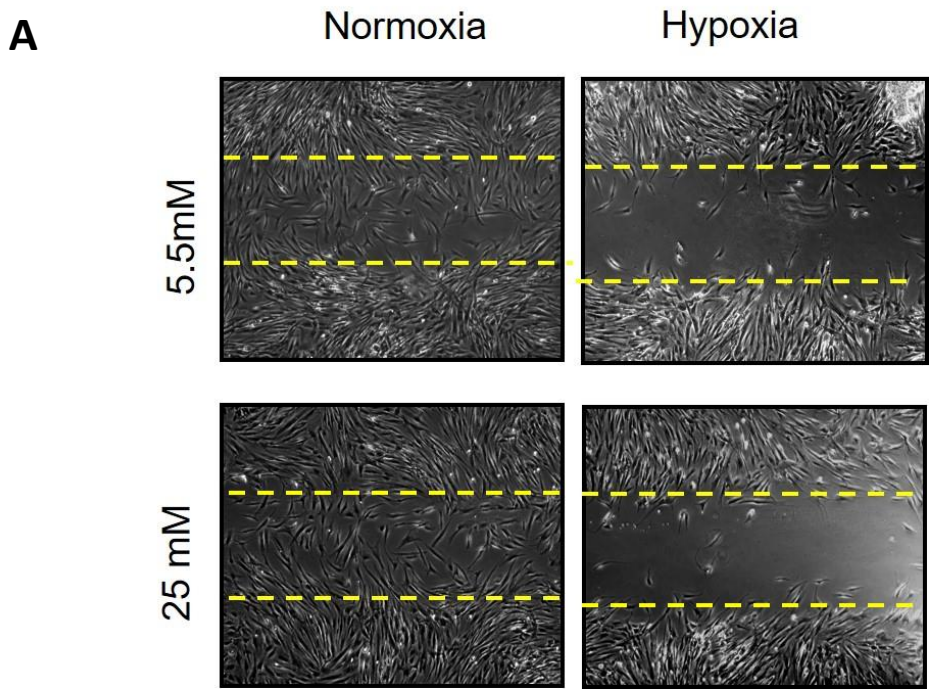

B

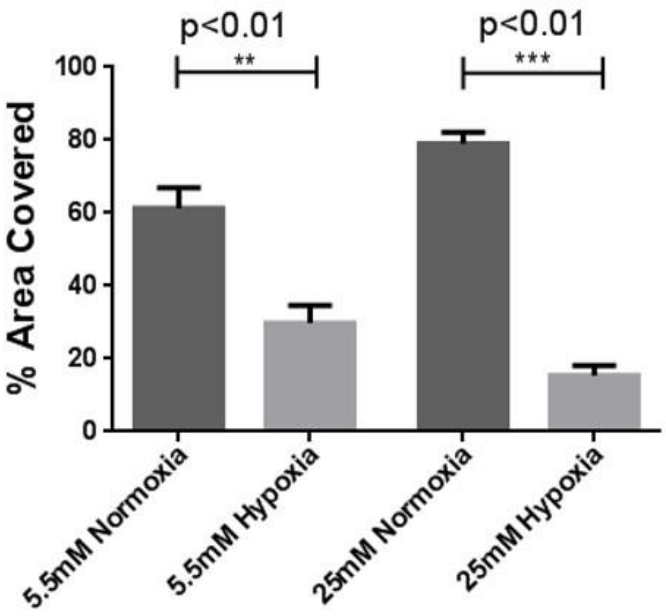
p<0.01
**
p<0.01
***
% Area Covered
100
80
60
40
20
0
5.5mM Normoxia
5.5mM Hypoxia
25mM Normoxia
25mM Hypoxia

C

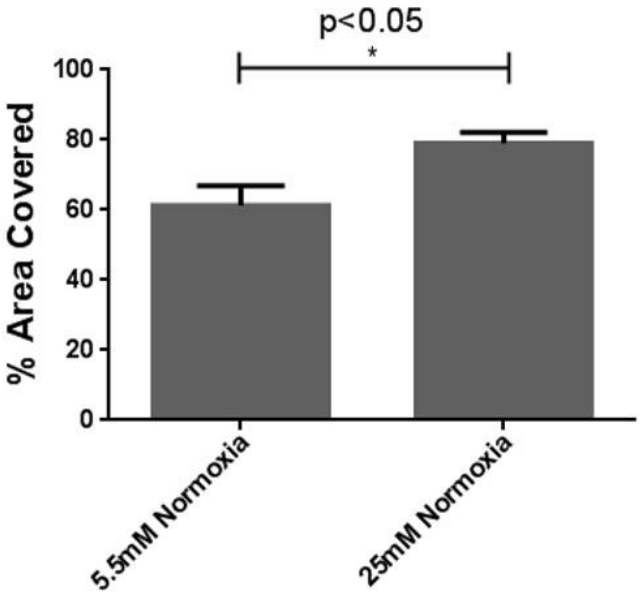
p<0.05
*
% Area Covered
100
80
60
40
20
0
5.5mM Normoxia
25mM Normoxia

D

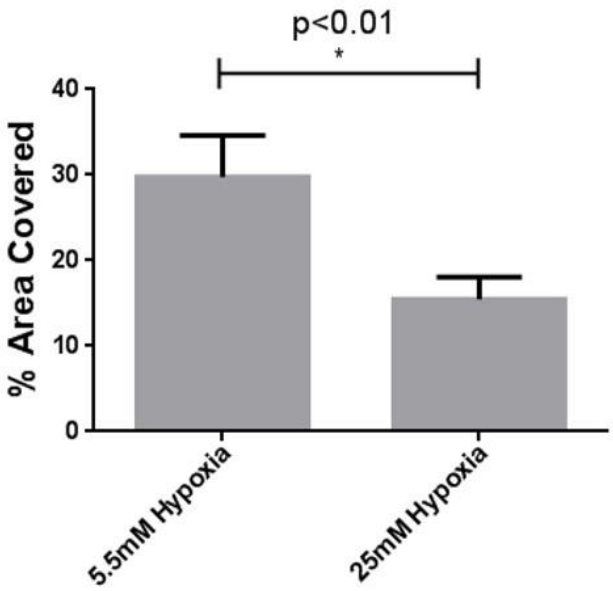

Figure 5.4.4 Effect of LG vs VHG in normoxia and hypoxia on fibroblast migration

(**A**) Representative phase contrast images of fibroblasts 24 hours following wounding. (**B**) Fibroblasts displayed a reduced migratory potential in hypoxic conditions (p=0.01, n=8 Mann-Whitney test). (**C**) Migration was increased in very high glucose compared to low glucose in normoxia (p=0.05, n=8 Mann-Whitney test). (**D**) The impairment in migration observed in hypoxic conditions (figure 5.4.6 **B**) was exaggerated by very high glucose (p=0.01, n=8 Mann-Whitney test).

5.4.5 Inhibitor dose-response effect on fibroblast migration

To examine the effect of TLR4 activation on fibroblast migration, a specific neutralising antibody and a selective antagonist were used. A preliminary experiment was conducted to confirm the optimum dose for each, informed by previous lab experience using these treatments. No statistical analysis was performed. A dose of 1μg/ml was selected for the TLR4 neutralising antibody (figure 5.4.5 **A**), and 10μg/ml for LPS-RS TLR4 antagonist (figure 5.4.5 **B**).

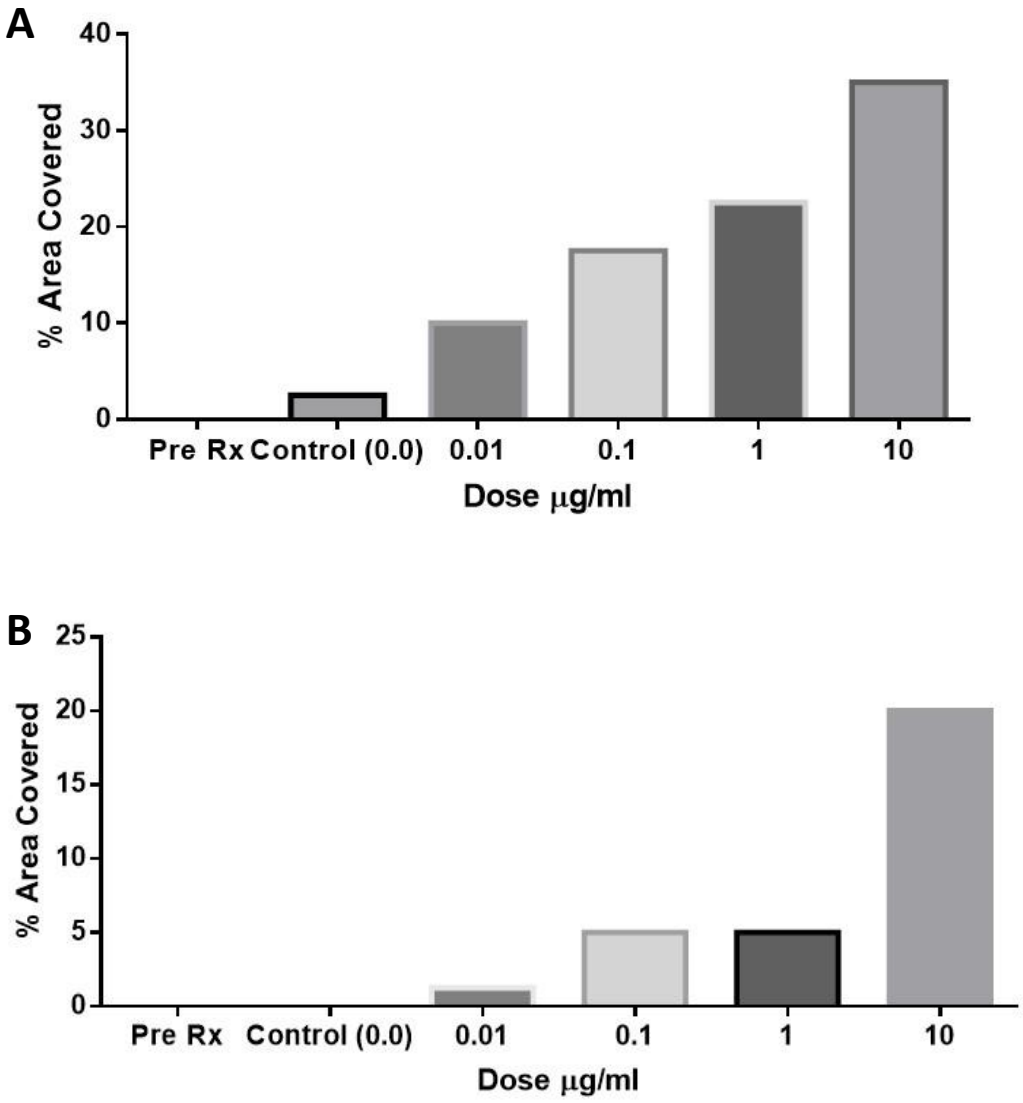

Figure 5.4.5 Dose response effect of TLR4 inhibitors on fibroblast migration

Dose-response effect on fibroblast migration in very high glucose hypoxic conditions of adding (**A**) A selective TLR4 neutralising antibody. A dose of 1μg/ml was selected. (**B**) The TLR4 antagonist LPS-RS, a dose of 10μg/ml was selected.

5.4.6 Effect of TLR4 pathway inhibition on fibroblast migration

Having established simulated hyperglycaemic ischaemic conditions significantly inhibit fibroblast migration (5.4.6), the effect of TLR4 activation and signalling was assessed through the addition of TLR4 neutralising antibody and TLR4 antagonist to the high glucose media in a hypoxic environment. Both compounds resulted in significant improvement in migration (figure 5.4.6 **B**) p=0.01. Migration was similarly improved by the addition of MYD88 inhibitory peptide (figure 5.4.6 **D**) p=0.001. TRIF inhibitory peptide had no beneficial effect on migration. TLR4 inhibition ameliorates the negative effect of hyperglycaemia and ischaemia on migration, and this occurs via the MYD88 dependant signalling pathway.

A

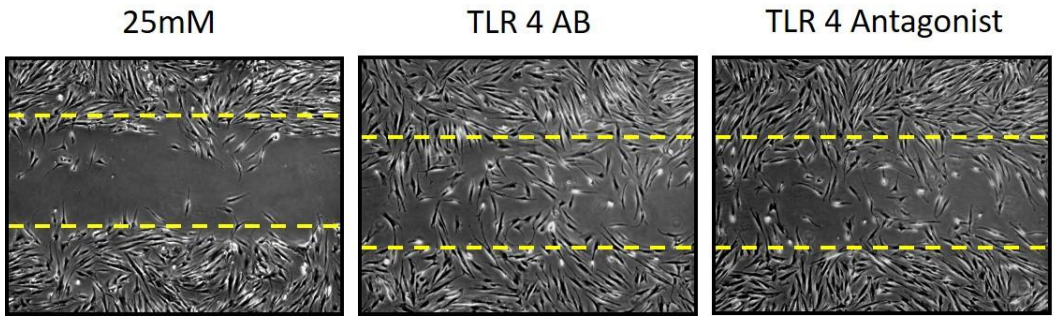

B

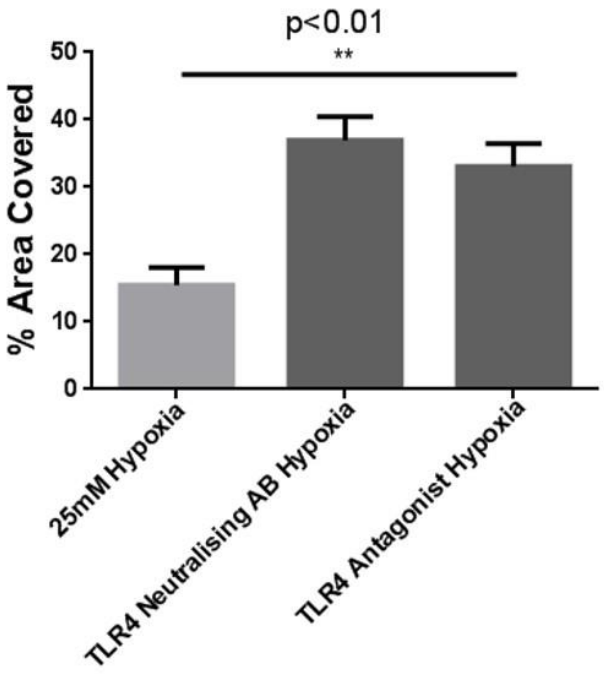
p<0.01
**
% Area Covered
50
40
30
20
10
0
25mM Hypoxia
TLR4 Neutralising AB Hypoxia
TLR4 Antagonist Hypoxia

C

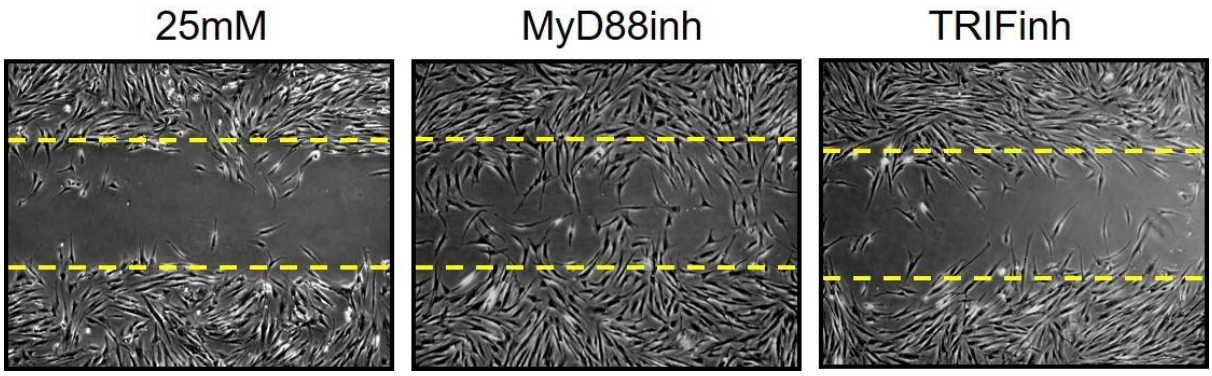
25mM
MyD88inh
TRIFinh

D

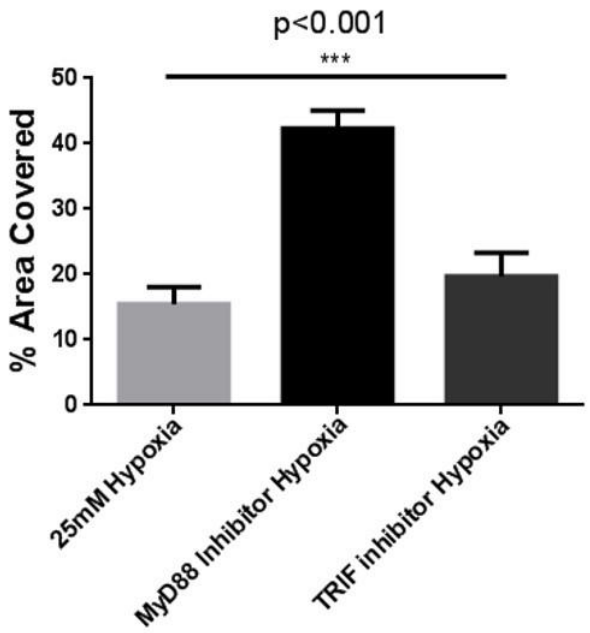

Figure 5.4.6 Effect of TLR4 and signalling pathway inhibition on fibroblast migration

The effect of inhibitor addition to the very high glucose media in hypoxic conditions on fibroblast migration. (**A**) Representative phase contrast images of fibroblasts 24 hours following wounding, comparing migration in TLR4 inhibitor groups vs control (**B**) The addition of TLR4 neutralising antibody or TLR4 antagonist significantly improved fibroblast migration (p=0.01, n=8 Kruskal-Wallis test). (**C**) Representative phase contrast images comparing TLR4 signalling pathway inhibitors vs control. (**D**) MYD88 inhibition significantly improves migration (p=0.001, n=8 Kruskal-Wallis test). Groups treated with TRIF inhibitory peptide demonstrated no improvement in migration. TLR4 inhibition attenuated the harmful effect of combined hyperglycamia and ischaemia, and this effect is mediated via the MYD88 dependant signalling pathway.

5.5 Discussion

In this chapter, the effect of simulated hyperglycaemia and ischaemia on fibroblast proliferation, migration and contraction was examined. The role of TLR4 activation and TLR4 signalling pathways in these cellular functional abilities was also assessed.

An increase in fibroblast proliferation in very high glucose conditions compared to low glucose in normoxia was found. The published literature offers conflicting evidence however. An increase in proliferation by high glucose, consistent with our observations has been reported in dermal fibroblasts (190), renal fibroblasts (191) and cardiac fibroblasts (192). In direct contradiction, others have reported inhibition of proliferation by high glucose in cardiac fibroblasts (193) and dermal fibroblasts (194). Another study noted a decrease in fibroblast proliferation in high glucose, however this effect was attenuated or reversed with the addition of FCS, which offered protection through increased cellular resilience to stress (195). Cells cultured from diabetics demonstrated reduced proliferation compared to non-diabetics, and this effect persisted even when both groups were cultured in high glucose (187). These differences and contradictions between groups only highlights the limitations of cell culture and in vitro studies in modelling complex disease patterns.

Once again unexpectedly the data suggested an inhibitory effect of hypoxia on fibroblast proliferation when combined with very high glucose. Hypoxia-induced increases in fibroblast proliferation are widely reported and often associated with abnormal healing processes such as hypertrophy and fibrosis (196). Studies utilising cells cultured from non-healing diabetic ulcers observe reduced proliferative and migratory capacity however (197), and no direct comparison of fibroblast proliferation in simulated hyperglycaemic ischaemic conditions has been reported previously. This novel finding suggests that the stimulatory effect of hypoxia is inhibited by the concurrent presence of hyperglycaemia.

The gel contraction assay suggested a trend towards increased contraction in hypoxic conditions in both low glucose and very high glucose environments, however this did not reach significance. Comparison of treatment groups across the full range of variable combinations utilising a Kruskal-Wallis test was significant however (figure

5.4.4 **D**). Published studies report the stimulatory effect of hypoxia on fibroblast contractile properties and differentiation to myofibroblasts through TGF-β activation of the SMAD pathways, leading to increased expression of α-smooth muscle actin (αSMA) (198). Other studies contradict this observation, reporting an inhibitory effect of hypoxia on contraction through inhibited myofibroblast differentiation (199). Our results are not conclusive in answering this discrepancy. The addition of TLR4 and TLR4 signalling inhibitors did not significantly alter contraction, suggesting the process of fibroblast differentiation is independent of TLR4 activation and signalling.

In normoxia, greater contraction ability was observed in the low glucose group, however this effect was not significant. An inhibitory effect of high glucose conditions has previously been reported in the literature in support of these findings (200). While trends in support of some published observations are seen, no significant differences between glucose concentrations and oxygen environments tested in this chapter on fibroblast contraction were demonstrated. No published study has reported the effect of combining hyperglycaemia and ischaemia, however these results remain inconclusive and further experimental repeats are required.

Very high glucose conditions led to a significantly increased fibroblast migration compared to low glucose in normoxia (figure 5.4.6 **C**). This effect was completely reversed however in hypoxia with a significantly reduced migration in the VHG hypoxia group (figure 5.4.6 **D**). This unexpected improvement in fibroblast migration by very high glucose conditions in normoxia, is contrary to several studies in which high glucose impeded migration through the overexpression of gap junction protein connexin 43 (Cx43) (201).

This outcome although unexpected, was very consistent. Multiple biological and temporal repeats using at least 3 separate lines of primary cultured fibroblasts produced remarkably similar results. It is possible the difference in observation between these results and others in the literature may be a consequence of experimental protocol. For instance, Mendoza-Naranjo et al (2013) reported inhibited migration in cultured fibroblasts at treatment glucose concentrations of 40mM, far exceeding the treatment dose of 25mM in this project (201). Xuan et al

(2014) reported an inhibition of migration at 30mM, however they observed a 3-day treatment exposure period, in comparison to the 24 hours in this protocol (195). It is also possible the process of primary culture may also have contributed.

It has previously been shown that hypoxia stimulates fibroblast migration, however cells harvested from diabetic animals failed to demonstrate this improved migratory property in hypoxia (189). The significant reduction in migration observed in this chapter by fibroblasts in high glucose and hypoxic conditions may in fact be due to the pathological combination of both factors, resulting in a deleterious signalling or phenotypic change to the cell.

A significant improvement in migration with the addition of TLR4 and MYD88 inhibitors was observed in simulated hyperglycaemia and ischaemia. TLR4 inhibition ameliorated the inhibitory effect of these conditions mediated through the MYD88 signalling pathway. The mechanism for this remains unclear and requires further investigation. The inhibitor doses were selected based on previous dose-response experiments performed within the group on other cell types. A preliminary dose-response experiment was done for this chapter to confirm the efficacy of these doses in fibroblasts. Formal studies were not repeated due to cost constraints.

5.6 Summary

Primary cultured human dermal fibroblast cell lines predominantly release IL-6 and IL-8 inflammatory cytokines. In this population, fibroblasts treated with very high glucose concentrations demonstrated increased proliferative capacity in normoxia, an effect which was completely reversed by the addition of hypoxia, with a significant reduction in proliferation measured. A similar observation occurred in the process of migration. A simulated diabetic-ischaemic environment resulted in a significant reduction in migration compared to very high glucose normoxic controls. These observations suggest a synergistic relationship between hypoxia and high glucose, with hyperglycaemia exaggerating the deleterious consequences of ischaemia. This effect appears to occur via the TLR4 MyD88 pro-inflammatory pathway.

Chapter 6

Murine model of diabetic ischaemic ulceration and the effect of endogenous TLR4 deletion

6.1 Introduction

As mentioned previously, *in vitro* studies utilising single cell types allow close manipulation of environmental conditions and give essential biological insight into the behaviour of cells under variable but specific experimental parameters. These studies are indispensable for the testing of individual receptors and downstream pathways and for the examination of physical cellular processes, such as migration. *In vitro* studies can model these processes in isolation under a variety of controlled specific conditions but cannot adequately replicate physiological complex tissue or organ level processes such as wound healing. As described in section 1.6, wound healing involves a complex interaction between multiple cell types and multiple complimentary cell processes such as phagocytosis, proliferation, migration, contraction and extracellular matrix production. These are closely regulated by cytokines, chemokines, growth factors and other inter-cell signalling processes, all with the correct temporal relationship.

A process of such overwhelming complexity that cannot be meaningfully recreated *in vitro* requires a whole organism study prior to human testing of disease specific therapeutic targets. It is therefore essential for *in vivo* studies to, as accurately as possible, model the pathology of human disease. The *in vitro* experiments presented in chapters 4 and 5 were conducted in very high glucose and hypoxic conditions (alongside relevant controls), *in vivo* studies however must reproduce the

hyperglycaemic and ischaemic conditions commonly found in the peripheral limb tissues of patients with chronic diabetic foot ulceration.

6.1.1 Murine models of diabetic ischaemic ulceration

Murine models of both type 1 and type 2 diabetes have been described (202). Type 1 diabetes is typically induced via the intraperitoneal injection of the diabetogenic antibiotic drug streptozotocin (STZ) and protocols include the single high dose intraperitoneal injection (at doses of 160-240mg/Kg) (203) and the multiple low dose STZ (20-40mg/Kg per day for 5 days) regime (204). The single high dose technique leads to rapid chemical destruction of pancreatic beta cells with a near immediate induction of severe hyperglycaemia (205). It is commonly utilised for beta cell transplantation models and for the testing of new insulin preparations (205) but is associated with increased morbidity such as drastic weight loss, diarrhoea, organ toxicity and sudden death, with a mortality of up to 20% (206). The low dose STZ dosing regime is described as producing a less severe diabetic phenotype but is associated with significantly less toxicity and reduced mortality (207). The diabetogenic effect is via an immune induced insulitis, a macrophage mediated T-lymphocyte cytotoxic destructive inflammatory response to pancreatic beta cells rather than direct toxicity (208). This method has been shown to induce a type 1 phenotype of diabetes in mice (209). A type 1 model is preferred in this study for continuity with in vitro studies, and because hyperglycaemia rather than insulin resistance is the pathological mechanism of interest.

Genetic models of type 1 diabetes in mice exist, the most extensively used is the autoimmune model non-obese diabetic (NOD) mouse (205). Murine models of type 2 diabetes utilise transgenic animals, examples include db/db mouse and the ob/ob mouse strains, both of which have an extreme obesity phenotype (205).

There are a variety of surgical hindlimb ischaemia models described in the literature, inducing differing severities of ischaemia. The described techniques differ in level of artery ligation, number of vessel levels ligated, the ligation of side branches and the ligation and excision of arteries (210). Recovery of hindlimb perfusion is observed

more readily in younger animals 6-8 weeks old compared to older individuals (8-10 months) (211).

Modelling chronic ischaemia is difficult due to the significant recovery potential of the mice, and techniques such as single level femoral ligation have been shown to exert little ischaemic effect due to the extensive collateral circulation (210). A model of high ligation and transection of the EIA proximal to the inferior epigastric and CFA bifurcation, with ligation and excision of the SFA in the C57BL/6 strain has been demonstrated to induce severe ischaemia that more closely resembles the chronic ischaemia found in human patients with PAD (212).

Murine models of diabetic wound healing are well described. Some protocols utilising digital image planimetry to measure wound area employ 9mm dorsal skin wounds inflicted on the animals back (122). While this allows larger wounds to be created and topical treatments and controls within the same animal, is clearly unsuitable to model diabetic ischaemia. Hindlimb models utilising induced ischaemia are however established, some utilise a 5mm thigh dorsal skin wound (143), others locate the wound more distally below the knee, at the expense of a smaller 4mm wound (52).

The model created for this project combines elements of all these techniques. Low dose multiple STZ regime was used to reduce animal morbidity and the potentially confounding effect of organ toxicity. The double ligation ischaemia model was chosen to more accurately model chronic ischaemia, and the wound created as distal as possible to better reflect foot ulceration.

6.2 Aims

The in-vitro experiments conducted in simulated high glucose and hypoxic conditions provided adequate proof of concept to justify progression to whole organism studies. Several murine models of diabetic hindlimb ischaemia have been described, with a variety of subtly different methods used to model diabetic ischaemic limb ulceration.

The first aim of this chapter therefore was to utilise aspects of previously described models to produce a validated model of chronic ulceration.

The second and most important aim was to utilise this model to determine the potential benefit of TLR4 antagonism on wound healing in chronic diabetic ischaemic ulceration. TLR4 antagonists are already available and have been evaluated in phase 3 clinical trials in the context of severe sepsis. Our aim is to again establish the proof of concept by first ascertaining the effect of endogenous TLR4 deletion through transgenic TLR4 -/- mice.

6.3 Methods

A more comprehensive description of methodologies is provided in section 2.3.

6.3.1 Induction of diabetes

Induction of type 1 diabetes was achieved through a low dose daily streptozotocin (STZ) intra-peritoneal injection method. Streptozotocin was reconstituted using a cold (5°C) 0.1M citrate buffer at pH 4.5, created through the addition of trisodium citrate (2.941g in 100ml distilled water) and citric acid monohydrate (2.1g in 100ml distilled water). The citrate buffer was used to reconstitute the STZ at a dose of 1g/ml. After aliquoting, STZ doses were stored at -20°C.

At first dosing, the individual 8-week-old male C57Bl/6 mice were weighed and a dose of 40mg/kg body weight STZ injected into the peritoneal cavity. The same dose was given for five consecutive days per animal. The animals were monitored for signs of distress or injury at least twice per day.

6.3.2 Post induction monitoring

Animals were observed and monitored throughout the experiment. A strict schedule was closely followed to ensure the well-being of subject animals was maintained, and that any of the common side effects of STZ use were detected. These include weight loss, respiratory distress, hypoglycaemia and sudden death. Any animal with >5%

weight loss detected requires euthanasia via a schedule 1 method as per project license protocol.

The STZ monitoring schedule was as follows:

Day 1	Weight		
Day 7	Weight		
Day 14	Weight	Urinalysis	Capillary blood glucose
Day 21	Weight	Urinalysis	
Day 28	Weight	Urinalysis	
Day 35 (day of surgery)	Weight		Capillary blood glucose

Table 6.3.2 Animal monitoring schedule

6.3.3 Induction of hindlimb ischaemia and infliction of lower limb wound

Diabetic animals at day 35 post first STZ injection, aged matched non-diabetic animals destined to become the non diabetic ischaemic cohort and TLR4 knock out animals day 35 post STZ injection underwent surgery to inflict hindlimb ischaemia and ipsilateral skin wounds. In addition, individuals in the non diabetic non ischaemic cohort had 4mm full thickness below knee wounds inflicted.

Prior to surgery, individual cages were moved through to a designated anaesthetic area outside of the operating room. All animals were weighed immediately prior to anaesthetic induction.

6.3.3.1 Induction of anaesthesia

Individuals were placed inside the anaesthetic chamber, where 2l/min O2 was applied as a pre-oxygenation step. Isoflurane gas was introduced, increasing

gradually to a minimum flow setting of 2 (maximum 5) on the anaesthetic machine. Once anaesthetised the animal was removed and placed on a warming mat and transferred to nasal gas anaesthetic using a scavenger circuit. Isoflurane anaesthesia was delivered driven via 2l/min O2 at setting of 2-5.

Anaesthesia was confirmed by applying toe pressure. Hind limb fur was shaved on the left limb (or both if bilateral wounds were created) and the limbs were fully extended and taped in place. The skin was cleansed with aqueous chlorhexidine. From this point full aseptic technique was observed.

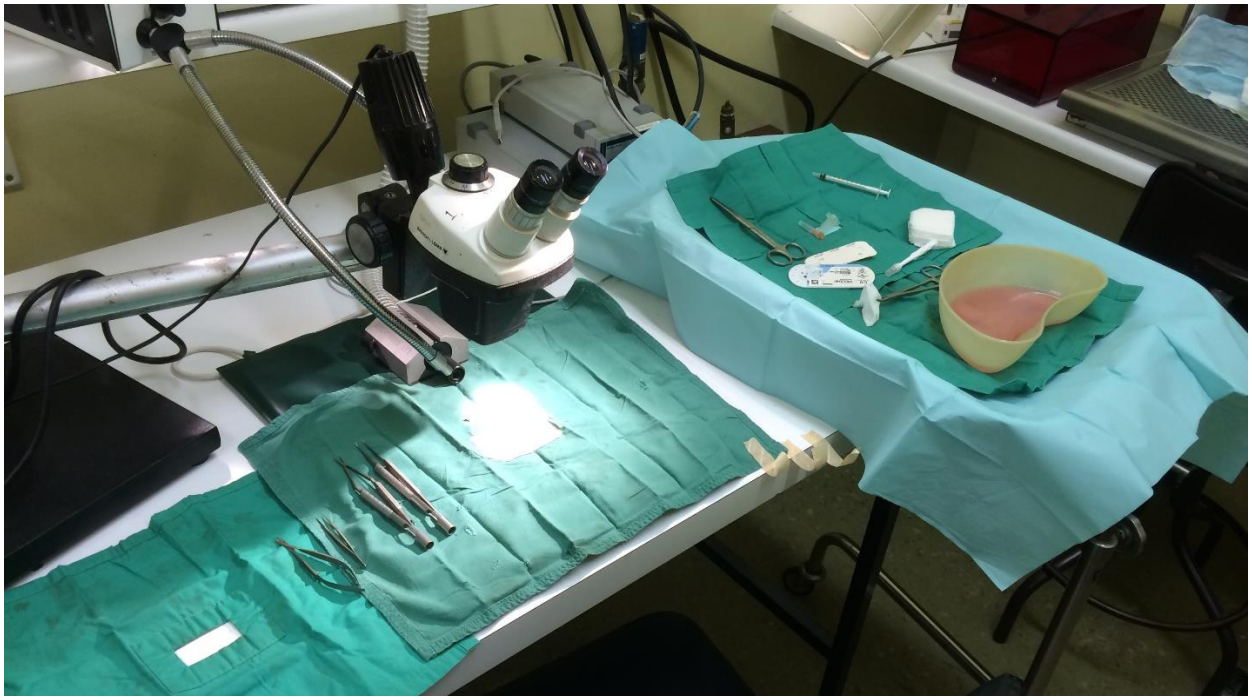

Figure 6.3.3.1 The operating room

Figure 6.3.3.1 A photograph demonstrating the pre-operative organisation of the operating room. Visible are the sterile drapes overlying the heat mat on which animals were placed in a supine position. The nasal gas anaesthesia and scavenger apparatus are located at the top of the heat mat. Additional lightening and x10 magnification microscope were arranged as seen.

6.3.3.2 Induction of hindlimb ischaemia

A 1cm longitudinal skin incision was made along the medial left thigh and the skin separated and undermined using blunt dissection. The artery was exposed by sweeping away the overlying fat pad using a peanut swab. The external iliac artery was located by continued proximal blunt dissection and separated from the vein by dissecting along its length. After isolating the artery, a 7-0 prolene suture was passed behind and tied proximally and again distally. The external iliac artery (EIA) was then divided between these sutures. The superficial femoral artery (SFA) was separated from the vein and isolated proximally after the common femoral (CFA) bifurcation, and distally at the above knee popliteal artery (figure 6.3.3.2 **A**). Without damaging the deep vein, the SFA was then completely excised (figure 6.3.3.2 **B**). Haemostasis was achieved and the wound closed using interrupted 3-0 vicryl rapide.

A

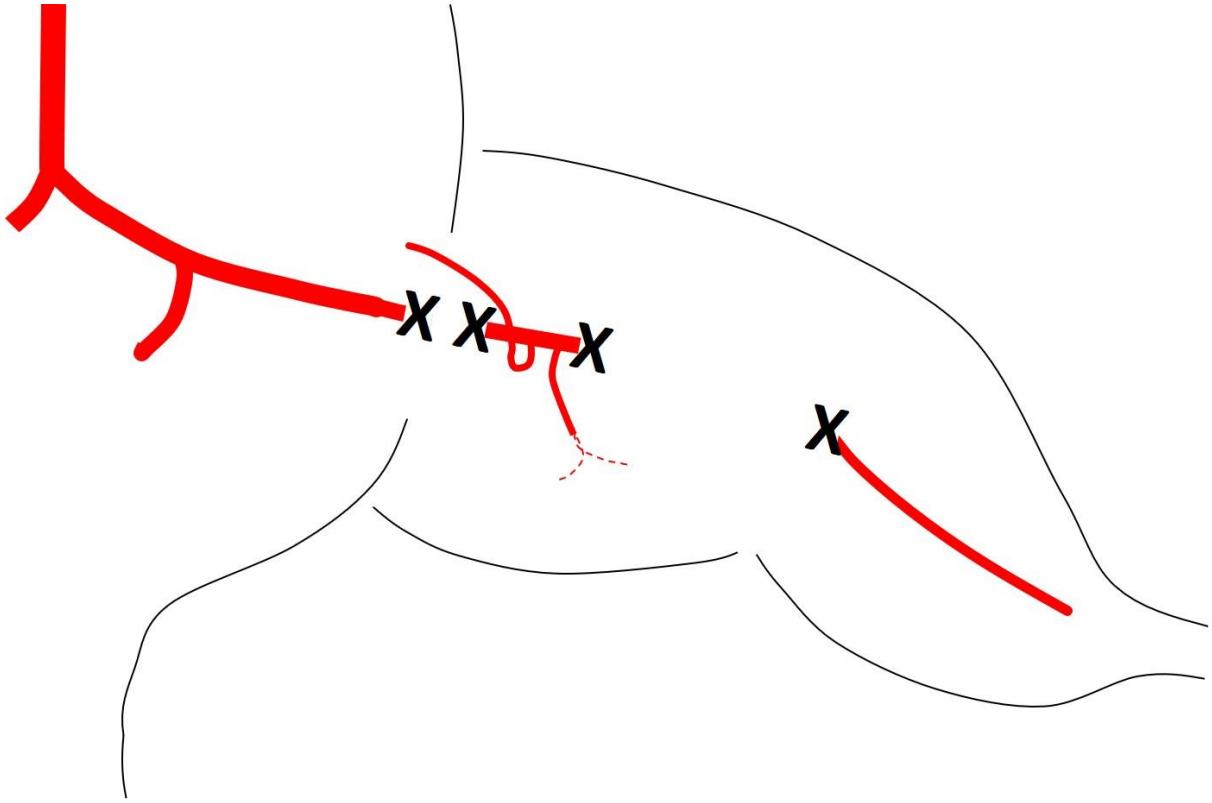

B

Figure 6.3.3.2 Mouse arterial ligation and excision

Figure 6.3.3.2 **A** diagrammatical representation of the levels of ligature placement and division of the artery, with representation of the excised section of SFA. **B** excised length of SFA on a cotton swab.

6.3.3.3 Infliction of below knee skin wound

Following closure of the operative wounds and while still anaesthetised, the securing tape was removed, and the animal placed in the right lateral position. The knee was located and a 4mm punch biopsy was used to remove a full thickness skin sample on the lateral aspect of the leg below the knee.

Prior to removal from nasal anaesthetic, a capillary blood glucose sample was taken via a tail pin prick, and a 40µL volume of buprenorphine (Temgesic®) was injected subcutaneously for post-operative analgesia. Laser doppler imaging was performed when available prior to recovery from anaesthetic to examine the perfusion of the operated limb and confirm induction of ischaemia (figure 6.4.3).

The animals were removed from nasal isoflurane anaesthesia and placed into a warmed recovery pen. Once fully recovered, they were returned to their individually ventilated cages and highlighted as post-operative animals to be closely observed.

6.3.4 Wound photography

A more detailed explanation of this method is outlined in section 2.3.5.1. Wounds were photographed using digital photography for subsequent wound area analysis. A standard measure was placed within the photograph to allow for size standardisation (figure 6.3.4). Wounds were photographed immediately post infliction of skin wound on day 0 while under anaesthesia, and on days 3, 7 and 14 post mortem after sacrifice using schedule 1 methods.

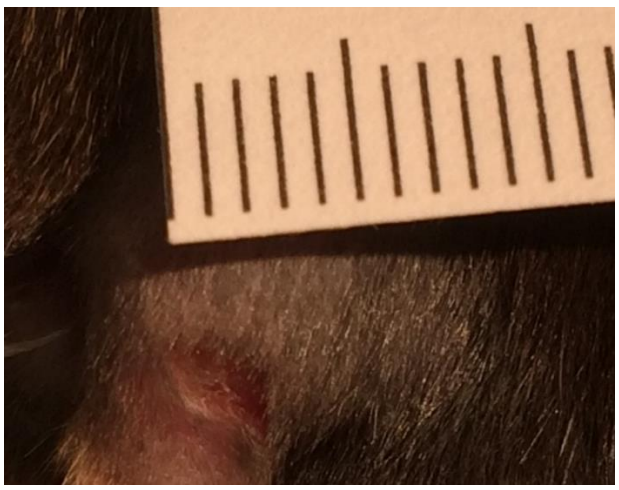

Figure 6.3.4 Wound digital photography incorporating measurement standard

Representative photograph of a mouse hindlimb wound containing a tape measure for accurate standard comparison in wound area measurement. This photograph depicts a day 3 wound in a diabetic ischaemic TLR4 knock out mouse.

6.3.5 Sample collection

The animals were euthanased using the schedule 1 methods of neck dislocation and aortic disruption under terminal anaesthesia. Post mortem the hindlimb wound was photographed as described in section 6.3.4. The ulcer was then circumferentially excised, fixed onto filter paper backing and placed into formalin. Skin biopsies from immediately adjacent to the ulcer excision site were taken and snap frozen in liquid nitrogen. They were subsequently placed in -80°C. Protein samples were liberated from the skin samples according to the tissue lysis protocol described in section 2.3.6.

6.3.6 Wound area planimetry

Wound areas were measured for each animal using ImageJ software. A more detailed explanation of this protocol is found in section 2.3.7. The images were magnified to improve accuracy and the tape measure used to calibrate each image to ensure standardised measurement. Due to the degree of variation in the day 0 initial wound areas, a mean starting wound area for each test group was calculated. Subsequent individual wound area measurements within that group were normalised against this starting mean. This ensured all groups day 0 wound area was assigned a value of 1, and comparisons between test groups was then possible. Subsequent data points are therefore expressed as relative mean wound areas, and the graphs demonstrate relative wound area reduction.

6.4 Results

6.4.1 Assessment of hyperglycaemia

Following the intra-peritoneal injection of STZ, animals were monitored as described in section 6.3.2. The successful induction of diabetes was confirmed through capillary blood glucose monitoring (CBG) and through the presence of glycosuria in urine. Figure 6.4.1 **A** demonstrates the glucose monitor used, and figure 6.4.1 **B** the urine test strips, along with the visual colour comparison method for interpretation.

A

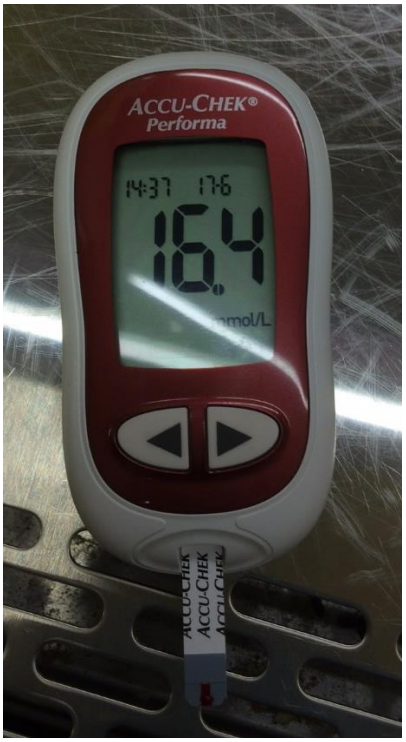

B

C

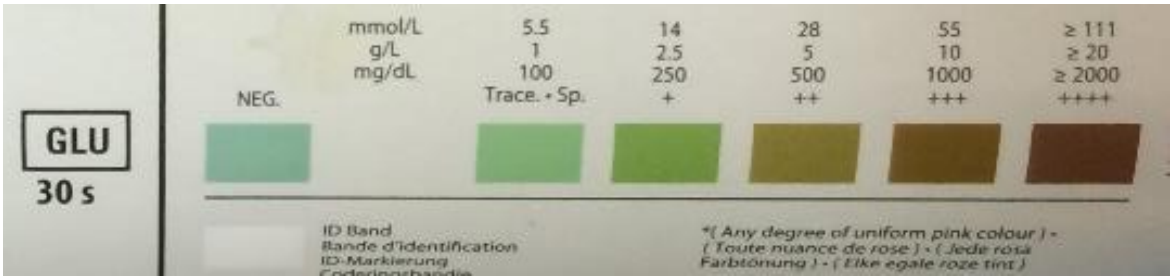

Figure 6.4.1.1 Capillary blood glucose test meter and urinary glucose test strips

Figure 6.4.1 **A** Photograph of portable capillary blood glucose monitor used for tail capillary blood sampling. **B** Photograph demonstrating urinalysis test strip comparison against colour key on test strip bottle. **C** The glycosuria colour comparison chart. The CBG tests were conducted at random, the fasting status of each animal was unknown.

6.4.1.2 Animal glycaemic control measurement

Diabetes was induced through a consecutive five-day dosing regimen of low dose (40mg/kg) intra-peritoneal STZ. Day one was considered as the first day of dosing. Random non-fasting capillary blood glucose measurements were taken on day 14 post first intraperitoneal injection of STZ. Glycosuria was assessed first at day 14 and at the intervals described in 6.3.2. Table 6.4.1.2 demonstrates the mean capillary blood glucose levels at each measurement interval. A urinary glucose reading of ++ or more and/or a random CBG measurement of >11.1mmol/L was taken to be diagnostic of the successful induction of diabetes (148).

	Pre Surgery				Post surgery		
	Day 14	**Day 21**	**Day 28**	**Day 35**	**Day 3**	**Day 7**	**Day 14**
Diabetic non ischaemic	**9.1**	**9.1**	**13.7**	**16.1**	**18.6**	**17.9**	**20.9**
Urinalysis	**+**	**++**	**++**	**++**			
Diabetic Ischaemic	**9.1**	**10.9**	**13.9**	**18.6**	**23.3**	**19.4**	**23.1**
Urinalysis	**++**	**++**	**+++**	**+++**			
TLR4 KO	**11.5**	**13.1**	**15.7**	**18.8**	**20.8**	**20.1**	**21.3**
Urinalysis	**+**	**++**	**++**	**+++**			

Table 6.4.1.2 Mean CBG measurements and urinalysis

Figure 6.4.1.2 Non-fasting capillary blood glucose measurements confirming induction of diabetes

Data illustrated in Table 6.4.1.2 and figure 6.4.1.2 demonstrates comparable mean random capillary blood glucose levels between groups with no statistical difference observed (p=0.17, 2way ANOVA). There was a trend for increasing CBG in all groups throughout the duration of the study period. There was a suggestion of a post-surgery peak in CBG levels at day 3, with this effect more pronounced in the DM-I group. By day 14 post-surgery CBG results had regained parity between groups.

The mean random non-fasting blood glucose measurements were comparable between the three diabetic treatment groups. Group mean results are presented as identification of individual mice was impossible owing to multi-occupancy cages. Data is therefore not available on an individual animal level, however the narrow error bars indicate there was little variation. By day 21 the mean observed glycosuria measurement across all groups was the ++ value set as diagnostic for successful diabetes induction. By day 28 the mean random non-fasting CBG measurement in all groups exceeded the 11.1mmol/L value used clinically as diagnostic for diabetes

(148). There appeared to be a post-operative peak in measured CBG, particularly in the diabetic ischaemic cohort, this reached a plateau by day 7.

Figure 6.4.2 Animal weight measurements

Diabetes was induced through a consecutive five-day dosing regimen of low dose (40mg/kg) intra-peritoneal STZ. Day one was considered as the first day of dosing. Multiple post-dosing assessments of weight were made following the schedule described above in section 6.3.2. Table 6.4.2.1 demonstrates the mean weight of groups at each monitoring interval following STZ administration.

Four weeks following induction of diabetes, animals in the relevant groups (diabetic ischaemic and TLR4 KO diabetic ischaemic) underwent surgical ligation of the right common femoral artery and excision of the superficial femoral artery to provoke hindlimb ischaemia. Animals in the non-diabetic group did not undergo STZ dosing and therefore received no specific pre-surgery monitoring. Table 6.4.2.2 lists the mean weight of animals in each group following surgery to induce hindlimb ischaemia. The TLR4 KO group were heavier than wild-type, attempts were made to weight match groups, however the differential growth rate between them made this particularly difficult.

	Day 1	Day 7	Day 14	Day 21	Day 28
Diabetic ischaemic	26.1g	25.7g	26.1g	26.6g	27.3g
Diabetic Non-ischaemic	25.7g	26.2g	26.7g	27.5g	27.6g
TLR4 KO (DM-I)	42.2g		40.0g		40.7g

Table 6.4.2.1 Mean weight at scheduled monitoring intervals post STZ dosing

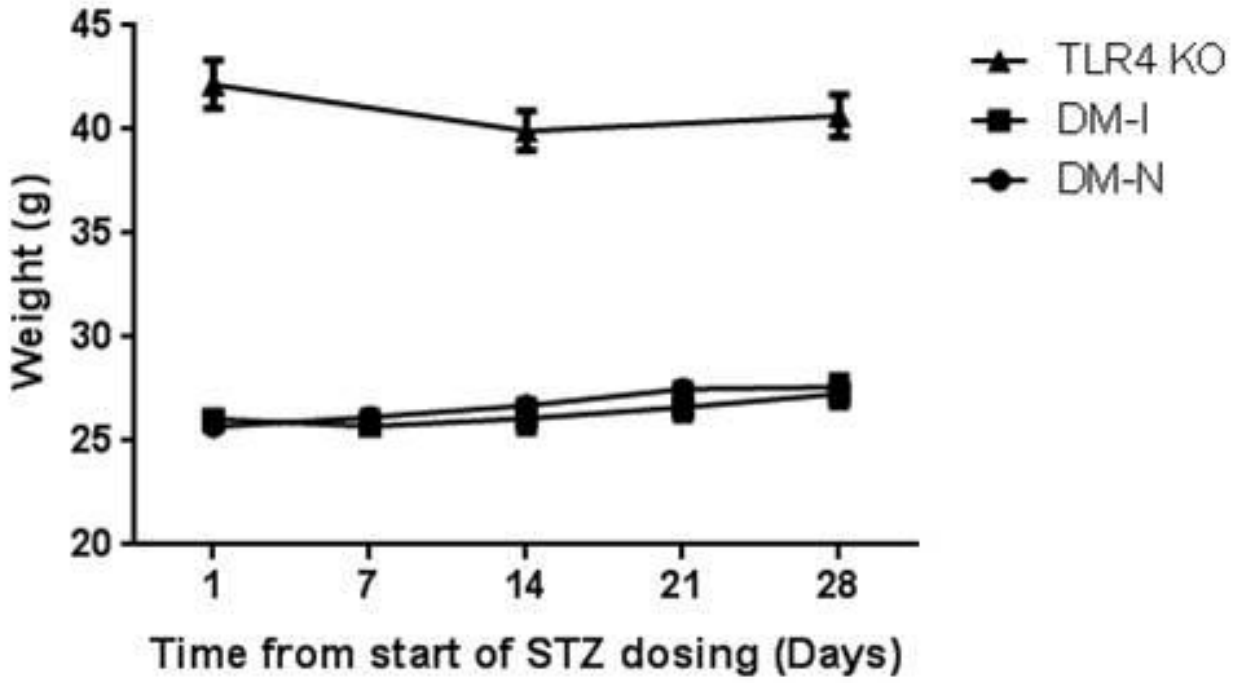

Figure 6.4.2.1 Weight change following diabetes induction

Table 6.4.2.1 and figure 6.4.2.1 document the progression of animal weight from the first day of dosing to day 28. There was no difference in age and starting weight between the diabetic ischaemic and diabetic non-ischaemic groups. An initial decrease in weight post-dosing was observed in the diabetic ischaemic group at day 7. This effect was not sustained, with weights regaining parity by day 28. TLR4 KO mice were significantly heavier than WT controls ($p=0.0001$, unpaired t test, $n=21$). The KO group exhibited a weight decrease post-dosing but failed to regain pre-STZ injection levels. This effect did not reach statistical significance.

	Day 0	Day 3	Day 7	Day 14
Diabetic ischaemic	27.4g	26.0g	25.9g	27.4g
Diabetic Non-ischaemic	27.7g	27.5g	27.9g	27.7g
Non-diabetic ischaemic	27.3g	27.1g	27.9g	30.3g
TLR4 KO (DMI)	41.3g	41.0g	39.3g	41.1g

Table 6.4.2.2 Mean weight at scheduled intervals post-induction of hindlimb ischaemia

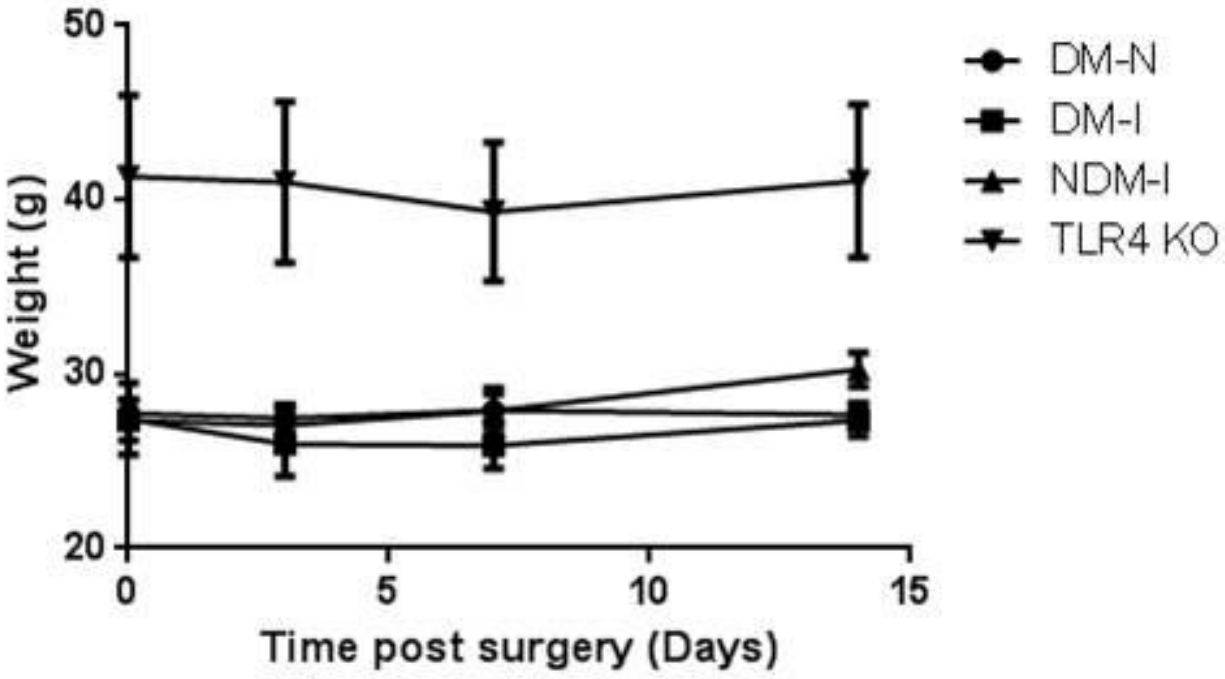

Figure 6.4.2.2 weight change following induction of hindlimb ischaemia

Table 6.4.2.2 and figure 6.4.2.2 demonstrate animal weights pre-surgery and at intervals of 3, 7- and 14-days post-surgical induction of hindlimb ischaemia. These represent the same individuals as those documented in figure 6.4.2.1 with the addition of the non-diabetic ischaemic cohort. At day 3 post surgery, animals in each group had lost weight, with animals in the diabetic ischaemic cohort observed to have reduced in weight by the greatest degree (5% pre-op body weight). This effect was/not significant (p=0.43, unpaired t-test, n=7). By day 14, diabetic animals had regained weight to pre-operative levels except in the TLR4 KO group. Non diabetic animals were also observed to gain weight, and by day 14 exceeded weights measured pre-surgery.

At day 7 after the induction of diabetes, animals in the group destined to undergo hindlimb ischaemia were observed to have lost weight. This effect was not seen in the comparable 'non-ischaemic group' however and was not sustained, with mean weights recovering by day 14. TLR4 KO animals were also observed to decrease in weight post STZ dosing but failed to recover to pre-dosing levels (figure 6.4.2.1). This effect was not statistically significant.

The surgical infliction of hindlimb ischaemia and a below the knee full thickness skin wound resulted in a decrease in weight in all groups (figure 6.4.2.2). This effect, although not statistically significant, appeared to be greatest in the diabetic groups, including TLR4 knock outs**.** The subsequent trend observed suggested these weights increased, however results after day 7 are difficult to interpret as experimental animal sacrifices resulted in a reducing population. Although the cages were chosen at random for sacrifice, there was considerable variation between individuals within each cage (from 33g to 48g). The sacrifice of larger individuals therefore affected the mean weight due to the small sample size.

6.4.3 Assessment of post-operative hindlimb ischaemia

Following induction of left hindlimb ischaemia through CFA ligation and SFA excision, the operated limb was imaged with a LASER doppler to confirm successful establishment of ischaemia. This was performed on all operated animals where available, prior to recovery from anaesthesia.

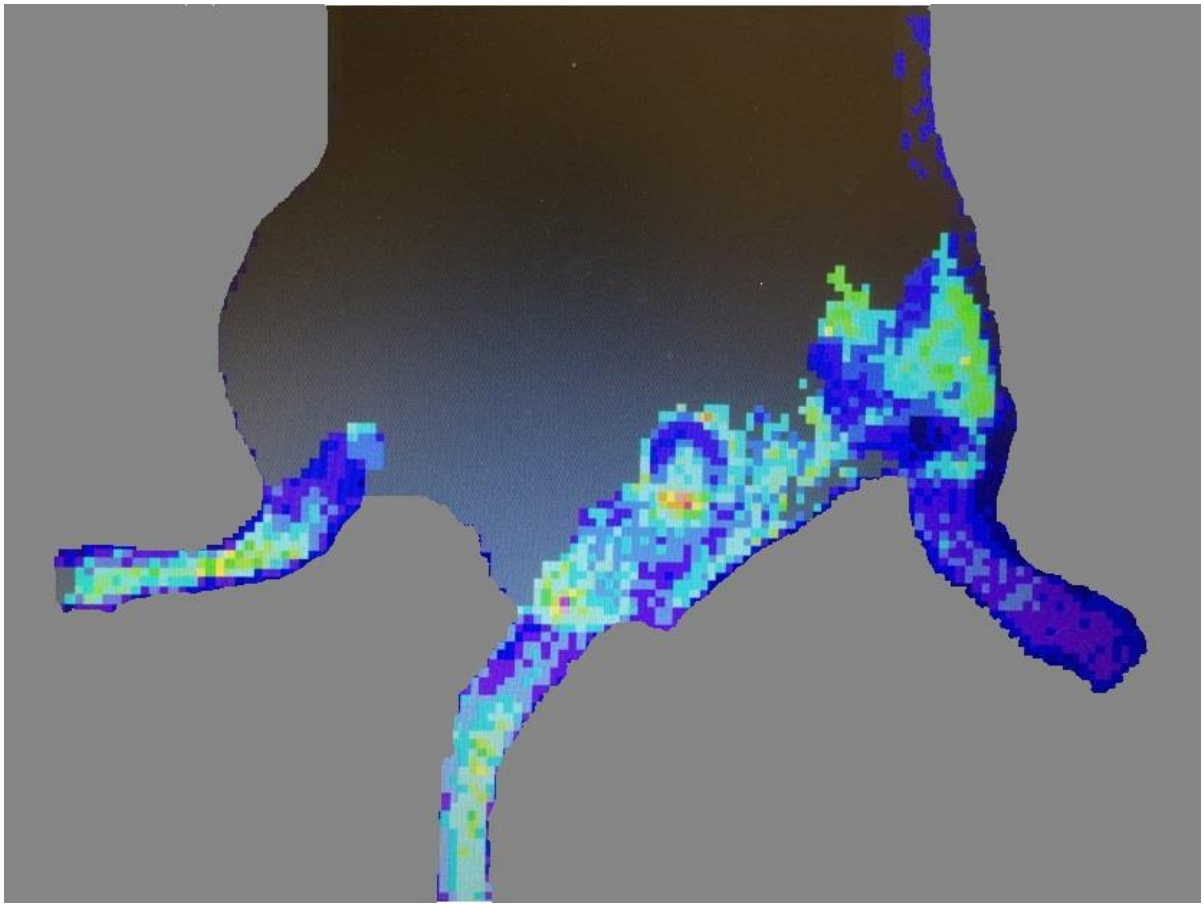

Figure 6.4.3 LASER doppler image post ligation of Left CFA and SFA excision

Figure 6.4.3 demonstrates a representative LASER doppler image post ligation of the left CFA and excision of the SFA, rendering the left limb ischaemic. In this image the fur of both lower limbs was shaved to allow visualisation of perfusion, and the animal is viewed lying supine. The left limb demonstrates no detectable blood flow indicating successful achievement of severe ischaemia.

LASER doppler images taken post operatively confirm establishment of severe hindlimb ischaemia. Previous work from this group has indicated rapid collateralisation and re-establishment of a degree of perfusion by day 7 in a similar

model of hindlimb ischaemia. In the context of co-existing diabetes, the degree of collateralisation throughout the time course remains unknown.

6.4.4 Murine diabetic-ischaemic model of lower limb ulceration

To determine the effect of diabetes and ischaemia on healing in a full-thickness lower limb wound, a murine model of induced diabetes and hindlimb ischaemia was created. To validate this model, diabetic-ischemic wound healing was compared to healing in diabetic non-ischaemic, non-diabetic ischaemic and non-diabetic non-ischaemic animals.

Diabetes was induced as described above utilising the repeat low-dose STZ regimen four weeks prior to induction of hindlimb ischaemia. Under isoflurane gas anaesthesia, the left common femoral artery was ligated with excision of the superficial femoral artery as described in section 2.3.4 and 6.3.3. A 4mm full thickness punch biopsy was taken below the knee at the time of surgery.

Photographs of each wound were taken prior to reversal of anaesthesia, and again at the time of sacrifice under terminal anaesthesia on day 3, 7, 14 post surgery.

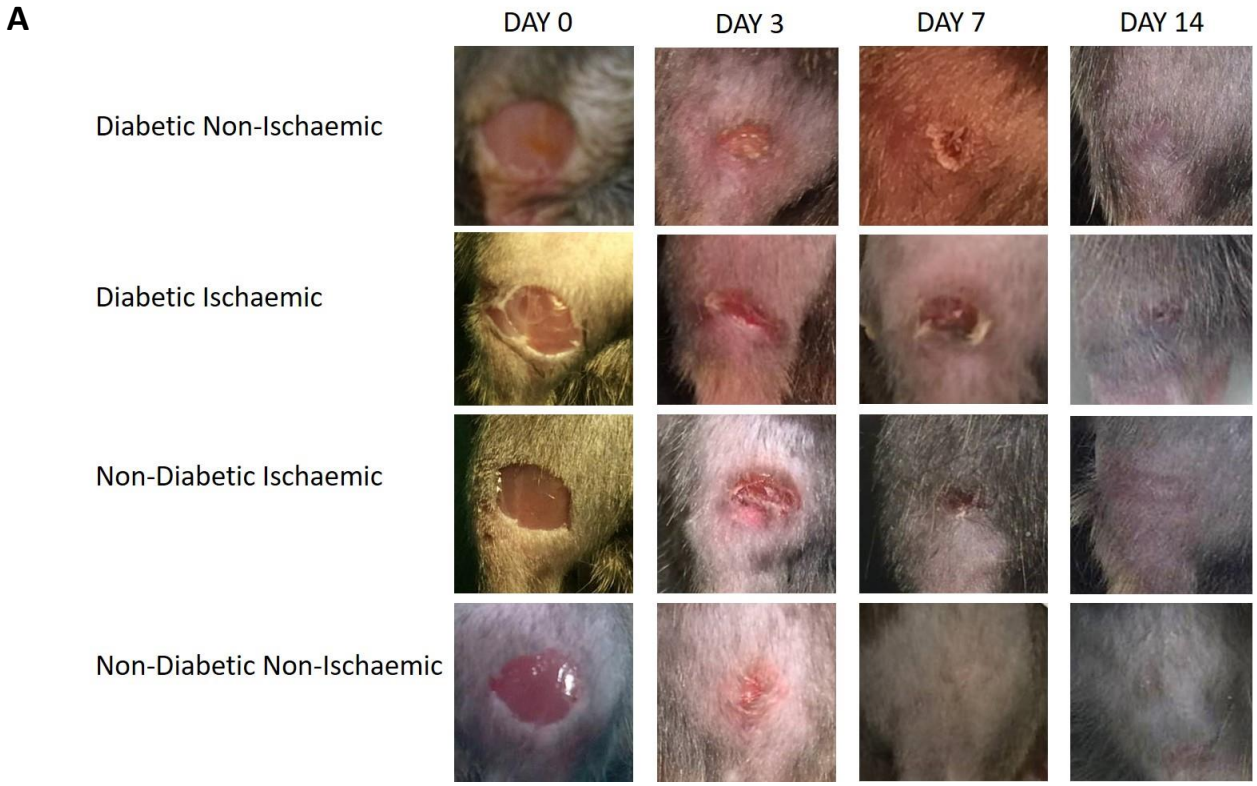

B

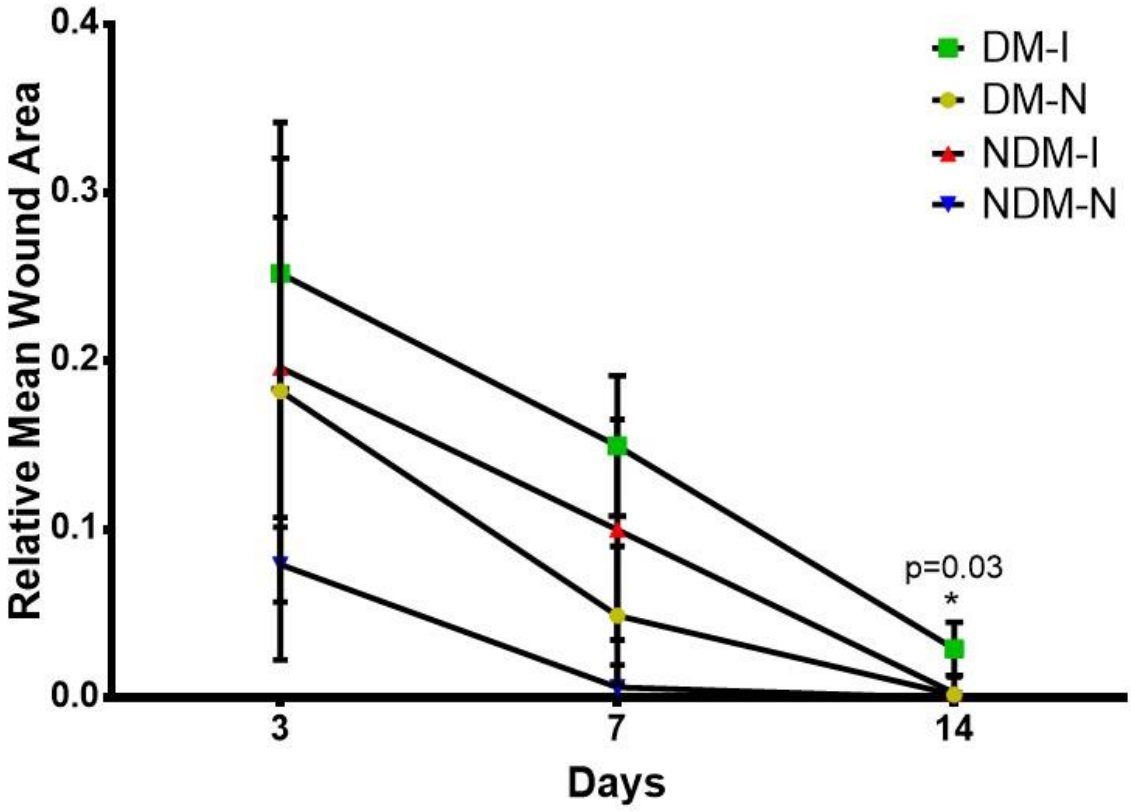

Figure 6.4.4 Diabetic-ischaemic conditions result in slower wound healing

Figure 6.4.4 **A** Representative photographic images demonstrating lower limb wound areas at perioperative (day 0) and 3,7 and 14 days post induction of hindlimb ischaemia. Control groups comparing diabetic and non-diabetic animals with or without ischaemia are represented. Images were obtained under anaesthesia (day 0), or terminal anaesthesia prior to sacrifice (days 3,7,14). **B** Comparison of relative mean wound areas between groups at highlighted time intervals. Analysis of wound area was conducted using image J software. A tape measure was included within each photograph for size comparison and accurate scaling (not shown). Animals with diabetic-ischaemic wounds had a significantly greater wound area at day 14 compared to other groups (p=0.03, Kruskal-Wallis test, n=4).

Animals with diabetes and hindlimb ischaemia were the only group to have wounds persist to day 14 (P=0.03). No animal in this group demonstrated complete wound healing (n=4). All wounds on animals from the other control groups healed by day 14. There was no significant difference between healing in diabetic non-ischaemic and non-diabetic ischaemic animals. All subjects in the non-diabetic non-ischaemic wounds had 100% wound closure at day 7.

Wound areas are represented as mean values, as the individuals within each group were not individually identifiable. The animals were housed in cages together by treatment group, therefore individual comparison of wound area reduction was not possible. As explained in section 6.3.6, these mean areas are then further represented relative to the starting (Day 0) mean wound area. The relative mean wound areas at each time point are therefore presented in figure 6.4.4 B, incorporating measurements from all individuals within the group.

The significant impairment in wound healing in the diabetic-ischaemic group suggests this may be a successful murine model of chronic diabetic-ischaemic ulceration. Further time points beyond 14 days, potentially up to 3 months are required to determine whether the effect is truly induction of a chronic wound, or simply significantly delayed wound healing. While no significant difference in wound area was observed between diabetes only and ischaemia only wounds, both groups failed to exhibit the rapid healing of animals in the non-diabetic non-ischaemic group. It is therefore possible that with a larger sample size this measured impairment in healing may reach statistical significance.

6.4.5 Effect of TLR4 knock-out on wound healing

The control experiments in wild-type male C56BL/6 strain mice described in figure 6.4.4 provided validation for this experimental protocol as a successful model of impaired wound healing in diabetic-ischaemic ulceration. The experiment was repeated utilising endogenously deleted TLR4 -/- mice on a background strain of C56BL/6. Male mice were exclusively used as before. Due to the slower growth rates of TLR4 KO animals compared to WT, the specimens could not be age matched. The TLR4 KO mice were aged approximately 14 months and are larger than control mice. Results are again expressed as relative mean wound areas.

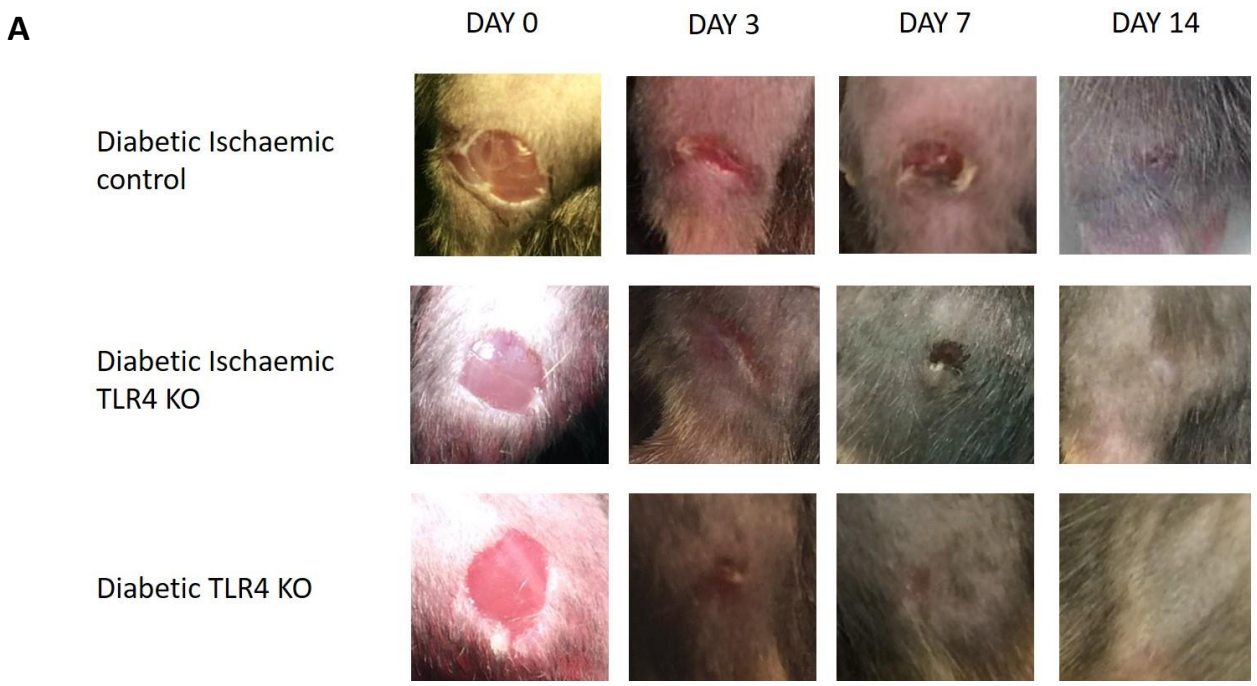

B

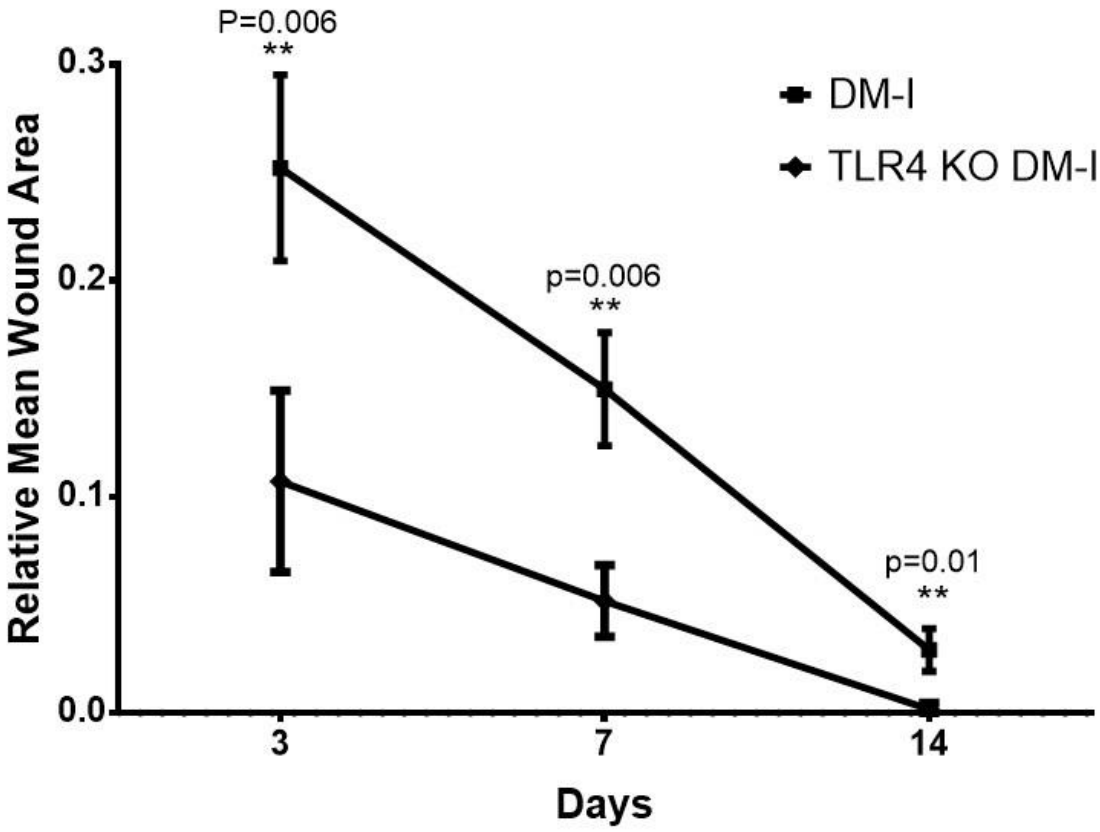

Figure 6.4.5 TLR4 knock-out significantly improves wound healing in diabetic-ischaemic conditions

Figure 6.4.5 **A** Representative photographic images comparing lower limb wound areas at time of operation (day 0), and post-operative days 3, 7 and 14. Diabetes and hindlimb ischaemia were induced in aged TLR4 KO mice as per previously described. Identical 4mm full thickness punch biopsy wounds were made on the contralateral non-ischaemic limb to provide a diabetic non-ischaemic TLR KO control. Images were obtained under anaesthesia as in figure 6.4.4. **B** Comparison of relative mean wound areas between WT diabetic ischaemic and TLR4 KO diabetic ischaemic wounds at days 3, 7 and 14. There was a significantly reduced wound area representing improved healing at each time point in the TLR4 KO mouse compared to WT (p=0.006, 0.006 and 0.01 at days 3, 7 and 14 respectively, Mann-Whitney test n=7 at each time point).

Endogenous TLR4 knock out was associated with an improvement in wound healing at each time point compared to comparable diabetic ischaemic wild type animals (figure 6.4.5 **B**). All wounds were healed by day 14.

6.4.6 Protein expression in wild-type vs TLR4 knock-out diabetic animals

Below knee skin samples were collected post mortem following ulcer excision. Biopsy samples underwent homogenisation as described in section 2.3.6. A comparison of day 3 post-operative TLR4 and cleaved caspase 3 tissue concentrations from diabetic non ischaemic, diabetic ischaemic and diabetic ischaemic TLR4 -/- animals is represented in figure 6.4.7. As expected TLR4 knock out animals did not express TLR4.

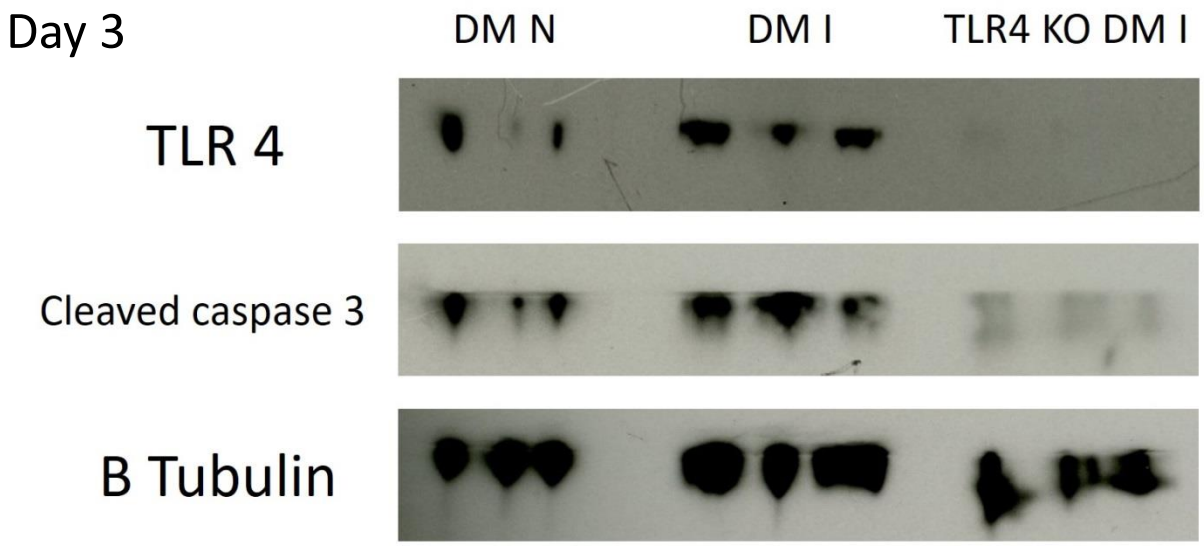

Figure 6.4.6 TLR4 expression and apoptosis appear increased in diabetic ischaemic wounds

Western blot analysis of TLR4 expression and cleaved caspase 3, an apoptotic marker, in tissue biopsies taken from diabetic non ischaemic, diabetic ischaemic and diabetic ischaemic TLR4 knock out animals on day 3 post skin wounding. Insufficient experimental repeats were conducted to statistically analyse these observations, however the trend appears to be a greater TLR4 expression in tissue from diabetic ischaemic wounds than from diabetic non ischaemic skin. It appeared cleaved caspase 3 concentration was increased in diabetic ischaemic tissue compared to diabetic only, and reduced in TLR4 knockout. As expected no TLR4 expression was observed in tissue from knock out animals.

TLR4 expression and cellular apoptosis appeared to be increased in diabetic ischaemic tissue and reduced under the same conditions in TLR4 knock out animals. Without statistical significance no firm conclusions can be made from these

observations, however the suggested trend closely correlates with the results of the *in vitro* experiments.

6.4.7 Temporal comparison between wild-type and TLR4 knock-out animals

Harvested tissue protein was used to compare TLR4 and cleaved caspase 3 expression between individuals sacrificed at each time point within treatment groups. Figure 6.4.6 demonstrates the expected absence of TLR4 expression in the knock-out animals, therefore TLR2 expression was examined instead to determine whether the absence of TLR4 results in a compensatory increase in TLR2.

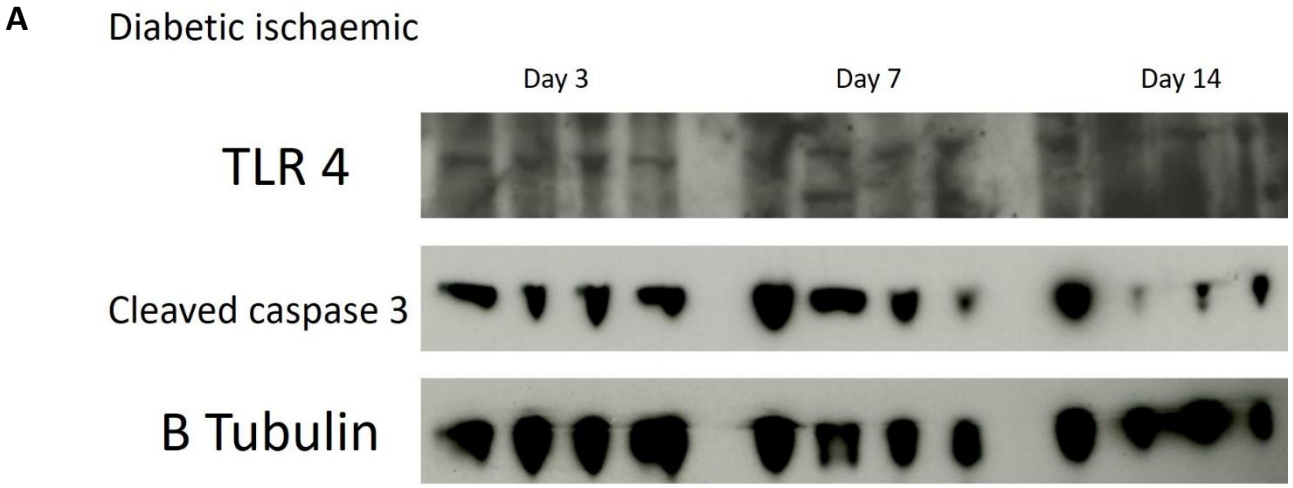

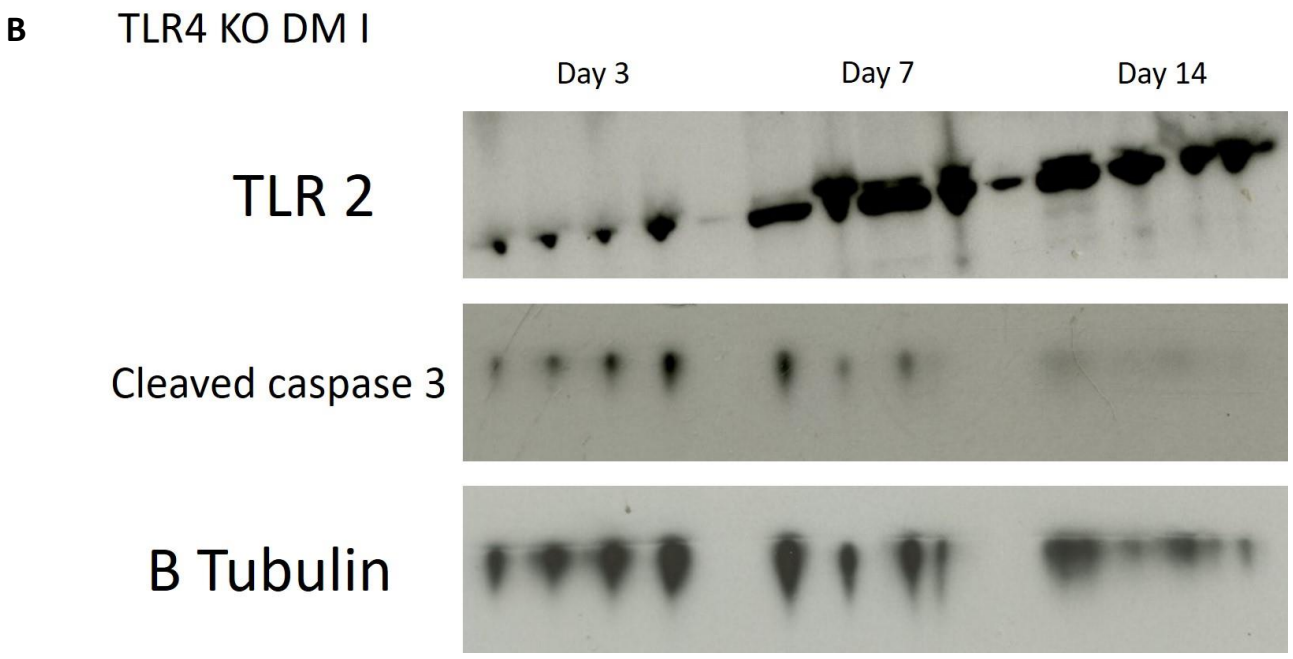

Figure 6.4.7 Increased TLR expression appears sustained to day 14 post wounding

Figure 6.4.7 **A** Western blot analysis comparing TLR4 protein expression and cleaved caspase 3 at days 3, 7 and 14 post skin wounding in wild-type diabetic ischaemic animals. It appears that TLR4 expression is maintained with comparable protein density bands observed at days 3, 7 and 14. Cleaved caspase 3 protein concentration appears to be greatest at days 3 and 7, with an observed decrease in protein band intensity by day 14, however no statistical analysis or densitometry comparisons can be performed due to lack of repeat data. **B** Western blot analysis comparing TLR2 protein expression and cleaved caspase 3 at days 3, 7 and 14 post skin wounding in TLR4 knock-out diabetic ischaemic animals. TLR2 appears to be readily expressed by the TLR4 endogenously deleted animals. TLR2 expression was greater at day 7 compared to day 3 and was sustained to day 14. Cleaved caspase 3 protein concentration appeared to be greatest at day 3. It had largely disappeared by day 14. Further conclusions and statistical measurements cannot be applied due to the unavailability of experimental repeats.

Both TLR4 in wild-type animals and TLR2 in TLR4 -/- animals appeared to be readily expressed. Expression was consistent throughout the duration of the experiment, possibly indicating the activation effect of ischaemia induction and wounding results in an upregulation of the receptors, subsequently sustained to at least 14 days. Further work is necessary to corroborate this. TLR2 expression appeared to peak at day 7 (figure 6.4.7 **B**), which may suggest a lag phase in TLR2 upregulation, however without further experimental repeats no firm conclusions can be drawn from this result. In diabetic ischaemic skin samples, the apoptosis marker cleaved caspase 3 appeared to decrease by day 14 (figure 6.4.7 **A**), an effect also observed in the TLR4 knock out samples at day 7 (figure 6.4.7.**B**). By day 14 cleaved caspase 3 protein was largely undetectable. This correlates to the pattern of wound healing demonstrated in figure 6.4.5 **A** and **B**.

6.5 Discussion

The aim of this chapter was to establish a murine model of chronic ulceration that closely resembles the non-healing foot ulcers commonly found in diabetic patients with concomitant ischaemia. This is an essential first process in the testing of novel therapeutic targets such as TLR4 inhibitors, prior to translation into first in human trials. Our murine diabetic ischaemic ulceration model was therefore chosen to be as close to the human pattern of disease as possible.

A type 1 phenotype of diabetes was chosen, as the *in vitro* focus had been on high glucose concentrations and thus hyperglycaemia, rather than the potentially confounding factors of insulin resistance or obesity. Likewise, from inception it was our intention to progress to TLR4 knock-out animals, therefore an induced model of type 1 diabetes removed the complexity of creating/obtaining double transgenic strains. The low dose multiple injection STZ regime was selected and written into the project license as it is associated with significantly less morbidity and mortality than the single large dose protocol. The low dose mechanism avoids the organ toxicity and significant initial hypoglycaemic events caused by insulin release during direct chemical destruction of the beta cells (205). The diabetogenic effect is produced by a progressive immune insulitis, and results in a gradual onset of hyperglycaemia better tolerated by the animal.

The strain and gender of the mice are essential to the consistency of the model, as there is considerable variation between strains in susceptibility and response to diabetes induction by STZ (206, 213, 214). Male mice are reported to be more sensitive to STZ and the C56BL/6 strain identified as particularly sensitive to its diabetogenic effects (206). There is also considerable variation between strains in the recovery from induction of hindlimb ischaemia, with C56BL/6 mice exhibiting a greater degree of pre-existing collateral vessels, resulting in less extreme ischaemia following femoral artery ligation (215).

The C56BL/6 strain was used in this model both for the response to STZ dosing and the availability of TLR4 -/- mice with C56BL/6 as the background strain. Male specimens were exclusively sourced. It is reported there is a greater incidence of

female animals of this strain developing dermatitis (141, 142). This was identified as a potential confounding factor within this study, as the outcome focussed primarily on wound healing.

The double ligation model of hindlimb Ischaemia was chosen as the collateral supply through the inferior epigastric artery and profunda femoris provides a pattern of ischaemia more closely reflective of chronic peripheral artery disease. Ligation of the external iliac and excision of the SFA results in severe ischaemia, however in this project it was tolerated well with no animals experiencing limb necrosis or requiring euthanasia. Our research group has used this method previously, having gathered experience of it directly from Dardik's group at Yale university (216).

The methods and schedule employed to measure the successful induction of diabetes were consistent with similar published studies. Significant glycosuria, defined as ++ or greater, was confirmed in all groups by day 21 and was maintained at each time point thereafter (table 6.4.1.2). Tail capillary blood glucose sampling demonstrated no significant difference in the mean measured blood glucose levels between each diabetic group (figure 6.4.1.2). The index figure of 11.1mmol/L for diabetes diagnosis on random non-fasting blood glucose measurement was achieved in all groups by day 28. Mean capillary blood glucose levels increased at each time point, until a plateaux was achieved at day 7 post op (day 42 post first STZ dose). This observation is consistent with the multiple low dose STZ regime, where STZ initiated immune-mediated insulitis causes gradual and progressive beta cell destruction, leading to rising CBG levels (205).

There appeared to be a post-operative peak in CBG in the diabetic ischaemic group observed on day 3 post op (table 6.4.1.2). This may represent a stress response following the trauma of hindlimb ligation and skin wounding, not seen in the diabetic non-ischaemic and TLR4 knock-out groups, possibly due to the exaggerated pro-inflammatory effect of diabetes and ischaemia.

Weights did not differ between control groups however TLR4 knock-out animals were significantly heavier (figure 6.4.2.1) and older (56 weeks vs 12 weeks) than wild-type controls. Post-dosing there was no-significant reduction in weight, with all

groups except TLR4 knock-outs gaining weight. There is no data to explain this observation, specifically in this group currently available in the literature. Pre-dose fasting is associated with significantly greater weight loss post STZ than non-fasted groups (217), however in this study all groups had free access to standard chow and water throughout. The effect of age on post-STZ weight loss has been examined in the C56BL/6 strain, where females aged 18 months were compared to 9-month-old individuals with no difference in weight observed between groups (218). At 9 months old however the control group in that study is considerably older than the 12-week-old wild-type group used in this project. It remains possible the sustained post STZ dosing weight loss effect observed in the aged TLR4 knock-out group is due to age rather than their transgenic status.

In wild-type animals, diabetes and hindlimb ischaemia was associated with a significant impairment in distal limb wound healing (figure 6.4.4 **A**). No individual in this group had achieved complete wound closure by day 14 ($p=0.03$). In comparison, all individuals in the diabetic non-ischaemic and the non-diabetic ischaemic group healed by day 14. Non-diabetic non-ischaemic mice achieved 100% wound closure by day 7 (figure 6.4.4 **B**). This provided adequate validation of this experimental protocol as a suitable murine model of impaired wound healing in diabetic ischaemic distal limb ulceration.

Identical experimental protocol was employed using a cohort of aged (56 weeks) male TLR4 deleted mice on a background strain of C56BL/6 with identical 4mm wounds inflicted. At each time point post wounding, wound area had significantly reduced in the diabetic ischaemic TLR4 knock-out group compared to the diabetic ischaemic wild-type group. Despite comparable mean CBG levels and identical patterns of hindlimb ischaemia between the two groups, all wounds had healed in the TLR4 KO cohort by day 14. Diabetic non-ischaemic wounds inflicted on the contralateral limb achieved 100% healing by day 7, comparable to the non-diabetic non-ischaemic wild-type control group (figure 6.4.5 **A**). This represents a considerable improvement in wound healing in diabetes irrespective of ischaemia. We therefore conclude that endogenous TLR4 deletion confers a beneficial effect on wound healing, but particularly in diabetic ischaemic conditions.

Protein analysis from skin tissue homogenates taken from the distal hindlimb suggested an increase in TLR4 expression and apoptosis in diabetic ischaemic tissue compared to diabetic non-ischaemic tissue, TLR4 KO animals did not express TLR4 (figure 6.4.6). While completely expected this was important to demonstrate, for both confidence in the KO animal, and to act as a negative control against the DM I and DM N groups. Apoptosis also appeared to be reduced in the TLR4 KO group compared to wild-type controls. Unfortunately, no firm conclusions can be drawn from this data and no statistical analysis possible due to the lack of experimental repeats. Irreversible physical loss of these irreplaceable protein samples has prevented the completion of necessary and desired repeat experiments. The trends presented however, are compelling.

The temporal trend in TLR4 expression was examined in the diabetic ischaemic wild-type cohort (figure 6.4.7 **A)**. It appeared that TLR4 was consistently expressed across all three time points, suggesting TLR4 upregulation is maintained out to at least day 14. The apoptosis marker cleaved caspase 3 appeared to be uniformly expressed at days 3 and 7, with a possible decrease in concentration by day 14. This correlates closely with the clinical appearance of the wounds (figure 6.4.4 **A**).

The same temporal trend was explored in the TLR4 KO cohort (figure 6.4.7 **B**). Cleaved caspase 3 concentration appeared to be reduced at each time point compared to wild-type, becoming weakly detectable by day 14, suggesting near complete resolution of apoptotic processes consistent with a healed wound. TLR2 expression was examined in this TLR4 KO population, as the possibility of a compensatory upregulation of TLR2 was of interest. It appeared TLR2 expression did not peak until day 7 and remained consistently expressed thereafter. The trend proposed by these observations is of a delayed but sustained increase in TLR2 expression. Further work is necessary to explore this further. As with figure 6.4.6, the lack of experimental repeats precludes substantial conclusions from this data.

A significant limitation with the conclusions from the *in vivo* studies presented in this chapter is the lack of corroborating evidence from histological studies. During the study design phase ulcer tissue collection post mortem was intended to be a crucial area of study in determining both the cellular components of inflammation through

H&E staining and receptor level examination using immunohistochemistry. Likewise, histological comparison between the human tissue biopsies presented in figure 3.4.1 and murine ulcerated skin would have given further credibility to the use of this model as an accurate representation of human disease. Ulcerated skin from every individual was excised post mortem and mounted on filter paper backing to maintain tissue architecture, before being placed in formalin. Unfortunately, the loss of these precious and irreplaceable samples has precluded the completion of this highly desirable aspect of the project. We aim to obtain this data in the future through further projects that utilise this model.

The lack of availability of age-matched knock out individuals was another limitation of this project. The considerable age difference between the wild-type and TLR4 knock-out animals potentially had an attenuating effect on the improvement in wound healing seen in the KO group. As discussed above, a study comparing 9 and 18-month-old STZ induced diabetic animals demonstrated significantly increased levels of oxidative stress in the aged group (218). Likewise, data from our own research group comparing the recovery from hindlimb ischaemia between aged and non-aged cohorts demonstrated a significantly impaired development of collateral circulation and hence capacity for ischaemia recovery in aged animals (216). The dramatic improvement in wound healing demonstrated by the TLR4 cohort is likely to be even more significant than these results report given their aged related disadvantages.

The choice of the multiple low dose STZ regime has been discussed previously in this chapter. It is considered to be a closer appropriation of autoimmune type 1 diabetes and avoids the considerable toxicity and mortality associated with the high dose protocol. There have been reports however of pancreatic beta cell recovery after STZ dosing, resulting in restoration of insulin secretion (219). This occurred following beta islet transplantation and became evident after removal of the transplant graft after 120 days. The mice presented in his chapter received no insulin replacement or any form of exogenous glycaemic control and were sacrificed at days 38 to 49 post first STZ dose. Peri mortem CBG measurement confirmed their ongoing diabetic status.

A significant limitation to using mouse surrogates to model human peripheral artery disease is the considerable collateralisation potential and recovery post ischaemia induction these animals possess. The surgical models for the creation of hindlimb ischaemia also lack the contributary adverse effects on the individual that other atherosclerotic risk factors such as hypertension, dyslipidaemia, age, family history and smoking pose in real-world disease. Some of these risk factors can be explored with the use of specific strains and enriched food, animal models, while essential for testing concepts in a pre-clinical setting, cannot guarantee translation to successful therapies in patients.

6.6 Summary

A murine model of progressive type 1 diabetes / hyperglycaemia and peripheral limb ischaemia results in significantly impaired wound healing and the creation of a non-healing lower limb wound at day 14. In this project, despite being considerably older, endogenously deleted TLR4 transgenic mice exhibited significantly improved wound healing in the same diabetic ischaemic conditions, suggesting a potential therapeutic benefit of TLR4 antagonism in chronic diabetic wounds.

This gives further evidence for the involvement of innate immune pattern recognition receptors in the pathogenesis of micro and macro vascular complications of diabetes, through their upregulation and activation, leading to excessive inflammation.

Chapter 7

General discussion and further work

7.1 General discussion

This thesis presents the results and conclusions of an *in vitro* and *in vivo* project designed to study the role of toll-like receptor 4 in diabetic foot ulceration. The project was in three parts.

Human tissue samples from ulcerated and intact, non-ischaemic skin from diabetics and non-diabetics were collected from patients undergoing major amputations for comparison of inflammatory cell infiltration, TLR4 expression and tissue distribution of TLR4.

In vitro, the effects of a high glucose environment and hypoxia on primary cultured human dermal fibroblasts were tested, along with the effect of those conditions on TLR4 expression, function and activation, by utilising selective inhibitors. Functional cell processes essential to wound healing such as migration, proliferation and contraction were tested in fibroblasts subjected to the simulated diabetic ischaemic conditions.

An *in vivo* model of wound healing was created to examine the effects of induced type 1 diabetes and surgical hindlimb ischaemia on distal limb ulceration. It was utilised to compare endogenously deleted TLR4 -/- mice with wild-type controls.

7.1.1 Diabetic foot ulceration

Diabetes is associated with the development of micro- and macro-vascular complications which carry considerable morbidity and mortality. Macrovascular complications include accelerated atherosclerosis, manifest as coronary artery

disease, cerebro-vascular disease and peripheral arterial disease. Microvascular complications include neuropathy, retinopathy and nephropathy (220). Having diabetes confers a 15-20% lifetime risk of developing foot ulceration and leads to a 20 times greater risk of major amputation compared to non-diabetics (18, 52).The development of foot ulcers is multifactorial, involving infection, trauma, micro- and macro-vascular insufficiency, immunological dysfunction and neuropathy (51, 221). Treatment consists of managing the predominant causes such as wound bed debridement, infection control, revascularisation and off-loading of the wound (221, 222). Despite current best medical and surgical intervention, 33% of these ulcers will fail to heal (223).

7.1.2 Wound healing

Wound healing in diabetes is significantly impaired with the observation that wounds fail to progress through the normal physiological phases of healing, often becoming stalled in the inflammatory phase (224). These wounds are characterised by excessive inflammation, with significantly prolonged and sustained neutrophil and macrophage infiltration observed (53). In addition to the cellular components, the hyper-inflammatory environment also comprises a dramatic increase in the release of pro-inflammatory cytokines IL-6, TNF-α and IL-1β and matrix metalloprotease (MMP) production (224). This results in exaggerated destruction of the extracellular matrix, impairment in granulation tissue formation and dysfunction of other processes crucial to healing such as fibroblast migration and proliferation, and collagen synthesis (224).

7.1.3 Toll like receptor 4

Diabetes is now widely considered a systemic pro-inflammatory condition. There is compelling evidence this effect is mediated through pattern recognition receptors of the innate immune system (89). In particular, TLR4 has been implicated in the systemic pathogenesis of diabetes and its complications particularly cardio-vascular

disease, retinopathy, neuropathy and nephropathy (163, 225). TLRs are key PRRs of the innate immune system, they activate through recognition of exogenous microbial components termed pathogen associated molecular patterns (PAMPS) (91). Binding PAMPS leads to activation of downstream signaling pathways, ultimately resulting in the release of pro-inflammatory cytokines such as IL-6 and TNF-α (97). In addition to the PAMPs, TLRs are also activated by a variety of host derived endogenous ligands termed damage associated molecular patterns (DAMPs). These are usually hidden from immune recognition but are exposed by tissue damage alerting the innate immune system to injury (98). The resulting inflammatory response is a physiological mechanism for the recruitment of immune cells and stimulation of the normal process of wound healing (98).

7.1.4 Human tissue

We observed increased inflammatory cell infiltrate in the diabetic-ischaemic human skin samples compared to non-ischaemic and non-diabetic samples. Morphological changes in both diabetic ulcerated and non-ulcerated tissues were also seen, such as peri-capillary tissue thickening. These observational studies provide supportive evidence for the hyperinflammatory and pathological nature of the healing process in diabetes, through the excessive and prolonged infiltration of innate immune cells such as neutrophils and macrophages, and absence of normal granulation tissue formation.

Immunohistochemistry studies demonstrated increased TLR4 expression in diabetic-ischaemic skin tissues when compared to the other groups. This is consistent with the hypothesis implicating TLR4 with the exaggerated cellular inflammation found in diabetes. The distribution of TLR4 expression concentrated within keratinocytes, endothelial and inflammatory cells is consistent with cell types known to freely express TLR4.

7.1.5 TLR4 activation and downstream pathway

High glucose conditions induced significant TLR4 protein expression in primary cultured human dermal fibrobasts in a dose-response fashion. The addition of hypoxia significantly increased TLR4 expression, signalling and activation. This was evident through increased MyD88 expression and NFkB activation, resulting in increased levels of caspase-3 and IL-6. These effects were inhibited by the addition of a specific TLR4 antibody and inhibitor, which also resulted in a decrease in the potent TLR4 endogenous ligand, HMBG1.

This data provides evidence for the mediation of the pro-inflammatory effect of high glucose and hypoxia signalling and actioning via TLR4 pathways, leading to increased and excessive inflammation via downstream production of cytokines such as IL-6.

A potential mechanism for this pathological hyperinflammatory effect in diabetes is through the release of pro-inflammatory cytokines via TLR4 activation. The subsequent recruitment of the innate immune cellular response results in further tissue damage and cellular apoptosis and the release of damage associated molecular patterns (DAMPS) such as HMGB1. These DAMPS act as potent ligands for ongoing TLR4 activation, resulting in the release of further pro-inflammatory cytokines, perpetuating a dysregulated positive feedback cycle of tissue damage-inflammation-tissue damage.

7.1.6 Functional consequences of TLR4

High glucose conditions led to an increase in fibroblast proliferation. There is conflicting evidence in the literature regarding the effects of high glucose and ischaemia when applied separately on fibroblast proliferation (191-197). In this study proliferation was significantly inhibited by the combination of high glucose and hypoxia. Contraction was non-significantly increased in hypoxic conditions irrespective of glucose environment. TLR4 inhibition did not influence contraction, leading to the conclusion that differentiation of fibroblasts into myofibroblasts occurs independently of TLR4 signalling.

Fibroblast migration was significantly impaired by combined high glucose and hypoxia, and this effect was ameliorated by the addition of a selective TLR4 antibody or inhibitor and MyD88 inhibitory peptide. The mechanism for this effect however remains uncertain. One study observed migration was impaired in fibroblasts cultured from diabetic animals in hypoxia and suggested this was due to increased oxidative stress (189). It is therefore possible that through this mechanism, inhibition of TLR4 mediated inflammation results in reduced oxidative stress.

Unexpectedly, migration was improved in high glucose conditions. This outcome was very consistent. Multiple biological and temporal repeats using at least 3 separate lines of primary cultured fibroblasts produced remarkably similar results, contrary to several published studies. One study reported inhibited migration in cultured fibroblasts at treatment glucose concentrations of 40mM, which far exceeds the treatment dose utilised in this project of 25mM (201). Another reported an inhibition of migration at 30mM glucose, however they evaluated a 3-day treatment exposure period, in comparison to the 24 hours in this project (195). The difference in observation between our project and others in the literature may therefore be a consequence of dose, exposure time and experimental protocol.

7.1.7 In vivo model of diabetic ischaemic ulceration

In vivo, the creation of hindlimb ischemia in induced type I diabetic mice resulted in significantly impaired wound healing compared to control conditions, and the formation of a non-healing wound at day 14. TLR4 knock out mice exhibited significantly improved wound healing at each time point in the same diabetic ischaemic conditions. This observation complements the results described in the *in vitro* studies and is consistent with the conclusion that exaggerated TLR4 mediated inflammation results in impaired wound healing.

7.1.8 Implications of this project

In this project, crucial aspects of both the pathological effect of high glucose and hypoxia *in vitro* and impaired diabetic ischaemic wound healing *in vivo* were ameliorated by inhibition or endogenous deletion of TLR4. We suggest this occurs via a reduction in the local and systemic hyper-inflammatory response that is observed in diabetic wounds.

TLR4 and TLR2 knock out has previously been shown to have a protective effect on wound healing in diabetic animals (122, 123). The data from this project suggests this beneficial effect also persists when ischaemia is applied, simulating the hyperglycaemic, locally ischaemic micro-environment of a diabetic foot wound.

This apparent synergistic effect between the innate inflammatory reaction to high glucose and hypoxia has significant clinical consequences. In addition to impaired wound healing, diabetic patients are observed to have poorer outcomes in other ischaemic pathologies such as acute myocardial infarction (226) and cerebro-vascular accident (227). This observation has led to the proposal of a two-hit hypothesis for the inflammatory basis of the clinical complications of diabetes. The process requires a subclinical 'priming' phase in diabetics of hyperglycaemia resulting in chronic low-grade inflammation and upregulated TLR4 expression. A second noxious stimulus such as infection, ischaemia or trauma, then triggers a significant TLR4 mediated response. TLR4 activation following injury is however an important physiological mechanism (91), with endogenous ligands such as HMBG1 released during tissue damage act as 'alarm signals' to precipitate a TLR mediated inflammatory response, recruiting innate immune cells and stimulating tissue healing.

In diabetes, the normal physiological healing process is instead characterised by pathological hyper-inflammation, preventing the progression of the normal phases of wound healing. TLR4 antagonism therefore presents a novel therapeutic target in diabetic ischaemic pathologies in both acute and chronic conditions.

The mechanism of how hyperglycaemia leads to TLR4 up-regulation remains uncertain. There is evidence high glucose induces TLR 2 and 4 expression through

increased oxidative stress, via the activation of protein kinase C (PKC) and NADPH oxidase activity (134). There is also considerable overlap and convergence between TLRs 2 and 4, and receptors for the advanced glycosylated end-products (RAGE), which utilise common signalling pathways to activate NFkB dependent gene expression (228). RAGEs are PRRs activated by a variety of ligands including advanced glycosylated end-products (AGE). These are protein, nucleic acid and fatty acid products produced non-enzymically in pro-oxidative environments, whose formation is accelerated by exposure to high glucose (228).

A number of highly potent endogenous ligands such as HMGB1 and S100 are common to TLRs 2 and 4 and RAGE (229). NFkB activation results in increased expression of TLR4 and TLR2, and it has been observed that TLR4 activation increases expression of TLR2 in endothelial cells (165). It is therefore possible that cross-talk between TLR2, TLR4 and RAGE and co-activation by ligands such as HMGB1 result in the over-expression of these pro-inflammatory receptors by high glucose.

The ultimate purpose of this project was not just to identify a potential mechanism for the hyperinflammatory destructive reactions that are observed in diabetic foot disease, but also the translation of this understanding into a genuine intervention for use in clinical practice. The poor healing outcomes, particularly in the diabetic patients with co-existent peripheral arterial disease requires the development of novel adjunctive therapies. The development of an off-the-shelf product such as a TLR4 antagonist treated dressing, which can be applied by community nurses, stable at room temperature and is readily available to patients in any part of the world, however inaccessible remains the goal.

7.2 Limitations

Specific experimental limitations are explored in more detail in the discussion section of each chapter.

The interpretation of immune cellular inflammation, TLR4 intensity and distribution in the human tissue analysis, is undoubtedly influenced by external variables not specifically controlled for in sample collection. Factors such as medications and doses, particularly of drugs known to modulate TLR4 function such as ACE inhibitors and statins were not matched between groups due to the small sample size. Similarly, the infection status of the ulcerated areas prior to amputation was not explored. Although biopsy samples were purposely taken away from areas of infection, the effect of bacterial colonisation is unclear. Infection, like ischaemia and trauma will result in activation of TLR4 inflammatory pathways.

A crucial piece of data missing from these results are the quantification of protein concentrations through Western Blot. Tissue samples were collected as a full-thickness skin biopsy sample from the amputated limbs in the same manner as histology samples, and immediately snap frozen in liquid nitrogen and stored in -80°C. Unfortunately, after tissue homogenisation and standardisation no results were obtained from multiple Western blot attempts. The failure of the protein quantification experiments almost certainly lies in the significant degradation of the proteins that occurred during both the storage, thawing and homogenising processes. These samples were collected over a period of 18 months and should have been prepared shortly after collection to avoid the damaging effect of prolonged storage.

Results from *in vitro* studies of the effect of high glucose and hypoxia on TLR4, its signalling pathway and endogenous ligands were presented as semi quantitative concentrations of protein expression rather than RNA RT-PCR. This was due to the consistency of band intensity patterns found on western blot, and the conclusion that gene transcription must also be increased as the protein expression is increased. The functional protein-level consequence of the exposure to study variables provides more information as post-transcriptional changes are also possible. Comparable

studies utilising similar experimental protocols in monocytes (134) and gingival fibroblasts (135) presented the effect of increasing glucose concentration on TLR4 gene expression and markers of its activation, and not the combination of high glucose and hypoxia represented in our study, which we have demonstrated results in a greater effect.

The exploration of the TLR4 downstream signalling mechanism presented in this study are only in the context of the migration assays. The inhibitory peptides were tested utilising the same methodology as that presented in figure 4.5.9, however experimental repeats yielded inconsistent protein concentrations after cell lysis and therefore shed doubt on the validity of these results. Subsequent repeat experiments remained inconclusive. Further work is necessary to re-examine these pathways in greater detail, however in this project time constraints meant TLR4 rather than its downstream mechanisms remained the priority and focus.

The TNFα and IL8 concentration measured by ELISA as illustrated in figure 5.4.2 was more variable and of a lower magnitude than that of IL6. The multicytokine array (figure 5.4.1) highlighted IL6 and IL8 as the significant cytokines produced by test populations of dermal fibroblasts, with TNFα produced to a comparatively minor degree. TNFα is cytokine known to be associated with TLR4 activation and signalling (170); it is therefore surprising its release under the same test conditions did not match that of IL6. It is possible this effect was artefact and a consequence of insufficient experimental repeats.

A significant limitation of the animal studies is the unfortunate lack of histological data on the density and duration of inflammatory cell infiltration. This was explored in chapter 3 in the human tissue samples and was intended to give further validation to this as a suitable small animal model of the human pattern of disease. Likewise, the comparison between wild-type and TLR4 would have provided crucial evidence regarding the cellular component of inflammation, possibly strengthening the evidence for the absence of TLR4 mediated inflammation as the mechanism for the significant improvement in wound healing observed. The loss of these irreplaceable

skin wound samples occurred as a consequence of an unavoidable prolonged absence from the lab and not technical or experimental failure.

The accuracy of mouse surrogates to model human peripheral artery disease is limited by the considerable collateralisation and rapid recovery following ischaemia induction these animals develop. More drastic ischaemia models can lead to extensive tissue loss, necrosis and autophagy and therefore a balance between rapid recovery and loss of the animal through euthanasia is necessary. The surgical models for the creation of hindlimb ischaemia also lack the systemic and multiorgan effects that long-term exposure to atherosclerotic risk factors such as hypertension, dyslipidaemia, age, family history and smoking pose in real-world disease. Some of these risk factors or their combinations can be included in the development of an atherosclerosis model. Due to these limitations, animal studies while essential for testing concepts in a pre-clinical setting, cannot guarantee translation to successful therapies in patients.

7.3 Further work

There are multiple areas of ongoing interest generated by this project. Some such as the mouse hindlimb histology analysis will be repeated during future projects with similar experimental design. Other interesting questions posed, but not explored due to time constraints include further examination of the effect of high glucose and hypoxia on TLR2 and RAGE receptors. These PRRs of the innate immune system are of considerable interest when contemplating the potential mechanism for the effect of high glucose and hypoxia on TLR4, and further dedicated study regarding their role is certainly warranted.

A specific focus on the endogenous ligands of TLR4 is also highly desirable to further examine the proposed underlying mechanism. Time constraints precluded further investigation of the other potent endogenous ligands of TLR4, TLR2 and RAGE, DAMPs such as HSP and S100 (230).

As mentioned above in section 7.2, re-examination of the TLR4 downstream signalling pathway is desirable to gain a better understanding of the role of MyD88 and TRIF in this process, including the potential of an additional therapeutic opportunity in the inhibition of down-stream signalling apparatus such as NFkB, given this pathway is common to TLR2 and RAGE, in addition to TLR4.

The purpose of this project was to ascertain the role of TLR4 in chronic non-healing diabetic wounds and to establish whether there is a therapeutic benefit to its inhibition. TLR4 knock out animals were therefore chosen as the first step to determine proof of concept. The next step is to utilise this model to administer TLR4 antagonists or inhibitors to the diabetic-ischaemic mouse wound. This is one of the priorities for subsequent projects and studies are already underway within our group to determine the optimum delivery method for TLR4 inhibitors. Potential mechanisms currently being explored by our biomaterials group include the use of polymer mesh scaffolds.

Given the systemic effect of hyperglycaemia, and the widespread expression of TLR4 by multiple cells types in tissues and organ beds throughout the body, there may ultimately be therapeutic potential in diabetes for systemic TLR4 inhibition in the prevention of micro- and macrovascular complications. This will certainly require further study. Projects aimed at examining the systemic effects of chronic ulceration are also needed and are in the design phase.

7.4 Conclusion

The clinical impact of this study goes beyond the introduction of an adjunctive therapy for chronic diabetic wounds. It provides evidence and potential mechanism for the excessive and destructive inflammatory processes seen in clinical practice associated with poorly controlled diabetes. This phenomenon is not limited to diabetes and ischaemia. Trauma and infection in diabetes, even with normal vascular supply, produces similarly destructive consequences. The addition of ischaemia only adds further significant challenge to successful wound healing.

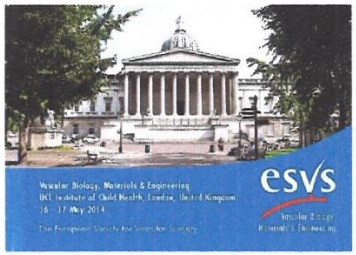

The Scientific Evaluation Committee of the European Society for Vascular Surgery at the Spring Meeting, London 16-17 May 2014 has awarded the

Oral Presentation Prize

to

Mark J. Poston

For the paper:

Hyperglycaemia exaggerates ischaemia induced tissue damage in dermal fibroblasts through MyD88 dependant Toll like receptor 4 activation

Janice Tsui

Thomas Schmitz-Rixen

17 May 2014

From: ESVS Secretary <esvs.secretary@btconnect.com>
Subject: World Federation Meeting in Cape Town
Date: Wed, 18 Jun 2014 11:53:09 +0100
To: <carla.kloeze@catharinaziekenhuis.nl>, <mjportou@doctors.org.uk>
Cc: 'ESVS administration' <administration@esvs.org>

Dear Carla and Mark,

I am writing to you about the World Federation Meeting in Cape Town, South Africa, in October (www.wfvscongress2014.co.za/) .

Amongst others, the ESVS is sponsoring two talks at the meeting to be given by presenters in prize sessions at our annual meeting in Budapest last year and at the Spring Meeting in London this year.

We would very much like to invite you to present your papers:

MJ Portou	Hyperglycaemia exaggerates ischaemia induced tissue da dermal fibroblasts through MyD88 dependant Toll-like r activation
Carla Kloeze, MSc; Elisabeth G. Klompenhouwer, MD; Peter Brands, MSc; Marc R.H.M. van Sambeek, MD, PhD; Philippe.W.M.Cuypers, MD, PhD; prof. Joep.A.W. Teijink, MD, PhD	Significant dose reduction during EVAR procedures by t disposable radiation absorbing surgical drapes

at the meeting, where you are asked to speak for 10 minutes each. Where the topic is not clinical you are asked to describe how your work can be translated into clinical practice.

ESVS will arrange and pay for a return economy flight to Cape Town, registration and accommodation for the meeting.

We hope you will join us in Cape Town, and look forward to hearing from you as soon as possible.

Best wishes,

Simon Parvin

Secretary General

European Society for Vascular Surgery

esvs

A leader in promoting optimal care for patients with vascular disease by supporting high quality research, providing educational opportunities, organising meetings, seminars, lectures, conferences and sponsoring the European Journal of Vascular and Endovascular Surgery.

B: Presentations/ Abstracts

Portou MJ, Yu R, Abraham D, Baker D, Tsui J. Hyperglycaemia induces increased TLR expression in human skin cells. Poster presentation at the ESVS Spring Meeting 2013, Frankfurt, Germany, May 2013.

Portou MJ, Yu R, Abraham D, Baker D, Tsui J. (2014) Toll-like receptor R antagonism significantly improves fibroblast migration in simulated diabetic ischaemic conditions. Oral presentation at the Society of Academic and Research Surgery meeting, Cambridge, January 2014.

Portou M, Yu R, Shi-wen X, Abraham D, Hamilton G, Baker D, Tsui J (2014). Hyperglycaemia results in an exaggerated response to ischemia in human dermal fibroblast through MyD88 dependant toll-like receptor 4 activation. Poster presentation at the ATVB Scientific Sessions 2014, Toronto, Canada. May 2014.

Portou M, Yu R, Shi-wen X, Abraham D, Hamilton G, Baker D, Tsui J (2014). Hyperglycaemia exaggerates ischemia-induced tissue damage in dermal fibroblast through MyD88 dependant toll-like receptor 4 activation. Oral presentation at the ESVS Spring meeting, London, May 2014. Winner of best oral presentation prize.

Portou MJ, Yu R, Shi-wen X, Abraham D, Baker D, Tsui J. Diabetes mellitus exaggerates ischaemia-induced inflammation and subsequent tissue damage. Poster presentation at the Vascular Society Annual Scientific meeting, Glasgow, November 2014.

Portou M J, Yu R, Shiwen X, Abrahams D, Hamilton G, Baker D, Tsui J. Hyperglycaemia exaggerates ischaemia induced tissue damage in dermal fibroblasts through MyD88 dependant Toll-like receptor 4 activation. World Federation of Vascular Societies, Stellenbosch, Cape Town. 2014.

Portou MJ, Yu R, Shi-wen X, Abraham D, Hamilton G, Baker D, Tsui J. Endogenous Toll-like receptor 4 deletion significantly improves wound healing in a murine model of diabetic-ischaemic ulceration. Oral presentation at the ESVS Spring meeting, Frankfurt, May 2015.

Published abstracts

Portou MJ, Yu R, Abraham D, Baker D, Tsui J. (2014) Toll-like receptor 4 antagonism significantly improves fibroblast migration in simulated diabetic ischaemic conditions. *British Journal of Surgery* 101, (S4), 33.

Portou MJ, Yu R, Shi-wen X, Abraham D, Hamilton G, Baker D, Tsui J. (2014) Hyperglycemia results in an exaggerated response to ischemia in human dermal fibroblasts through MyD88 dependent Toll-like receptor 4 activation. *ATVB* 34, A210.

Portou MJ, Yu R, Shi-wen X, Abraham D, Hamilton G, Baker D, Tsui J. (2014) Hyperglycaemia exaggerates ischaemia induced tissue damage in dermal fibroblasts through MyD88 dependant Toll-like receptor 4 activation. *European Journal of Vascular & Endovascular Surgery* 47, 697-8.

Portou MJ, Shi-wen X, Abraham D, Hamilton G, Baker D, Tsui J. (2015) Diabetes mellitus exaggerates ischaemia induced inflammation and subsequent tissue damage. *British Journal of Surgery* 102 (S2), 17.

Published Manuscripts

Portou M J, Baker D, Abraham D, Tsui J. The innate immune system, toll-like receptors and dermal wound healing: A review. *Vascular pharmacology*. 71 (2015) 31-36.

Kanapathy M, Portou M J, Tsui J, Richards T. Diabetic foot ulceration in conjunction with lymphoedema- pathophysiology and treatment. *Chronic wound care management and research*. June 2015:2 1-8.

Portou MJ, Yu R, Baker D, Shiwen X, Abraham D, Tsui J. Hyperglycaemia and ischaemia impair wound healing via toll-like receptor 4 pathway activation. *European Journal of Vascular & Endovascular Surgery.* Submitted (2019). Manuscript number EJEVS13226R.

C: Publications

Vascular Pharmacology 71 (2015) 31–36

Contents lists available at ScienceDirect

Vascular Pharmacology

journal homepage: www.elsevier.com/locate/vph

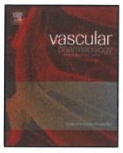

Review

The innate immune system, toll-like receptors and dermal wound healing: A review☆

M.J. Portou [a,*], D. Baker [a], D. Abraham [b], J. Tsui [a]

[a] Royal Free Vascular, Division of Surgery and Interventional Science, Royal Free Campus, UCL, London, UK
[b] Centre for Rheumatology and Connective Tissue Disease, UCL, London, UK

ARTICLE INFO

Article history:
Received 16 November 2014
Received in revised form 5 February 2015
Accepted 8 February 2015
Available online 11 April 2015

Keywords:
Wound healing
Innate immune system
Diabetes

ABSTRACT

Wound healing is a complex physiological process comprised of discrete but inter-related and overlapping stages, requiring exact timing and regulation to successfully progress, yet occurs spontaneously in response to injury. It is characterised by four phases, coagulation, inflammation, proliferation and remodelling. Each phase is predominated by particular cell types, cytokines and chemokines. The innate immune system represents the first line of defence against invading microorganisms. It is entirely encoded with the genome, and comprised of a cellular response with specificity provided by pattern recognition receptors (PRRs) such as toll-like receptors (TLRs). TLRs are activated by exogenous microbial pathogen associated molecular patterns (PAMPs), initiating an immune response through the production of pro-inflammatory cytokines and further specialist immune cell recruitment. TLRs are also activated by endogenous molecular patterns termed damage associated molecular patterns (DAMPs). These ligands, usually shielded from the immune system, act as alarm signals alerting the immune system to damage and facilitate the normal wound healing process. TLRs are expressed by cells essential to wound healing such as keratinocytes and fibroblasts, however the specific role of TLRs in this process remains controversial. This article reviews the current knowledge on the potential role of TLRs in dermal wound healing where inflammation arising from pathogenic activation of these receptors appears to play a role in chronic ulceration associated with diabetes, scar hypertrophy and skin fibrosis.

Contents

1. Introduction

Wound healing is a complex physiological process comprised of discrete but inter-related and overlapping stages, requiring exact timing and regulation to successfully progress, yet occurs spontaneously in response to injury. It is characterised by four phases, coagulation, inflammation, proliferation and remodelling. Each phase is predominated by particular cell types, cytokines and chemokines.

Mammals and higher organisms have evolved complex immune defences against pathogenic microbial organisms in the form of the antibody based adaptive immune system and the innate immune system, a primitive evolutionary cellular based system. Pattern recognition receptors (PRRs) on the cell surface of innate immune cells recognise discrete microbial molecular patterns triggering their activation termed

☆ 'This article is based on a presentation at the 8th International Workshop on Cardiovascular Biology & Translational Medicine held in London in September 2013.'

* Corresponding author at: Royal Free Vascular, Division of Surgery and Interventional science, 9th Floor Royal Free Hospital, Pond Street, London NW3 2QG, UK.
E-mail address: mjportou@doctors.org.uk (M.J. Portou).

http://dx.doi.org/10.1016/j.vph.2015.02.007
1537-1891/

pathogen associated molecular patterns (PAMPS). A group of highly conserved and prime PRRs are toll-like receptors (TLRs). In addition to PAMPs, TLRs also recognise a rage of endogenous self derived molecular patterns released in response to tissue and cellular damage, termed damage associated molecular patterns (DAMPs).

TLRs are expressed by cells comprising the dermis and epidermis of the skin, in addition to the immune cells that reside within the skin or those that are recruited from circulation. The activation and timing of specific TLRs and the presence of conditions affecting TLR expression and activation determine whether TLR activation promotes or inhibits the wound healing process, leading to chronic wounds.

2. Normal dermal wound healing

Immediately following trauma to the skin, platelets aggregate at the site of injury with haemostasis achieved following local vasoconstriction and activation of the clotting cascade, resulting in fibrin clot formation [1]. The inflammatory phase of wound healing begins with release of proinflammatory cytokines such as platelet derived growth factor (PDGF), transforming growth factor (TGF-β), fibroblast growth factor (FGF), epidermal growth factor (EGF) and Interleukin 8 (IL-8/CXCL-8) from the newly formed clot and directly from the damaged tissues [2]. These act as potent chemotactic signals to immediately recruit neutrophils to the wound [3]. Circulating polymorphonuclear neutrophils (PMN) begin migration within minutes from the blood into the immature wound bed formed by the clot, peaking within the first 24 h [4]. The neutrophils now present in the wound provide a crucial defence against microbial invasion following disruption to the skins natural barrier function, clearing both pathogen and tissue debris by phagocytosis [2,5].

The process of platelet de-granulation, activation of the complement cascade, and the migration and signalling of PMNs results in the further production of chemotactic factors such as complement component 5 (C5), fibrin by products and TGF-βc [6]. These chemokines along with chemokine (C-C motif) ligand 5 (CCL5) produced by keratinocytes, recruit monocytes to the wound, which under the influence of local cytokines undergo differentiation to become mature wound macrophages [6,7]. By days three to five following injury, tissue macrophages become the dominant cell type [8]. Wound macrophages continue the process of wound bed clearance through phagocytosis of apoptotic cells including the early phase PMNs, tissue debris and microbial organisms [8]. In addition, macrophages also directly aid the debridement of injured and devitalised tissue through release of protease and metalloprotease enzymes [8,9]. Over and above their phagocytic role, an important initial function of wound macrophages is the release of cytokines which further aid the recruitment and activation of inflammatory cells [2]. As the inflammatory phase progresses, macrophages produce important growth factors such as KGF, TGF-β, VEGF and PDGF which stimulate fibroblast and keratinocyte growth and migration and the process of angiogenesis [1]. It is therefore considered that macrophages are responsible for the transition to the proliferative phase of wound healing [2].

The late inflammatory phase becomes characterised by infiltration of T-lymphocytes under the influence of IL-1, which peak at day 7 after injury. At this stage there is considerable temporal overlap between the late inflammatory, proliferative and early remodelling phases of normal wound healing. [10]. As described, the inflammatory phase involves a well characterised sequence of immune cell infiltration, neutrophils followed by macrophages then finally T-lymphocytes [2].

Like macrophages, T-lymphocytes appear to have a complex yet significant role in the normal process of wound healing, however these processes, functions and pathways remain poorly understood. Studies utilising *In vivo* murine knock-out models have suggested that absent or delayed T-lymphocyte wound infiltration results in an impairment of the healing process [2]. However there appears to be differential roles of CD4+ T helper and CD8+ cytotoxic T cells, with CD4+ cells found to have a positive promoting effect on healing, and CD8+ cells an inhibitory effect [11]. In addition, T-lymphocytes have a regulatory effect on inflammation and fibrosis and a dermal subgroup of gamma delta T cells produce keratinocyte growth factor (KGF) and insulin-like growth factor 1 which stimulate keratinocyte proliferation, promoting healing [12].

Central to the proliferative phase of wound healing is the formation of granulation tissue. Dermal fibroblast proliferation, migration and differentiation (into contractile myofibroblasts) occurs under the influence of growth factors such as fibronectin, PDGF, FGF, TGF-β and C5a, as inflammatory cytokine release diminishes [13]. Fibroblasts are crucial for the production of extracellular matrix comprised of collagen, glycosaminoglycans, proteoglycans, fibronectin and elastin [14]. Angiogenesis occurs as dermal endothelial cells migrate into the newly forming extracellular matrix under the influence of macrophage derived angiogenic factor, forming new capillaries [8].

During the proliferative phase, wound contraction is an important process that occurs through the action of myofibroblasts, differentiated from mesenchymal fibroblast cell lines [15]. Myofibroblasts, unlike fibroblasts express the contractile protein α smooth muscle actin (αSMA) and as the wound matures are gradually lost from the granulation tissue [15].

Restoration of the skins crucial barrier function requires successful epidermal keratinocyte migration, proliferation and differentiation to cover the newly formed granulation tissue and extracellular matrix in a process termed re-epithelialisation [16]. In intact skin, keratinocytes are closely attached to adjacent epithelial cells through desmosomes, and to the extra cellular matrix of the underlying basement membrane by hemidesmosomes [17]. Following injury, keratinocytes become mobilized by undergoing phenotypic changes favouring detachment in a process that remains incompletely understood. However cytokines such as IL-1, IL-6 and TNF-α produced in inflammatory phase seem to help modulate the migratory phenotype of keratinocytes [17]. Migration and proliferation are influenced by growth factors such as IGF1 and epidermal growth factors (EGF) [18]. In addition, EGF, KGF and TGF-β have important pro-migratory or pro-proliferative effects on keratinocytes [17]. Essential to the process of keratinocyte migration is production of proteases such as collagenases and matrix metalloproteases [19]. These degrade adhesions between the keratinocyte and the newly formed extracellular matrix to permit cell movement [16]. Disruption of the basement membrane after injury requires migrating keratinocytes to utilize fibronectin, vitronectin and fibrin components of the provisional extracellular matrix for attachment through focal integrin receptors [16]. Closely following migration is rapid proliferation and basement membrane repair through laminin production [20]. Keratinocyte differentiation and keratin production occurs as the epidermal barrier and normal stratified architecture is restored [21].

The remodelling phase is the longest phase of the wound healing process, continuing for weeks to months [8]. This phase is characterised by reduced proliferation and inflammation, active re-organisation of the extracellular matrix and regression of the newly formed capillaries as the nutrient requirements of the wound site reduce [8].

Type III collagen produced by fibroblasts during the proliferative phase is gradually replaced by structural type I collagen, through the action of collagenases and matrix-metalloproteases [16]. During remodelling, collagen becomes more organised and increasingly cross-linked strengthening the scar; fibronectin disappears, and hyaluronic acid and glycosaminoglycans are replaced by proteoglycans. The result is the re-organisation of the extracellular matrix to an architecture more closely resembling normal tissue [2].

3. The innate immune system and the skin

3.1. The innate immune system

Mammals and other higher vertebrate organisms have evolved complex immune defences against invading pathogenic microorganisms,

comprised of the innate and adaptive immune systems [22]. The innate immune system is in evolutionary terms primitive and unlike the clonal selection antibody-based response of the adaptive immune system, is entirely encoded within the genome [23]. Innate immunity comprises the entire immune response of invertebrate organisms, however in higher species it provides the first line of defence against infectious pathogens and aids adaptive responses through antigen presentation, with the adaptive response concerned with later stages of infection, providing a targeted and specific response and immunological memory [22].

The innate immune system is comprised of numerous different cellular components such as neutrophils, eosinophils, basophils, mast cells, monocytes, macrophages, dendritic cells, NK cells, gamma delta T cells, B-1 cells [24]. Rather than coordinating a non-specific pro-inflammatory or phagocyte response, cell activation, pathogen recognition and a specificity of the innate immunity is conferred by the presence of specific receptors expressed by these immune cells termed pattern recognition receptors (PRRs) [25,26].

3.2. Toll-like receptors

Toll-like receptors (TLRs) are key pattern recognition receptors of the innate immune system [27]. Other examples of PRRs include scavenger receptors (SRs), C-type lectin receptors (CLRs), NOD-like receptors (NLRs) and B2 integrins [26]. These receptors are highly conserved in evolution and recognise discrete molecular components of invading pathogens termed pathogen associated molecular patterns (PAMPs), such as lipids, lipopeptides, proteins and nucleic acids [22,27]. The recognition of microbial PAMPs by PRRs leads to activation of specific signalling pathways and a variety of cell dependent responses, including pro-inflammatory cytokine release, phagocytosis and antigen presentation [26].

The Toll-like receptor family consists of thirteen identified members of which ten are expressed in humans [24]. TLRs are located either at the cell surface (TLRs 1,2, 4, 5, 6) or in the intracellular compartment (TLRs 3, 7, 8, 9) primarily on exosomes and endoplasmic reticulum [28,29]. TLRs are transmembrane proteins consisting of an ectodomain comprising leucine-rich repeats, a transmembrane domain and an intracellular (TIR) domain [28]. The binding of TLR ligands results in activation through the recruitment of specific adaptor molecules such as myeloid differentiation factor 88 (MyD88), MyD88 adaptor like (MAL), TIR domain-containing adapter-inducing interferon-β (TRIF) and TRIF adaptor molecule (TRAM) to the intracellular domain [28,30]. All TLRs except TLR3 utilize one of two signalling pathways, the MyD88 dependent and MyD88 independent (TRIF) pathways, resulting in the activation of nuclear transcription factors such as NFkB, JNK and MAPK [28]. TLR3 signals solely through the TRIF pathway [27]. The result is proinflammatory cytokine and type 1 interferon gene induction [22].

TLRs efficiently recognise distinct components of pathogens that are essential to their metabolism, preventing mutations rendering them undetectable [31]. TLRs 1, 2 and 6 recognise gram positive bacteria cell wall constituents such as lipoproteins, peptidoglycans and lipoteichoic acid [31]. TLR4 is activated by the gram negative bacteria cell wall component lipopolysaccharide (LPS) [32] and TLR5 bacterial flagellin [31]. The intracellular TLRs 3, 7 and 8 recognise double and single stranded viral RNA, and TLR9 non-methylated CpG dinucleotides present in bacterial DNA [31,33].

In addition to exogenous microbial PAMP ligands, TLRs are also activated by a range of endogenous ligands released as a result of tissue and cellular injury termed damage associated molecular patterns (DAMPs). These are usually hidden from recognition, however following injury they are released or revealed, triggering a TLR mediated inflammatory response [31]. It has been suggested DAMPs act as danger signals, released by injured tissues, alerting the immune system of damage [34]. The resulting sterile inflammation is a key stimulator for the recruitment of innate immune inflammatory cells and initiation of the wound healing process [31]. DAMPs identified as TLR ligands include the extracellular matrix constituent hyaluronic acid, HMGB1 (a nuclear protein), Heat shock proteins (HSPs) 60 and 70, oxidised LDL, fibrinogen and fibronectin [35].

3.3. Toll-like receptors and the skin

Intact skin provides an external barrier to the environment, preventing infection by the majority of pathogenic bacteria, viruses and fungi [36]. In addition to this physical defence, cells of the innate immune system present in skin such as dermal mast cells, phagocytes and dendritic cells such as Langerhans cells of the epidermis, and those readily recruited from blood such as neutrophils, macrophages, basophils, eosinophils, NK cells and gamma-delta T cells all express TLRs for pattern recognition [31]. On detection of invading microbial pathogens through recognition of PAMPs, TLR activation results in the initiation of a pro-inflammatory defence response, promoting phagocytosis, immune cell recruitment and antigen presentation [36]. In addition to immune cells, TLRs are also widely expressed by a variety of non-immune cells contained within both the epidermis and dermis which are vital to wound healing [37].

The epidermis is primarily comprised of keratinocytes, which have been demonstrated to express TLRs 1–6 and TLR9 and 10 [38]. Unlike specialist immune cells, keratinocytes and other epithelial cells comprise the boundary and interface with the external environment and are under constant exposure to microbes and PAMPS [31]. They are able to maintain a delicate balance between tolerance of commensal organisms and the detection of infection and injury and subsequent inflammatory response [31]. The relative expression of TLRs by keratinocytes also seems to vary depending on position of the cell, for instance TLR5 is predominantly expressed in the basal layers, whereas TLR9 is expressed to a greater degree by more differentiated cells of the upper epidermal layers [39]. It does appear however all TLRs are functional, and produce distinct immune responses [40]. For instance, activation of keratinocyte TLRs 2, 3, 4, 5 and 9 by their respective ligands resulted in TNF-α, IL-8, CCL2 (basophil chemokine) and CCL20 (macrophage inflammatory protein-3) release [40]. TLR3 and TLR9 activation produced CXCL9 and CXCL10, involved in T-memory cell activation and type 1 interferon production [40].

Fibroblasts located in the dermis produce extra cellular matrix constituents, cytokines, growth factors and have a crucial role in the wound healing process as described above. They have been found to express the full range of human TLRs from 1 to 10 [41]. Studies have demonstrated *in vitro* activation of TLRs 2, 3, 4, 5 and 9 resulted in production of interferon-γ, CXCL9, CXCL10 and CXCL11, important in the recruitment of T-cells and NK cells [40]. TLR4 activation in dermal fibroblasts has been demonstrated to result in IL-6, IL-8 and monocyte chemotactic protein (MCP) [42]. Microvascular cells such as dermal endothelial cells have been shown to highly express TLR4 and to a lesser extent TLR2. *In vitro* treatment with the exogenous TLR4 ligand LPS resulted in NFkB activation. Likewise exposure to the endogenous derived ligand hyaluronan induced IL-8, a potent chemokine, stimulating the recognition of tissue injury and promoting initiation of the early stages of the wound healing process [43].

3.4. Toll-like receptors and wound healing

As previously described, recognition of endogenous ligands by TLRs on both immune and non-immune cells of the skin provide alarm signals *via* TLR activation and resulting sterile inflammation alerting to tissue injury. However, the effect of TLR activation on the wound healing process extends beyond the initial recognition of cellular damage, and it appears depending on the location, timing and degree of activation may have a promoting or inhibiting effect on the process of wound healing and tissue regeneration [44] (Table 1).

Table 1
Summary of TLR wound healing studies.

Study	TLR	Model	Wound	Findings
Dasu et al. (2010) [44]	2	*In vivo* murine, knock out	Diabetic	TLR2 knock out was beneficial for wound healing in diabetes induced animals
Dasu et al. (2013) [45]	4	*In vivo* murine, knock out	Diabetic	TLR4 knock out improves wound healing and reduces inflammation in diabetic mice
Suga et al. (2013) [7]	2 and 4	*In vivo* murine, knock out	Non-diabetic	TLR 2 and 4 knock out impaired wound healing at days 3 and 7. TLR4 rather than TLR2 regulates healing through TGF-β and CCL5
Chen et al. (2013) [43]	4	*In vitro*, *In vivo* murine, knock out	Non-diabetic	Injury stimulates TLR4 mRNA expression in keratinocytes. Wound healing is prolonged in TLR4 deficient mice.
Sato et al. (2010) [31]	9	*In vivo* murine, knock out	Non-diabetic	Wounds treated with TLR9 agonists exhibit accelerated healing. TLR9 deficient animals demonstrate delayed wound healing
Lin et al. (2011) [47]	3	*In vivo* murine	Non-diabetic	Wound healing is significantly delayed in TLR3 deficient mice compared to wild type
Lin et al. (2012) [48]	3	*In vivo* murine, human	Non-diabetic	Topical application of TLR3 agonist accelerated wound healing when applied to human and mouse wounds TLR3 deficiency inhibited wound healing

In vitro and *in vivo* data has suggested that TLR4 becomes upregulated within the first 12–24 h following injury and slowly decreases to baseline at day 10, and is primarily concentrated in epidermal keratinocytes [45]. The same study demonstrated significantly impaired wound healing in TLR4 deficient mice at days 1–5, with no difference seen from wild type at 10 days [45]. An altered pattern of cytokine release and inflammatory cell infiltration was observed with decreased IL-1β and IL-6, and an increase in neutrophil, macrophage and T-cell infiltrates in the wounds of knockout animals at discreet time points [45]. Another study also observed impairment in wound healing in TLR2 and TLR4 deficient mice at days 3 and 7, but observed a decrease in neutrophil and macrophage infiltration, and reduced TGF-β and CCL5 expression [7]. Activation of TLR4 and TLR2 appears therefore to have a beneficial effect on wound healing in the early stages following acute injury, at least in absence of other influences on TLR expression, signalling and activation.

However the story does not end there. Controversy exists as to the exact effect of TLR4 and TLR2 in the wound healing process. Given the seemingly important regulatory role of TLR4 and TLR2 in initiating the early stages of wound healing, it perhaps seems counter-intuitive that wound healing was significantly improved in TLR2 deficient mice with induced diabetes compared to diabetic wild-type animals [46]. The same effect was also observed in diabetic TLR4 deficient mice [47] in apparent contradiction of the studies described above.

In addition to decreased healing time, the wounds from TLR2 deficient mice also demonstrated significantly reduced NFkB activation, IL-6 and TNF-α release [46]. In the same study when comparing wild-type diabetic mice to non-diabetic controls, TLR2 mRNA and protein expression was significantly increased, along with markers of activation such as increased expression of MyD88, IRAK and NFkB [46]. Likewise, TLR4 mRNA and protein expression, IL-6, TNF-α and NFkB activation was increased in wild-type diabetic compared to non-diabetic animals, with a corresponding reduction in IL-6, TNF-α and NFkB activity in the TLR4 deficient diabetic populations [47].

These studies demonstrated significantly increased TLR2, TLR4 and MyD88 expression in diabetic compared to non-diabetic wounds and suggests in diabetes, TLR2 and TLR4 mediated hyperinflammation results in an impairment of wound healing. Persistent activation of TLR2 and TLR4 is also associated with other chronic non-healing wounds such as chronic venous ulceration [48].

Wound healing studies utilising TLR3 deficient mice resulted in significantly delayed wound healing compared to wild-type controls, led to decreased neutrophil and macrophage recruitment, and reduced CXCL2, CCL2 and CCL3 chemokines [49]. Further to this effect, the TLR3 agonist poly(I:C) significantly accelerated wound healing when applied topically to human and mouse wounds compared to control and resulted in greater neutrophil and macrophage recruitment and upregulated CXCL2 [50].

TLR9 deficient mice demonstrated delayed wound healing compared to wild-type [33]. In addition, topical administration of the TLR9 agonist CpG ODN to wounds resulted in significantly improved healing times, increased macrophage infiltration and increased production of VEGF [33].

4. Non-healing, hypertrophy and other wound complications

Chronic wounds such as foot ulceration are a frequent and challenging complication of diabetes with a life time risk of between 15 and 25% [51,52]. This translates to a 20× greater risk of major amputation compared to non-diabetics, and remains the most common cause of hospitalisation amongst diabetic patients [6]. Diabetic foot ulcers are multifactorial in causation, although a predomination for either neuropathy or ischaemia often exists [6]. The result is a wound characterised by poor healing, with the progression of the normal process stalled, or failed to initiate, leading to a chronic, static wound.

The diabetic wound environment differs from the normal acute wound process through a prolonged and persistent inflammatory phase (Fig. 1). There is an exaggerated and sustained neutrophil and macrophage infiltration, which in a db/db mouse model was demonstrated to be associated with deregulated and prolonged chemokine expression, such as macrophage inflammatory protein 2 and macrophage chemoattractant protein 1 [53].

Although the initial infiltration of immune cells is impaired, once activated the result is a hyperinflammatory response with elevated inflammatory cytokine production of TNF-α, IL-1β and IL-6, and increased NFkB regulated matrix metalloprotease (MMP) production leading to excessive extracellular matrix destruction and grossly impaired granulation tissue formation [6]. Neutrophils in particular appear to contribute to these destructive wound conditions through upregulated release of MMP-8 and downregulated release of the MMP inhibitor TIMP1 in chronic wounds [54]. The resulting hostile environment of excess inflammatory cytokine production (TNF-α, IL-6) also impairs other events and processes crucial to healing such as fibroblast migration and proliferation, collagen synthesis and promotes apoptosis in fibroblasts and vascular precursor cells [6].

Diabetic ulceration is an example of chronic inflammation directly leading to a significant impairment in the healing process and the creation of a chronic non-healing wound. As previously described, there is compelling evidence this pathological inflammation is mediated *via* excessive TLR activation. Another consequence of abnormal TLR mediated inflammation on the wound healing process is in *over* healing in the form of hypertrophic scar formation [42]. Hypertrophic scars develop following trauma as a result of excessive production of ECM components such as collagen, and although the mechanism remains unclear, are associated with prolonged inflammation and bacterial contamination [42]. Comparison of hypertrophic and normal scar tissue from burns patients demonstrated increased TLR4 staining in hypertrophic tissues and increased TLR4 and MyD88 mRNA in fibroblasts isolated from hypertrophic scars [42]. A corresponding increase in pro-inflammatory cytokines such as PGE2, IL-6, IL-8 and MCP-1 were also

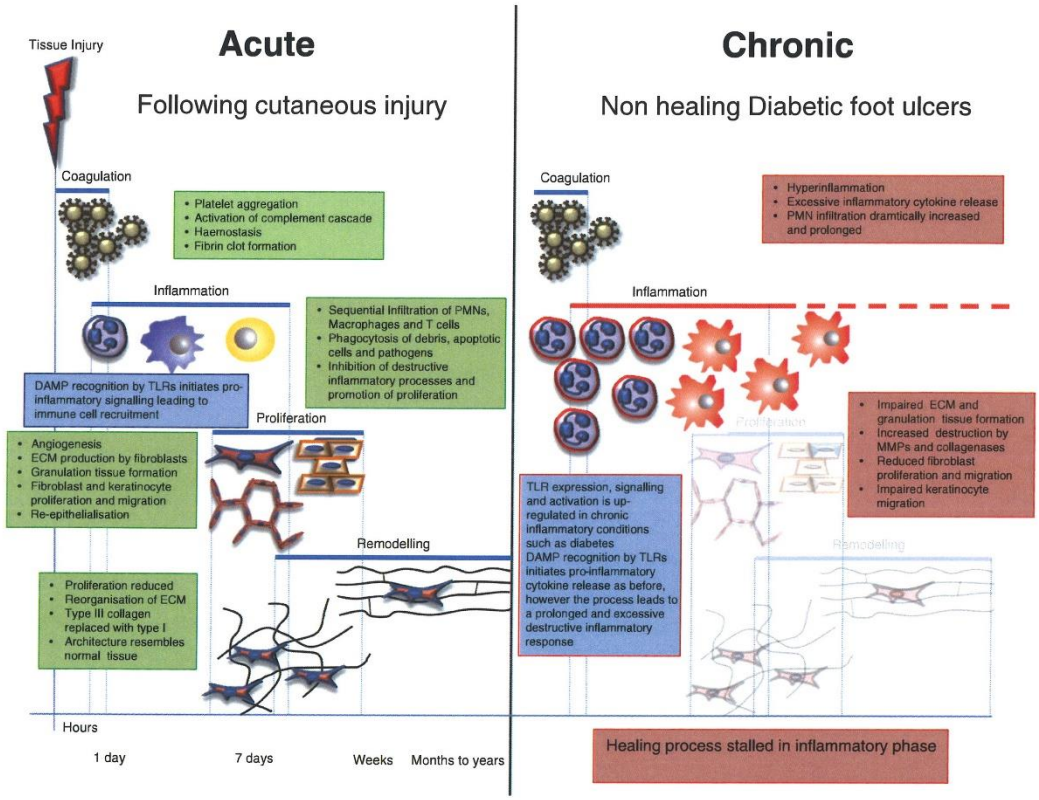

Fig. 1. A comparison betwen the progressing and overlapping stages of normal wound healing following acute tissue injury and chronic, non-healing diabetic wounds.

detected. It is therefore suggested that persistent TLR4 activation in dermal fibroblasts leads to hypertrophic scarring, possibly through the increased production of growth factors by supporting cells [42].

Another example of a maladaptive healing response that occurs in response to chronic inflammation is fibrosis. TLR activation is implicated in fibrotic abnormal healing responses in specific organs such as the liver, following repeated tissue injury [31]. TLR4 in particular is thought to contribute to the fibrotic reaction through chronic activation from the continuous translocation of gut bacteria associated with chronic liver diseases, and as demonstrated by the protective effect of TLR4 knock out in animal models of liver injury [31]. There does however appear to be a differential TLR effect on fibrosis depending on the organ involved, with TLR9 implicated in lung fibrosis, and TLRs 2 and 4 likely to have a greater effect in acute renal inflammation rather than chronic kidney fibrotic responses, where evidence is conflicting [31].

The role of TLRs in fibrotic skin reactions has been of particular interest in conditions such as systemic sclerosis. TLR4 activation has been implicated by murine models of skin fibrosis utilising bleomycin, through increased hyaluronan production, a potent TLR4 endogenous ligand [55]. In addition, studies utilising human tissue biopsies from scleroderma patients have demonstrated TLR4 and associated adaptor molecules are overexpressed in affected skin, and correlate with disease progression [56]. *In vitro* studies in ex-planted scleroderma fibroblasts have shown activation of TLR4 resulted in increased collagen production and gene expression of factors associated with ECM production and remodelling, in addition to an increased susceptibility to the effects of TGF-β [57]. Recent work has also identified TLR4 as a crucial mechanism through which in scleroderma, injured keratinocytes interact with fibroblasts through increased production of the protein S100A9, a known ligand of TLR4, leading to increased production of the pro-fibrotic gene CCN2 [58].

It is therefore proposed that in chronic fibrotic skin diseases such as scleroderma, persistent TLR4 activation through endogenous ligand stimulation results in altered response to TGF-β, and subsequent dysregulated production and remodelling of the extracellular matrix, leading to profound skin fibrosis.

5. Conclusion

Wounds that fail to heal, such as chronic diabetic ulcers, do not progress through the normal stages of the healing process described in detail earlier in this review. It is clear the innate immune system and the pattern recognition receptors that confer specificity such as toll-like receptors have a crucial role in the initiation and regulation of normal wound healing, however the role of the innate immune response in chronic wounds remains controversial.

In addition to the excess morbidity and mortality associated with foot ulceration and subsequent amputation, and with the global burden of diabetes set to reach 350 million people, non-healing wounds of all aetiology are set to remain an enormous economic liability for

healthcare systems around the world. Manipulation of the innate immune response therefore represents a potential novel therapeutic opportunity to reduce the hyperinflammation associated with chronic wounds, and to restart the normal wound healing process.

The impact of dysregulated TLR activation and subsequent chronic inflammation on the wound healing process appears to be significantly more complex however, when the pathological yet intuitively opposed outcomes of non-healing, hypertrophy and fibrosis can all occur in different disease phenotypes within the same tissue, the skin.

References

[1] Hubner G, Brauchle M, Smola H, Madlener M, Fassler R, Werner S. Differential regulation of pro-inflammatory cytokines during wound healing in normal and glucocorticoid-treated mice. Cytokine 1996;8(7):548–56.
[2] Guo S, Dipietro LA. Factors affecting wound healing. J Dent Res 2010;89(3):219–29.
[3] Roupe KM, Nybo M, Sjobring U, Alberius P, Schmidtchen A, Sorensen OE. Injury is a major inducer of epidermal innate immune responses during wound healing. J Invest Dermatol 2010;130(4):1167–77.
[4] Kim MH, Liu W, Borjesson DL, Curry FR, Miller LS, Cheung AL, Liu FT, Isseroff RR, Simon SI. Dynamics of neutrophil infiltration during cutaneous wound healing and infection using fluorescence imaging. J Invest Dermatol 2008;128(7):1812–20.
[5] Segal AW. How neutrophils kill microbes. Annu Rev Immunol 2005;23:197–223.
[6] Acosta JB, del Barco DG, Vera DC, Savigne W, Lopez-Saura P, Guillen Nieto G, Schultz GS. The pro-inflammatory environment in recalcitrant diabetic foot wounds. Int Wound J 2008;5(4):530–9.
[7] Suga H, Sugaya M, Fujita H, Asano Y, Tada Y, Kadono T, Sato S. TLR4, rather than TLR2, regulates wound healing through TGF-beta and CCL5 expression. J Dermatol Sci 2014;73(2):117–24.
[8] DiPietro LA. Wound healing: the role of the macrophage and other immune cells. Shock 1995;4(4):233–40.
[9] Deodhar AK, Rana RE. Surgical physiology of wound healing: a review. J Postgrad Med 1997;43(2):52–6.
[10] Fishel RS, Barbul A, Beschorner WE, Wasserkrug HL, Efron G. Lymphocyte participation in wound healing. Morphologic assessment using monoclonal antibodies. Ann Surg 1987;206(1):25–9.
[11] Park JE, Barbul A. Understanding the role of immune regulation in wound healing. Am J Surg 2004;187(5A):11S–6S.
[12] Jameson J, Havran WL. Skin gammadelta T-cell functions in homeostasis and wound healing. Immunol Rev 2007;215:114–22.
[13] Traversa B, Sussman G. The role of growth factors, cytokines and proteases in wound management. Prim Intention 2001;9(4):161–7.
[14] Wild T, Rahbarnia A, Kellner M, Sobotka L, Eberlein T. Basics in nutrition and wound healing. Nutrition 2010;26(9):862–6.
[15] Gilbane AJ, Denton CP, Holmes AM. Scleroderma pathogenesis: a pivotal role for fibroblasts as effector cells. Arthritis Res Ther 2013;15(3):215.
[16] O'Toole EA. Extracellular matrix and keratinocyte migration. Clin Exp Dermatol 2001;26(6):525–30.
[17] Raja Sivamani K, Garcia MS, Isseroff RR. Wound re-epithelialization: modulating keratinocyte migration in wound healing. Front Biosci 2007;12:2849–68.
[18] Haase I, Evans R, Pofahl R, Watt FM. Regulation of keratinocyte shape, migration and wound epithelialization by IGF-1- and EGF-dependent signalling pathways. J Cell Sci 2003;116(Pt 15):3227–38.
[19] Martins VL, Caley M, O'Toole EA. Matrix metalloproteinases and epidermal wound repair. Cell Tissue Res 2013;351(2):255–68.
[20] Amano S, Akutsu N, Ogura Y, Nishiyama T. Increase of laminin 5 synthesis in human keratinocytes by acute wound fluid, inflammatory cytokines and growth factors, and lysophospholipids. Br J Dermatol 2004;151(5):961–70.
[21] Usui ML, Mansbridge JN, Carter WG, Fujita M, Olerud JE. Keratinocyte migration, proliferation, and differentiation in chronic ulcers from patients with diabetes and normal wounds. J Histochem Cytochem 2008;56(7):687–96.
[22] Akira S, Uematsu S, Takeuchi O. Pathogen recognition and innate immunity. Cell 2006;124(4):783–801.
[23] Staros EB. Innate immunity: new approaches to understanding its clinical significance. Am J Clin Pathol 2005;123(2):305–12.
[24] Spirig R, Tsui J, Shaw S. The emerging role of TLR and innate immunity in cardiovascular disease. Cardiol Res Pract 2012;2012:181394.
[25] Gordon S. Pattern recognition receptors: doubling up for the innate immune response. Cell 2002;111(7):927–30.
[26] Areschoug T, Gordon S. Pattern recognition receptors and their role in innate immunity: focus on microbial protein ligands. Contrib Microbiol 2008;15:45–60.
[27] Patel H, Shaw SG, Shi-Wen X, Abraham D, Baker DM, Tsui JC. Toll-like receptors in ischaemia and its potential role in the pathophysiology of muscle damage in critical limb ischaemia. Cardiol Res Pract 2012;2012:121237.
[28] Navi A, Patel H, Shaw S, Baker D, Tsui J. Therapeutic role of toll-like receptor modification in cardiovascular dysfunction. Vascul Pharmacol 2013;58(3):231–9.
[29] Mann DL. The emerging role of innate immunity in the heart and vascular system: for whom the cell tolls. Circ Res 2011;108(9):1133–45.
[30] De Nardo D, De Nardo CM, Nguyen T, Hamilton JA, Scholz GM. Signaling crosstalk during sequential TLR4 and TLR9 activation amplifies the inflammatory response of mouse macrophages. J Immunol 2009;183(12):8110–8.
[31] Huebener P, Schwabe RF. Regulation of wound healing and organ fibrosis by toll-like receptors. Biochim Biophys Acta 2013;1832(7):1005–17.
[32] Alexander C, Rietschel ET. Bacterial lipopolysaccharides and innate immunity. J Endotoxin Res 2001;7(3):167–202.
[33] Sato T, Yamamoto M, Shimosato T, Klinman DM. Accelerated wound healing mediated by activation of toll-like receptor 9. Wound Repair Regen 2010;18(6):586–93.
[34] Matzinger P. The danger model: a renewed sense of self. Science 2002;296(5566):301–5.
[35] Dasu MR, Ramirez S, Isseroff RR. Toll-like receptors and diabetes: a therapeutic perspective. Clin Sci (Lond) 2012;122(5):203–14.
[36] Terhorst D, Kalali BN, Ollert M, Ring J, Mempel M. The role of toll-like receptors in host defenses and their relevance to dermatologic diseases. Am J Clin Dermatol 2010;11(1):1–10.
[37] Pasparakis M, Haase I, Nestle FO. Mechanisms regulating skin immunity and inflammation. Nat Rev Immunol 2014;14(5):289–301.
[38] Miller LS, Modlin RL. Human keratinocyte toll-like receptors promote distinct immune responses. J Invest Dermatol 2007;127(2):262–3.
[39] Miller LS, Sorensen OE, Liu PT, Jalian HR, Eshtiaghpour D, Behmanesh BE, Chung W, Starner TD, Kim J, Sieling PA, et al. TGF-alpha regulates TLR expression and function on epidermal keratinocytes. J Immunol 2005;174(10):6137–43.
[40] Miller LS, Modlin RL. Toll-like receptors in the skin. Semin Immunopathol 2007;29(1):15–26.
[41] Jang S, Park JS, Won YH, Yun SJ, Kim SJ. The expression of toll-like receptors (TLRs) in cultured human skin fibroblast is modulated by histamine. Chonnam Med J 2012;48(1):7–14.
[42] Wang J, Hori K, Ding J, Huang Y, Kwan P, Ladak A, Tredget EE. Toll-like receptors expressed by dermal fibroblasts contribute to hypertrophic scarring. J Cell Physiol 2011;226(5):1265–73.
[43] Taylor KR, Trowbridge JM, Rudisill JA, Termeer CC, Simon JC, Gallo RL. Hyaluronan fragments stimulate endothelial recognition of injury through TLR4. J Biol Chem 2004;279(17):17079–84.
[44] Dasu MR, Isseroff RR. Toll-like receptors in wound healing: location, accessibility, and timing. J Invest Dermatol 2012;132(8):1955–8.
[45] Chen L, Guo S, Ranzer MJ, DiPietro LA. Toll-like receptor 4 has an essential role in early skin wound healing. J Invest Dermatol 2013;133(1):258–67.
[46] Dasu MR, Thangappan RK, Bourgette A, DiPietro LA, Isseroff R, Jialal I. TLR2 expression and signaling-dependent inflammation impair wound healing in diabetic mice. Lab Invest 2010;90(11):1628–36.
[47] Dasu MR, Jialal I. Amelioration in wound healing in diabetic toll-like receptor-4 knockout mice. J Diabetes Complications 2013;27(5):417–21.
[48] Pukstad BS, Ryan L, Flo TH, Stenvik J, Moseley R, Harding K, Thomas DW, Espevik T. Non-healing is associated with persistent stimulation of the innate immune response in chronic venous leg ulcers. J Dermatol Sci 2010;59(2):115–22.
[49] Lin Q, Fang D, Fang J, Ren X, Yang X, Wen F, Su SB. Impaired wound healing with defective expression of chemokines and recruitment of myeloid cells in TLR3-deficient mice. J Immunol 2011;186(6):3710–7.
[50] Lin Q, Wang L, Lin Y, Liu X, Ren X, Wen S, Du X, Lu T, Su SY, Yang X, et al. Toll-like receptor 3 ligand polyinosinic:polycytidylic acid promotes wound healing in human and murine skin. J Invest Dermatol 2012;132(8):2085–92.
[51] Fadini GP, Albiero M, Menegazzo L, Boscaro E, Pagnin E, Iori E, Cosma C, Lapolla A, Pengo V, Stendardo M, et al. The redox enzyme p66Shc contributes to diabetes and ischemia-induced delay in cutaneous wound healing. Diabetes 2010;59(9):2306–14.
[52] O'Loughlin A, McIntosh C, Dinneen SF, O'Brien T. Review paper: basic concepts to novel therapies: a review of the diabetic foot. Int J Low Extrem Wounds 2010;9(2):90–102.
[53] Wetzler C, Kampfer H, Stallmeyer B, Pfeilschifter J, Frank S. Large and sustained induction of chemokines during impaired wound healing in the genetically diabetic mouse: prolonged persistence of neutrophils and macrophages during the late phase of repair. J Invest Dermatol 2000;115(2):245–53.
[54] Nwomeh BC, Liang HX, Cohen IK, Yager DR. MMP-8 is the predominant collagenase in healing wounds and nonhealing ulcers. J Surg Res 1999;81(2):189–95.
[55] Yoshizaki A, Iwata Y, Komura K, Ogawa F, Hara T, Muroi E, Takenaka M, Shimizu K, Hasegawa M, Fujimoto M, et al. CD19 regulates skin and lung fibrosis via toll-like receptor signaling in a model of bleomycin-induced scleroderma. Am J Pathol 2008;172(6):1650–63.
[56] Stifano G, Affandi AJ, Mathes AL, Rice LM, Nakerakanti S, Nazari B, Lee J, Christmann RB, Lafyatis R. Chronic toll-like receptor 4 stimulation in skin induces inflammation, macrophage activation, transforming growth factor beta signature gene expression, and fibrosis. Arthritis Res Ther 2014;16(4):R136.
[57] Bhattacharyya S, Kelley K, Melichian DS, Tamaki Z, Fang F, Su Y, Feng G, Pope RM, Budinger GR, Mutlu GM, et al. Toll-like receptor 4 signaling augments transforming growth factor-beta responses: a novel mechanism for maintaining and amplifying fibrosis in scleroderma. Am J Pathol 2013;182(1):192–205.
[58] Nikitorowicz-Buniak J, Shiwen X, Denton CP, Abraham D, Stratton R. Abnormally differentiating keratinocytes in the epidermis of systemic sclerosis patients show enhanced secretion of CCN2 and S100A9. J Invest Dermatol 2014;134(11):2693–702.

Chronic Wound Care Management and Research

Dovepress
open access to scientific and medical research

Open Access Full Text Article

REVIEW

Diabetic foot ulcers in conjunction with lower limb lymphedema: pathophysiology and treatment procedures

Muholan Kanapathy[1]
Mark J Portou[1,2]
Janice Tsui[1,2]
Toby Richards[1,2]

[1]Division of Surgery and Interventional Science, University College London, [2]Department of Vascular Surgery, Royal Free London NHS Foundation Trust Hospital, London, UK

Abstract: Diabetic foot ulcers (DFUs) are complex, chronic, and progressive wounds, and have a significant impact on morbidity, mortality, and quality of life. A particular aspect of DFU that has not been reviewed extensively thus far is its management in conjunction with peripheral limb edema. Peripheral limb edema is a feature of diabetes that has been identified as a significant risk factor for amputation in patients with DFU. Three major etiological factors in development of lymphedema with concurrent DFU are diabetic microangiopathy, failure of autonomic regulation, and recurrent infection. This review outlines the pathophysiology of lymphedema formation in patients with DFU and highlights the cellular and immune components of impaired wound healing in lymphedematous DFU. We then discuss the principles of management of DFU in conjunction with lymphedema.

Keywords: diabetic foot ulcer, lymphedema, chronic wound, wound management

Introduction

Globally, approximately 370 million people have diabetes and this number is on the rise.[1] Diabetes UK estimates that by 2030, nearly 552 million people worldwide will have diabetes.[2] In the UK alone, approximately 2% of the population is estimated to have diabetes, of which 15% will develop foot ulceration at some point in their lives.[3] Overall, 8% of hospital admissions involve patients with diabetes.

Diabetic foot ulcers (DFUs) are complex, chronic, and progressive wounds, and have a significant impact on morbidity, mortality, and quality of life.[4,5] Diabetic patients have a 20-fold increased risk of amputation compared with non-diabetics, and DFU directly leads to 6,000 amputations per year in England alone.[6] The prognosis often remains poor despite amputation. Historical data demonstrate 50% mortality at 2 years following major amputation,[7] and an overall decrease in 5-year survival of 41%–70% has been reported.[8] Even between diabetic populations, the presence of DFU represents an approximately 50% increased mortality risk.[9]

The economic burden of DFU management is significant. In the UK, an estimated £639–£662 million was spent in 2010–2011 on the management of DFU and subsequent amputation, representing 0.6%–0.7% of the entire National Health Service annual budget.[6] In the USA, 33% of the $116 billion total health care spend on diabetes is on the management of foot ulceration.[10]

Peripheral limb edema is a feature of DFU and despite the lack of an estimate of its incidence or prevalence in DFU, it has been identified as a significant risk factor for amputation in patients with DFU.[11,12] Diabetes, however, has been identified as a comorbidity in 23.5% of patients with lymphedema in a multicenter study of 1,000 patients

Correspondence: Mark J Portou
Department of Vascular Surgery, Royal Free London NHS Foundation Trust Hospital, London NW3 2QG, UK
Email mjportou@doctors.org.uk

with chronic leg ulcers and is also reported to be a significant comorbidity in breast cancer survivors with lymphedema.[13,14] The resistance of diabetic ulcers to healing is undoubtedly multifactorial, but having concurrent lymphedema further impairs the wound healing process.[11,12] This review outlines the pathophysiology of lymphedema formation in DFU and the principles of management of DFU in conjunction with lymphedema.

Pathophysiology of lymphedema formation in DFU

DFU has traditionally been linked to peripheral vascular disease, peripheral neuropathy, and infection.[3] Peripheral vascular disease is more common in patients with diabetes and is traditionally classified into macrovascular and microvascular complications. Neuropathy affects the motor, sensory, and autonomic nerves and their associated functions, with local trauma and pressure in the neuropathic foot being the leading factors in the development of DFU. Recurrent infection in the functionally immunosuppressed diabetic can have devastating sequelae.[15]

Lymphedema is a condition of localized fluid retention and tissue swelling caused by a compromised lymphatic system. Primary lymphedema develops as result of lymphatic abnormalities from congenital hypoplasia, aplasia, or valvular incompetence that could present at birth or later in life. Secondary lymphedema occurs due to recurrent infection and inflammation, parasitic infection, malignancy, trauma, or iatrogenic causes, resulting in failure to drain protein-rich lymphatic fluid from the interstitium, leading to edema of the affected site. Secondary lymphedema is seen in patients with lymphedematous DFU.

The pathophysiology of DFU in conjunction to lymphedema has not been widely discussed, although several studies have been undertaken to better understand the development of peripheral limb edema in diabetes. This section explores the pathophysiology of lymphedema in DFU, focusing on the three major underlying etiologies of DFU, ie, diabetic microangiopathy, failure of autonomic regulation, and recurrent infection. We then highlight the cellular and immune component of impaired wound healing in lymphedematous DFU.

Diabetic microangiopathy and lymphedema

The important role of hyperglycemia in the development and progression of microvascular complications has been clearly established.[16] In the hyperglycemic state, abnormal glucose metabolism leads to production of advanced glycation end products. These, among other consequences, interfere with vascular remodeling, which has been proposed as a mechanism for development of diabetic microangiopathy.[17] Microangiopathy alters the structure and function of the microvasculature, leading to loss of the vascular barrier and tone regulation, resulting in increased capillary filtration of fluid into the tissues.[17]

When the capillary filtration rate exceeds the rate of lymphatic drainage, fluid accumulates in the intercellular space, leading to edema, which is governed by Starling's principle of fluid exchange (equation 1). Starling's principle states that fluid transport across the exchange vessel wall is driven by the hydraulic pressure gradient and opposed by the colloid osmotic pressure gradient between the plasma and the interstitium.[18] In diabetic microangiopathy, the hydraulic conductance of the capillary wall (L_p) is increased due to structural and functional impairment, resulting in an increased capillary filtration rate.

$$\text{Starling's equilibrium: } J_v = L_p S ([P_c - P_i] - \sigma [\pi_p - \pi_i]) \quad (1)$$

where J_v is the capillary filtration rate, L_p is the hydraulic conductance of the capillary wall, S is the surface area, P is the pressure within the capillary (c) or interstitium (i), σ is the osmotic reflection coefficient of the capillary wall, and π is the osmotic pressure of plasma (p) or interstitial fluid (i).

This is further exacerbated by the increased resting blood flow in the skin, the capillary filtration rate, and the hydrostatic pressure in the lower limbs compared with the upper limbs, leading to lower limb lymphedema.[19–21]

Microangiopathy also affects endothelial function with increased capillary permeability to large proteins and molecules in diabetic patients, a feature that can be seen by the transcapillary escape rate of radiolabelled albumin.[22,23] Removal and drainage of interstitial albumin appears to be delayed in diabetic patients, suggesting a defect in lymphatic function due to overflow saturation of the lymph pumps.[22] Hence, although diabetes does not cause direct damage to the lymphatic vessels, the processes of normal interstitial fluid homeostasis are affected with the increase in transport capacity that overwhelms the drainage system. This has been demonstrated by the improvement of edema and notable reduction in local capillary filtration with drugs acting on capillary permeability such as O-(beta-hydroxyethyl)-rutosides and Pycnogenol in subjects with diabetic microangiopathy.[24–26] Reduction in lymphedema was accompanied by improvement in ulcer healing.[25]

Diabetic neuropathy and lymphedema

The pathogenesis of diabetic neuropathy is thought to involve disturbance in the metabolism and vasculature of nerve tissue due to excessive glucose uptake, leading to damage of peripheral nerves.[27] The functional subunit in lymphatic vessels is the lymphangion, wall of which consists of smooth muscle cells that propel lymph in a peristaltic manner, contraction of which is under neural control.[22] Analogous to the blood vessels, the peripheral lymphatic vessels and smooth muscle subunits are under autonomic control. Diabetic neuropathy can lead to lymphatic pump failure, impairing interstitial fluid uptake from the distal part of the limb and disrupting lymphatic fluid transport along the lymphatic vessels.[22] The disorder in absorption and transport of lymphatic fluid is analogous to direct neural injury with sympathetic denervation interruption seen in trauma where management by complex physical decongestion therapy with manual lymphatic drainage (MLD) results in clinical improvement.[28]

Recurrent infection and lymphedema

Patients with DFU are predisposed to recurrent wound infections, contributed to by the open wound and immunological perturbation. The shift in balance between the host defense system and bacterial load in the wound favors soft tissue infection which leads to destruction of host tissue. Recurrent soft tissue infection invariably damages the lymphatic system located in the dermal layer of the skin. The affected lymphatics become inflamed, dilated, and filled with exudate, chiefly neutrophils and monocytes. Abnormal accumulation of interstitial fluid, proteins, growth factors and other active peptide moieties, glycosaminoglycans, and particulate matter also includes bacteria. The overload and failure of lymphatic intestinal drainage with accumulation of these larger elements leads to occlusion of the lymphatic system and stasis, providing an ideal microenvironment for bacterial growth, commonly group A β-hemolytic *Streptococcus* and *Staphylococcus aureus*.[29–31] Accumulation of lymphatic fluid within the interstitium stimulates fibroblasts, keratinocytes, and adipocytes, leading to deposition of collagen and glycosaminoglycans within the skin and subcutaneous tissue.[31] This is accompanied by chronic inflammation, involving lymphocytes, monocyte/macrophages, and dendritic cells. These inflammatory cells produce several inflammatory cytokines related to fibrosis, such as connective tissue growth factor, transforming growth factor-β, and platelet-derived growth factor, besides upregulating the cellular proliferation and migration of fibroblasts.[31] The outcome of this is further soft tissue destruction, which exacerbates the lymphedema. Lymphatic dysfunction also impairs the local immune response, which plays a permissive role in propagation of bacterial and fungal invasion, further worsening the existing lymphatic dysfunction leading to a chronic state with reduced reversibility of the edema.[31]

Impaired wound healing in lymphedematous DFU

Wound healing is a complex physiological process involving numerous types of cells, growth factors, and cytokines, each of which is required at the correct time and for the appropriate duration. Impaired wound healing in the lymphedematous DFU is attributed to altered function at the cellular level, compounded by the inflammatory reaction and impaired immune system. This section exemplifies the cellular and immunological aspects of impaired wound healing in lymphedematous DFU through two important mechanistic processes of wound healing: the gap junctional protein and the Toll-like receptors (TLRs) of the innate immune system.

Cellular component in DFU and lymphedema

Accumulation of fluid in the interstitial space results in abnormal function at both the tissue and cellular level.[32] The ensuing increase in physical distance between tissue channels can affect metabolic exchange, impairing the delivery of oxygen and nutrients and the discharge of toxins and inhibitory factors, with a resultant shift toward anaerobic metabolism. Likewise, the wider separation between cells affects the exchange of gases between plasma membranes. Given that the rich microvascular network in the skin is located in the papillary dermal layer, formation of interstitial edema that increases intercellular spaces affects oxygenation to the epidermal layer of the skin.[33] This leads to alteration of the tissue properties in response to external pressure, predisposing to ulcer formation. This is particularly true in weight-bearing areas such as the plantar surface of the foot, which is the commonest location for DFU.[33]

Important transmembrane proteins involved in the passage of nutrients between cells and gaseous exchange are the connexin family of gap junctional proteins. Gap junctions are highly specialized structures, made up of channels spanning adjacent cell membranes, leaving a 2–4 nm extracellular "gap", hence their name.[34] These channels are assembled of transmembrane proteins called "connexins", which are described in terms of molecular mass (Cx43 represents the connexin protein of 43 kDa). As the key mechanism of cellular communication, connexins are involved in epidermal

innate immunity, inflammation control, and wound repair.[35] A wide range of connexins are found within the skin (including Cx26, 30, 30.3, 31.1, 32, 37, 40, 43, and 45), with Cx43 being the most ubiquitous and found in dermal fibroblasts, blood vessels, and appendages such as sweat glands, sebaceous glands, hair follicles, mast cells, and activated leukocytes, as well as epidermal keratinocytes.[36,37] Connexins are associated with the pathogenesis of both type 1 and type 2 diabetes, and are directly linked to wound healing. Abnormal upregulation of Cx43 seen in diabetic wounds binds cells together and prevents migration of keratinocytes from the wound edge, delaying re-epithelialization and the wound healing process.[38,39] Preventing upregulation of Cx43 expression in a diabetic wound has been reported to increase the rate of re-epithelialization in a mouse model.[40]

Three connexin isoforms, Cx37, Cx43, and C47, have been shown to be involved in development and function of the lymphatics.[41] Loss of function in knockout mice results in widely dilated superficial lymphatics in the skin and severe lymphedema due to complete absence of valve formation.[41,42] Mutation experiments on connexins, on the other hand, resulted in impaired uptake of lymphatic fluid without obvious anatomical defect involving the lymphatic vessels.[43] Data suggest that coordinated function of gap junctions is needed to mediate the propagation of spontaneous contractions in the lymphatic vasculature.[44] Although these in vivo studies have demonstrated the effect of deletion of connexin, it is still unknown if the changes in expression of connexin seen in chronic wounds affect lymphangiogenesis.

Innate immune system in DFU and lymphedema

Persistent and excessive inflammation results in disruption of wound healing in diabetes. DFU become stalled in the inflammatory phase of wound healing, fails to progress, and a chronic ulcer results. This excessive "hyperinflammation" is mediated in part by the TLRs of the innate immune system. TLRs are key pattern recognition receptors of the innate immune system, which confer specificity to the innate immune system through recognition of discrete molecular patterns such as microbial cell wall constituents.[45] Stimulation of TLRs results in activation of a variety of cell-dependent responses, including antigen presentation and activation of a potent pro-inflammatory cascade, with release of inflammatory cytokines, such as interleukin-6 and tumor necrosis factor-α, and phagocytosis.[46]

In addition to exogenous microbial ligands known as pathogen-associated molecular patterns, TLRs also recognize endogenous "self" patterns that are released in response to tissue damage, known as damage-associated molecular patterns (DAMPs).[46] DAMPs act as danger signals triggered by tissue damage, and initiate a TLR-mediated inflammatory response, that in turn alerts the immune system to the presence of tissue injury.[47] Under normal circumstances, the resulting influx of inflammatory cells and stimulates a sterile inflammatory reaction to control bacterial infection and remove debris. Activation of DAMP TLRs is regarded as essential for initiation of the wound healing process.[48] However, in diabetes, controversy exists as to whether TLR-mediated inflammation has a beneficial or inhibitory effect on wound healing.[49] In animal studies, TLR2 and TLR4 inhibition or knock-out has a detrimental effect on the wound healing process for up to 7 days following injury, indicating the importance of TLR2 and TLR4 in the early phases of wound healing.[50,51] However, in diabetes-induced mice, TLR2 and TLR4 deletion conferred an apparent protective effect, demonstrated by significantly improved wound healing and a reduction in the pro-inflammatory environment of the wound, compared with wild-type diabetic rodents.[52,53]

In lymphedema, DAMPs such as high-mobility group box 1 and heat-shock protein appear elevated in response to lymphatic stasis.[54] Inhibition of high-mobility group box 1 leads to a significant reduction in inflammatory lymphangiogenesis, suggesting a negative role for DAMPs in promoting lymphangiogenesis besides provocating chronic inflammatory response in chronic lymphedema.[54] Studies in a mouse model of post-surgical lymphedema deficient for TLR2, TLR4, and TLR9 demonstrated significantly worse effects post injury compared with those in a wild-type model, as evidenced by increased tissue edema, reduced lymphangiogenesis, increased fibrosis, and increased leucocyte infiltration but reduced monocyte infiltration.[55] The data suggest a role for TLRs in the normal repair of lymphatic injury and resolution of lymphedema.[55]

Consequently, although TLRs appear to have a role in normal inflammation and swelling, their role in the diabetic patient with lymphedema may be confused, and the excessive TLR-mediated inflammation associated with diabetes is counterproductive with resultant chronic lymphedema.

Principles of management

While the current standard of care for DFU is well established by clinical guidelines and pathways and a recent systematic review by Braun et al, there remains a lack of high-quality evidence on the management of DFU in conjunction with lymphedema.[5,56]

Best practice management for DFU with or without lymphedema includes rapid assessment and correction where possible (or necessary) of macrovascular arterial insufficiency. The importance of wound assessment, debridement and cleansing, recognition and treatment of infection, revascularization, and selection of an appropriate dressing to achieve optimal healing is undeniable. However, managing DFU requires comprehensive attention with good diabetic control, offloading strategies, and an integrated approach to wound care.[56] This section highlights the principles of management of DFU in conjunction with lymphedema.

Glycemic control

Evidence for the benefit of good glycemic control is well established.[57] Randomized controlled trials (RCTs) such as the Diabetes Control and Complication Trial in type 1 diabetes demonstrated a significant reduction in development of microvascular complications such as retinopathy, nephropathy, and microalbuminuria and in neurological complications such as neuropathy in the intensive therapy groups.[16] The UK Prospective Diabetes Study in type 2 diabetes similarly demonstrated a significant reduction in "any diabetes related end-point", progression of retinopathy, and microalbuminuria in the tightly controlled treatment arm, regardless of treatment modality.[16] While no studies have examined the effect of tight glycemic control on the development, progression, and treatment of lymphedema in DFU, it seems intuitive that a reduction in the risk of diabetes-related microangiopathic complications and in the secondary consequences of hyperglycemia, such as cellulitis and other skin infections, through long-term close glycemic control will benefit the prevention and treatment of lymphedema.

Decongestion therapy

Decongestion therapies, including compression bandaging, MLD, and physical exercises, improve dermal lymphatic plexus lymph flow and have been the accepted non-surgical method to manage lymphedema.[58] MLD involves specialized rhythmic pumping techniques to massage the affected area and enhance the flow of lymph from the peripheries toward the heart. This gentle skin massage encourages superficial lymphatic contraction, thereby increasing lymph drainage.[59] Current imaging studies with near-infrared fluorescence have demonstrated the positive effect of MLD in increasing lymphatic vessel contractility and lymph velocity, leading to resolution of clinical symptoms.[60,61] The benefit of MLD in lymphedema secondary to complex regional pain syndrome, a clinical condition characterized by post-traumatic diffuse pain with autonomic and vasomotor changes, indicates that MLD could also benefit edema due to autonomic impairment as seen in DFU.[62] Conversely, a recent systematic review of the RCTs evaluating the effects of MLD on breast cancer-related secondary lymphedema indicates that MLD does not prevent or treat lymphedema.[63] However, there were clinical and statistical inconsistencies between the various studies, confounding the evaluation of the reviewed studies.[63]

Compression therapy has been advocated for the management of lymphedema and in the management of high perfusion microangiopathy in patients with DFU. Compression therapy with elastic stockings reduces capillary leakage and formation of edema, and may retard the progression of diabetic microangiopathy.[64] Use of stiff, short-stretch bandages with high working pressure and low resting pressure provides resistance to the accumulation of interstitial fluid while stimulating the rhythmic contraction of lymphatic collectors during exercise.[65] Working pressure is determined by the resistance provided by the bandage against the underlying muscle contraction, while the pressure exerted on tissue at rest is the resting pressure.[65] Two RCTs have shown that compression therapy with the use of intermittent pneumatic compression (IPC) is effective in reducing healing time for DFU in addition to reducing lymphedema.[66,67] The mechanism of action of IPC is believed to include enhancement of fibrinolysis and venous outflow, thereby reducing edema.[67,68] IPC simulates the effect of walking and weight-bearing on the venous system by the intermittent compression-decompression cycle. However, compression therapy is limited in the presence of peripheral vascular disease. One RCT evaluated the effect of compressed air massage on the rate of diabetic ulcer healing, with all patients receiving standard medical and surgical treatment, while in addition, one group received air massage at 100 kPa for 15–20 minutes for 5 days per week. This study found a significant reduction in time to DFU healing, with an average time of 58.1 days in patients (n=28) receiving compressed air massage, while those patients (n=27) receiving only standard wound care averaged 82.7 days until ulcer healing.[66] Compressed air massage has been shown to significantly improve local skin blood flow measured using laser Doppler fluxmetry.[66] Another double-blind RCT compared healing at 12 weeks between a pulsatile pneumatic foot compression system with a bladder that inflates to 160 mmHg for 2 seconds to empty the veins of the foot, repeating the cycle every 20 seconds for 8 hours a day in 52 patients, against a non-functioning

foot compression device in 45 patients. This study found a significant increase in healing efficacy in patients with DFU,[67] along with a significant reduction in edema in the study arm receiving IPC therapy.

Limb offloading is a common strategy in the management of diabetic foot disease, and standard offloading devices are believed to reduce edema by enabling patients to remain relatively mobile; however, there are no objective published data confirming this.[69] An alternative view is that immobilization of the ankle reduces function of the calf muscle pump, impairing venous return, potentially resulting in increased foot edema.[69]

Surgical management

Surgical management of DFU with lymphedema can be divided into debridement, debulking, and a microsurgical approach. Wound debridement is considered part of standard DFU care. Debridement, the most important intervention for decreasing the risk of limb amputation in patients with DFU, involves the removal of callus and necrotic tissue, and reduction of bacterial biofilm.[70] Debridement may be surgical, enzymatic (collagenase), autolytic (ie, occlusive), or biologic (larval). The different types of debridement for DFU, along with their advantages and disadvantages, have been recently reviewed by Yazdanpanah et al.[71]

Debulking surgery, such as the Charles procedure, which involves extensive excision of subcutaneous tissue followed by skin grafting, may be the simplest approach to reducing the volume of lymphedematous limbs but often results in substantial morbidity. Treatment of secondary lymphedema in the presence of DFU using the Charles procedure was described in a case report; however, it is an aggressive treatment with a prolonged treatment course.[72] The debulking procedure is particularly useful for ulcers with deep sinuses in the presence of chronic lymphedema where excision of the ulcer along with the sinus tract can be performed as a combined debulking procedure.[73]

Microsurgical techniques for treating lymphedema consist of lymphovenous anastomosis and vascularized lymph node transfer. Lymphovenous anastomosis creates a detour route from the lymphatics to the vein at the peripheral region of the affected limb, thereby increasing lymphatic drainage. Lymphovenous anastomosis has minimal morbidity; however, several studies have found that it is less effective in advanced-stage lymphedema, hence less likely to benefit patients with both lymphedema and DFU.[74] Vascularized lymph node transfer, a relatively new surgical treatment for lymphedema, involves transfer of lymph nodes to the lymphedematous limbs followed by microanastomosis of blood vessels. Despite promising outcomes in the clinical setting, the interaction between the transferred lymph nodes and the lymphatic system in the transfer site is not yet well understood.[74] Lahteenvuo et al and Honkonen et al showed that the transferred lymph nodes produce vascular endothelial growth factor-C, inducing lymphangiogenesis which may facilitate canalization of recipient lymphatic vessels to the lymph node.[75,76] Lin et al and Cheng et al hypothesized that the transferred lymph nodes act as "lymph pumps", ejecting the absorbed lymph fluid from the surrounding interstitial tissue into the venous circulation via the lymphovenous communication.[77,78] Despite the encouraging results in treating lymphedema, the reported clinical studies involve only patients with chronic lymphedema secondary to iatrogenic injury, which does not reflect the exact pathophysiology of lymphedema associated with a DFU. Furthermore, the surgical complexity and potential morbidity at the donor site of vascularized lymph node transfer may complicate its application.

Conclusion

Foot ulceration represents a significant burden of morbidity and excess mortality for diabetic patients, and is an enormous challenge for health care providers. There is significant overlap in the pathophysiology of both DFU and lymphedema, but further research is needed to better our understanding. The treatment strategies outlined here address the management of DFU in conjunction with lower limb lymphedema; however, novel strategies such as manipulation of innate immune inflammatory pathways through modulation of TLR and connexin regulation therapies have the potential to benefit both these pathologies. Our understanding of lymphatic biology in relation to chronic ulcers has to be advanced with further research, as it holds immense benefit for both patients and the health care system.

Disclosure

None of the authors have any commercial associations or financial relationships that would create a conflict of interest with regard to the work presented in this article.

References

1. Bakker K, Apelqvist J, Schaper NC. Practical guidelines on the management and prevention of the diabetic foot 2011. *Diabetes Metab Res Rev*. 2012;28 Suppl 1:225–231.
2. Diabetes UK. State of the nation. 2012. Available from: https://www.diabetes.org.uk/documents/reports/state-of-the-nation-2012.pdf. Accessed June 25, 2015.

3. Edwards J, Stapley S. Debridement of diabetic foot ulcers. *Cochrane Database Syst Rev*. 2010;1:CD003556.
4. Jeffcoate WJ, Harding KG. Diabetic foot ulcers. *Lancet*. 2003; 361(9368):1545–1551.
5. Lepow BD, Downey M, Yurgelon J, Klassen L, Armstrong DG. Bioengineered tissues in wound healing: a progress report. *Expert Rev Dermatol*. 2011;6(3):255–262.
6. Kerr M. Foot care for people with diabetes: The economic case for change. 2012. Available from: https://www.diabetes.org.uk/documents/nhs-diabetes/footcare/footcare-for-people-with-diabetes.pdf. Accessed June 25, 2015.
7. Waugh NR. Amputations in diabetic patients – a review of rates, relative risks and resource use. *Community Med*. 1988;10(4):279–288.
8. Alavi A, Sibbald RG, Mayer D, et al. Diabetic foot ulcers: Part I Pathophysiology and prevention. *J Am Acad Dermatol*. 2014;70(1):1.e1–e18.
9. Iversen MM, Tell GS, Riise T, et al. History of foot ulcer increases mortality among individuals with diabetes: ten-year follow-up of the Nord-Trondelag Health Study, Norway. *Diabetes Care*. 2009;32(12):2193–2199.
10. Armstrong DG, Kanda VA, Lavery LA, Marston W, Mills JL Sr, Boulton AJ. Mind the gap: disparity between research funding and costs of care for diabetic foot ulcers. *Diabetes Care*. 2013;36(7): 1815–1817.
11. Apelqvist J, Larsson J, Agardh CD. Medical risk factors in diabetic patients with foot ulcers and severe peripheral vascular disease and their influence on outcome. *J Diabetes Complications*. 1992;6(3): 167–174.
12. Apelqvist J, Larsson J, Agardh CD. The importance of peripheral pulses, peripheral oedema and local pain for the outcome of diabetic foot ulcers. *Diabet Med*. 1990;7(7):590–594.
13. Ridner SH, Dietrich MS. Self-reported comorbid conditions and medication usage in breast cancer survivors with and without lymphedema. *Oncol Nurs Forum*. 2008;35(1):57–63.
14. Jockenhofer F, Gollnick H, Herberger K, et al. Aetiology, comorbidities and cofactors of chronic leg ulcers: retrospective evaluation of 1000 patients from 10 specialised dermatological wound care centers in Germany. *Int Wound J*. December 5, 2014. [Epub ahead of print.]
15. Margolis DJ, Kantor J, Berlin JA. Healing of diabetic neuropathic foot ulcers receiving standard treatment. A meta-analysis. *Diabetes Care*. 1999;22(5):692–695.
16. Skyler J. Effects of glycaemic control on diabetes complications and on the prevention of diabetes. *Clin Diabetes*. 2004;22(4):5.
17. Di Mario U, Pugliese G. Pathogenetic mechanisms of diabetic microangiopathy. *Int Congr Ser*. 2003;1253:171–182.
18. Mortimer PS, Levick JR. Chronic peripheral oedema: the critical role of the lymphatic system. *Clin Med*. 2004;4(5):448–453.
19. Belcaro G, Nicolaides AN, Volteas N, Leon M. Skin flow the venoarteriolar response and capillary filtration in diabetics. A 3-year follow-up. *Angiology*. 1992;43(6):490–495.
20. Jorneskog G, Fagrell B. Discrepancy in skin capillary circulation between fingers and toes in patients with type 1 diabetes. *Int J Microcirc Clin Exp*. 1996;16(6):313–319.
21. Rendell M, Bamisedun O. Diabetic cutaneous microangiopathy. *Am J Med*. 1992;93(6):611–618.
22. Valensi P, Behar A, Attalah M, Cohen-Boulakia F, Paries J, Attali JR. Increased capillary filtration of albumin in diabetic patients – relation with gender, hypertension, microangiopathy, and neuropathy. *Metabolism*. 1998;47(5):503–507.
23. Cosson E, Cohen-Boulakia F, Tarhzaoui K, et al. Capillary endothelial but not lymphatic function is restored under rosiglitazone in Zucker diabetic fatty rats. *Microvasc Res*. 2009;77(2):220–225.
24. Incandela L, Cesarone MR, DeSanctis MT, Belcaro G, Dugall M, Acerbi G. Treatment of diabetic microangiopathy and edema with HR (Paroven, Venoruton; 0-(beta-hydroxyethyl)-rutosides): a prospective, placebo-controlled, randomized study. *J Cardiovasc Pharmacol Ther*. 2002;7 Suppl 1:S11–S15.
25. Belcaro G, Cesarone MR, Ledda A, et al. 5-Year control and treatment of edema and increased capillary filtration in venous hypertension and diabetic microangiopathy using O-(beta-hydroxyethyl)-rutosides: a prospective comparative clinical registry. *Angiology*. 2008;59 Suppl 1: 14s–20s.
26. Cesarone MR, Belcaro G, Rohdewald P, et al. Improvement of diabetic microangiopathy with Pycnogenol: a prospective, controlled study. *Angiology*. 2006;57(4):431–436.
27. Rahimi Z, Moradi M, Nasri H. A systematic review of the role of renin angiotensin aldosterone system genes in diabetes mellitus, diabetic retinopathy and diabetic neuropathy. *J Res Med Sci*. 2014;19(11): 1090–1098.
28. Trettin H. [Neurologic principles of edema in inactivity]. *Z Lymphol*. 1992;16(1):14–16. German.
29. Suma TK, Shenoy RK, Varghese J, Kuttikkal VV, Kumaraswami V. Estimation of ASO titer as an indicator of streptococcal infection precipitating acute adenolymphangitis in brugian lymphatic filariasis. *Southeast Asian J Trop Med Public Health*. 1997;28(4):826–830.
30. Vaqas B, Ryan TJ. Lymphoedema: pathophysiology and management in resource-poor settings – relevance for lymphatic filariasis control programmes. *Filaria J*. 2003;2(1):4.
31. Saito Y, Nakagami H, Kaneda Y, Morishita R. Lymphedema and therapeutic lymphangiogenesis. *Biomed Res Int*. 2013;2013:804675.
32. Macdonald JM, Sims N, Mayrovitz HN. Lymphedema, lipedema, and the open wound: the role of compression therapy. *Surg Clin North Am*. 2003;83(3):639–658.
33. Chao CY, Zheng YP, Cheing GL. The association between skin blood flow and edema on epidermal thickness in the diabetic foot. *Diabetes Technol Ther*. 2012;14(7):602–609.
34. Mese G, Richard G, White TW. Gap junctions: basic structure and function. *J Invest Dermatol*. 2007;127(11):2516–2524.
35. Martin PE, Easton JA, Hodgins MB, Wright CS. Connexins: sensors of epidermal integrity that are therapeutic targets. *FEBS Lett*. 2014; 588(8):1304–1314.
36. Richard G. Connexins: a connection with the skin. *Exp Dermatol*. 2000;9(2):77–96.
37. Salomon D, Masgrau E, Vischer S, et al. Topography of mammalian connexins in human skin. *J Invest Dermatol*. 1994;103(2):240–247.
38. Wright JA, Richards T, Becker DL. Connexins and diabetes. *Cardiol Res Pract*. 2012;2012:496904.
39. Wang CM, Lincoln J, Cook JE, Becker DL. Abnormal connexin expression underlies delayed wound healing in diabetic skin. *Diabetes*. 2007;56(11):2809–2817.
40. Becker DL, Thrasivoulou C, Phillips AR. Connexins in wound healing; perspectives in diabetic patients. *Biochim Biophys Acta*. 2012;1818(8):2068–2075.
41. Kanady JD, Simon AM. Lymphatic communication: connexin junction, what's your function? *Lymphology*. 2011;44(3):95–102.
42. Kanady JD, Dellinger MT, Munger SJ, Witte MH, Simon AM. Connexin37 and Connexin43 deficiencies in mice disrupt lymphatic valve development and result in lymphatic disorders including lymphedema and chylothorax. *Dev Biol*. 2011;354(2):253–266.
43. Ostergaard P, Simpson MA, Brice G, et al. Rapid identification of mutations in GJC2 in primary lymphoedema using whole exome sequencing combined with linkage analysis with delineation of the phenotype. *J Med Genet*. 2011;48(4):251–255.
44. Ferrell RE, Baty CJ, Kimak MA, et al. GJC2 missense mutations cause human lymphedema. *Am J Hum Genet*. 2010;86(6):943–948.
45. Patel H, Shaw SG, Shi-Wen X, Abraham D, Baker DM, Tsui JC. Toll-like receptors in ischaemia and its potential role in the pathophysiology of muscle damage in critical limb ischaemia. *Cardiol Res Pract*. 2012;2012:121237.
46. Areschoug T, Gordon S. Pattern recognition receptors and their role in innate immunity: focus on microbial protein ligands. *Contrib Microbiol*. 2008;15:45–60.
47. Matzinger P. The danger model: a renewed sense of self. *Science*. 2002;296(5566):301–305.

48. Huebener P, Schwabe RF. Regulation of wound healing and organ fibrosis by toll-like receptors. *Biochim Biophys Acta*. 2013;1832(7):1005–1017.
49. Dasu MR, Isseroff RR. Toll-like receptors in wound healing: location, accessibility, and timing. *J Invest Dermatol*. 2012;132(8):1955–1958.
50. Suga H, Sugaya M, Fujita H, et al. TLR4, rather than TLR2, regulates wound healing through TGF-beta and CCL5 expression. *J Dermatol Sci*. 2014;73(2):117–124.
51. Chen L, Guo S, Ranzer MJ, DiPietro LA. Toll-like receptor 4 has an essential role in early skin wound healing. *J Invest Dermatol*. 2013;133(1):258–267.
52. Dasu MR, Thangappan RK, Bourgette A, DiPietro LA, Isseroff R, Jialal I. TLR2 expression and signaling-dependent inflammation impair wound healing in diabetic mice. *Lab Invest*. 2010;90(11):1628–1636.
53. Dasu MR, Jialal I. Amelioration in wound healing in diabetic toll-like receptor-4 knockout mice. *J Diabetes Complications*. 2013;27(5):417–421.
54. Zampell JC, Yan A, Avraham T, et al. Temporal and spatial patterns of endogenous danger signal expression after wound healing and in response to lymphedema. *Am J Physiol Cell Physiol*. 2011;300(5):C1107–C1121.
55. Zampell JC, Elhadad S, Avraham T, et al. Toll-like receptor deficiency worsens inflammation and lymphedema after lymphatic injury. *Am J Physiol Cell Physiol*. 2012;302(4):C709–C719.
56. Braun LR, Fisk WA, Lev-Tov H, Kirsner RS, Isseroff RR. Diabetic foot ulcer: an evidence-based treatment update. *Am J Clin Dermatol*. 2014;15(3):267–281.
57. Bretzel RG. Intensive insulin regimens: evidence for benefit. *Int J Obes Relat Metab Disord*. 2004;28 Suppl 2:S8–S13.
58. Rockson SG. Lymphedema. *Am J Med*. 2001;110(4):288–295.
59. Benton D, Avery G. Quality, research and ritual in nursing. *Nurs Stand*. 1993;7(49):29–30.
60. Tan IC, Maus EA, Rasmussen JC, et al. Assessment of lymphatic contractile function after manual lymphatic drainage using near-infrared fluorescence imaging. *Arch Phys Med Rehabil*. 2011;92(5):756–764. e751.
61. Unno N, Nishiyama M, Suzuki M, et al. A novel method of measuring human lymphatic pumping using indocyanine green fluorescence lymphography. *J Vasc Surg*. 2010;52(4):946–952.
62. Duman I, Ozdemir A, Tan AK, Dincer K. The efficacy of manual lymphatic drainage therapy in the management of limb edema secondary to reflex sympathetic dystrophy. *Rheumatol Int*. 2009;29(7):759–763.
63. Huang TW, Tseng SH, Lin CC, et al. Effects of manual lymphatic drainage on breast cancer-related lymphedema: a systematic review and meta-analysis of randomized controlled trials. *World J Surg Oncol*. 2013;11:15.
64. Belcaro G, Christopoulos A, Nicolaides AN. Diabetic microangiopathy treated with elastic compression – a microcirculatory evaluation using laser-Doppler flowmetry, transcutaneous PO2/PCO2 and capillary permeability measurements. *Vasa*. 1990;19(3):247–251.
65. Partsch H, Moffatt C. An overview of the science behind compression bandaging for lymphoedema and chronic oedema. In: Glover D, editor. *Best Practice for the Management of Lymphoedema*. 2nd ed, International Lymphoedema Framework; 2012. Available from: http://www.lympho.org/mod_turbolead/upload/file/Resources/Compression%20bandaging%20-%20final.pdf. Accessed June 25, 2015.
66. Mars M, Desai Y, Gregory MA. Compressed air massage hastens healing of the diabetic foot. *Diabetes Technol Ther*. 2008;10(1):39–45.
67. Armstrong DG, Nguyen HC. Improvement in healing with aggressive edema reduction after debridement of foot infection in persons with diabetes. *Arch Surg*. 2000;135(12):1405–1409.
68. Comerota AJ, Chouhan V, Harada RN, et al. The fibrinolytic effects of intermittent pneumatic compression: mechanism of enhanced fibrinolysis. *Ann Surg*. 1997;226(3):306–313.
69. Ho TK, Leigh RD, Tsui J. Diabetic foot disease and oedema. *Br J Diabetes Vasc Dis*. 2013;13(1):45–50.
70. Alavi A, Sibbald RG, Mayer D, et al. Diabetic foot ulcers: Part II Management. *J Am Acad Dermatol*. 2014;70(1):21. e21–e24.
71. Yazdanpanah L, Nasiri M, Adarvishi S. Literature review on the management of diabetic foot ulcer. *World J Diabetes*. 2015;6(1):37–53.
72. Lin CT, Ou KW, Chang SC. Diabetic foot ulcers combination with lower limb lymphedema treated by staged Charles procedure: case report and literature review. *Pak J Med Sci*. 2013;29(4):1062–1064.
73. Karnasula VM. Management of ulcers in lymphoedematous limbs. *Indian J Plast Surg*. 2012;45(2):261–265.
74. Ito R, Suami H. Overview of lymph node transfer for lymphedema treatment. *Plast Reconstr Surg*. 2014;134(3):548–556.
75. Lahteenvuo M, Honkonen K, Tervala T, et al. Growth factor therapy and autologous lymph node transfer in lymphedema. *Circulation*. 2011;123(6):613–620.
76. Honkonen KM, Visuri MT, Tervala TV, et al. Lymph node transfer and perinodal lymphatic growth factor treatment for lymphedema. *Ann Surg*. 2013;257(5):961–967.
77. Lin CH, Ali R, Chen SC, et al. Vascularized groin lymph node transfer using the wrist as a recipient site for management of postmastectomy upper extremity lymphedema. *Plast Reconstr Surg*. 2009;123(4):1265–1275.
78. Cheng MH, Chen SC, Henry SL, Tan BK, Lin MC, Huang JJ. Vascularized groin lymph node flap transfer for postmastectomy upper limb lymphedema: flap anatomy, recipient sites, and outcomes. *Plast Reconstr Surg*. 2013;131(6):1286–1298.

D: Patient consent form and information pack

Royal Free and University College Medical School
UNIVERSITY COLLEGE LONDON

Address for Correspondence:
University Department of Surgery
Royal Free Campus
The Royal Free Hospital
Pond Street,
London NW3 2QG
Telephone: 020 77940500
Facsimile: 02074726711

PATIENT
INFORMATION
SHEET

Study Title: A study of tissue damage in peripheral vascular disease and diabetes

You are invited to participate in a research study. This information sheet explains why we are conducting this study and how it is being done. Please take some time to read the information carefully and to decide whether you would like to take part or not. Please discuss it with your family and friends as you wish and ask us if you have any questions.

What is the purpose of this study?

The aim of this project is to study some aspects of peripheral vascular disease and diabetes which are not well understood. Peripheral vascular disease is a common condition where the blood supply to the legs is impaired and the leg muscles are damaged. Diabetes is another common condition which results in the body being unable to control blood sugar levels correctly. Despite current treatment options, both conditions can lead to significant tissue damage. We aim to study the mechanisms that are involved in causing muscle damage secondary to peripheral vascular disease and/or diabetes. A better understanding of these mechanisms may improve treatment for this disease in the future.

Why have I been chosen?

You have been invited to take part either because you suffer from peripheral vascular disease and/or diabetes which has caused problems severe enough to require an amputation. This allows us to collect suitable samples for analyses.

Do I have to take part?

You do not have to take part in this study if you do not want to. If you decide to take part you may withdraw at any time without giving a reason. Your decision to take part or not will not affect your care in any way.

What will happen to me if I take part?

Tissue samples from the amputated limb will be taken during the operation. These are for the study and not part of the treatment. None of these should cause any ill effect or additional discomfort and will not affect your recovery from your operation.

What do I have to do?

You do not have to do anything more than you need to for your operation.

Royal Free and University College
Medical School
UNIVERSITY COLLEGE LONDON
Address for Correspondence:
University Department of Surgery
Royal Free Campus
The Royal Free Hospital
Pond Street,
London NW3 2QG
Telephone: 020 77940500
Facsimile: 02074726711

Date: 25 Sept 2008

What are the possible disadvantages and risks in taking part?

The tissue samples will be taken from the amputated leg during surgery when you are anaesthetized and so will not cause any discomfort. Your treatment and recovery will not be affected.

What are the possible benefits of taking part?

This study will help us improve treatment for this condition in the future. However, at this stage, there will be no immediate benefits to you.

What if something goes wrong?

This study does not involve any extra treatment or any high-risk procedures so nothing is likely to go wrong. However, if you wish to complain about any aspect of the way you have been approached or treated during the course of this study, the normal National Health Service complaints mechanisms may be available to you.

Will taking part in this study be kept confidential?

Any information collected about you during the course of the research will be kept strictly confidential.

What happens to the results of the research study?

Results from this study will be published in a medical journal in approximately a year's time. However you will not be identified in any report or publication. If you wish to know the outcome of the study, you can do so by contacting us.

Who is organizing and funding the research?

This study is organised and funded by the Vascular Unit of the Department of Surgery.

Who has reviewed the study?

The Research Ethics Committee of the Royal Free Hospital has reviewed this study.

If you have any questions or queries at any stage, please contact:

Miss Janice Tsui
University Department of Surgery
Royal Free Hospital
Pond Street
London NW3 2QG

Tel: 020-7794-0500 Ext 33938

You will be given a copy of the information sheet and a signed consent form to keep. Thank you very much for taking part in this study.

Royal Free and University College
Medical School
UNIVERSITY COLLEGE LONDON
Address for Correspondence:
University Department of Surgery
Royal Free Campus
The Royal Free Hospital
Pond Street,
London NW3 2QG
Telephone: 020 77940500
Facsimile: 02074726711

Consent Form

Project Title: Study of Tissue Damage in Peripheral Vascular Disease and Diabetes

Researcher: Miss Janice Tsui & _____

1. I confirm that I have read and understood the information sheet provided for the above study and have had the opportunity to ask questions. ☐
2. I confirm that I have had sufficient time to consider whether or not I want to be included with the study. ☐
3. I understand that my participation is voluntary and that I am free to withdraw at any time, without giving any reasons, without my medical care or legal rights being affected. ☐
4. I understand that sections of my medical notes may be looked at by responsible individuals from NHS or from regulatory authorities where it is relevant to my taking part in the research. I understand that samples of my muscle may be kept up to 6 months for other studies. ☐
5. I agree to take part in the above study. ☐

Name of patient	Date	Signature
Name of person taking consent	Date	Signature

Royal Free and University College
Medical School
UNIVERSITY COLLEGE LONDON
Address for Correspondence:
University Department of Surgery,
Royal Free Campus
The Royal Free Hospital
Pond Street,
London NW3 2QG
Telephone: 020 77940500
Facsimile: 02074726711

Consent Form

Project Title: Study of Tissue Damage in Peripheral Vascular Disease and Diabetes

Researcher: Miss Janice Tsui & _____

1. I confirm that I have read and understood the information sheet provided for the above study and have had the opportunity to ask questions. ☐
2. I confirm that I have had sufficient time to consider whether or not I want to be included with the study. ☐
3. I understand that my participation is voluntary and that I am free to withdraw at any time, without giving any reasons, without my medical care or legal rights being affected. ☐
4. I understand that sections of my medical notes may be looked at by responsible individuals from NHS or from regulatory authorities where it is relevant to my taking part in the research. I understand that samples of my muscle may be kept up to 6 months for other studies. ☐
5. I agree to take part in the above study. ☐

Name of patient	Date	Signature

Name of person taking consent	Date	Signature

Patient Data

Sample Type: Normal ☐ Ischaemic ☐ Number:

Information sheet/ Consent: Yes ☐ No ☐

Hospital Number: Ethnic Group:

Name: Sex: Male ☐ Female ☐

Date of Birth:

PMH Date of onset:

- Bleeding Disorders ☐
- Diabetes ☐ _____
- IHD ☐ _____
- CVA ☐ _____
- Hypertension ☐ _____
- Other _____

Medications

Smoking Hx

Fontaine Classification

Investigations

- ABPI:
- Duplex:
- Angiogram:
- Coronary Angiogram:
- ECG:

E: Personal licence

SOCIETY OF Biology

This is to certify that

Mark James Portou

has been assessed as having satisfactorily completed accredited training for personnel working under the Animals (Scientific Procedures) Act 1986

Modules: **1, 2, 3 & 4 (General Principles)**

Species: **rat & mouse**

Training organised by: **Biological Services, UCL**

Certificate Number: **UCL/13/074**

Date: **16-18 April 2013**

Course Organiser

For the Society of Biology

This is <u>not</u> a licence to perform procedures under the Animals (Scientific Procedures) Act 1986

Incorporated by Royal Charter
Registered Charity No. 277981

UNIVERSITY COLLEGE LONDON
ROYAL FREE CAMPUS
CBU
Duncan Moore
DATE: 3/12/13.
cc. JP + SG.

Home Office

No. PIL 70/25983

ANIMALS (SCIENTIFIC PROCEDURES) ACT 1986

PERSONAL LICENCE

to

carry out regulated procedures on living animals.

In pursuance of the powers vested in him by the above Act, the Secretary of State hereby licenses

Dr M J Portou
UCL C/O D P Moore,Comparative Biology
UCL, Royal Free Campus, Medicine
Rowland Hill Street
Hampstead, London
NW3 2PF

to apply regulated procedures of the category or categories specified in column a of paragraph 8 of the attached Schedule to the kinds of animals in column b of the same paragraph at places specified in authorised project licences subject to the restrictions and provisions contained in the Act, and subject also to the limitations and conditions contained in this licence and to such other conditions as the Secretary of State may from time to time prescribe.

This licence shall be in force until revoked by the Secretary of State and shall be periodically reviewed by him.

Home Office
2 Marsham Street
London SW1P 4DF

For the Secretary of State

25 November 2013

NB. This licence does not authorise the licensee to perform any of the procedures specified in it unless they are carried out in the course of a project for which there is a project licence in force under the Act.

Home Office

PIL 70/25983
25 November 2013

Personal Licence - Additional Conditions

Any additional conditions that may apply to this licence are set out below.

Home Office

No. PIL 70/25983

8. The techniques and animals for which you have authority

Date Granted:	25 November 2013

Category	a. Procedure	b. Animal(s)
A	Minor/minimally invasive procedures not requiring sedation, analgesia or general anaesthesia	Mice
B	Minor/minimally invasive procedures involving sedation, analgesia or brief general anaesthesia Plus - surgical procedures conducted under brief non-recovery general anaesthesia	Mice
C	Surgical procedures involving general anaesthesia Plus – administration and maintenance of balanced or prolonged general anaesthesia	Mice

Home Office

Animals in Science Regulation Unit
Home Office Science
ASRU (Mail Point 20B)
4th Floor, SW Seacole Building 2 Marsham Street,
London SW1P 4DF
Tel 020 7035 0477 Fax 0870 336 9155

Dr M J Portou
C/O Mr Moore
Royal Free & University
College Medical School
Comparative Biology Unit
Rowland Hill Street LONDON
NW3 2PF

Your Reference

Our Reference PIL 70/25983

Date 25 November 2013

Dear Dr Portou

ANIMALS (SCIENTIFIC PROCEDURES) ACT 1986

I am pleased to inform you that the Secretary of State has granted you a personal licence.

You should check through your licence carefully for any endorsements on this licence in relation to animal types, licence category and the conditions attached to it. A personal licence on its own does not authorise you to perform regulated procedures on protected animals. You may perform only procedures of the category specified by it if the procedure is applied as part of a programme of work specified in a project licence authorising the application, as part of that programme, of a regulated procedure of that description to an animal of that description. The application of unauthorised regulated procedures is a contravention of the Act and may result in prosecution and/or variation, suspension or revocation of your licence.

You are required to keep a record of all regulated procedures that you have carried out. This information must be made readily available to the Inspector or Secretary of State when required. If you cease to carry out work requiring a licence (for example leaving the UK to work abroad) you must return your licence to the Home Office.

As soon as you cease to work at the establishment given as the primary availability on your licence, or it ceases to be the place where you wish your licence to be primarily available, you must notify the Home Office, as this change will affect the fees charged. If the establishment shown on your licence ceases to be your sole or primary place of work then the holder of the establishment licence may request the Home Office to revoke your licence. You must therefore be certain that your personal licence is in force before carrying out regulated procedures by confirming with your primary establishment.

No other person may perform, either in whole or in part, any procedure authorised by your personal licence. The only exceptions are certain specific tasks of a non-technical nature. No other delegation is permitted (see Guidance on the Operation of the Act).

Should you wish any part of this licence to be amended, you must apply to the Home Office giving details of the changes requested and using the Application for change(s) to a Personal Licence form located at: http://www.homeoffice.gov.uk/science-research/animal-research/

Yours sincerely

J. Sabu

Mrs J Sabu

Bibliography

1. Raghav A, Khan ZA, Labala RK, Ahmad J, Noor S, Mishra BK. Financial burden of diabetic foot ulcers to world: a progressive topic to discuss always. Ther Adv Endocrinol Metab. 2018;9(1):29-31.
2. Mortality GBD, Causes of Death C. Global, regional, and national age-sex specific all-cause and cause-specific mortality for 240 causes of death, 1990-2013: a systematic analysis for the Global Burden of Disease Study 2013. Lancet. 2015;385(9963):117-71.
3. WHO global report on diabetes: 2018 [Available from: http://apps.who.int/iris/bitstream/handle/10665/204871/9789241565257_eng.pdf;jsessionid=A229DE3E80BEC5034F70ED464AEC4E0F?sequence=1.
4. Zajuc J. Main events in history of diabetes mellitus in: Principles of Diabetes Mellitus2010.
5. Cho NH, Shaw JE, Karuranga S, Huang Y, da Rocha Fernandes JD, Ohlrogge AW, et al. IDF Diabetes Atlas: Global estimates of diabetes prevalence for 2017 and projections for 2045. Diabetes Res Clin Pract. 2018;138:271-81.
6. American Diabetes A. Diagnosis and classification of diabetes mellitus. Diabetes Care. 2004;27 Suppl 1:S5-S10.
7. Shi Y, Hu FB. The global implications of diabetes and cancer. Lancet. 2014;383(9933):1947-8.
8. Wang G. Raison d'etre of insulin resistance: the adjustable threshold hypothesis. J R Soc Interface. 2014;11(101):20140892.
9. Rother KI. Diabetes treatment--bridging the divide. N Engl J Med. 2007;356(15):1499-501.
10. Ahlqvist E, Storm P, Karajamaki A, Martinell M, Dorkhan M, Carlsson A, et al. Novel subgroups of adult-onset diabetes and their association with outcomes: a data-driven cluster analysis of six variables. Lancet Diabetes Endocrinol. 2018;6(5):361-9.
11. King P, Peacock I, Donnelly R. The UK prospective diabetes study (UKPDS): clinical and therapeutic implications for type 2 diabetes. Br J Clin Pharmacol. 1999;48(5):643-8.
12. Strongman H, Christopher S, Majak M, Williams R, Bahmanyar S, Linder M, et al. Pioglitazone and cause-specific risk of mortality in patients with type 2 diabetes: extended analysis from a European multidatabase cohort study. BMJ Open Diabetes Res Care. 2018;6(1):e000481.
13. Copenhaver M, Hoffman RP. Type 1 diabetes: where are we in 2017? Transl Pediatr. 2017;6(4):359-64.
14. Leal J, Gray AM, Clarke PM. Development of life-expectancy tables for people with type 2 diabetes. Eur Heart J. 2009;30(7):834-9.
15. Vestberg D, Rosengren A, Eeg-Olofsson K, Miftaraj M, Franzen S, Svensson AM, et al. Body mass index as a risk factor for coronary events and mortality in patients with type 1 diabetes. Open Heart. 2018;5(1):e000727.
16. Young BA, Lin E, Von Korff M, Simon G, Ciechanowski P, Ludman EJ, et al. Diabetes complications severity index and risk of mortality, hospitalization, and healthcare utilization. Am J Manag Care. 2008;14(1):15-23.

17. American Diabetes A. Economic Costs of Diabetes in the U.S. in 2017. Diabetes Care. 2018;41(5):917-28.
18. Fowler MJ. Microvascular and Macrovascular Complications of Diabetes. Clinical Diabetes 2008((2)):77-82.
19. Khalil SA, Megallaa MH, Rohoma KH, Guindy MA, Zaki A, Hassanein M, et al. Prevalence of Chronic Diabetic Complications in Newly Diagnosed versus Known Type 2 Diabetic Subjects in a Sample of Alexandria Population, Egypt. Curr Diabetes Rev. 2019;15(1):74-83.
20. Maffi P, Secchi A. The Burden of Diabetes: Emerging Data. Dev Ophthalmol. 2017;60:1-5.
21. Heydari. Chronic complications of diabetes mellitus in newly diagnosed patients. International Journal of Diabetes Mellitus. 2010;2(1):61-3.
22. Porta M, Curletto G, Cipullo D, Rigault de la Longrais R, Trento M, Passera P, et al. Estimating the delay between onset and diagnosis of type 2 diabetes from the time course of retinopathy prevalence. Diabetes Care. 2014;37(6):1668-74.
23. Wang W, Lo ACY. Diabetic Retinopathy: Pathophysiology and Treatments. Int J Mol Sci. 2018;19(6).
24. Lim A. Diabetic nephropathy - complications and treatment. Int J Nephrol Renovasc Dis. 2014;7:361-81.
25. Papatheodorou K, Banach M, Bekiari E, Rizzo M, Edmonds M. Complications of Diabetes 2017. J Diabetes Res. 2018;2018:3086167.
26. Komici K, Femminella GD, de Lucia C, Cannavo A, Bencivenga L, Corbi G, et al. Predisposing factors to heart failure in diabetic nephropathy: a look at the sympathetic nervous system hyperactivity. Aging Clin Exp Res. 2018.
27. Shakher J, Stevens MJ. Update on the management of diabetic polyneuropathies. Diabetes Metab Syndr Obes. 2011;4:289-305.
28. Ziegler D, Landgraf R, Lobmann R, Reiners K, Rett K, Schnell O, et al. Painful and painless neuropathies are distinct and largely undiagnosed entities in subjects participating in an educational initiative (PROTECT study). Diabetes Res Clin Pract. 2018;139:147-54.
29. Tesfaye S, Chaturvedi N, Eaton SE, Ward JD, Manes C, Ionescu-Tirgoviste C, et al. Vascular risk factors and diabetic neuropathy. N Engl J Med. 2005;352(4):341-50.
30. Nathan DM, Group DER. The diabetes control and complications trial/epidemiology of diabetes interventions and complications study at 30 years: overview. Diabetes Care. 2014;37(1):9-16.
31. Abraira C, Duckworth WC, Moritz T, Group V. Glycaemic separation and risk factor control in the Veterans Affairs Diabetes Trial: an interim report. Diabetes Obes Metab. 2009;11(2):150-6.
32. Testa R, Bonfigli AR, Prattichizzo F, La Sala L, De Nigris V, Ceriello A. The "Metabolic Memory" Theory and the Early Treatment of Hyperglycemia in Prevention of Diabetic Complications. Nutrients. 2017;9(5).
33. Bailey C. Glycaemic memory The British Journal of Diabetes & Vascular Disease. 2008;8(5):242-7.
34. McClelland AD, Kantharidis P. microRNA in the development of diabetic complications. Clin Sci (Lond). 2014;126(2):95-110.
35. Beltrami C, Angelini TG, Emanueli C. Noncoding RNAs in diabetes vascular complications. J Mol Cell Cardiol. 2015;89(Pt A):42-50.

36. Mitsios JP, Ekinci EI, Mitsios GP, Churilov L, Thijs V. Relationship Between Glycated Hemoglobin and Stroke Risk: A Systematic Review and Meta-Analysis. J Am Heart Assoc. 2018;7(11).
37. Huang D, Refaat M, Mohammedi K, Jayyousi A, Al Suwaidi J, Abi Khalil C. Macrovascular Complications in Patients with Diabetes and Prediabetes. Biomed Res Int. 2017;2017:7839101.
38. Jensen LO, Maeng M, Thayssen P, Tilsted HH, Terkelsen CJ, Kaltoft A, et al. Influence of diabetes mellitus on clinical outcomes following primary percutaneous coronary intervention in patients with ST-segment elevation myocardial infarction. Am J Cardiol. 2012;109(5):629-35.
39. Beckman JA, Creager MA, Libby P. Diabetes and atherosclerosis: epidemiology, pathophysiology, and management. JAMA. 2002;287(19):2570-81.
40. Heller SR, Group AC. A summary of the ADVANCE Trial. Diabetes Care. 2009;32 Suppl 2:S357-61.
41. Duckworth W, Abraira C, Moritz T, Reda D, Emanuele N, Reaven PD, et al. Glucose control and vascular complications in veterans with type 2 diabetes. N Engl J Med. 2009;360(2):129-39.
42. Action to Control Cardiovascular Risk in Diabetes Study G, Gerstein HC, Miller ME, Byington RP, Goff DC, Jr., Bigger JT, et al. Effects of intensive glucose lowering in type 2 diabetes. N Engl J Med. 2008;358(24):2545-59.
43. Boussageon R, Bejan-Angoulvant T, Saadatian-Elahi M, Lafont S, Bergeonneau C, Kassai B, et al. Effect of intensive glucose lowering treatment on all cause mortality, cardiovascular death, and microvascular events in type 2 diabetes: meta-analysis of randomised controlled trials. BMJ. 2011;343:d4169.
44. Brownlee M. The pathobiology of diabetic complications: a unifying mechanism. Diabetes. 2005;54(6):1615-25.
45. Giacco F, Brownlee M. Oxidative stress and diabetic complications. Circ Res. 2010;107(9):1058-70.
46. Morley RL, Sharma A, Horsch AD, Hinchliffe RJ. Peripheral artery disease. BMJ. 2018;360:j5842.
47. McDermott MM, Greenland P, Liu K, Guralnik JM, Criqui MH, Dolan NC, et al. Leg symptoms in peripheral arterial disease: associated clinical characteristics and functional impairment. JAMA. 2001;286(13):1599-606.
48. NICE. Critical limb ischaemia in peripheral vascular disease 2013 [Available from: www.nice.org.uk.
49. Norgren L, Hiatt WR, Dormandy JA, Nehler MR, Harris KA, Fowkes FG, et al. Inter-society consensus for the management of peripheral arterial disease. Int Angiol. 2007;26(2):81-157.
50. Motsumi MJ, Naidoo NG. Pattern and distribution of peripheral arterial disease in diabetic patients with critical limb ischemia (rutherford clinical category 4-6). S Afr J Surg. 2017;55(3):48-54.
51. O'Loughlin A, McIntosh C, Dinneen SF, O'Brien T. Review paper: basic concepts to novel therapies: a review of the diabetic foot. The international journal of lower extremity wounds. 2010;9(2):90-102.
52. Fadini GP, Albiero M, Menegazzo L, Boscaro E, Pagnin E, Iori E, et al. The redox enzyme p66Shc contributes to diabetes and ischemia-induced delay in cutaneous wound healing. Diabetes. 2010;59(9):2306-14.

53. Acosta JB, del Barco DG, Vera DC, Savigne W, Lopez-Saura P, Guillen Nieto G, et al. The pro-inflammatory environment in recalcitrant diabetic foot wounds. Int Wound J. 2008;5(4):530-9.
54. Kerr M. Footcare in Diabetes: The economic case for change 2012 [Available from: http://www.professionalevents.co.uk/_images/_products2downloads/88_208.pdf.
55. Edmonds ME, Foster AV. Diabetic foot ulcers. BMJ. 2006;332(7538):407-10.
56. Adiewere P, Gillis RB, Imran Jiwani S, Meal A, Shaw I, Adams GG. A systematic review and meta-analysis of patient education in preventing and reducing the incidence or recurrence of adult diabetes foot ulcers (DFU). Heliyon. 2018;4(5):e00614.
57. Pendsey SP. Understanding diabetic foot. Int J Diabetes Dev Ctries. 2010;30(2):75-9.
58. Allan J, Munro W, Figgins E. Foot deformities within the diabetic foot and their influence on biomechanics: A review of the literature. Prosthet Orthot Int. 2016;40(2):182-92.
59. Arosi I, Hiner G, Rajbhandari S. Pathogenesis and Treatment of Callus in the Diabetic Foot. Curr Diabetes Rev. 2016;12(3):179-83.
60. Brownrigg JR, Apelqvist J, Bakker K, Schaper NC, Hinchliffe RJ. Evidence-based management of PAD & the diabetic foot. Eur J Vasc Endovasc Surg. 2013;45(6):673-81.
61. Prompers L, Schaper N, Apelqvist J, Edmonds M, Jude E, Mauricio D, et al. Prediction of outcome in individuals with diabetic foot ulcers: focus on the differences between individuals with and without peripheral arterial disease. The EURODIALE Study. Diabetologia. 2008;51(5):747-55.
62. NICE. Diabetic foot problems: prevention and management NICE guideline [NG19]. 2016.
63. Smith-Strom H, Iversen MM, Igland J, Ostbye T, Graue M, Skeie S, et al. Severity and duration of diabetic foot ulcer (DFU) before seeking care as predictors of healing time: A retrospective cohort study. PLoS One. 2017;12(5):e0177176.
64. Pickwell KM, Siersma VD, Kars M, Holstein PE, Schaper NC, Eurodiale c. Diabetic foot disease: impact of ulcer location on ulcer healing. Diabetes Metab Res Rev. 2013;29(5):377-83.
65. Game F. Classification of diabetic foot ulcers. Diabetes Metab Res Rev. 2016;32 Suppl 1:186-94.
66. Ince P, Abbas ZG, Lutale JK, Basit A, Ali SM, Chohan F, et al. Use of the SINBAD classification system and score in comparing outcome of foot ulcer management on three continents. Diabetes Care. 2008;31(5):964-7.
67. Lavery LA, Armstrong DG, Harkless LB. Classification of diabetic foot wounds. J Foot Ankle Surg. 1996;35(6):528-31.
68. Bolton LL. Quality Randomized Clinical Trials of Topical Diabetic Foot Ulcer Healing Agents. Adv Wound Care (New Rochelle). 2016;5(3):137-47.
69. Hubner G, Brauchle M, Smola H, Madlener M, Fassler R, Werner S. Differential regulation of pro-inflammatory cytokines during wound healing in normal and glucocorticoid-treated mice. Cytokine. 1996;8(7):548-56.
70. Guo S, Dipietro LA. Factors affecting wound healing. Journal of dental research. 2010;89(3):219-29.

71. Roupe KM, Nybo M, Sjobring U, Alberius P, Schmidtchen A, Sorensen OE. Injury is a major inducer of epidermal innate immune responses during wound healing. J Invest Dermatol. 2010;130(4):1167-77.
72. Kim MH, Liu W, Borjesson DL, Curry FR, Miller LS, Cheung AL, et al. Dynamics of neutrophil infiltration during cutaneous wound healing and infection using fluorescence imaging. J Invest Dermatol. 2008;128(7):1812-20.
73. Segal AW. How neutrophils kill microbes. Annu Rev Immunol. 2005;23:197-223.
74. Suga H, Sugaya M, Fujita H, Asano Y, Tada Y, Kadono T, et al. TLR4, rather than TLR2, regulates wound healing through TGF-beta and CCL5 expression. J Dermatol Sci. 2014;73(2):117-24.
75. DiPietro LA. Wound healing: the role of the macrophage and other immune cells. Shock. 1995;4(4):233-40.
76. Deodhar AK, Rana RE. Surgical physiology of wound healing: a review. J Postgrad Med. 1997;43(2):52-6.
77. Fishel RS, Barbul A, Beschorner WE, Wasserkrug HL, Efron G. Lymphocyte participation in wound healing. Morphologic assessment using monoclonal antibodies. Ann Surg. 1987;206(1):25-9.
78. Park JE, Barbul A. Understanding the role of immune regulation in wound healing. Am J Surg. 2004;187(5A):11S-6S.
79. Jameson J, Havran WL. Skin gammadelta T-cell functions in homeostasis and wound healing. Immunol Rev. 2007;215:114-22.
80. Otranto D, Tarsitano E, Traversa D, Giangaspero A, De Luca F, Puccini V. Differentiation among three species of bovine Thelazia (Nematoda: Thelaziidae) by polymerase chain reaction-restriction fragment length polymorphism of the first internal transcribed spacer ITS-1 (rDNA). International journal for parasitology. 2001;31(14):1693-8.
81. Wild T, Rahbarnia A, Kellner M, Sobotka L, Eberlein T. Basics in nutrition and wound healing. Nutrition. 2010;26(9):862-6.
82. Gilbane AJ, Denton CP, Holmes AM. Scleroderma pathogenesis: a pivotal role for fibroblasts as effector cells. Arthritis Res Ther. 2013;15(3):215.
83. O'Toole EA. Extracellular matrix and keratinocyte migration. Clin Exp Dermatol. 2001;26(6):525-30.
84. Raja, Sivamani K, Garcia MS, Isseroff RR. Wound re-epithelialization: modulating keratinocyte migration in wound healing. Front Biosci. 2007;12:2849-68.
85. Haase I, Evans R, Pofahl R, Watt FM. Regulation of keratinocyte shape, migration and wound epithelialization by IGF-1- and EGF-dependent signalling pathways. J Cell Sci. 2003;116(Pt 15):3227-38.
86. Martins VL, Caley M, O'Toole EA. Matrix metalloproteinases and epidermal wound repair. Cell Tissue Res. 2013;351(2):255-68.
87. Amano S, Akutsu N, Ogura Y, Nishiyama T. Increase of laminin 5 synthesis in human keratinocytes by acute wound fluid, inflammatory cytokines and growth factors, and lysophospholipids. Br J Dermatol. 2004;151(5):961-70.
88. Usui ML, Mansbridge JN, Carter WG, Fujita M, Olerud JE. Keratinocyte migration, proliferation, and differentiation in chronic ulcers from patients with diabetes and normal wounds. J Histochem Cytochem. 2008;56(7):687-96.

89. Wetzler C, Kampfer H, Stallmeyer B, Pfeilschifter J, Frank S. Large and sustained induction of chemokines during impaired wound healing in the genetically diabetic mouse: prolonged persistence of neutrophils and macrophages during the late phase of repair. The Journal of investigative dermatology. 2000;115(2):245-53.
90. Nwomeh BC, Liang HX, Cohen IK, Yager DR. MMP-8 is the predominant collagenase in healing wounds and nonhealing ulcers. J Surg Res. 1999;81(2):189-95.
91. Portou MJ, Baker D, Abraham D, Tsui J. The innate immune system, toll-like receptors and dermal wound healing: A review. Vascular pharmacology. 2015;71:31-6.
92. Akira S, Uematsu S, Takeuchi O. Pathogen recognition and innate immunity. Cell. 2006;124(4):783-801.
93. Staros EB. Innate immunity: New approaches to understanding its clinical significance. Am J Clin Pathol. 2005;123(2):305-12.
94. Spirig R, Tsui J, Shaw S. The Emerging Role of TLR and Innate Immunity in Cardiovascular Disease. Cardiology research and practice. 2012;2012:181394.
95. Gordon S. Pattern recognition receptors: doubling up for the innate immune response. Cell. 2002;111(7):927-30.
96. Areschoug T, Gordon S. Pattern recognition receptors and their role in innate immunity: focus on microbial protein ligands. Contributions to microbiology. 2008;15:45-60.
97. Patel H, Shaw SG, Shi-Wen X, Abraham D, Baker DM, Tsui JC. Toll-like receptors in ischaemia and its potential role in the pathophysiology of muscle damage in critical limb ischaemia. Cardiology research and practice. 2012;2012:121237.
98. Navi A, Patel H, Shaw S, Baker D, Tsui J. Therapeutic role of toll-like receptor modification in cardiovascular dysfunction. Vascular pharmacology. 2013;58(3):231-9.
99. Mann DL. The emerging role of innate immunity in the heart and vascular system: for whom the cell tolls. Circ Res. 2011;108(9):1133-45.
100. De Nardo D, De Nardo CM, Nguyen T, Hamilton JA, Scholz GM. Signaling crosstalk during sequential TLR4 and TLR9 activation amplifies the inflammatory response of mouse macrophages. J Immunol. 2009;183(12):8110-8.
101. Huebener P, Schwabe RF. Regulation of wound healing and organ fibrosis by toll-like receptors. Biochimica et biophysica acta. 2013;1832(7):1005-17.
102. Alexander C, Rietschel ET. Bacterial lipopolysaccharides and innate immunity. J Endotoxin Res. 2001;7(3):167-202.
103. Sato T, Yamamoto M, Shimosato T, Klinman DM. Accelerated wound healing mediated by activation of Toll-like receptor 9. Wound repair and regeneration : official publication of the Wound Healing Society [and] the European Tissue Repair Society. 2010;18(6):586-93.
104. Matzinger P. The danger model: a renewed sense of self. Science. 2002;296(5566):301-5.
105. Dasu MR, Ramirez S, Isseroff RR. Toll-like receptors and diabetes: a therapeutic perspective. Clin Sci (Lond). 2012;122(5):203-14.
106. Salaun B, Romero P, Lebecque S. Toll-like receptors' two-edged sword: when immunity meets apoptosis. Eur J Immunol. 2007;37(12):3311-8.

107. Yuan J, Najafov A, Py BF. Roles of Caspases in Necrotic Cell Death. Cell. 2016;167(7):1693-704.
108. Haase R, Kirschning CJ, Sing A, Schrottner P, Fukase K, Kusumoto S, et al. A dominant role of Toll-like receptor 4 in the signaling of apoptosis in bacteria-faced macrophages. J Immunol. 2003;171(8):4294-303.
109. Yang Y, Lv J, Jiang S, Ma Z, Wang D, Hu W, et al. The emerging role of Toll-like receptor 4 in myocardial inflammation. Cell Death Dis. 2016;7:e2234.
110. Yao L, Lu P, Ling EA. Melatonin Suppresses Toll Like Receptor 4-Dependent Caspase-3 Signaling Activation Coupled with Reduced Production of Proinflammatory Mediators in Hypoxic Microglia. PLoS One. 2016;11(11):e0166010.
111. Li C, Che LH, Ji TF, Shi L, Yu JL. Effects of the TLR4 signaling pathway on apoptosis of neuronal cells in diabetes mellitus complicated with cerebral infarction in a rat model. Sci Rep. 2017;7:43834.
112. Terhorst D, Kalali BN, Ollert M, Ring J, Mempel M. The role of toll-like receptors in host defenses and their relevance to dermatologic diseases. American journal of clinical dermatology. 2010;11(1):1-10.
113. Pasparakis M, Haase I, Nestle FO. Mechanisms regulating skin immunity and inflammation. Nat Rev Immunol. 2014;14(5):289-301.
114. Miller LS, Modlin RL. Human keratinocyte Toll-like receptors promote distinct immune responses. J Invest Dermatol. 2007;127(2):262-3.
115. Miller LS, Sorensen OE, Liu PT, Jalian HR, Eshtiaghpour D, Behmanesh BE, et al. TGF-alpha regulates TLR expression and function on epidermal keratinocytes. J Immunol. 2005;174(10):6137-43.
116. Miller LS, Modlin RL. Toll-like receptors in the skin. Seminars in immunopathology. 2007;29(1):15-26.
117. Jang S, Park JS, Won YH, Yun SJ, Kim SJ. The Expression of Toll-Like Receptors (TLRs) in Cultured Human Skin Fibroblast is Modulated by Histamine. Chonnam Med J. 2012;48(1):7-14.
118. Wang J, Hori K, Ding J, Huang Y, Kwan P, Ladak A, et al. Toll-like receptors expressed by dermal fibroblasts contribute to hypertrophic scarring. J Cell Physiol. 2011;226(5):1265-73.
119. Taylor KR, Trowbridge JM, Rudisill JA, Termeer CC, Simon JC, Gallo RL. Hyaluronan fragments stimulate endothelial recognition of injury through TLR4. J Biol Chem. 2004;279(17):17079-84.
120. Dasu MR, Isseroff RR. Toll-like receptors in wound healing: location, accessibility, and timing. The Journal of investigative dermatology. 2012;132(8):1955-8.
121. Chen L, Guo S, Ranzer MJ, DiPietro LA. Toll-like receptor 4 has an essential role in early skin wound healing. J Invest Dermatol. 2013;133(1):258-67.
122. Dasu MR, Thangappan RK, Bourgette A, DiPietro LA, Isseroff R, Jialal I. TLR2 expression and signaling-dependent inflammation impair wound healing in diabetic mice. Lab Invest. 2010;90(11):1628-36.
123. Dasu MR, Jialal I. Amelioration in wound healing in diabetic toll-like receptor-4 knockout mice. Journal of diabetes and its complications. 2013;27(5):417-21.
124. Pukstad BS, Ryan L, Flo TH, Stenvik J, Moseley R, Harding K, et al. Non-healing is associated with persistent stimulation of the innate immune response in chronic venous leg ulcers. J Dermatol Sci. 2010;59(2):115-22.

125. Lin Q, Fang D, Fang J, Ren X, Yang X, Wen F, et al. Impaired wound healing with defective expression of chemokines and recruitment of myeloid cells in TLR3-deficient mice. J Immunol. 2011;186(6):3710-7.
126. Lin Q, Wang L, Lin Y, Liu X, Ren X, Wen S, et al. Toll-like receptor 3 ligand polyinosinic:polycytidylic acid promotes wound healing in human and murine skin. J Invest Dermatol. 2012;132(8):2085-92.
127. Smith PK, Krohn RI, Hermanson GT, Mallia AK, Gartner FH, Provenzano MD, et al. Measurement of protein using bicinchoninic acid. Anal Biochem. 1985;150(1):76-85.
128. Rath A, Glibowicka M, Nadeau VG, Chen G, Deber CM. Detergent binding explains anomalous SDS-PAGE migration of membrane proteins. Proc Natl Acad Sci U S A. 2009;106(6):1760-5.
129. Weber K, Osborn M. The reliability of molecular weight determinations by dodecyl sulfate-polyacrylamide gel electrophoresis. J Biol Chem. 1969;244(16):4406-12.
130. lifesciences GH. Amersham™ ECL™ Prime Western blotting detection reagent 2012 [Available from: https://cdn.gelifesciences.com/dmm3bwsv3/AssetStream.aspx?mediaformatid=10061&destinationid=10016&assetid=15681.
131. Boukamp P, Petrussevska RT, Breitkreutz D, Hornung J, Markham A, Fusenig NE. Normal keratinization in a spontaneously immortalized aneuploid human keratinocyte cell line. J Cell Biol. 1988;106(3):761-71.
132. Joshi D, Patel H, Baker DM, Shiwen X, Abraham DJ, Tsui JC. Development of an in vitro model of myotube ischemia. Lab Invest. 2011;91(8):1241-52.
133. Devaraj S, Venugopal SK, Singh U, Jialal I. Hyperglycemia induces monocytic release of interleukin-6 via induction of protein kinase c-{alpha} and -{beta}. Diabetes. 2005;54(1):85-91.
134. Dasu MR, Devaraj S, Zhao L, Hwang DH, Jialal I. High glucose induces toll-like receptor expression in human monocytes: mechanism of activation. Diabetes. 2008;57(11):3090-8.
135. Jiang SY, Wei CC, Shang TT, Lian Q, Wu CX, Deng JY. High glucose induces inflammatory cytokine through protein kinase C-induced toll-like receptor 2 pathway in gingival fibroblasts. Biochemical and biophysical research communications. 2012;427(3):666-70.
136. Cory G. Scratch-wound assay. Methods Mol Biol. 2011;769:25-30.
137. Liang CC, Park AY, Guan JL. In vitro scratch assay: a convenient and inexpensive method for analysis of cell migration in vitro. Nat Protoc. 2007;2(2):329-33.
138. Feoktistova M, Geserick P, Leverkus M. Crystal Violet Assay for Determining Viability of Cultured Cells. Cold Spring Harb Protoc. 2016;2016(4):pdb prot087379.
139. Eming SA, Martin P, Tomic-Canic M. Wound repair and regeneration: mechanisms, signaling, and translation. Sci Transl Med. 2014;6(265):265sr6.
140. Nyati KK, Masuda K, Zaman MM, Dubey PK, Millrine D, Chalise JP, et al. TLR4-induced NF-kappaB and MAPK signaling regulate the IL-6 mRNA stabilizing protein Arid5a. Nucleic Acids Res. 2017;45(5):2687-703.
141. Hampton AL, Hish GA, Aslam MN, Rothman ED, Bergin IL, Patterson KA, et al. Progression of ulcerative dermatitis lesions in C57BL/6Crl mice and the development

of a scoring system for dermatitis lesions. J Am Assoc Lab Anim Sci. 2012;51(5):586-93.
142. Sundberg JP, Taylor D, Lorch G, Miller J, Silva KA, Sundberg BA, et al. Primary follicular dystrophy with scarring dermatitis in C57BL/6 mouse substrains resembles central centrifugal cicatricial alopecia in humans. Vet Pathol. 2011;48(2):513-24.
143. Barcelos LS, Duplaa C, Krankel N, Graiani G, Invernici G, Katare R, et al. Human CD133+ progenitor cells promote the healing of diabetic ischemic ulcers by paracrine stimulation of angiogenesis and activation of Wnt signaling. Circulation research. 2009;104(9):1095-102.
144. Murray-Lyon IM, Eddleston AL, Williams R, Brown M, Hogbin BM, Bennett A, et al. Treatment of multiple-hormone-producing malignant islet-cell tumour with streptozotocin. Lancet. 1968;2(7574):895-8.
145. Emanueli C, Graiani G, Salis MB, Gadau S, Desortes E, Madeddu P. Prophylactic gene therapy with human tissue kallikrein ameliorates limb ischemia recovery in type 1 diabetic mice. Diabetes. 2004;53(4):1096-103.
146. Emanueli C, Salis MB, Pinna A, Stacca T, Milia AF, Spano A, et al. Prevention of diabetes-induced microangiopathy by human tissue kallikrein gene transfer. Circulation. 2002;106(8):993-9.
147. Lawrence RD. Renal Threshold for Glucose: Normal and in Diabetics. Br Med J. 1940;1(4140):766-8.
148. WHO. Definition and diagnosis of diabetes mellitus and intermediate hyperglycaemia 2006 [Available from: https://www.who.int/diabetes/publications/diagnosis_diabetes2006/en/.
149. Ferguson MW, Herrick SE, Spencer MJ, Shaw JE, Boulton AJ, Sloan P. The histology of diabetic foot ulcers. Diabet Med. 1996;13 Suppl 1:S30-3.
150. Mendoza Y, Valdés Pérez C, Rodríguez Corrales E, Suárez Alba J, García Ojalvo A, Garcia del Barco D, et al. Histological and Transcriptional Expression differences between Diabetic Foot and Pressure Ulcers2013. 296 p.
151. Szasz T, Wenceslau CF, Burgess B, Nunes KP, Webb RC. Toll-Like Receptor 4 Activation Contributes to Diabetic Bladder Dysfunction in a Murine Model of Type 1 Diabetes. Diabetes. 2016;65(12):3754-64.
152. Panzer R, Blobel C, Folster-Holst R, Proksch E. TLR2 and TLR4 expression in atopic dermatitis, contact dermatitis and psoriasis. Exp Dermatol. 2014;23(5):364-6.
153. Tellechea A, Kafanas A, Leal EC, Tecilazich F, Kuchibhotla S, Auster ME, et al. Increased skin inflammation and blood vessel density in human and experimental diabetes. The international journal of lower extremity wounds. 2013;12(1):4-11.
154. . !!! INVALID CITATION !!! {}.
155. Venardos N, Deng XS, Yao Q, Weyant MJ, Reece TB, Meng X, et al. Simvastatin reduces the TLR4-induced inflammatory response in human aortic valve interstitial cells. J Surg Res. 2018;230:101-9.
156. Yang J, Huang C, Yang J, Jiang H, Ding J. Statins attenuate high mobility group box-1 protein induced vascular endothelial activation : a key role for TLR4/NF-kappaB signaling pathway. Mol Cell Biochem. 2010;345(1-2):189-95.
157. Ajamieh H, Farrell G, Wong HJ, Yu J, Chu E, Chen J, et al. Atorvastatin protects obese mice against hepatic ischemia-reperfusion injury by Toll-like receptor-4 suppression and endothelial nitric oxide synthase activation. J Gastroenterol Hepatol. 2012;27(8):1353-61.

158. Katsargyris A, Klonaris C, Tsiodras S, Bastounis E, Giannopoulos A, Theocharis S. Statin treatment is associated with reduced toll-like receptor 4 immunohistochemical expression on carotid atherosclerotic plaques: a novel effect of statins. Vascular. 2011;19(6):320-6.
159. Ji Y, Liu J, Wang Z, Liu N. Angiotensin II induces inflammatory response partly via toll-like receptor 4-dependent signaling pathway in vascular smooth muscle cells. Cell Physiol Biochem. 2009;23(4-6):265-76.
160. Yang S, Li R, Qu X, Tang L, Ge G, Fang W, et al. Fosinoprilat alleviates lipopolysaccharide (LPS)-induced inflammation by inhibiting TLR4/NF-kappaB signaling in monocytes. Cell Immunol. 2013;284(1-2):182-6.
161. Eissler R, Schmaderer C, Rusai K, Kuhne L, Sollinger D, Lahmer T, et al. Hypertension augments cardiac Toll-like receptor 4 expression and activity. Hypertens Res. 2011;34(5):551-8.
162. Ceriello A, Motz E. Is oxidative stress the pathogenic mechanism underlying insulin resistance, diabetes, and cardiovascular disease? The common soil hypothesis revisited. Arterioscler Thromb Vasc Biol. 2004;24(5):816-23.
163. Lucas K, Maes M. Role of the Toll Like receptor (TLR) radical cycle in chronic inflammation: possible treatments targeting the TLR4 pathway. Molecular neurobiology. 2013;48(1):190-204.
164. Creely SJ, McTernan PG, Kusminski CM, Fisher f M, Da Silva NF, Khanolkar M, et al. Lipopolysaccharide activates an innate immune system response in human adipose tissue in obesity and type 2 diabetes. American journal of physiology Endocrinology and metabolism. 2007;292(3):E740-7.
165. Fan J, Frey RS, Malik AB. TLR4 signaling induces TLR2 expression in endothelial cells via neutrophil NADPH oxidase. The Journal of clinical investigation. 2003;112(8):1234-43.
166. Ding Y, Subramanian S, Montes VN, Goodspeed L, Wang S, Han C, et al. Toll-like receptor 4 deficiency decreases atherosclerosis but does not protect against inflammation in obese low-density lipoprotein receptor-deficient mice. Arterioscler Thromb Vasc Biol. 2012;32(7):1596-604.
167. Davis JE, Gabler NK, Walker-Daniels J, Spurlock ME. Tlr-4 deficiency selectively protects against obesity induced by diets high in saturated fat. Obesity (Silver Spring). 2008;16(6):1248-55.
168. Boxman IL, Ruwhof C, Boerman OC, Lowik CW, Ponec M. Role of fibroblasts in the regulation of proinflammatory interleukin IL-1, IL-6 and IL-8 levels induced by keratinocyte-derived IL-1. Arch Dermatol Res. 1996;288(7):391-8.
169. Kubo K, Kuroyanagi Y. A study of cytokines released from fibroblasts in cultured dermal substitute. Artif Organs. 2005;29(10):845-9.
170. He W, Qu T, Yu Q, Wang Z, Lv H, Zhang J, et al. LPS induces IL-8 expression through TLR4, MyD88, NF-kappaB and MAPK pathways in human dental pulp stem cells. Int Endod J. 2013;46(2):128-36.
171. Fahey TJ, 3rd, Turbeville T, McIntyre K. Differential TNF secretion by wound fibroblasts compared to normal fibroblasts in response to LPS. J Surg Res. 1995;58(6):759-64.
172. Navi A AD, Shi-wen X, Hamilton G, Baker D, Tsui J. Critical role of Toll-like receptor 4 in ischemia-induced skeletal muscle damage. ATVB 2014;34:A148.

173. Trengove NJ, Langton SR, Stacey MC. Biochemical analysis of wound fluid from nonhealing and healing chronic leg ulcers. Wound Repair Regen. 1996;4(2):234-9.
174. Spence VA, Walker WF. Tissue oxygen tension in normal and ischaemic human skin. Cardiovasc Res. 1984;18(3):140-4.
175. D'Eri A, Martini R, Cordova RM, Trevisan G, Andreozzi GM. [Evaluation of cutaneous necrosis risk in peripheral arterial diseases]. Minerva Cardioangiol. 2002;50(3):239-44.
176. Mast BA, Schultz GS. Interactions of cytokines, growth factors, and proteases in acute and chronic wounds. Wound Repair Regen. 1996;4(4):411-20.
177. Schmidt M, Gutknecht D, Simon JC, Schulz JN, Eckes B, Anderegg U, et al. Controlling the Balance of Fibroblast Proliferation and Differentiation: Impact of Thy-1. The Journal of investigative dermatology. 2015;135(7):1893-902.
178. Singer AJ, Clark RA. Cutaneous wound healing. N Engl J Med. 1999;341(10):738-46.
179. Mariggio MA, Cassano A, Vinella A, Vincenti A, Fumarulo R, Lo Muzio L, et al. Enhancement of fibroblast proliferation, collagen biosynthesis and production of growth factors as a result of combining sodium hyaluronate and aminoacids. Int J Immunopathol Pharmacol. 2009;22(2):485-92.
180. Dale PD, Sherratt JA, Maini PK. Role of fibroblast migration in collagen fiber formation during fetal and adult dermal wound healing. Bull Math Biol. 1997;59(6):1077-100.
181. Bainbridge P. Wound healing and the role of fibroblasts. J Wound Care. 2013;22(8):407-8, 10-12.
182. Xu J, Clark RA. Extracellular matrix alters PDGF regulation of fibroblast integrins. J Cell Biol. 1996;132(1-2):239-49.
183. McHarg S, Hopkins G, Lim L, Garrod D. Down-regulation of desmosomes in cultured cells: the roles of PKC, microtubules and lysosomal/proteasomal degradation. PLoS One. 2014;9(10):e108570.
184. Li B, Wang JH. Fibroblasts and myofibroblasts in wound healing: force generation and measurement. J Tissue Viability. 2011;20(4):108-20.
185. Darby IA, Laverdet B, Bonte F, Desmouliere A. Fibroblasts and myofibroblasts in wound healing. Clin Cosmet Investig Dermatol. 2014;7:301-11.
186. Tomasek JJ, Gabbiani G, Hinz B, Chaponnier C, Brown RA. Myofibroblasts and mechano-regulation of connective tissue remodelling. Nat Rev Mol Cell Biol. 2002;3(5):349-63.
187. Loots MA, Lamme EN, Mekkes JR, Bos JD, Middelkoop E. Cultured fibroblasts from chronic diabetic wounds on the lower extremity (non-insulin-dependent diabetes mellitus) show disturbed proliferation. Arch Dermatol Res. 1999;291(2-3):93-9.
188. Fowlkes V, Clark J, Fix C, Law BA, Morales MO, Qiao X, et al. Type II diabetes promotes a myofibroblast phenotype in cardiac fibroblasts. Life Sci. 2013;92(11):669-76.
189. Lerman OZ, Galiano RD, Armour M, Levine JP, Gurtner GC. Cellular dysfunction in the diabetic fibroblast: impairment in migration, vascular endothelial growth factor production, and response to hypoxia. The American journal of pathology. 2003;162(1):303-12.

190. Kruse CR, Singh M, Sorensen JA, Eriksson E, Nuutila K. The effect of local hyperglycemia on skin cells in vitro and on wound healing in euglycemic rats. J Surg Res. 2016;206(2):418-26.
191. Han DC, Isono M, Hoffman BB, Ziyadeh FN. High glucose stimulates proliferation and collagen type I synthesis in renal cortical fibroblasts: mediation by autocrine activation of TGF-beta. J Am Soc Nephrol. 1999;10(9):1891-9.
192. Li J, Dai Y, Su Z, Wei G. MicroRNA-9 inhibits high glucose-induced proliferation, differentiation and collagen accumulation of cardiac fibroblasts by down-regulation of TGFBR2. Biosci Rep. 2016;36(6).
193. Zhang X, Stewart JA, Jr., Kane ID, Massey EP, Cashatt DO, Carver WE. Effects of elevated glucose levels on interactions of cardiac fibroblasts with the extracellular matrix. In Vitro Cell Dev Biol Anim. 2007;43(8-9):297-305.
194. Sibbitt WL, Jr., Mills RG, Bigler CF, Eaton RP, Griffey RH, Vander Jagt DL. Glucose inhibition of human fibroblast proliferation and response to growth factors is prevented by inhibitors of aldose reductase. Mech Ageing Dev. 1989;47(3):265-79.
195. Xuan YH, Huang BB, Tian HS, Chi LS, Duan YM, Wang X, et al. High-glucose inhibits human fibroblast cell migration in wound healing via repression of bFGF-regulating JNK phosphorylation. PLoS One. 2014;9(9):e108182.
196. Bodempudi V, Hergert P, Smith K, Xia H, Herrera J, Peterson M, et al. miR-210 promotes IPF fibroblast proliferation in response to hypoxia. Am J Physiol Lung Cell Mol Physiol. 2014;307(4):L283-94.
197. Hehenberger K, Heilborn JD, Brismar K, Hansson A. Inhibited proliferation of fibroblasts derived from chronic diabetic wounds and normal dermal fibroblasts treated with high glucose is associated with increased formation of l-lactate. Wound Repair Regen. 1998;6(2):135-41.
198. Zhao B, Guan H, Liu JQ, Zheng Z, Zhou Q, Zhang J, et al. Hypoxia drives the transition of human dermal fibroblasts to a myofibroblast-like phenotype via the TGF-beta1/Smad3 pathway. Int J Mol Med. 2017;39(1):153-9.
199. Modarressi A, Pietramaggiori G, Godbout C, Vigato E, Pittet B, Hinz B. Hypoxia impairs skin myofibroblast differentiation and function. The Journal of investigative dermatology. 2010;130(12):2818-27.
200. Deveci M, Gilmont RR, Dunham WR, Mudge BP, Smith DJ, Marcelo CL. Glutathione enhances fibroblast collagen contraction and protects keratinocytes from apoptosis in hyperglycaemic culture. Br J Dermatol. 2005;152(2):217-24.
201. Mendoza-Naranjo A, Cormie P, Serrano AE, Wang CM, Thrasivoulou C, Sutcliffe JE, et al. Overexpression of the gap junction protein Cx43 as found in diabetic foot ulcers can retard fibroblast migration. Cell biology international. 2012;36(7):661-7.
202. Siqueira MF, Li J, Chehab L, Desta T, Chino T, Krothpali N, et al. Impaired wound healing in mouse models of diabetes is mediated by TNF-alpha dysregulation and associated with enhanced activation of forkhead box O1 (FOXO1). Diabetologia. 2010;53(2):378-88.
203. Graham ML, Janecek JL, Kittredge JA, Hering BJ, Schuurman HJ. The streptozotocin-induced diabetic nude mouse model: differences between animals from different sources. Comp Med. 2011;61(4):356-60.

204. Rossini AA, Like AA, Chick WL, Appel MC, Cahill GF, Jr. Studies of streptozotocin-induced insulitis and diabetes. Proceedings of the National Academy of Sciences of the United States of America. 1977;74(6):2485-9.
205. King AJ. The use of animal models in diabetes research. Br J Pharmacol. 2012;166(3):877-94.
206. Deeds MC, Anderson JM, Armstrong AS, Gastineau DA, Hiddinga HJ, Jahangir A, et al. Single dose streptozotocin-induced diabetes: considerations for study design in islet transplantation models. Lab Anim. 2011;45(3):131-40.
207. Motyl K, McCabe LR. Streptozotocin, type I diabetes severity and bone. Biol Proced Online. 2009;11:296-315.
208. Ihm SH, Lee KU, Rhee BD, Min HK. Initial role of macrophage in the development of anti-beta-cell cellular autoimmunity in multiple low-dose streptozotocin-induced diabetes in mice. Diabetes Res Clin Pract. 1990;10(2):123-6.
209. Sheshala R, Peh KK, Darwis Y. Preparation, characterization, and in vivo evaluation of insulin-loaded PLA-PEG microspheres for controlled parenteral drug delivery. Drug Dev Ind Pharm. 2009;35(11):1364-74.
210. Goto T, Fukuyama N, Aki A, Kanabuchi K, Kimura K, Taira H, et al. Search for appropriate experimental methods to create stable hind-limb ischemia in mouse. Tokai J Exp Clin Med. 2006;31(3):128-32.
211. Niiyama H, Huang NF, Rollins MD, Cooke JP. Murine model of hindlimb ischemia. Journal of visualized experiments : JoVE. 2009(23).
212. Brenes RA, Jadlowiec CC, Bear M, Hashim P, Protack CD, Li X, et al. Toward a mouse model of hind limb ischemia to test therapeutic angiogenesis. Journal of vascular surgery. 2012;56(6):1669-79; discussion 79.
213. Chitaley K, Luttrell I. Strain differences in susceptibility to in vivo erectile dysfunction following 6 weeks of induced hyperglycemia in the mouse. J Sex Med. 2008;5(5):1149-55.
214. Qi Z, Fujita H, Jin J, Davis LS, Wang Y, Fogo AB, et al. Characterization of susceptibility of inbred mouse strains to diabetic nephropathy. Diabetes. 2005;54(9):2628-37.
215. Helisch A, Wagner S, Khan N, Drinane M, Wolfram S, Heil M, et al. Impact of mouse strain differences in innate hindlimb collateral vasculature. Arterioscler Thromb Vasc Biol. 2006;26(3):520-6.
216. Navi A, Yu, R, Abraham D, Shi-Wen X, Baker, D, Tsui, J. Mouse Model of Ischaemia-induced Skeletal Muscle Damage. ESVS Spring Meeting, London. 2014.
217. Chaudhry ZZ, Morris DL, Moss DR, Sims EK, Chiong Y, Kono T, et al. Streptozotocin is equally diabetogenic whether administered to fed or fasted mice. Lab Anim. 2013;47(4):257-65.
218. Wu J, Zhang R, Torreggiani M, Ting A, Xiong H, Striker GE, et al. Induction of diabetes in aged C57B6 mice results in severe nephropathy: an association with oxidative stress, endoplasmic reticulum stress, and inflammation. The American journal of pathology. 2010;176(5):2163-76.
219. Yin D, Tao J, Lee DD, Shen J, Hara M, Lopez J, et al. Recovery of islet beta-cell function in streptozotocin- induced diabetic mice: an indirect role for the spleen. Diabetes. 2006;55(12):3256-63.

220. WHO. Global report on diabetes 2016 [Available from: http://apps.who.int/iris/bitstream/10665/204874/1/WHO_NMH_NVI_16.3_eng.pdf?ua=1.
221. Boyko EJ, Ahroni JH, Stensel V, Forsberg RC, Davignon DR, Smith DG. A prospective study of risk factors for diabetic foot ulcer. The Seattle Diabetic Foot Study. Diabetes care. 1999;22(7):1036-42.
222. Brem H, Sheehan P, Boulton AJ. Protocol for treatment of diabetic foot ulcers. American journal of surgery. 2004;187(5A):1S-10S.
223. Sheehan P, Jones P, Caselli A, Giurini JM, Veves A. Percent change in wound area of diabetic foot ulcers over a 4-week period is a robust predictor of complete healing in a 12-week prospective trial. Diabetes care. 2003;26(6):1879-82.
224. Hinchliffe RJ, Valk GD, Apelqvist J, Armstrong DG, Bakker K, Game FL, et al. A systematic review of the effectiveness of interventions to enhance the healing of chronic ulcers of the foot in diabetes. Diabetes/metabolism research and reviews. 2008;24 Suppl 1:S119-44.
225. Rosa Ramirez S, Ravi Krishna Dasu M. Toll-like receptors and diabetes complications: recent advances. Curr Diabetes Rev. 2012;8(6):480-8.
226. Donahoe SM, Stewart GC, McCabe CH, Mohanavelu S, Murphy SA, Cannon CP, et al. Diabetes and mortality following acute coronary syndromes. Jama. 2007;298(7):765-75.
227. Arnold M, Mattle S, Galimanis A, Kappeler L, Fischer U, Jung S, et al. Impact of admission glucose and diabetes on recanalization and outcome after intra-arterial thrombolysis for ischaemic stroke. International journal of stroke : official journal of the International Stroke Society. 2014;9(8):985-91.
228. van Beijnum JR, Buurman WA, Griffioen AW. Convergence and amplification of toll-like receptor (TLR) and receptor for advanced glycation end products (RAGE) signaling pathways via high mobility group B1 (HMGB1). Angiogenesis. 2008;11(1):91-9.
229. Martinotti S, Patrone M, Ranzato E. Emerging roles for HMGB1 protein in immunity, inflammation, and cancer. ImmunoTargets and therapy. 2015;4:101-9.
230. Erridge C. Endogenous ligands of TLR2 and TLR4: agonists or assistants? J Leukoc Biol. 2010;87(6):989-99.